

**SYSTEM-DEPENDENT METABOLISM OF DRUGS BY CYTOCHROME
P450: THE MECHANISTIC BASIS FOR WHY HUMAN LIVER
MICROSOMES ARE SUPERIOR TO HUMAN HEPATOCYTES AT
METABOLIZING MIDAZOLAM BUT INFERIOR AT METABOLIZING
DESLORATADINE**

BY

©2015

FARAZ KAZMI

Submitted to the graduate degree program in Pharmacology, Toxicology & Therapeutics
and the Graduate Faculty of the University of Kansas in partial fulfillment of the
requirements for the degree of Doctor of Philosophy.

Committee Co-chair: Gregory Reed, Ph.D.

Committee Co-chair: Andrew Parkinson, Ph.D.

Scott Weir, Pharm.D., Ph.D.

Jed Lampe, Ph.D.

Jeffrey Krise, Ph.D.

Date Defended: April 27th, 2015

The Dissertation Committee for FARAZ KAZMI

certifies that this is the approved version of the following dissertation:

**SYSTEM-DEPENDENT METABOLISM OF DRUGS BY CYTOCHROME
P450: THE MECHANISTIC BASIS FOR WHY HUMAN LIVER
MICROSOMES ARE SUPERIOR TO HUMAN HEPATOCYTES AT
METABOLIZING MIDAZOLAM BUT INFERIOR AT METABOLIZING
DESLORATADINE**

Committee Co-chair: Gregory Reed, Ph.D.

Committee Co-chair: Andrew Parkinson, Ph.D.

Date Approved: April 27th, 2015

ABSTRACT

In the pharmaceutical industry, pooled human liver microsomes (HLM) and pooled cryopreserved human hepatocytes (CHH) are the most commonly used test systems to measure the in vitro metabolic intrinsic clearance (CL_{int}) of investigational new drugs in order to identify drug candidates with favorable pharmacokinetic properties such as once-a-day dosing and low oral dose. However, both HLM and CHH have been shown to underpredict the in vivo clearance of drugs. For drugs whose clearance is predominantly determined by P450 enzymes, metabolic clearance in CHH would be expected to equal that in HLM even if both test systems underpredicted (or overpredicted) in vivo clearance. Curiously, in the case of drugs with high intrinsic clearance (CL_{int}), CHH underpredict in vivo clearance to a greater extent than HLM. Such system-dependent clearance has been reported for midazolam, a high CL_{int} drug that is the most widely used CYP3A4/5 substrate for both the in vitro and in vivo assessment of drug-drug interactions (DDIs). Previous investigators have proposed that the system-dependent clearance of midazolam is due to permeability- or cofactor-restricted clearance in CHH (i.e., clearance in hepatocytes is limited by membrane permeability or the availability of NADPH). The objective of this dissertation research was to determine the mechanism underlying the system-dependent clearance of midazolam. Studies of midazolam clearance in HLM and CHH confirmed previous reports that midazolam clearance is almost an order of magnitude lower in CHH than HLM, a system-dependent difference that was much more pronounced than with other CYP3A4/5 substrates (namely alfentanil, nifedipine and verapamil). In vitro to in vivo extrapolation (IVIVE) of clearance established that HLM accurately predicted the in vivo clearance of midazolam whereas CHH underpredicted

midazolam clearance by a factor of 5. Permeabilizing CHH by sonication or treatment with the pore-forming agent saponin did not increase the rate of midazolam metabolism, even in the presence of excess NADPH. Furthermore, the rate of midazolam uptake by CHH was found to greatly exceed the rate of midazolam metabolism, and microsomes isolated from pooled CHH had comparable CYP3A4/5 activity towards midazolam as microsomes prepared directly from human liver. These results suggested that neither membrane permeability nor intracellular cofactor availability were likely explanations for the system-dependent clearance of midazolam.

The impact of in vitro incubation conditions on P450 activity, namely the ionic strength of the incubation buffer and the effect of cell culture media, was evaluated as a possible explanation for the system-dependent clearance of midazolam. As part of this investigation, a cell culture medium was sought that was capable of increasing midazolam clearance in CHH. Compared with KHB (the medium used in the initial experiment), Williams' E medium supported similar rates of midazolam metabolism but the other three media examined, namely Waymouth's, MCM+ and DMEM, supported lower rates of midazolam metabolism. In other words, none of the media examined corrected the system-dependent clearance of midazolam (and three of them made matters worse). In general, P450 activities in HLM were maximal at 50 mM phosphate buffer, with the exception of CYP3A4/5 and CYP2E1, where the enzymatic activities increased with increasing buffer ionic strength. The activity of these two enzymes was markedly decreased when HLM were incubated in Waymouth's, MCM+ or DMEM (the same three media that decreased the rate of midazolam metabolism in CHH). The effect of certain cell culture media on reducing midazolam clearance in both HLM and CHH was not

observed with other CYP3A4/5 substrates (namely alfentanil, nifedipine, verapamil, testosterone and atorvastatin). The kinetics of midazolam metabolism in HLM in the presence of various cell culture media suggested that both MCM+ and Williams' E medium contained an inhibitory substance as evidenced by a marked increase in K_m compared with 50 mM phosphate buffer. Studies with complete versions or salt-only versions of each medium on CYP3A4/5 activity in HLM further suggested the presence of an inhibitory component in certain cell culture media. Although, this dissertation research was unsuccessful in identifying a the cell culture medium that corrected the system-dependent clearance of midazolam, it disproved two previous explanations for this phenomenon and formed the basis for recommending valuable improvements for the conduct of in vitro metabolism studies, such as ideal buffering conditions for HLM and the use of Williams' E media for studies in CHH.

In an effort to identify a CYP3A4/5 substrate with the same system-dependent clearance characteristics as midazolam, the CYP3A4/5 substrate loratadine was examined in CHH. The rate of conversion of loratadine to desloratadine by CHH varied depending on the culture medium in a manner similar to that observed with all other CYP3A4/5 substrates except midazolam. In these studies of loratadine metabolism in hepatocytes, 3-hydroxydesloratadine was detected, which was unexpected because no prior in vitro test system (such as HLM or recombinant CYP enzymes) or non-clinical species in vivo had been previously shown to support its formation. 3-Hydroxydesloratadine is the major human metabolite of desloratadine, and the enzyme responsible for its formation had not been identified despite this being a postmarketing requirement imposed by the FDA on the manufacturer Schering-Plough. Capitalizing on the detection of

3-hydroxydesloratadine in incubations with CHH, studies were conducted to elucidate the enzymology of 3-hydroxydesloratadine formation and to evaluate the potential of desloratadine to be the victim or perpetrator of drug interactions. These studies established that the conversion of desloratadine to 3-hydroxydesloratadine is catalyzed by CYP2C8 but only after desloratadine is converted to an *N*-glucuronide by UGT2B10. Formation of 3-hydroxydesloratadine could be blocked with inhibitors of either CYP2C8 or UGT2B10. Recombinant CYP2C8 formed 3-hydroxydesloratadine only when co-incubated with recombinant UGT2B10 and HLM formed 3-hydroxydesloratadine only when supplemented with both NADPH and UDP-GlcUA (the cofactors to support CYP and UGT enzymes). The formation of 3-hydroxydesloratadine was proposed to follow a three step process: *N*-glucuronidation of desloratadine by UGT2B10, followed by 3-hydroxylation by CYP2C8 and a de-conjugation event to form 3-hydroxydesloratadine. Desloratadine was found to be a weak inhibitor of CYP2B6, CYP2D6 and CYP3A4/5, but a potent and selective inhibitor of UGT2B10. Further studies with inhibitors of UGT2B10 and UGT1A4 established that UGT2B10 is the sole UGT responsible for supporting the CYP2C8-dependent formation of 3-hydroxydesloratadine. In addition to solving a long-standing mystery surrounding the enzymology of 3-hydroxydesloratadine formation, the results of this dissertation have implications on the labeling of desloratadine and, more importantly, provide a pathway for investigating the genetic basis of the impaired metabolism of desloratadine (the so-called poor metabolizer phenotype) observed in a small percentage of patients taking desloratadine. Furthermore, the identification of desloratadine as a UGT2B10 selective inhibitor advances the field of UGT research

towards the goal of identifying a selective inhibitor of each UGT enzyme for use in in vitro metabolism studies.

Dedicated to my family

“Every container becomes tightly packed with what is put in it, except for the container of knowledge, for surely it expands.” – Ali ibn Abi Talib (AS)

ACKNOWLEDGEMENTS

First and foremost, I would like to express my deepest gratitude to **Andrew Parkinson**. I owe my career to your mentorship and guidance, and for that I can never thank you enough. You had the foresight to recognize the potential a novice scientist in the drug inhibition group at XenoTech had, and by taking me under your wing, you fostered that potential into something tangible. You made science fun, not only because of your infectious curiosity of how things work, but because of your magnetic personality and legendary storytelling. I consider myself fortunate to have landed a job at the company you founded and even more fortunate to be (dare I say) your last graduate student. I've often heard you use the phrase that you are 'the luckiest person in the world'. I genuinely consider myself truly lucky to have crossed paths with you. I would be remiss in not also thanking your better half, **Kay Parkinson**. Thank you both for your generosity and welcoming me into your XenoTech family.

To my dissertation committee members: **Greg Reed, Jed Lampe, Scott Weir** and **Jeff Krise** – thank you for your encouragement and support. I couldn't have asked for a better dissertation committee. Thank you also to the Pharmacology, Toxicology and Therapeutics department at KUMC, for welcoming me into your graduate studies family as an industrial student.

To my XenoTech colleagues, first and foremost I would like to thank **Phyllis Yerino** for helping me with my dissertation research. As someone who completes roughly five Ph.D.'s worth of work every week, your help and insight were invaluable. I have to also thank **Joanna Barbara**, for enduring my exciting method development requests and

working miracles with mass spectrometry – all on short notice. To my brother-in-arms (i.e. fellow graduate student) **Brian Ogilvie**, thank you for being my sounding board, answering my questions, and for all of your advice. My thanks also to **Matt Beck**, for helping color and format many figures in this dissertation. I would also like to thank the management at XenoTech, for use of their laboratory and for supporting my dissertation research. To everyone else, past or present, at XenoTech that helped me get this far, my sincerest thanks.

I would also like to thank **Brandy Paris** and **Oliver Parkinson** for figure preparation and data analysis assistance during the preparation of this dissertation.

To my parents, my siblings, my in-laws and the rest of my family – thank you for your constant love and support, none of this would have been possible without it.

Lastly, to my dear wife **Batool** – your constant love, support and encouragement has always kept me anchored and grounded, and my heartfelt thanks for always believing in me. To my little children, **Taha** and **Fatima** – daddy loves you and always be good.

TABLE OF CONTENTS

ABSTRACT	III
ACKNOWLEDGEMENTS	IX
LIST OF ABBREVIATIONS	XVI
LIST OF TABLES	XIX
LIST OF FIGURES	XXII
LIST OF EQUATIONS	XXIX
Chapter 1 : BACKGROUND AND INTRODUCTION	1
1.1. Cytochrome P450 enzymes and drug-drug interactions	2
1.2. Uridine diphosphate glucuronosyltransferase (UGT) enzymes and their interplay with P450 metabolism	6
1.3. Types of in vitro drug metabolism studies and test systems	12
1.4. In vitro intrinsic clearance (CL_{int}) and its relationship to K_m and V_{max} , and in vivo clearance	15
1.5. The importance of membrane partitioning and enzyme inhibition in determining in vitro CL_{int}	20
1.6. Extrapolation of in vitro CL_{int} to in vivo clearance (IVIVE) – models and the importance of R_b , Q_H and f_{ub}	34
1.7. The underprediction of in vivo hepatic intrinsic clearance (CL_H)	57
1.8. Mechanisms of P450 and UGT inhibition	80
1.9. Regulatory perspective on P450 and UGT inhibition	86
1.10. Statement of purpose	91
Chapter 2 : MATERIALS AND METHODS	93
Chapter 3 : TEST SYSTEM-DEPENDENT DRUG CLEARANCE PART 1: MIDAZOLAM CLEARANCE IN HUMAN HEPATOCYTES IS	

RESTRICTED COMPARED WITH HUMAN LIVER MICROSOMES BUT NOT BY CELL PERMEABILITY OR COFACTOR AVAILABILITY	121
ABSTRACT	122
INTRODUCTION	124
RESULTS	127
3.1. Comparison of midazolam and dextromethorphan clearance in HLM and CHH.	127
3.2. Assessment of CYP3A4/5 activity in microsomes prepared from CHH compared with a standard preparation of HLM.	133
3.3. Determining the effect of membrane permeabilization and cofactor supplementation on midazolam metabolism in CHH.	135
3.4. Assessment of midazolam uptake into CHH.	137
3.5. Clearance of four CYP3A4/5 substrates in HLM and CHH.	139
3.6. Assessment of midazolam N-glucuronide as an inhibitor of CYP3A4/5 activity	145
DISCUSSION	148
Chapter 4 : TEST SYSTEM-DEPENDENT DRUG CLEARANCE PART 2: THE EFFECT OF BUFFER IONIC STRENGTH AND VARIOUS CELL CULTURE MEDIA ON THE IN VITRO METABOLISM OF CYTOCHROME P450 SUBSTRATES IN HUMAN LIVER MICROSOMES AND CRYOPRESERVED HUMAN HEPATOCYTES	155
ABSTRACT	156
INTRODUCTION	158
RESULTS	161
4.1. Effects of buffer ionic strength and pH on midazolam 1'-hydroxylation by HLM	161

4.2. Effects of buffer ionic strength and cell culture media on various P450 activities in HLM	165
4.3. Effects of various cell culture media on P450 activities in CHH.	169
4.4. Effects of buffer ionic strength and cell culture media on the metabolism of multiple CYP3A4/5 substrates in HLM and HS9	171
4.5. Effects of various cell culture media on the metabolism of multiple CYP3A4/5 substrates in CHH.	175
4.6. Effects of cell culture media on the kinetics of midazolam and chlorzoxazone metabolism in HLM	178
4.7. Evaluating cell culture media for the presence of CYP3A4/5 modulators	184
4.8. Effects of buffer ionic strength and cell culture media on midazolam metabolism by HLM, rCYP3A4 and rCYP3A5 with and without cytochrome b ₅ .	187
4.9. Effects of cell culture media on midazolam hydroxylation by HLM lacking CYP3A5	190
4.10. Detection of 3-hydroxydesloratadine during the assessment of cell culture media on loratadine metabolism in CHH.	192
DISCUSSION	194
Chapter 5 : A LONG-STANDING MYSTERY SOLVED: THE FORMATION OF 3-HYDROXYDESLORATADINE IS CATALYZED BY CYP2C8 BUT PRIOR GLUCURONIDATION OF DESLORATADINE BY UGT2B10 IS AN OBLIGATORY REQUIREMENT	203
ABSTRACT	204
INTRODUCTION	206
RESULTS	209
5.1. Determination of an in vitro test system capable of producing 3-hydroxydesloratadine.	209
5.2. Assessment of the kinetics of 3-hydroxydesloratadine formation.	211

5.3. Assessment of the species specificity of 3-hydroxydesloratadine formation.	213
5.4. Identification of the enzyme responsible for 3-hydroxydesloratadine formation using recombinant enzymes.	216
5.5. Identification of the enzyme responsible for 3-hydroxydesloratadine formation using chemical inhibitors.	218
5.6. Correlation of 3-hydroxydesloratadine formation with known CYP2C8 activities.	224
5.7. Determining the reason why 3-hydroxydesloratadine forms in hepatocytes but not in subcellular fractions.	228
5.8. Identification of the UGT enzymes involved in 3-hydroxydesloratadine formation.	232
DISCUSSION	235
Chapter 6 : FURTHER CHARACTERIZATION OF THE METABOLISM OF DES Loratadine AND ITS Cytochrome P450 AND UDP- Glucuronosyltransferase (UGT) Inhibitor Potential: Identification of Desloratadine as a Selective UGT2B10 Inhibitor	244
ABSTRACT	245
INTRODUCTION	246
RESULTS	250
6.1. Assessment of desloratadine as an inhibitor of seven P450 enzymes.	250
6.2. Assessment of desloratadine as an inhibitor of CYP2C8 in human hepatocytes.	254
6.3. Assessment of desloratadine as an inhibitor of nine UGT enzymes.	256
6.4. Further characterization of the UGT enzymes involved in 3-hydroxydesloratadine formation.	259
DISCUSSION	262

Chapter 7 : CONCLUSIONS AND FUTURE DIRECTIONS	268
7.1. Summary and overall conclusions	269
7.2. Future directions	278
7.3. Final thoughts	285
REFERENCES	286
APPENDIX I: PERMISSION FOR ARTICLE REPRODUCTION (CHAPTER 5)	332

LIST OF ABBREVIATIONS

Abbreviation	Full name
[S]	Substrate concentration
1-ABT	1-Aminobenzotriazole
AMP	Adenosine monophosphate
ATP	Adenosine triphosphate
AUC	Area under the curve
CDCA	Chenodeoxycholic acid
CHH	Cryopreserved human hepatocytes
CL	Clearance (units of volume per unit time; e.g., L/h)
CL _H	In vivo hepatic clearance of drug from whole blood
CL _{H,int}	In vivo hepatic intrinsic clearance of drug from whole blood
CL _{int}	In vitro intrinsic metabolic clearance
CL _{U,int}	In vitro intrinsic clearance of unbound drug
C _{max}	Maximum drug concentration in blood or plasma after an oral or intravenous dose
DDI	Drug-drug interaction
DMEM	Dulbecco's modified Eagle's medium
D _N	Dispersion number
EDTA	Ethylenediaminetetraacetic acid
EM	Extensive metabolizer
EMA	European Medicines Agency
ER	Endoplasmic reticulum
ESI	Electrospray ionization
FAD	Flavin adenine dinucleotide

FDA	U.S. Food and Drug Administration
F_H	Hepatic availability
FMO	Flavin-containing monooxygenase
f_{UB}	Fraction of unbound drug in whole blood
$f_{U_{hep}}$	Fraction of unbound drug in an in vitro incubation of hepatocytes
$f_{U_{inc}}$	Fraction of unbound drug in an in vitro incubation
$f_{U_{mic}}$	Fraction of unbound drug in an in vitro incubation of microsomes
f_{Up}	Fraction of unbound drug in plasma
HEPES	4-(2-hydroxyethyl)-1-piperazineethanesulfonic acid
HLM	Human liver microsomes
HPGL	Amount of hepatocytes per gram of liver (million cells/g liver)
HS9	Human liver S9 fraction
IC_{50}	Concentration of inhibitor that causes 50% inhibition of enzyme activity
IDA	Information dependent acquisition
ITS	Insulin-transferrin-sodium selenite supplement
IVIVE	In vitro to in vivo extrapolation
k_{el}	Elimination rate constant (units of reciprocal time; e.g., min^{-1})
KHB	Krebs-Henseleit buffer
K_i	Inhibition constant and indicator of the potency of an inhibitor
K_i	Potency of enzyme inactivation by an inhibitor for MDI
K_{inact}	Maximal rate of enzyme inactivation over time (min^{-1})
K_m	Substrate concentration that gives a reaction rate equal to half of V_{max}
LC-MS/MS	Liquid chromatography tandem mass spectrometry
MCM+	Modified Chee's Medium with ITS supplement

MDI	Metabolism-dependent inhibition
MPPGL	Amount of microsomal protein per gram of liver (mg/g liver)
MRM	Multiple reaction monitoring
NA	Not applicable
NADH	Nicotinamide adenine dinucleotide reduced form
NADP	Nicotinamide adenine dinucleotide phosphate
NADPH	Nicotinamide adenine dinucleotide phosphate reduced form
ND	Not determined
OATP	Organic anion transporting polypeptide
P450	Cytochrome P450
PBSF	Physiologically based scaling factor
PM	Poor metabolizer
Q _H	Hepatic blood flow
R _b	Blood-to-plasma drug concentration ratio
RCF	Relative centrifugal force
rpm	Revolutions per minute
t _{1/2}	Half-life (units of time)
TDI	Time-dependent inhibition
TPSA	Topological polar surface area
UDP	Uridine diphosphate
UDP-GlcUA	Uridine diphosphate glucuronic acid
UGT	Uridine diphosphate-glucuronosyltransferase
V _d	Volume of distribution
V _{max}	Maximum velocity (rate) of an enzyme catalyzed reaction

LIST OF TABLES

Table 1.1. The effect of correcting for microsomal partitioning on drug clearance based on measurements of the <i>in vitro</i> half-life of paroxetine (high partitioning) and tienilic acid (low partitioning) by human liver microsomes (HLM) at 0.1 and 1.0 mg protein/mL	31
Table 1.2. Methods to calculate the <i>in vitro</i> free fraction of drug in the presence of microsomes (f_{Umic}).	32
Table 1.3. Physiological data and physiologically based scaling factors (PBSF) for <i>in vitro</i> to <i>in vivo</i> extrapolation (IVIVE)	43
Table 1.4. Examples of hepatically cleared drugs classified as having a low, medium or high hepatic extraction ratio based on intravenous dosing	51
Table 1.5. Comparison of <i>in vitro</i> intrinsic clearance (based on V_{max}/K_m) by microsomes and hepatocytes prepared from the same four human livers.	60
Table 1.6. Estimates of <i>in vivo</i> clearance ($CL_{H,int}$) from <i>in vitro</i> clearance values (CL_{int}) determined from V_{max}/K_m for P450 marker substrates with human liver microsomes and their relationship to hepatic blood flow (Q_H)	73
Table 1.7. FDA and EMA models for the prediction of clinically significant P450 and UGT inhibition	89
Table 2.1. Salt composition and ionic strength of various cell culture media	117

Table 2.2. Individual human donor information for CYP2C8 and UGT2B10 correlation analysis.	118
Table 2.3. Analytical conditions for the measurement of P450 activity in HLM and CHH by LC-MS/MS with electrospray ionization (ESI)	119
Table 2.4. Experimental conditions for measuring UGT activity for enzyme inhibition and metabolism studies in human liver microsomes (HLM) by LC-MS/MS with electrospray ionization (ESI)	120
Table 3.1. Summary of scaled values of in vivo hepatic intrinsic clearance ($CL_{H,int}$) from values of in vitro intrinsic clearance (CL_{int}) determined with cryopreserved human hepatocytes and human liver microsomes	132
Table 3.2. Comparison of metabolic rates between microsomes isolated from cryopreserved human hepatocytes and a standard preparation of pooled human liver microsomes with two concentrations of midazolam (CYP3A4/5) and dextromethorphan (CYP2D6)	134
Table 3.3. Characteristics of the four CYP3A4/5 substrates used in measurements of intrinsic metabolic clearance in human liver microsomes and cryopreserved human hepatocytes	141
Table 3.4. Estimates of intrinsic clearance of four CYP3A4/5 substrates by human liver microsomes (HLM) and cryopreserved human hepatocytes (CHH) based on in vitro half-life.	143

Table 3.5. Observed blood clearance of four CYP3A4/5 substrates following intravenous administration and blood clearance predicted from in vitro half-lived in human liver microsomes (HLM) and cryopreserved human hepatocytes (CHH)	144
Table 4.1. The effect of various cell culture media on the viability of pooled cryopreserved human hepatocytes (1 million cells/mL) over a 240-min incubation period	177
Table 4.2. Summary of kinetic constants (K_m and V_{max}) and scaled values of hepatic clearance (CL_{int}) based on V_{max}/K_m for midazolam and chlorzoxazone metabolism by human liver microsomes incubated in 50 mM phosphate buffer or various cell culture media	182
Table 4.3. Ion concentration and ionic strength of cell culture medium composed of salts only	186
Table 5.1. Chemical inhibition and formation of 3-hydroxydesloratadine in cryopreserved human hepatocytes (CHH) and recombinant enzymes	217
Table 6.1. Assessment of desloratadine as an inhibitor of P450 and UGT enzymes in pooled human liver microsomes (HLM)	252

LIST OF FIGURES

- Figure 1.1. Role of CYP2C9 and CYP2C8 in the formation of 4'-hydroxydiclofenac 11
- Figure 1.2. The effect of membrane partitioning of a drug into microsomes on its in vitro half-life, the apparent incubation volume ($V_{d,app}$) and clearance: The top panel represents total drug concentration and the bottom panel represents unbound (free) drug concentration. 27
- Figure 1.3. The impact of membrane partitioning on the time course of disappearance of paroxetine (left panel) and tienilic acid (right panel) by human liver microsomes at two protein concentrations (0.1 and 1.0 mg/mL). 29
- Figure 1.4. Differences between plasma and blood clearance for a drug excluded from erythrocytes (Panel A), a drug evenly distributed between plasma and erythrocytes (Panel B) and a drug preferentially distributed in erythrocytes. 41
- Figure 1.5. The mutual impact of intrinsic clearance (CL_{int}) and the unbound fraction of drug in blood (f_{uB}) on hepatic extraction ratio (E_H ; left axis) and hepatic clearance (CL_H ; right axis) 50
- Figure 1.6. Relationship between unbound intrinsic clearance ($CL_{u, int}$) in human hepatocytes and microsomes from the same four donors. 61
- Figure 1.7. Current paradigm for performing in vitro P450 and UGT inhibition studies 84

Figure 1.8. Theoretical prediction of drug-drug interactions involving P450 and UGT inhibition on the basis of inhibitory potency	90
Figure 3.1. The in vitro clearance of midazolam (top) and dextromethorphan (bottom) at 1 μ M and plasma C_{max} in cryopreserved human hepatocytes (CHH)	129
Figure 3.2. The in vitro clearance of midazolam (top) and dextromethorphan (bottom) at 1 μ M in pooled human liver microsomes	130
Figure 3.3. Kinetics of 1'-hydroxymidazolam (CYP3A4/5) formation (top) and dextrorphan (CYP2D6) formation (bottom) pooled human liver microsomes	131
Figure 3.4. The effects of membrane permeabilization by sonication or saponin treatment and cofactor supplementation on the in vitro metabolism of midazolam in cryopreserved human hepatocytes	136
Figure 3.5. The contribution of metabolism and uptake as determined by whole-system loss versus medium loss of midazolam (1 μ M) in cryopreserved human hepatocytes (1 million cells/mL)	138
Figure 3.6. The in vitro clearance of the CYP3A4/5 substrates midazolam, alfentanil, nifedipine and verapamil at 1 μ M in human liver microsomes (top) and cryopreserved human hepatocytes (bottom)	142
Figure 3.7. Evaluation of midazolam N-glucuronide as an inhibitor of CYP3A4/5 activity toward midazolam 1'-hydroxylation (top), midazolam 4-hydroxylation	

(middle) and nifedipine oxidation (bottom) in human liver microsomes (HLM)

146

Figure 4.1. The effect of phosphate buffer (top), potassium chloride (middle) and pH (bottom) on midazolam hydroxylation in human liver microsomes (HLM) 163

Figure 4.2. The effect of different concentrations of phosphate buffer (5-200 mM, pH 7.4) and five cell culture media on CYP enzyme activity in human liver microsomes. 167

Figure 4.3. The effect of various media on multiple P450 activities in human hepatocytes over time 170

Figure 4.4. The effect of phosphate buffer concentration (5-200 mM, pH 7.4 and cell culture media on the metabolism of six CYP3A4/5 substrates by human liver microsomes (top) and human S9 fraction (bottom). 173

Figure 4.5. The effect of cell culture media on the metabolism of six CYP3A4/5 substrates in cryopreserved human hepatocytes. 176

Figure 4.6. Kinetics of midazolam 1'-hydroxylation (CYP3A4/5; top) and chlorzoxazone 6-hydroxylation (CYP2E1; bottom) by pooled human liver microsomes incubated in 50 mM phosphate buffer or various cell culture media 180

Figure 4.7. Effects of cell culture media on the kinetics of midazolam 1'-hydroxylation and chlorzoxazone hydroxylation in human liver microsomes: Ratio of V_{max} ,

K_m and CL_{int} (V_{max}/K_m) values in media and those determined in 50 mM phosphate buffer.	183
Figure 4.8. The effect of complete versions or salt-only versions of cell culture media on the metabolism of six CYP3A4/5 substrates by human liver microsomes	185
Figure 4.9. The effect of buffer ionic strength and various media on CYP3A4/5 midazolam metabolism in HLM, rCYP3A4 and rCYP3A5	189
Figure 4.10. Effects of cell culture media on midazolam hydroxylation by human liver microsomes lacking CYP3A5.	191
Figure 4.11. The effect of various cell culture media on desloratadine (top) and 3-hydroxydesloratadine (bottom) formation from loratadine in cryopreserved human hepatocytes	193
Figure 4.12. Schematic representation of the hepatocyte relay method to measure the in vitro half-life of metabolically stable drugs	202
Figure 5.1. The formation of 3-hydroxydesloratadine over time in cryopreserved human hepatocytes (CHH), human liver microsomes (HLM) and human S9 fraction (HS9).	210
Figure 5.2. Determination of the enzyme kinetics for the formation of 3-hydroxydesloratadine from desloratadine in cryopreserved human hepatocytes (CHH).	212

Figure 5.3. Formation of 3-hydroxydesloratadine in pooled cryopreserved mouse, rat, rabbit, dog, minipig, monkey and human hepatocytes.	214
Figure 5.4. Formation of 5- and 6-hydroxydesloratadine in hepatocytes from mouse, rat, rabbit, dog, minipig, monkey and human.	215
Figure 5.5. Effect of specific P450 chemical inhibitors on formation of 3-hydroxydesloratadine in pooled cryopreserved human hepatocytes (CHH).	220
Figure 5.6. The effect of various P450 chemical inhibitors on 5-hydroxydesloratadine, 6-hydroxydesloratadine and 3-hydroxydesloratadine O-glucuronide formation in cryopreserved human hepatocytes (CHH).	223
Figure 5.7. Correlation between CYP2C8 activity and 3-hydroxydesloratadine formation in individual donor cryopreserved human hepatocytes (CHH)	225
Figure 5.8. Correlation between CYP2C8 activity, UGT2B10 activity and 3-hydroxydesloratadine formation in individual donor cryopreserved human hepatocytes (CHH)	226
Figure 5.9. Correlation of N-desalkylamodiaquine formation with 6 α -hydroxypaclitaxel formation in a panel of individual donor cryopreserved human hepatocytes (CHH).	227

Figure 5.10. Formation of 3-hydroxydesloratadine in saponin treated or sonicated cryopreserved human hepatocytes (CHH) followed by addition of NADPH and/or UDP-GlcUA.	230
Figure 5.11. Time course of 3-hydroxydesloratadine formation in HLM (0.1 mg/mL) and HS9 (1 mg/mL) with or without NADPH and/or UDP-GlcUA.	231
Figure 5.12. Assessment of 3-hydroxydesloratadine formation with a panel of recombinant UGT enzymes supplemented with recombinant CYP2C8.	233
Figure 5.13. Proposed metabolic scheme for the formation of 3-hydroxydesloratadine and its glucuronide in human hepatocytes and liver subcellular fractions.	234
Figure 6.1. The metabolic scheme for the conversion of desloratadine to 3-hydroxydesloratadine	249
Figure 6.2. Assessment of the inhibition of P450 enzymes by desloratadine.	251
Figure 6.3. Evaluation of desloratadine as an inhibitor of CYP2C8 activity toward amodiaquine (left) and paclitaxel (right) in cryopreserved human hepatocytes	255
Figure 6.4. Evaluation of desloratadine (10 μ M) as an inhibitor of UGT enzymes in human liver microsomes	257
Figure 6.5. IC ₅₀ determination of the UGT2B10 inhibition potential by desloratadine in HLM	258

Figure 6.6. The effect of the UGT1A4 inhibitor hecogenin and the UGT2B10 inhibitor nicotine on the formation of 3-hydroxydesloratadine by NADPH- and UDP-GlcUA-fortified human liver microsomes (HLM) 261

Figure 7.1. Analogs of desloratadine to investigate the site of N-glucuronidation that supports the CYP2C8-dependent formation of 3-hydroxydesloratadine 282

LIST OF EQUATIONS

Equation 1.1	15
Equation 1.2	15
Equation 1.3	15
Equation 1.4	15
Equation 1.5	15
Equation 1.6	16
Equation 1.7	16
Equation 1.8	22
Equation 1.9	25
Equation 1.10	25
Equation 1.11	25
Equation 1.12	37
Equation 1.13	37
Equation 1.14	40
Equation 1.15	40
Equation 1.16	45

Equation 1.17	45
Equation 1.18	45
Equation 1.19	46
Equation 1.20	47
Equation 1.21	47
Equation 1.22	47
Equation 1.23	47
Equation 1.24	49
Equation 1.25	49
Equation 1.26	56
Equation 1.27	59
Equation 1.28	65
Equation 1.29	66
Equation 1.30	66
Equation 1.31	66
Equation 1.32	66
Equation 1.33	86

Equation 1.34	87
Equation 2.1	114
Equation 2.2	114
Equation 2.3	114
Equation 2.4	115
Equation 2.5	115
Equation 2.6	115
Equation 2.7	115
Equation 2.8	115
Equation 2.9	116

CHAPTER 1 : BACKGROUND AND INTRODUCTION

1.1. Cytochrome P450 enzymes and drug-drug interactions

Cytochrome P450 enzymes (P450 enzymes) are a superfamily of heme-containing proteins that catalyze the biotransformation of many endobiotics and xenobiotics (foreign chemicals such as drugs). P450 enzymes are expressed throughout the body; however they are most prominently expressed in the hepatic endoplasmic reticulum, which serves as the primary site of drug metabolism (the next most important site being the intestinal epithelium) (Paine et al., 2006; Parkinson et al., 2013). The P450 enzymes are the most actively studied drug-metabolizing enzymes because they are responsible for the biotransformation of the vast majority of therapeutic drugs. Roughly 80% of the oxidative metabolism of all drugs involves xenobiotic-metabolizing P450 enzymes (the major ones are CYP1A1, 1A2, 1B1, 2A6, 2B6, 2C8, 2C9, 2C19, 2D6, 2E1, 2J2, 3A4 and 3A5), with CYP2D6 and CYP3A4/5 accounting for the metabolism of over half of all small-molecule drugs (Wilkinson, 2005; Gonzalez et al., 2011; Parkinson et al., 2013). The fact that a limited number of xenobiotic-metabolizing enzymes catalyze the vast majority of oxidative drug metabolism underscores their broad substrate specificity. In contrast, P450 enzymes that specialize in the synthesis and degradation of endobiotics (such as steroid hormones, and bile acids) have highly restricted substrate specificity, such as CYP19 (aromatase) which can metabolize testosterone or androstenedione to estrogens but is generally not involved in xenobiotic metabolism (Gonzalez et al., 2011). Biotransformation by drug-metabolizing enzymes with broad substrate specificities is important for converting drugs and the large number of lipophilic xenobiotics in the diet (such as alkaloids and flavonoids) into hydrophilic compounds (metabolites) than can be readily eliminated in urine or bile. P450 enzymes accomplish this primarily through the oxidation of xenobiotics in the

following basic reaction: $\text{RH} + \text{O}_2 + \text{NADPH} + \text{H}^+ \rightarrow \text{ROH} + \text{H}_2\text{O} + \text{NADP}^+$. At the endoplasmic reticulum, P450 enzymes receive electrons for the above basic reaction from the cofactor reduced nicotinamide adenine dinucleotide phosphate (NADPH) via the flavoprotein NADPH-cytochrome P450 reductase (Parkinson et al., 2013). The biotransformation of xenobiotics by enzymes that catalyze hydrolysis (e.g. carboxylesterases), reduction (e.g. carbonyl reductases), and oxidation (e.g. P450 enzymes) reactions is known as Phase I metabolism. Phase II metabolism refers to conjugation reactions, such as the addition of a glucuronic acid moiety by UDP-glucuronosyltransferases (UGT), or sulfation by sulfotransferases. The terms Phase I and Phase II should not be interpreted as one reaction preceding the other, as there are instances in the literature where Phase II reactions precede Phase I reactions and the classification system has been the subject of criticism (Josephy et al., 2005; Ogilvie et al., 2006; Parkinson et al., 2013).

The ability of a drug to cause clinically relevant drug-drug interactions (DDIs) involves the evaluation of that drug's perpetrator and victim potential. Victim drugs are those whose clearance is predominantly through a single route of elimination, an example of which is metabolism by a single P450 enzyme. Partial or complete elimination of that pathway of clearance, either by genetic polymorphism of that particular P450 or due to inhibition by a concomitantly administered drug, can result in a marked decrease in clearance of the victim drug. This in turn leads to an increase in systemic exposure to the victim drug (as measured by the area under plasma-time concentration curve [AUC]) and can result in exaggerated pharmacological effects or toxicity. Terfenadine, cisapride and astemizole are all examples of drugs that have been withdrawn from the market due to their high

victim potential because they are extensively metabolized by CYP3A4 and interactions with inhibitors of CYP3A4, such as the antimycotic ketoconazole and the antibiotic erythromycin, has led to serious (even lethal) ventricular arrhythmias (characterized by QT prolongation and torsade de pointes) (Huang et al., 2008; Ogilvie et al., 2008). Perpetrators are drugs or factors that alter the clearance of a victim drug, such as genetic polymorphisms, inhibitory drugs, inducing drugs and agents involved in transporter interactions. The calcium channel blocker mibefradil is the only drug withdrawn from the U.S. market due to its perpetrator potential; it causes prolonged inactivation of CYP3A4 because it is a mechanism-based inhibitor (Huang et al., 2008; Ogilvie et al., 2008). Genetic polymorphisms can be viewed as perpetrators of DDIs because deficiency in a given metabolic pathway, such as those individuals that have a poor metabolizer (PM) or intermediate (IM) metabolizer genotype, can result in a decrease in clearance and consequently an increase in systemic exposure to victim drugs. Polymorphisms that result in the over-expression of a metabolic pathway of clearance, such as those individuals that have an ultra-rapid metabolizer (UM) genotype, can also act as perpetrators of DDIs because this can result in an increase in clearance leading to a decrease in exposure to victim drugs. Both of the aforementioned genetic polymorphisms (PMs & UMs) are analogous to the use of inhibitory and inducing drugs respectively as perpetrators of DDIs. Of the P450 enzymes, polymorphisms in CYP2C8, CYP2C9, CYP2C19 and CYP2D6 are common and have a clinically significant impact (Muszkat et al., 2007; Zhou, 2009b; Zhou, 2009a; Zi et al., 2010; Aquilante et al., 2013; Parkinson et al., 2013).

DDIs can be classified as either pharmacodynamic (PD) or pharmacokinetic (PK), where the former involves altered pharmacological effects, an example of which is the interaction

between non-steroidal anti-inflammatory drugs (NSAIDs) and acetylsalicylic acid (aspirin). The administration of an NSAID such as ibuprofen can lead to specific reversible inhibition of COX1 which prevents acetylation and irreversible inhibition of COX1 by acetylsalicylic acid, which in turn leads to an increased risk of cardiovascular disease due to the continued production of COX1-mediated thromboxane A₂ (Catella-Lawson et al., 2001; Cascorbi, 2012). Another example is the increased risk of serotonin syndrome that has been reported to result from interactions between MAO inhibitors (Beasley et al., 1993). Pharmacokinetic DDIs involve alterations in the absorption, distribution, metabolism and elimination of drugs, particularly through inhibition or induction of xenobiotic-metabolizing enzymes or transporters. Inhibition of drug-metabolizing enzymes such as P450 enzymes by perpetrator drugs can lead to supra-pharmacological concentrations of a victim drug, which may result in an exaggerated pharmacological response or toxicity, whereas induction can lead to sub-pharmacological concentrations of a victim drug, which may result in loss of therapeutic efficacy (the opposite pharmacological outcome occurs when a metabolite of the drug is the pharmacologically active component). Victim drugs that have a narrow therapeutic index (the dosage range spanning the minimum threshold dose for efficacy to maximum tolerated dose without adverse effect), such as phenytoin, digoxin, and warfarin, are particularly susceptible to pharmacokinetic DDIs as slight alterations in drug clearance by perpetrator inhibitors or inducers can lead to adverse effects or changes in efficacy.

1.2. Uridine diphosphate glucuronosyltransferase (UGT) enzymes and their interplay with P450 metabolism

Uridine diphosphate glucuronosyltransferase (UGT) enzymes catalyze the conjugation of glucuronic acid to xenobiotics. This particular reaction requires the cofactor UDP-glucuronic acid (UDP-GlcUA), but conjugation has been shown to occur with UDP-glucose, UDP-xylose and UDP-galactose (Mackenzie et al., 2005). UGTs are located in the endoplasmic reticulum of liver and other tissues such as kidney, gastrointestinal tract, lungs, prostate, mammary glands, skin, brain, spleen, and nasal mucosa (Parkinson et al., 2013). Contrary to the cytoplasm-facing P450 enzymes, UGT enzymes are located on the luminal side of the endoplasmic reticulum and are the second most actively studied drug-metabolizing enzymes, next to P450. The luminal orientation of UGTs suggests that a nucleotide transporter may be involved in shuttling the cofactor UDP-GlcUA to the site metabolism, and removing the byproduct UDP (because UDP-GlcUA is synthesized in the cytosol). In support of a such a transport mechanism, it was recently reported that a transporter (possibly the same as *in vivo*) may be involved in the uptake of UDP-GlcUA by inside-out microsomes (Rowland et al., 2015). The spatial differences between P450 and UGT suggest that metabolites produced by P450 diffuse across the ER membrane to access UGT enzymes on the luminal side (in the case of sequential Phase I to Phase II metabolism). This spatial difference may also contribute to the consistent *in vitro* underprediction of *in vivo* UGT-mediated clearance (Miners et al., 2010a). There are several factors that may affect UGT-mediated clearance in test systems such as liver microsomes and hepatocytes: 1) the permeability of microsomal membranes to allow free access of the cofactor UDP-GlcUA as well as the aglycone substrate, 2) the effect of long-

chain unsaturated fatty acids present in in vitro incubations, and 3) the homo- or heterodimerization of UGT proteins in the ER. Other factors may also affect the glucuronidation clearance such as UDP-GlcUA concentration, membrane composition, microsomal membrane partitioning of a substrate, buffer composition, ionic strength, pH, organic solvents (used to dissolve substrates), β -glucuronidase activity and glucuronide stability (Miners et al., 2010a). The impact of many of these factors can be minimized with controlled in vitro experimental conditions, for example the limitation of cofactor availability is bypassed by adding saturating concentrations of UDP-GlcUA (2-5 mM). However the byproduct of glucuronidation reactions, namely UDP, has been reported to competitively inhibit the binding of UDP-GlcUA to UGT enzymes and very high concentrations of UDP-GlcUA (8-20 mM) are required to overcome this effect (Fujiwara et al., 2008). The in vitro CL_{int} for zidovudine glucuronidation in HLM were shown to vary 6-fold depending on the incubation conditions, leading to a 3-4 fold underprediction to the in vivo clearance rate (Miners et al., 2006). The prediction of in vivo UGT-mediated drug clearance is generally more accurate with hepatocytes than with microsomes, although both test systems underpredict the in vivo rate of clearance, with the exception of zidovudine, whose clearance is accurately predicted with hepatocytes (Miners et al., 2006). The glucuronidation of xenobiotics by HLM is latent, meaning that it can be stimulated by detergents, such as CHAPS and Brij-58, and the pore-forming peptide alamethicin. These reagents are thought to permeabilize inside-out microsomes and thereby increase access of UGT enzymes to UDP-GlcUA (Parkinson et al., 2013). However treatment of HLM with detergents abolishes P450 activity, a property that is not

shared by alamethicin, leading to the wide use of this pore-forming peptide in studies of drug glucuronidation by microsomes.

The mammalian UGT gene superfamily contains four families and to date at least 22 human UGT enzymes have been identified, of which the major xenobiotic metabolizing UGTs are UGT1A1, 1A3, 1A4, 1A6, 1A7, 1A8, 1A9, 1A10, 2B4, 2B7, 2B10, 2B11, 2B15, 2B17, and 2B28 (Parkinson et al., 2013). Several of these enzymes have also been identified as being polymorphic, such as UGT1A1 where the UGT1A1*28 allele (a loss-of-function variant) is an important risk factor for irinotecan toxicity (Parkinson et al., 2013). Glucuronidation of xenobiotics typically occurs at nucleophilic oxygen, nitrogen and sulfur sites, leading to *O*-, *N*-, and *S*-glucuronides, respectively, although the *C*-glucuronidation of phenylbutazone by UGT1A9 has been reported (Nishimura and Naito, 2006). The most common reactions are *O*- and *N*-glucuronidation. Kaivosaari and colleagues (2011) reviewed the *N*-glucuronidation of drugs, which occurs to a much greater extent than was first appreciated. Historically, UGT1A4 was thought to be the only human UGT capable of forming *N*-glucuronides; however, it is now known that several UGT enzymes including UGT1A3, 1A9, 2B4, 2B7 and 2B10 can also form *N*-glucuronides (Zhou et al., 2010; Kaivosaari et al., 2011). Nevertheless, UGT1A4 and UGT2B10 catalyze the majority of *N*-glucuronidation reactions. UGT1A4 generally catalyzes the *N*-glucuronidation of drugs with low affinity, high capacity whereas UGT2B10 is considered a high affinity, low capacity enzyme. Accordingly, under clinical conditions, UGT2B10 – the high affinity enzyme – may play an important role in the *N*-glucuronidation of drugs, which are present at relatively low concentrations. In contrast to rodents, humans, monkeys, rabbits and, to a lesser extent dogs, can catalyze the *N*-glucuronidation of

tertiary amines. Consequently, the formation of quaternary ammonium glucuronides occurs in humans and some nonclinical species but not in rats or mice (Zhou et al., 2010; Parkinson et al., 2013).

There are several examples of interplay between P450 and UGT enzymes, where some glucuronide conjugates have been found to be substrates for Phase I oxidation or further Phase II metabolism. For example, estradiol 17 β -glucuronide has been shown to be sulfonated by sulfotransferases in Wag/Rij rats (Sun et al., 2006). Furthermore, the secondary metabolite 4-hydroxydiclofenac acyl glucuronide can be formed either by glucuronidation followed by P450 metabolism or vice versa. This can confound the analysis of the CYP2C9 marker substrate diclofenac in test systems that support both P450 and UGT metabolism (such as hepatocytes) or in vivo, because the 4'-hydroxylation of diclofenac can be catalyzed by CYP2C9 (acting on the parent drug) or CYP2C8 (acting on the acyl glucuronide). When the conjugate is hydrolyzed (which can occur by β -glucuronidase in the lumen of the endoplasmic reticulum or in the gastrointestinal tract), it is not possible to discern whether 4'-hydroxydiclofenac was formed by CYP2C9 or CYP2C8 (Kumar et al., 2002) as shown in Figure 1.1. There are several other examples where glucuronidation effectively converts a CYP2C9 substrate into a CYP2C8 substrate or inhibitor. CYP2C8 has been shown to metabolize several glucuronides (the aglycones of which are typically CYP2C9 substrates), including naproxen acyl glucuronide, estradiol 17 β -glucuronide and gemfibrozil glucuronide (Delaforge et al., 2005; Kochansky et al., 2005; Ogilvie et al., 2006). The example of gemfibrozil glucuronide is particularly interesting because the CYP2C8-mediated hydroxylation of gemfibrozil-1-O- β -glucuronide leads to the formation of a reactive metabolite, a benzylic radical, that causes

irreversible inhibition of this enzyme (Ogilvie et al., 2006; Baer et al., 2009). Gemfibrozil and its glucuronide are also substrates and inhibitors of OATP1B1 (Shitara et al., 2004) and this, in combination with CYP2C8 inactivation, accounts for the pharmacokinetic interaction between gemfibrozil and several statin drugs, particularly the OATP1B1 and CYP2C8 substrate cerivastatin (Tornio et al., 2008). Clopidogrel is another example of a clinically used drug whose glucuronide is a mechanism-based inhibitor of CYP2C8 (Tornio et al., 2014). Like gemfibrozil, clopidogrel also increases the incidence of fatal cases of rhabdomyolysis when coadministered with cerivastatin. Kazmi et al. (2010) also identified an N-carbamoyl-glucuronide of a drug candidate that caused mechanism-based inhibition of CYP2C8 in vitro, although its clinical significance is unknown.

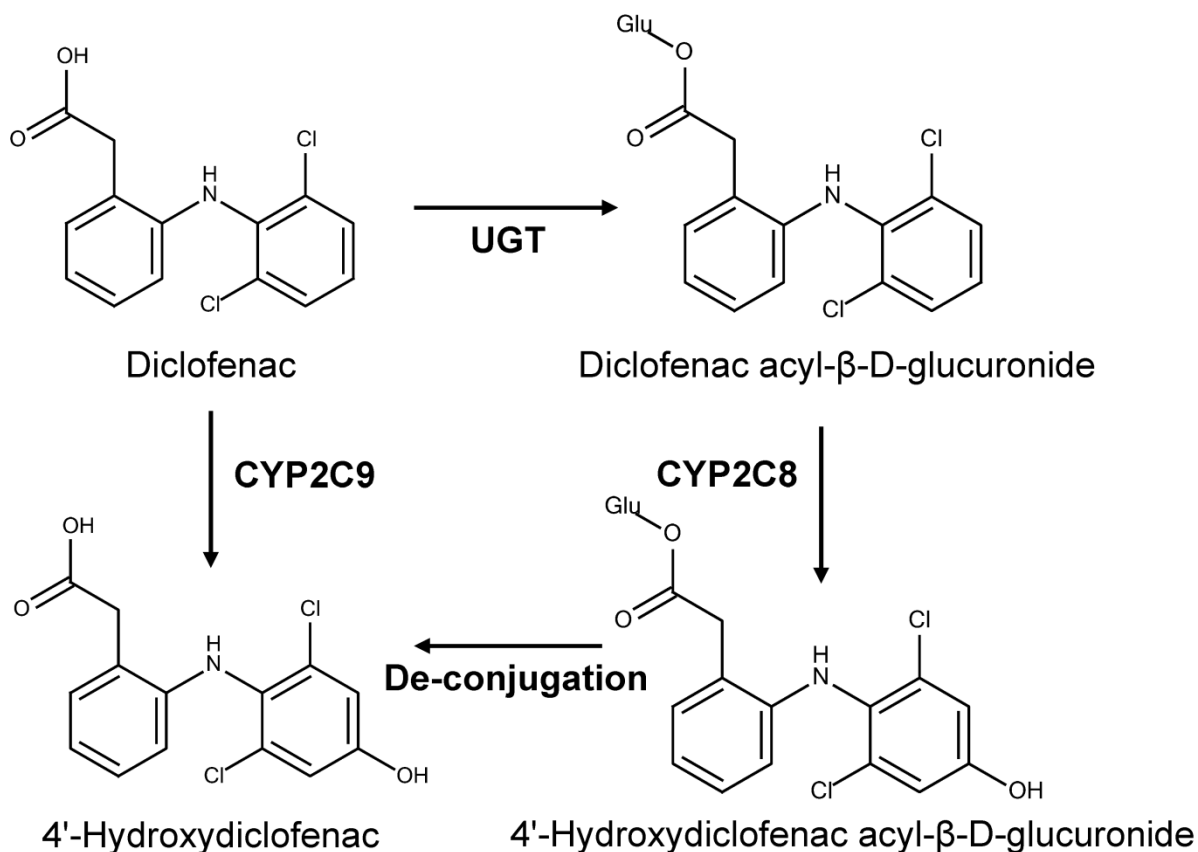


Figure 1.1. Role of CYP2C9 and CYP2C8 in the formation of 4'-hydroxydiclofenac

The schematic depicts the two pathways for the production of 4'-hydroxydiclofenac, the *in vitro* metabolite typically used to assess CYP2C9 activity in human liver microsomes. The first pathway involves direct oxidation by CYP2C9, whereas the second pathway involves oxidation of diclofenac acyl glucuronide by CYP2C8, followed by hydrolysis (de-conjugation) of the glucuronide moiety.

1.3. Types of in vitro drug metabolism studies and test systems

In vitro studies of drug metabolism are conducted for the following purposes:

1. To compare species differences in metabolite profile to examine the potential for the formation of human-predominant or human-specific metabolites;
2. To measure intrinsic metabolic clearance (CL_{int}) to identify drug candidates with desirable pharmacokinetic properties (those consistent with once-a-day dosing and low oral dose);
3. To identify the individual enzyme or enzymes responsible for drug metabolism (by the process of reaction phenotyping or enzyme mapping) to assess the victim potential of a drug (*i.e.*, its potential to be the object of drug-drug interactions or genetic polymorphisms in the expression of drug-metabolizing enzymes);
4. To establish the sample-to-sample variation in the activity of cytochrome P450 (P450) and UDP-glucuronosyltransferase (UGT) enzymes in a bank of human liver microsomes to support reaction phenotyping studies (correlation analysis);
5. To identify which enzymes can be reversibly or irreversibly inhibited by a drug to assess its perpetrator potential (*i.e.*, its potential to be the precipitant of drug-drug interactions);
6. To identify which enzymes can be induced by a drug to assess its perpetrator potential (information that can also be obtained by measuring changes in mRNA levels).

The first three studies involve measurements of the metabolism of the drug or drug candidate under investigation. The latter three studies involve measurements of the metabolism of marker substrates (substrates specifically metabolized by a single enzyme). The latter two studies focus largely on the ability of a drug to inhibit or induce P450 enzymes because changes in P450 activity can be large, prolonged and they can affect the disposition of a large number of other drugs (Parkinson et al., 2013). However, an evaluation of the ability of drugs to inhibit (or possibly induce) UGT and, on a case-by-case basis, other drug-metabolizing enzymes is becoming more common. The metabolism of drugs can be studied in vitro with various test systems including subcellular fractions, such as microsomes and post-mitochondrial (S9) fraction from liver, small intestine, kidney and other tissues, hepatocytes and recombinant or purified enzymes. Such studies can serve a number of purposes, as described below. One application involves the use of in vitro systems to determine metabolic intrinsic clearance (CL_{int}) based on measurements of V_{max}/K_m , $v/[S]$ or in vitro half-life (discussed in the next section and Chapter 2). In vitro CL_{int} values are widely used to predict the in vivo hepatic clearance of drugs, which is used prospectively to select for further development those drug candidates that are expected to possess commercially desirable pharmacokinetic properties, such as a half-life consistent with once-a-day administration and a low oral clearance to reduce dose.

Studies with recombinant enzymes, microsomes, S9 fraction and hepatocytes provide information on rates of drug metabolism. Studies in suspended hepatocytes can also provide information on the rate of cellular uptake of the drug by passive diffusion and transporters whereas studies in cultured hepatocytes (confluent monolayers) can provide

information on rates of uptake and biliary excretion. In the case of acidic and zwitterionic drugs, the rate of transporter-mediated uptake into hepatocytes can provide important information on the rate-determining step in hepatic clearance. In the case of neutral and basic drugs, uptake into hepatocytes and ion partitioning into lysosomes can provide valuable information on the potential for a large volume of distribution, which is a particular characteristic of lipophilic amines (cationic amphiphilic drugs with a $\log P > 1$ and $pK_a > 6$) (Kazmi et al., 2013). Studies with microsomes and hepatocytes have also been conducted in the presence of plasma to achieve the same concentration of unbound drug in vitro that is present in plasma in vivo (Skaggs et al., 2006; Lu et al., 2007; Kazmi et al., 2009; Mao et al., 2012).

Measurements of in vitro metabolic CL_{int} with human liver microsomes and hepatocytes systematically underpredict in vivo hepatic clearance. The underprediction stems in part from attributing the rate-determining step in the clearance of acidic and zwitterionic drug to metabolism rather than transporter-mediated uptake; an underprediction that is evident with both human and rat in vitro test systems. In the case of neutral and basic drugs, however, a systematic underprediction of in vivo metabolic clearance is observed with human but not rat test systems, which suggests human liver microsomes and hepatocytes have low in vitro enzyme activities relative to those in vivo. This issue is discussed in the next sections.

1.4. In vitro intrinsic clearance (CL_{int}) and its relationship to K_m and V_{max} , and in vivo clearance

In pharmacokinetic terms, clearance (CL), the volume of plasma or blood cleared of drug per unit time (e.g., L/h), has many mathematical definitions including that shown in Equation 1.1, in which clearance is the term relating the rate of elimination of a drug from plasma (in units of mg/h) to the concentration of drug in plasma (in units of mg/L):

$$\textit{Elimination rate} = \textit{clearance} \cdot \textit{drug concentration} \quad \textbf{Equation 1.1}$$

The same relationship can be applied to enzymatic rates where the elimination rate is represented by reaction velocity (v) and drug concentration is represented by substrate concentration (S); in this case clearance is termed intrinsic clearance (CL_{int}):

$$v = CL_{int} \cdot [S] \quad \textbf{Equation 1.2}$$

Hence,

$$CL_{int} = \frac{v}{[S]} \quad \textbf{Equation 1.3}$$

The relationship between v and $[S]$ is also given by the Michaelis-Menten equation:

$$v = \frac{V_{max} \cdot [S]}{K_m + [S]} \quad \textbf{Equation 1.4}$$

Equation 1.4 and Equation 1.5 can be combined so that CL_{int} can be related to the terms V_{max} and K_m , which is accomplished by dividing each side of the Michaelis-Menten equation by $[S]$, which gives Equation 1.5:

$$CL_{int} = \frac{v}{[S]} = \frac{V_{max}}{K_m + [S]} \quad \textbf{Equation 1.5}$$

which, by multiplying by K_m/K_m , can be expressed as follows:

$$CL_{int} = \frac{v}{[S]} = \frac{V_{max}}{K_m} \cdot \frac{K_m}{K_m + [S]} \quad \text{Equation 1.6}$$

Alternatively,

$$\frac{V_{max}}{K_m} = \frac{v}{[S]} \cdot \frac{K_m + [S]}{K_m} \quad \text{Equation 1.7}$$

The terms $K_m+[S]/K_m$ and $K_m/K_m+[S]$ are correction factors to convert CL_{int} values determined by $v/[S]$ to CL_{int} values determined by V_{max}/K_m and *vice versa*, respectively. There are two basic in vitro procedures to measure metabolic CL_{int} of drugs by liver microsomes, recombinant enzymes, and hepatocytes: one involves measuring V_{max} and K_m , and the other involves measuring the rate of reaction at a single substrate concentration. In the former case, CL_{int} is based on V_{max}/K_m ; in the latter case it is based on $v/[S]$. However, from Equation 1.5 it is apparent that these two terms are not identical and, furthermore, in accordance with Equation 1.6 and Equation 1.7, they will differ depending on the value of $[S]$ relative to K_m (which determines the values of the correction factors $K_m/K_m+[S]$ in Equation 1.6 and $K_m+[S]/K_m$ in Equation 1.7). For example, if $[S] = K_m$ then the value of CL_{int} based on $v/[S]$ will be half of that based on V_{max}/K_m (because the term $K_m/K_m+[S]$ is 0.5). If $[S] = 1/10 K_m$ then CL_{int} based on $v/[S]$ will be 0.909 of that based on V_{max}/K_m (*i.e.*, it's within 10%), which is why CL_{int} based on $v/[S]$ should be conducted with $[S]$ equal to $1/10 K_m$ or less. The lower the concentration of $[S]$ relative to K_m the closer values of CL_{int} based on $v/[S]$ equal those based on V_{max}/K_m . Strictly speaking, a CL_{int} value exactly equal to V_{max}/K_m could not be achieved experimentally because, from Equation 1.5, we see that $CL_{int} = V_{max}/K_m$ only when $[S] = 0$, which is meaningless from an experimental perspective but it illustrates that values of V_{max}/K_m

represent an upper limit of CL_{int} . Although this upper limit cannot be achieved based on measurements of $v/[S]$, it is important to note that, when $[S]$ is $1/10 K_m$ or less, CL_{int} values based on $v/[S]$ are within 10% of V_{max}/K_m , the maximum value of CL_{int} for any given reaction.

There are physiologically based scaling factors (PBSFs; shown in Table 1.3) to extrapolate the in vitro value of metabolic CL_{int} to $CL_{H,int}$, the in vivo hepatic intrinsic clearance of drug from whole blood (by the process known as in vitro to in vivo extrapolation or IVIVE). In vitro metabolic CL_{int} and its in vivo counterpart $CL_{H,int}$ are measures of the ability of the liver to clear a drug by metabolism *in the absence of any restrictions on delivery of the drug to the intracellular hepatic drug-metabolizing enzymes imposed by blood flow, permeability, binding of the drug to plasma proteins or cellular components such as proteins, lipids, and organelles (such as lysosomes) or cofactor availability*. These restrictions cannot be ignored during the process of IVIVE to estimate the actual hepatic clearance in vivo (CL_H). There are two major restrictions on the in vivo hepatic clearance of a drug, namely hepatic blood flow and binding of the drug to plasma proteins and erythrocytes. Hepatic blood flow (abbreviated Q_H) imposes an upper limit on the hepatic clearance of drugs ($Q_H = 90L/h$ in humans); drugs cannot be eliminated by the liver any faster than blood flow can deliver them to the liver. The binding of some – but not all – drugs to plasma proteins impedes their hepatic uptake and, hence, their metabolic and biliary clearance by the liver. These restrictions on hepatic clearance are discussed in connection with IVIVE in the next section.

The uptake of some drugs into liver is mediated by transporters, such as OATPs. For drugs with low passive permeability, transporter-mediated uptake can be a rate-

determining step in hepatic clearance. The predictive value of in vitro metabolic CL_{int} data also depends on the importance of hepatic metabolic clearance relative to other routes of clearance, such as renal and biliary clearance (renal, biliary and metabolic clearance are the three major clearance pathways). The predictive value of in vitro CL_{int} data determined with NADPH-fortified liver microsomes or recombinant/purified cytochrome P450 enzymes further depends on the importance of P450-dependent metabolism relative to other routes of metabolism. Obach (1999) summarized the assumptions inherent in the use of NADPH-fortified microsomes to the measurement of CL_{int} (all of which can also be extended to recombinant/purified P450 enzymes) as follows:

1. Metabolic clearance is the major mechanism of clearance (*i.e.*, $CL_{metabolism} \gg CL_{renal} + CL_{biliary} + CL_{other}$);
2. The liver is the major organ of clearance (*i.e.*, $CL_{hepatic} \gg \sum CL_{all\ other\ organs}$);
3. Oxidative metabolism predominates over other metabolic routes such as direct conjugation, reduction, hydrolysis, etc.;
4. Rates of metabolism and enzyme activities in vitro are truly reflective of those that exist in vivo.
5. The concentration of drug used to measure CL_{int} based on in vitro half-life is well below K_m ;
6. There is no significant product inhibition or irreversible enzyme inactivation during prolonged incubations to measure in vitro half-life.

Obach also pointed out that a tenet of the well-stirred and parallel-tube models of hepatic extraction is that the unbound concentration of drug in plasma is equal to the unbound concentration in hepatocytes. Therefore, facilitated transport processes that could

possibly be responsible for drug uptake or drug efflux from hepatocytes are not accounted for in in vitro studies with microsomes or recombinant enzymes (or with hepatocytes depending on the experimental design).

In vitro CL_{int} is usually determined from V_{max}/K_m or in vitro half-life. Both methods are widely used to measure in vitro CL_{int} with liver microsomes and recombinant/purified enzymes. In contrast, the measurement of CL_{int} in hepatocytes is usually based on in vitro half-life (substrate disappearance) because measuring the rate of formation of primary metabolites in hepatocytes can be complicated by a lag in their formation and their further metabolism (e.g., conjugation) to secondary metabolites. Each method has its advantages and disadvantages. The first method (V_{max}/K_m) generally involves the measurement of metabolite formation at multiple substrate concentrations under initial-rate conditions (a single, short incubation time). The second method (*in vitro* half-life) usually involves the measurement of substrate disappearance at a single, low concentration of drug at multiple time points (typically with much longer incubation times than those used to determine V_{max} and K_m). Some investigators use abbreviated procedures to estimate CL_{int} in which in vitro half-life is measured with only two time points (e.g., zero and 30 min) or in which the rate of metabolite formation (v) is measured at a single substrate concentration (ideally one that is well below K_m) and CL_{int} is based on $v/[S]$. Estimates of CL_{int} based on in vitro half-life or $v/[S]$ give slightly lower values of CL_{int} than that based on V_{max}/K_m , the magnitude of which depends on the concentration of substrate relative to K_m .

1.5. The importance of membrane partitioning and enzyme inhibition in determining in vitro CL_{int}

The degree of membrane partitioning of drugs to microsomes is dependent on the concentration of microsomal protein (the fraction of unbound drug, $f_{u_{mic}}$, decreases with increasing protein concentration) and the drug's lipophilicity and charge at pH 7.4 (Obach, 1996; Obach, 1997; Obach, 1999; Austin et al., 2002; Hallifax and Houston, 2006; Gertz et al., 2008; Nagar and Korzekwa, 2012). Basic (cationic) drugs tend to partition into microsomes more extensively than acidic (anionic) drugs; the former, being positively charged, are attracted to the negatively charged phospholipids in the membrane whereas the latter, being negatively charged, are repelled. Several endpoints, such as the kinetic constants K_m , K_i and K_i , are affected by microsomal partitioning, but others are not. For example, if in vitro experiments are performed at 0.1 and 1.0 mg microsomal protein/mL with a drug that is 20% bound at the lower protein concentration ($f_{u_{mic}} = 0.8$) and 80% bound at the 10-fold higher protein concentration ($f_{u_{mic}} = 0.2$), the four-fold difference in $f_{u_{mic}}$ would cause a four-fold increase in K_m (in studies of the drug's metabolism) and a four-fold increase in K_i or K_i for P450 enzymes inhibited reversibly or irreversibly by the drug. These concentration-dependent effects on K_m , K_i and K_i can be corrected by taking $f_{u_{mic}}$ into account and expressing these constants on the basis of the unbound drug concentration (Obach, 1996; Obach, 1997; Obach, 1999; McLure et al., 2000; Austin et al., 2002; Di Marco et al., 2003; Margolis and Obach, 2003; Hallifax and Houston, 2006; Howgate et al., 2006; Brown et al., 2007a; Brown et al., 2007b).

Microsomal partitioning (often all microsomal binding) affects in vitro clearance but it does not affect in vitro half-life, which seems counterintuitive. How is this possible? Microsomal

partitioning affects CL_{int} by changing the apparent volume of the incubation ($V_{d,app}$), which is the in vitro equivalent of V_d , the in vivo volume of distribution. This is illustrated in Figure 1.2, which depicts the in vitro metabolism (disappearance) of a drug (1 μM) under the conditions noted above: incubations are performed at two concentrations of microsomal protein, namely 0.1 mg protein/mL (with $f_{u,mic} = 0.8$) and 1.0 mg protein/mL (with $f_{u,mic} = 0.2$). The upper panel in Figure 1.2 depicts substrate disappearance based on the total concentration of drug (starting with 1 μM for both protein concentrations); the lower panel depicts substrate disappearance based on the unbound concentration (starting with 0.8 μM at 0.1 mg protein/mL and 0.2 μM at 1.0 mg/mL). Both graphs are semi-log plots and substrate disappearance conforms to a first-order elimination process (which gives a straight line). In both cases, increasing the concentration of microsomes tenfold shortened the in vitro half-life from 25 min (at 0.1 mg/mL) to 10 min (at 1.0 mg/mL). When CL_{int} is determined based on total drug concentration (1 μM), V_{inc} is 1 mL for both concentrations of microsomes; hence, the 2.5-fold difference in half-life translates to a 2.5-fold difference in CL_{int} (Figure 1.2, upper panel). In contrast, when CL_{int} is determined based on the unbound drug concentration (0.8 μM at 0.1 mg/mL and 0.2 μM at 1.0 mg/mL), the apparent incubation volume ($V_{inc,app}$) increases fourfold (from 1.25 mL at 0.1 mg/mL to 5.0 mL at 1.0 mg/mL); now the 2.5-fold difference in half-life combined with the four-fold difference in the apparent incubation volume translates into a 10-fold difference in CL_{int} (Figure 1.2, lower panel). The important point illustrated in Figure 1.2 is that a 10-fold increase in the concentration of microsomes results in a 10-fold increase in clearance only when the fraction of unbound drug is taken into account. When such clearance values are expressed on a per-mg-protein basis, the same result is obtained regardless

of the concentration of microsomes. Without correcting for such partitioning, values of CL_{int} will decrease with increasing microsomal protein concentration.

Figure 1.3 shows the elimination of tienilic acid (0.5 μ M) and paroxetine (0.2 μ M) when incubated with human liver microsomes at 0.1 and 1.0 mg/mL (Parkinson et al., 2011). Tienilic acid is a substrate and metabolism-dependent inhibitor of CYP2C9 whereas paroxetine is a substrate and metabolism-dependent inhibitor of CYP2D6. The key parameters for this experiment are summarized in Table 1.1. A visual inspection of Figure 1.3 reveals that increasing the concentration of human liver microsomes 10-fold markedly increased the rate of elimination of tienilic acid but only marginally increased the rate of elimination of paroxetine. Table 1.1 shows that increasing the concentration of human liver microsomes 10-fold increased the rate of elimination of paroxetine only 2.6 fold (k_{el} increased from 0.028 min^{-1} to 0.073 min^{-1} and half-life decreased by the same factor from 25 to 9.5 min). This difference can largely be attributed to membrane partitioning of paroxetine, a lipophilic amine that is predominantly positively charged at pH 7.4, to microsomal protein and the negatively charged phospholipids. Partitioning of paroxetine into microsomes was determined experimentally (discussed later in this section); the unbound fraction ($f_{u_{mic}}$) was 0.45 and 0.14 at 0.1 and 1.0 mg microsomal protein/mL, respectively (Table 1.1). These values were used to calculate the in vitro clearance of unbound paroxetine as follows:

$$CL_{u_{int}} = \frac{CL_{int}}{f_{u_{mic}}} \quad \text{Equation 1.8}$$

Without correction for microsomal partitioning, CL_{int} of paroxetine at the lower concentration of HLM (280 μ L/min/mg microsomal protein) was 3x greater than CL_{int} at the higher concentration of HLM (83 μ L/min/mg microsomal protein). However, when

corrected for membrane partitioning, paroxetine clearance was roughly the same at both microsomal concentrations ($CL_{U_{int}} = \sim 600 \mu\text{L}/\text{min}/\text{mg}$ microsomal protein).

Table 1.1 shows that increasing the concentration of HLM 10-fold actually increased the rate of elimination of tienilic acid 24 fold (k_{el} increased from 0.014 min^{-1} to 0.033 min^{-1} and half-life decreased from 50 to 2.1 min). CL_{int} at the higher protein concentration was more than twice that at the lower protein concentration (330 versus $140 \mu\text{L}/\text{min}/\text{mg}$ microsomal protein). This 2.4-fold difference cannot be attributed to microsomal partitioning. No membrane partitioning of tienilic acid was measurable at 0.1 mg microsomal protein/mL and only 12% partitioning was evident at 1.0 mg microsomal protein/mL; such low microsomal partitioning is characteristic of acidic drugs. In contrast to the situation with paroxetine, correcting CL_{int} values for microsomal partitioning in the case of tienilic acid made the discrepancy worse (but only slightly): $CL_{U_{int}}$ at the lower and higher protein concentration were 140 and $375 \mu\text{L}/\text{min}/\text{mg}$ microsomal protein (compared with uncorrected values of 140 and 330) (Table 1.1). The 2.7 fold discrepancy in $CL_{U_{int}}$ is likely due to the partial inactivation of CYP2C9 by tienilic acid, the extent of which increases with decreasing concentration of microsomes (Parkinson et al., 2011).

The in vitro half-life studies with tienilic acid and paroxetine shown in Figure 1.3 underscore some important principles:

1. If $f_{u_{mic}}$ is not taken into account then estimates of in vitro CL_{int} will often depend on the concentration of liver microsomes (*i.e.*, they will decrease with increasing protein concentration). This will be particularly apparent with basic drugs (like paroxetine), which tend to partition into microsomes to a greater extent than acidic drug (like tienilic acid). The importance of correcting for membrane partitioning

applies also to studies with recombinant enzymes and hepatocytes. Correcting in vitro CL_{int} values for f_{umic} (according to Equation 1.8) is important regardless of whether they are based on in vitro half-life, $v/[S]$ or V_{max}/K_m .

2. When an increase in microsomal protein concentration does not cause a corresponding increase in metabolic rate based on the total (nominal) concentration of substrate, as in the case of paroxetine, this is a good indication that microsomal partitioning is lowering the free (unbound) concentration of substrate and thereby restricting the enzyme's access to substrate.
3. When an increase in microsomal protein concentration causes a supra-proportional increase in metabolic rate, as in the case of tienilic acid, this is a good indication that the substrate inactivates the enzyme, the extent of which decreases with increasing concentration of microsomal protein (for reasons detailed in Parkinson et al. (2011)).
4. To avoid a departure from first-order elimination kinetics, measurements of in vitro half-life should be based on initial rates of substrate disappearance. A departure from first-order elimination kinetics (as indicated by deviation from a straight line on a semi-log plot of [Drug] *versus* time) can occur for three main reasons:
 - a. The substrate can be converted to a metabolite that causes reversible enzyme inhibition;
 - b. The substrate causes irreversible enzyme inactivation;
 - c. There is spontaneous (drug-independent) loss of enzyme activity.

The partitioning of drugs into microsomes (*i.e.*, the fraction of free drug in a microsomal incubation) can be determined experimentally by equilibrium dialysis, ultrafiltration or ultracentrifugation. Alternatively, $f_{u_{mic}}$ values can be estimated for any concentration of microsomal protein (C_p) based on $\log P$ or $\log D_{7.4}$ values. Values of $\log P$ (the log octanol-water partition coefficient of neutral [unionized] drug) and $\log D_{7.4}$ (the log octanol-water partition coefficient of both neutral and ionized [total] drug at pH 7.4) can be determined experimentally or estimated with free software programs such as MarvinSketch 5.9.0 (ChemAxon, Cambridge, MA [www.chemaxon.com]). For basic drugs, estimates of $f_{u_{mic}}$ are based on $\log P$ whereas $\log D_{7.4}$ is used to estimate $f_{u_{mic}}$ for acidic drugs. In the case of neutral drugs, either $\log P$ or $\log D_{7.4}$ can be used because the values are identical. As shown in Table 1.2, several equations to determine $f_{u_{mic}}$ have been reported in the literature. Estimates of $f_{u_{mic}}$ tend to become less reliable with highly lipophilic drugs ($\log P$ or $\log D_{7.4} > 5$).

The unbound fraction of drug in the extracellular medium of in vitro incubations of hepatocytes ($f_{u_{hep}}$) can be estimated from the following equations (Kilford et al., 2008);

$$f_{u_{hep}} = \frac{1}{1 + \frac{K_p \cdot V_R}{K_a \cdot P} \left(\frac{1 - f_{u_{mic}}}{f_{u_{mic}}} \right)} \quad \text{Equation 1.9}$$

$$f_{u_{hep}} = \frac{1}{1 + K_a \cdot V_R \cdot 10^{0.072 \log P / D^2 + 0.067 \log P / D - 1.126}} \quad \text{Equation 1.10}$$

$$f_{u_{hep}} = \frac{1}{1 + 125 \cdot \left(0.005 \cdot \frac{n}{V} \right) \cdot 10^{0.072 \log P / D^2 + 0.067 \log P / D - 1.126}} \quad \text{Equation 1.11}$$

where K_p is the ratio of the concentration of drug in hepatocytes *versus* the concentration of drug in medium, K_a is a microsomes-to-hepatocytes scaling factor (= 125 for 1 mg microsomal protein/mL and 1 million hepatocytes/mL), V_R is the ratio of the volume of hepatocytes to the volume of medium (= 0.005 for 1 million cells/mL), P is the concentration of microsomal protein used to measure or estimate $f_{u_{mic}}$, n is the number of million hepatocytes in the incubation, V is the incubation volume and $\log P/D$ is the $\log P$ value for basic drugs and the $\log D_{7.4}$ value for acidic and neutral drugs. The application of $f_{u_{hep}}$ to values of in vitro half-life determined with hepatocytes is analogous to the application of $f_{u_{mic}}$ to values in vitro half-life determined with microsomes (Table 1.2); the end result being an estimate of CL_{int} based on the unbound concentration of drug in the in vitro incubation system.

The term $f_{u_{hep}}$, the fraction unbound in hepatocytes, can be misleading. It is a measure of the unbound concentration of drug in the medium, not in the hepatocyte. The equations for calculating $f_{u_{hep}}$ (Equation 1.9, Equation 1.10 and Equation 1.11) are based on experiments with inactive or disrupted hepatocytes. Consequently, they do not account for active processes such as transporter-mediated uptake or ion-partitioning into acidic lysosomes, processes that lead to drug accumulation in hepatocytes (Kazmi et al., 2013). Suffice it to say here that, in the case of drugs that are actively transported into hepatocytes, such as the OATP substrate atorvastatin, the concentration of unbound drug in the hepatocyte incubation medium and the rate of metabolic clearance both decrease with increasing concentration of hepatocytes and do so to a much greater extent than is observed with non-transported drugs (Nordell et al., 2013).

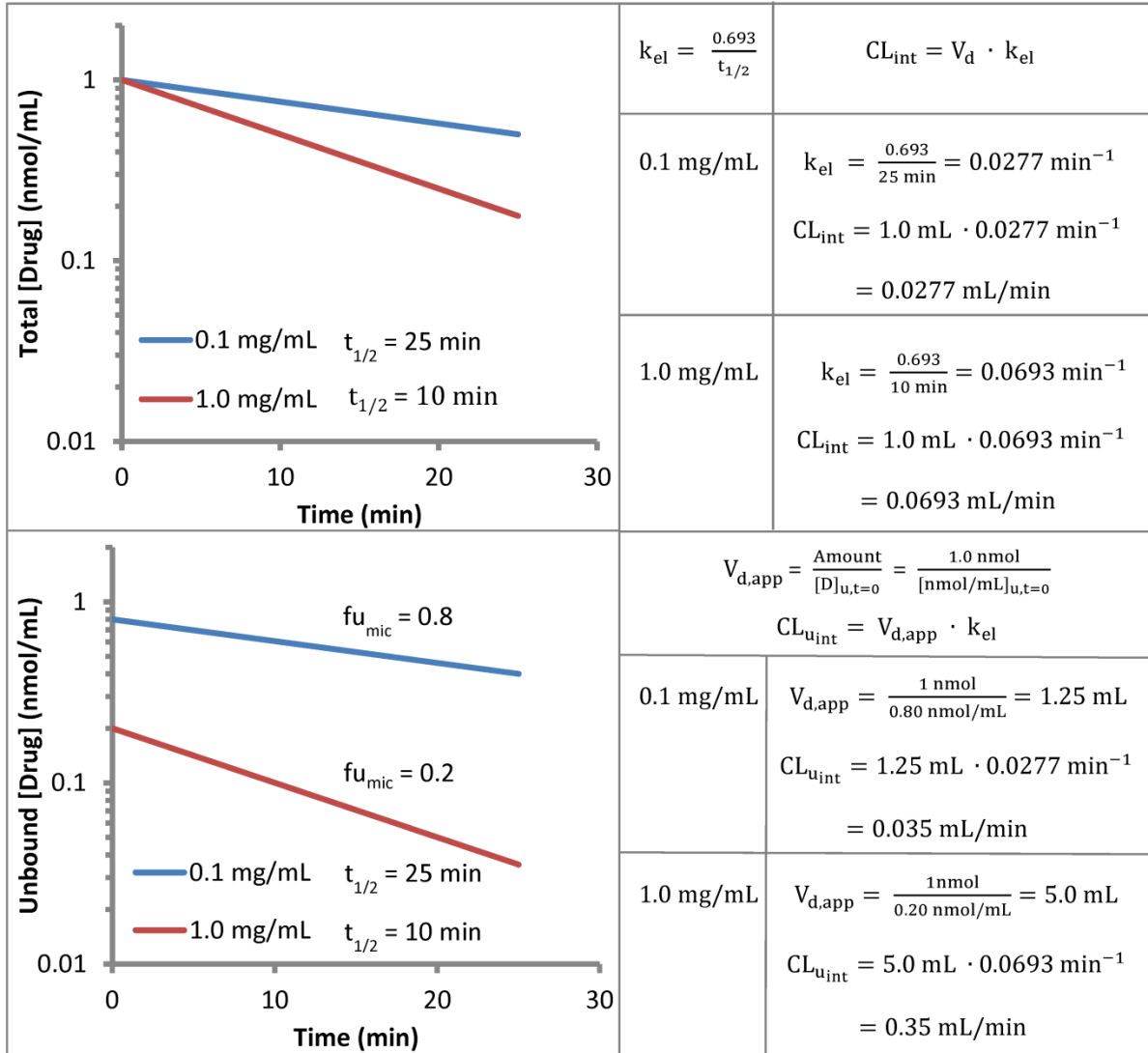


Figure 1.2. The effect of membrane partitioning of a drug into microsomes on its in vitro half-life, the apparent incubation volume ($V_{d,app}$) and clearance: The top panel represents total drug concentration and the bottom panel represents unbound (free) drug concentration.

The time course of disappearance of a drug is shown for two concentrations of liver microsomes (0.1 and 1.0 mg protein/mL). The fraction of unbound drug ($f_{u,mic}$) is 0.8 at 0.1 mg protein/mL and 0.2 at 1.0 mg protein/mL. When corrected for membrane partitioning, the elimination rate constant (k_{el}) and, hence, half-life ($t_{1/2}$) do not change; the lines in the bottom panel have the same slope as those in the top panel. However, the apparent incubation volume ($V_{d,app}$) increases in proportion to $f_{u,mic}$. Without correcting for

membrane partitioning (top panel), the 10-fold increase in microsomal protein concentration caused only a 2.5-fold increase in intrinsic clearance (CL_{int}). With the correction for $f_{u,mic}$ (bottom panel), the 10-fold increase in microsomal protein concentration caused a 10-fold increase in CL_{int} .

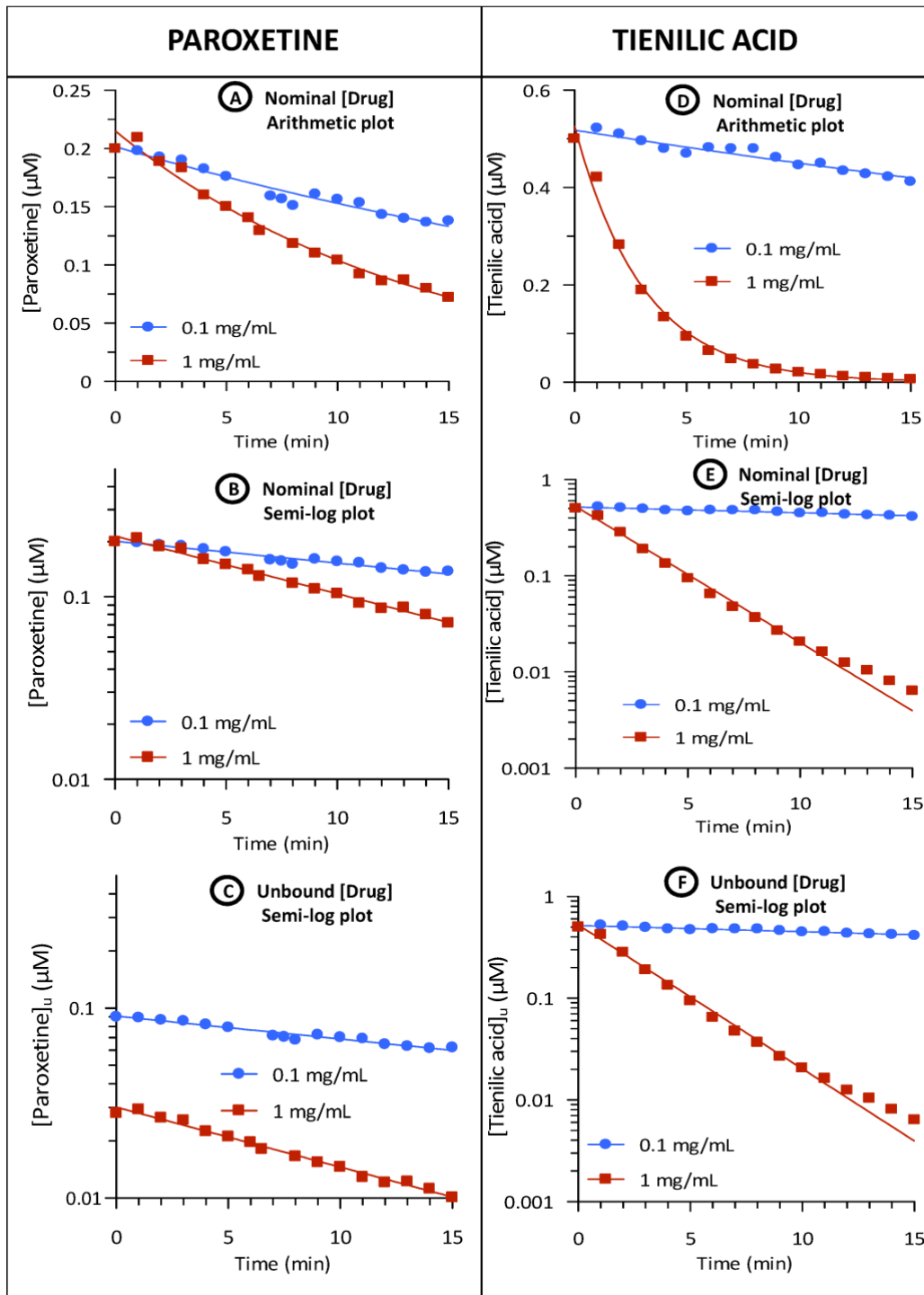


Figure 1.3. The impact of membrane partitioning on the time course of disappearance of paroxetine (left panel) and tienilic acid (right panel) by human liver microsomes at two protein concentrations (0.1 and 1.0 mg/mL).

Tienilic acid is a substrate for – and a metabolism-dependent inhibitor of – CYP2C9; it partitions only marginally (12%) into human liver microsomes at 1 mg protein/mL. Paroxetine is a substrate for – and a metabolism-dependent inhibitor – of CYP2D6; it partitions extensively into human liver microsomes (55% and 86% at 0.1 and 1.0 mg/mL, respectively). In the case of tienilic acid, increasing the concentration of human liver microsomes 10 fold caused more than a 10-fold decrease in half-life. In the case of paroxetine, increasing the concentration of human liver microsomes 10 fold caused only a 2.6-fold decrease in half-life. However, when corrected for partitioning into microsomes ($f_{u\text{mic}}$), the intrinsic clearance ($CL_{u\text{int}}$) at 1.0 mg/mL was comparable to that at 0.1 mg/mL. Values are presented in Table 1.1. Data are from Parkinson et al. (2011).

Table 1.1. The effect of correcting for microsomal partitioning on drug clearance based on measurements of the *in vitro* half-life of paroxetine (high partitioning) and tienilic acid (low partitioning) by human liver microsomes (HLM) at 0.1 and 1.0 mg protein/mL

Substrate	[HLM] (mg/mL)	$f_{u_{mic}}^1$	$[S]_T$ and $[S]_U$ (μM) ²	<i>In vitro</i> half- life ($t_{1/2}$)	Elimination rate constant (k_{el})	CL_{int} ($\mu L/min$ /mg protein)	CLu_{int} ($\mu L/min$ /mg protein)	Unbound $CL_{H,int}$ (Multiple of Q_H)
Tienilic acid	0.1	1.0	0.50 0.50	50 min	0.014 min^{-1}	140	140	554 L/h (~6 x Q_H)
	1.0	0.88	0.50 0.44	2.1 min	0.330 min^{-1}	340	375	1,490 L/h (~17 x Q_H)
Paroxetine	0.1	0.45	0.20 0.09	25 min	0.028 min^{-1}	280	620	2,460 L/h (~27 x Q_H)
	1.0	0.14	0.20 0.028	9.5 min	0.073 min^{-1}	43	521	2,060 L/h (~23 x Q_H)

¹ Fraction unbound in microsomes (determined experimentally)

² $[S]_T$ and $[S]_U$ are the total and unbound substrate concentration, respectively

$$CL_{int} = k_{el} \cdot \frac{\text{volume of incubation } (\mu L)}{\text{mg microsomal protein in the incubation}}$$

$$CLu_{int} = \frac{CL_{int}}{f_{u_{mic}}}$$

$$CL_{H,int} = CL_{int} \cdot PBSF(66,000) \cdot 60 \text{ min/h} \cdot 10^{-6} \text{ L}/\mu L$$

$$Q_H = \text{hepatic blood flow} = 90 \text{ L/h}$$

Table 1.2. Methods to calculate the in vitro free fraction of drug in the presence of microsomes ($f_{u_{mic}}$).

Reference	Neutral
Austin <i>et al.</i> , 2005	$f_{u_{mic}} = \left[\frac{1}{1 + C_p \times 10^{0.56 \times \log P / D_{7.4} - 1.41}} \right]$
Hallifax and Houston, 2006	$f_{u_{mic}} = \left[\frac{1}{1 + C_p \times 10^{0.072 \times \log P / D_{7.4}^2 + 0.067 \times \log P / D_{7.4} - 1.126}} \right]$
Turner <i>et al.</i> , 2007	$f_{u_{mic}} = \left[\frac{1}{1 + C_p \times 10^{0.46 \times \log P - 1.51}} \right]$
Poulin and Haddad, 2011	<p>Where:</p> $f_{u_{mic}} = \left[\frac{1}{P_{ma}} \right]$ $P_{ma} = F_{wm} + \frac{P_{nla} \times F_{nlm}}{1 + I_m}$
Reference	Bases
Austin <i>et al.</i> , 2005	$f_{u_{mic}} = \left[\frac{1}{1 + C_p \times 10^{0.56 \times \log P - 1.41}} \right]$
Hallifax and Houston, 2006	$f_{u_{mic}} = \left[\frac{1}{1 + C_p \times 10^{0.072 \times \log P^2 + 0.067 \times \log P - 1.126}} \right]$
Turner <i>et al.</i> , 2007	$f_{u_{mic}} = \left[\frac{1}{1 + C_p \times 10^{0.58 \times \log P - 2.02}} \right]$
Poulin and Haddad, 2011	<p>Where:</p> $f_{u_{mic}} = \left[\frac{1}{P_{ma}} \right]$ $P_{ma} = F_{wm} + \frac{P_{nla} \times F_{nlm} + I_m \times P_{apla} \times F_{aplm}}{1 + I_m}$

Reference	Acids
Austin <i>et al.</i> , 2005	$f_{u_{mic}} = \left[\frac{1}{1 + C_p \times 10^{0.56 \times \log D - 1.41}} \right]$
Hallifax and Houston, 2006	$f_{u_{mic}} = \left[\frac{1}{1 + C_p \times 10^{0.072 \times \log D^2 + 0.067 \times \log D - 1.126}} \right]$
Turner <i>et al.</i> , 2007	$f_{u_{mic}} = \left[\frac{1}{1 + C_p \times 10^{0.20 \times \log P - 1.54}} \right]$
Poulin and Haddad, 2011	<p>Where:</p> $f_{u_{mic}} = \left[\frac{1}{P_{ma}} \right]$ $P_{ma} = F_{wm} + \frac{P_{nla} \times F_{nlm}}{1 + I_m}$

Note: logP is the log *n*-octanol-water partition ratio of unionized (neutral) drug (usually determined at a pH where the unionized form of the drug predominates). logD is the log *n*-octanol-buffer partition ratio of total (unionized + ionized) drug at pH 7.4. For neutral drugs logP = logD_{pH 7.4}. C_p is the microsomal protein concentration (mg/mL); P_{ma} is the medium-aqueous phase partition coefficient; F_{wm} is the fractional volume of water equivalent in the incubation medium; F_{nlm} is the fractional volume of neutral lipids equivalent in the incubation medium; F_{aplm} is the fractional volume of acidic phospholipids equivalent in the incubation volume; P_{nla} is the ratio of a drug between the neutral lipids and the aqueous phase in the incubation medium (estimated from logP at 37°C; logP_{37°C} = logP_{25°C} + 0.009/°C × Δ°C); I_m is the ionization term for the incubation medium where I_m = 0 for neutrals, I_m = 10^{pKa-pH} for bases, and I_m = 10^{pH-pKa} for acids; P_{apla} is the ratio of a drug between the acidic phospholipids and aqueous phase in the incubation medium calculated as described by Poulin and Haddad (2011)

1.6. Extrapolation of in vitro CL_{int} to in vivo clearance (IVIVE) – models and the importance of R_b , Q_H and f_{uB}

There are two major restrictions on hepatic drug clearance in vivo, namely hepatic blood flow and plasma protein binding. Hepatic blood flow imposes an upper limit on the hepatic clearance of drugs; drugs cannot be eliminated by the liver any faster than blood flow can deliver them to the liver (90 L/h in humans). The binding of some – but not all – drugs to plasma proteins impedes their hepatic uptake and, hence, their metabolic and biliary clearance by the liver.

According to Ramanathan and Vachharajani (2010), the binding of drugs to plasma proteins can be classified as follows:

Very highly bound >99%

Highly bound = 95-99%

Moderately highly bound = 85-95%

Poorly bound <80%

It is widely accepted that unbound drug concentration determines the efficacy or toxicity of a drug; this is known as the free-drug hypothesis or principle (Trainor, 2007). The metabolism of drugs by cytochrome P450 and most other drug-metabolizing enzymes occurs intracellularly where the measurement of unbound drug concentration is difficult. The pharmacokinetics of drugs and the clearance of drugs from blood, the so-called central compartment, are typically based on measurements of total drug concentrations in plasma and measurements of the unbound concentration of drugs in plasma (f_{uP}) and

R_b , the ratio of the concentration of drug in whole blood and plasma (discussed later in this section). Although plasma contains more than 60 different soluble proteins, f_{up} is largely determined by the binding of drugs to three proteins, namely albumin, α_1 -acid glycoprotein (α AGP) and, to a lesser extent, lipoproteins (Ramanathan and Vachharajani, 2010). Although albumin and α AGP have been shown to bind both acidic and basic drugs, albumin preferentially binds acidic drugs and α AGP generally binds basic drugs. Lipoproteins generally bind neutral, lipophilic drugs (Ermondi et al., 2004; Ramanathan and Vachharajani, 2010). The concentration of albumin (MW 67 kDa) is so high (35-50 mg/mL; 500-700 μ M) that drugs rarely saturate binding to this plasma protein. The concentration of α AGP (MW 38-48 kDa), which is quite variable and influenced by several disease states, is normally much lower (0.4-1 mg/mL; 12-31 μ M) and saturation of binding is more likely. Albumin is often described as a low affinity, high capacity binding protein whereas α AGP is high affinity, low capacity binding protein. Lastly, lipoproteins play a role in the plasma binding of various lipophilic drugs, and include high density lipoproteins (HDL), low density lipoproteins (LDL) and very low density lipoproteins (VLDL), which have circulating levels less than 5 mg/mL. In contrast to albumin and α AGP, lipoproteins do not have specific drug-binding sites; rather drugs partition nonspecifically into the lipid core, a process that is unlikely to be saturated (Ramanathan and Vachharajani, 2010).

There is little question that binding of certain acidic (anionic) drugs to albumin and binding of certain basic (cationic) drugs to α AGP can restrict rates of hepatic clearance. For example, the hepatic clearance of warfarin, which binds with high affinity to albumin, is highly correlated with the concentration of free (unbound) warfarin in plasma (Routledge et al., 1979) whereas the hepatic clearance of 7-hydroxystaurosporine (UCN-01) is

restricted by its high affinity binding to α AGP (Fuse et al., 1998; Fuse et al., 1999). The latter is interesting because high affinity binding of 7-hydroxystaurosporine to α AGP occurs in humans but not in nonclinical species. However, the fraction of unbound drug in plasma, as determined by various in vitro techniques (equilibrium dialysis, ultrafiltration and ultracentrifugation), may underestimate the fraction of drug available for hepatic uptake and clearance. In the hepatic sinusoids a drug may bind to active uptake transporters (such as OATP1B1 and 1B3) with higher affinity than it binds to albumin or other plasma proteins. Binding affinity to albumin (the equilibrium dissociation constant K_D) is determined by k_{off}/k_{on} (the ratio of the first order rate constant for dissociation and the second order rate constant for association of the albumin-drug complex). With a sufficiently high k_{off} , a drug can dissociate during its transit through the liver and can enter the liver under so-called sink conditions (conditions under which the loss of unbound drug due to hepatic uptake is replaced by dissociation of the plasma protein-drug complex during its transit through the liver). Baker and Parton (2007) reported that, for most drugs, k_{off} is not low enough ($<1 \text{ s}^{-1}$) to limit the hepatic extraction of plasma protein-bound drugs; however, in some cases, k_{on} can be sufficiently high for plasma proteins to compete with hepatic uptake by transporters and passive diffusion. Baker and Parton (2007) concluded that, for many drugs, values of f_{uP} tend to underestimate the amount of drug available for hepatic uptake and that k_{off} is a better indicator of the maximum amount of drug available for hepatic uptake during the passage of blood through the liver. Unfortunately, whereas f_{uP} is known for most approved drugs, k_{off} is known for relatively few drugs. As discussed later, if the unbound concentration of drug in plasma at equilibrium underestimates the

fraction of drug available for hepatic uptake then the use of f_{uB} in IVIVE will lead to underpredictions of hepatic clearance *in vivo*.

The vast majority of pharmacokinetic studies are based on measurements of the time course of changes in the concentration of drug in plasma rather than whole blood, which is technically more difficult to work with. However, hepatic drug clearance *in vivo* is evaluated in terms of hepatic *blood* flow, not hepatic *plasma* flow. Consequently, drug concentrations in plasma must be converted to drug concentrations in blood, which is based on R_b , the blood-to-plasma concentration ratio:

$$R_b = \frac{[Drug]_{Blood}}{[Drug]_{Plasma}} \quad \text{Equation 1.12}$$

Hence,

$$[Drug]_{Blood} = [Drug]_{Plasma} \cdot R_b \quad \text{Equation 1.13}$$

R_b can be determined experimentally (with *in vivo* or, more commonly, *in vitro* samples) or it can be estimated based on the properties of the drug (whether it's neutral, basic, acidic or zwitterionic) and based on the fact that plasma accounts for ~55% of blood volume with cells (mainly erythrocytes) accounting for ~45% (Table 1.3). In the case of acidic and zwitterionic drugs, estimates of R_b are based on the assumption that these drugs, which are charged at pH 7.4, do not readily penetrate into blood cells but are largely confined to plasma (where they bind extensively to albumin); accordingly, R_b is assumed to be 0.55 for acidic and zwitterionic drugs (Hallifax et al., 2010). In the case of neutral and basic drugs, R_b is assumed to be 1.0 because these drugs often (but not always) freely diffuse in and out of erythrocytes and are evenly distributed between plasma and erythrocytes (Hallifax et al., 2010). From time to time the assumed values of R_b (as opposed to the experimentally determined values) can produce misleading

predictions of in vivo hepatic clearance; notably when the value of R_b is greater than unity, which occurs when certain drugs bind preferentially (but reversibly) to erythrocytes (either to the surface or to intracellular sites). In such cases, estimates of blood clearance from measurements of plasma clearance can exceed hepatic blood flow, which can give the false impression that non-hepatic clearance mechanisms must also contribute to the drug's clearance. The basis for this over-prediction is illustrated in Figure 1.4, which depicts the in vivo plasma and blood clearance of three drugs, A, B and C. The first drug (an acidic or zwitterionic drug) is excluded from erythrocytes; for simplicity its R_b value is set to 0.5. The second drug (a neutral or basic drug) is distributed evenly between plasma and blood; hence, its R_b value is 1.0. The third drug is a basic drug that binds preferentially to erythrocytes (but not in a restricted manner); its R_b value is set to 2.0. For illustrative purposes, all three drugs are flow-limited, hepatically cleared drugs such that, in all three cases, their clearance from blood is 90 L/h, which corresponds to hepatic blood flow. What is the plasma clearance of each drug? In the case of Drug B, which is evenly distributed between plasma and erythrocytes ($R_b = 1.0$), plasma clearance equals blood clearance (90 L/h). In the case of Drug A, which is largely excluded from erythrocytes ($R_b = 0.5$), plasma clearance is half hepatic blood flow (and close to hepatic plasma flow). In the case of Drug C, which is preferentially distributed in erythrocytes, plasma clearance is 180 L/h, which is *twice* hepatic blood flow. If Drug C were assumed to have an R_b value of 1.0, its clearance from blood would be estimated to equal its clearance from plasma (180 L/h). Given that the estimated blood clearance is twice hepatic blood flow, it might be incorrectly assumed that Drug C must be cleared by renal excretion or extrahepatic metabolism; *i.e.*, some mechanism in addition to hepatic clearance.

It is apparent from Figure 1.4 that the drug's half-life (and, hence, k_{el}) is the same regardless of whether the concentrations of drug are measured in plasma or blood; this is true across all values of R_b . However, whether the concentrations of drug are measured in plasma or blood affects the apparent volume of distribution and it is differences in V_d that cause changes in clearance between blood and plasma.

It is noteworthy that the pharmacokinetic behavior of Drugs B and C in Figure 1.4 assumes that the portion of drug in erythrocytes is just as available for uptake into hepatocytes as the portion of drug in plasma. Although this might seem counter-intuitive, the clinical observation that the hepatic clearance of many basic/neutral drugs does in fact occur at rates equal to hepatic blood flow (as represented by Drug B) or greater than hepatic blood flow (as represented by Drug C) establishes that the localization of drugs in erythrocytes is not necessarily an impediment to their hepatic uptake. However, there are also drugs that bind preferentially to erythrocytes ($R_b > 1$) but the binding is restrictive, meaning dissociation of the drug from erythrocytes is slow compared with the transit time of blood through the liver. Drugs with large blood-to-plasma concentration ratios (some more than an order of magnitude) and drugs with slow rates of erythrocyte partitioning are reviewed in Hinderling (1997). They include chlorthalidone, dorzolamide and methazolamide, diuretic drugs that bind with high affinity to carbonic anhydrase, an abundant enzyme in erythrocytes, and have R_b values of 30.7, >100 and 241, respectively.

Finally, it is worth noting that R_b , the blood-to-plasma concentration ratio, is also used to convert plasma clearance (CL_P) to blood clearance (CL_B) and unbound fraction of drug in blood (f_{uB}) from unbound fraction in plasma (f_{uP}) as follows:

$$CL_B = \frac{CL_P}{R_b} \quad \text{Equation 1.14}$$

$$fu_B = \frac{fu_P}{R_b} \quad \text{Equation 1.15}$$

As noted above, Equation 1.14 is appropriate for drugs with an $R_b > 1$ only if the preferential binding of the drug to erythrocytes is not restrictive (*i.e.*, if dissociation of the drug from erythrocytes is not slow compared with the transit time of blood through the liver) (Hinderling, 1997).

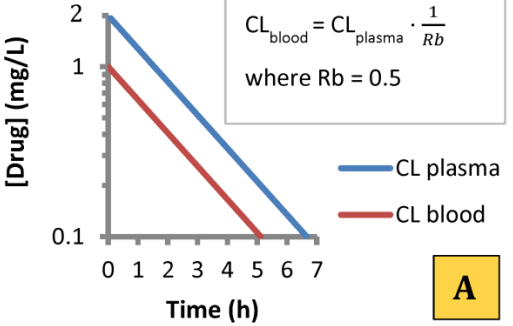
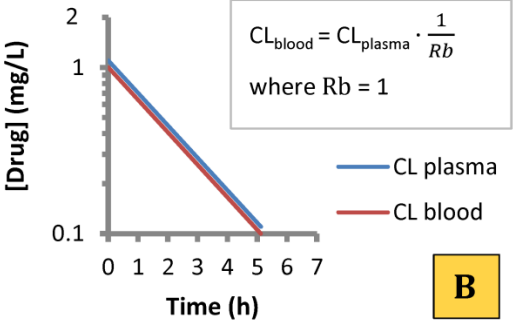
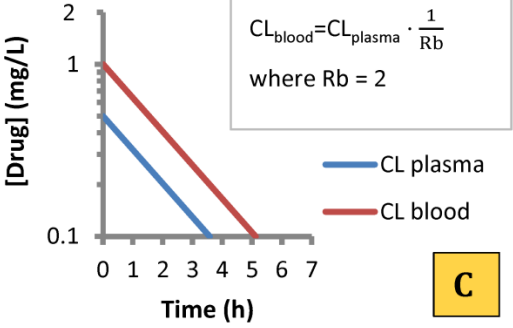
Dose = 200 mg $t_{1/2} = 1.54 \text{ h}$ $k_{el} = 0.45 \text{ h}^{-1}$	$V_d = \frac{\text{Dose (mg)}}{[\text{Drug}]_{t=0} \text{ (mg/L)}}$	$CL = V_d \cdot k_{el}$	$R_b = \frac{[\text{Drug}]_{\text{blood}}}{[\text{Drug}]_{\text{plasma}}}$
 <p style="text-align: right;">A</p>	$V_{d,\text{plasma}} = \frac{200 \text{ mg}}{2 \text{ mg/L}} = 100 \text{ L}$ $CL_{\text{plasma}} = 100 \text{ L} \cdot 0.45 \text{ h}^{-1} = 45 \text{ L} \cdot \text{h}^{-1}$ $V_{d,\text{blood}} = \frac{200 \text{ mg}}{1 \text{ mg/L}} = 200 \text{ L}$ $CL_{\text{blood}} = 200 \text{ L} \cdot 0.45 \text{ h}^{-1} = 90 \text{ L} \cdot \text{h}^{-1}$		
 <p style="text-align: right;">B</p>	$V_{d,\text{plasma}} = \frac{200 \text{ mg}}{1 \text{ mg/L}} = 200 \text{ L}$ $CL_{\text{plasma}} = 200 \text{ L} \cdot 0.45 \text{ h}^{-1} = 90 \text{ L} \cdot \text{h}^{-1}$ $V_{d,\text{blood}} = \frac{200 \text{ mg}}{1 \text{ mg/L}} = 200 \text{ L}$ $CL_{\text{blood}} = 200 \text{ L} \cdot 0.45 \text{ h}^{-1} = 90 \text{ L} \cdot \text{h}^{-1}$		
 <p style="text-align: right;">C</p>	$V_{d,\text{plasma}} = \frac{200 \text{ mg}}{0.5 \text{ mg/L}} = 400 \text{ L}$ $CL_{\text{plasma}} = 400 \text{ L} \cdot 0.45 \text{ h}^{-1} = 180 \text{ L} \cdot \text{h}^{-1}$ $V_{d,\text{blood}} = \frac{200 \text{ mg}}{1 \text{ mg/L}} = 200 \text{ L}$ $CL_{\text{blood}} = 200 \text{ L} \cdot 0.45 \text{ h}^{-1} = 90 \text{ L} \cdot \text{h}^{-1}$		

Figure 1.4. Differences between plasma and blood clearance for a drug excluded from erythrocytes (Panel A), a drug evenly distributed between plasma and erythrocytes (Panel B) and a drug preferentially distributed in erythrocytes.

Panel A depicts the situation for most acidic/zwitterionic drugs. Panel B depicts the situation with many basic/neutral drugs. Panel C depicts the situation with a small number of basic/neutral drugs that distribute preferentially into erythrocytes compared with

plasma. Note that plasma clearance is half the rate of blood clearance in Panel A (45 *versus* 90 L/h); is equal to blood clearance in Panel B (90 L/h) but *exceeds* total blood flow by a factor of two in Panel C (180 L/h *versus* 90 L/h). In all three cases the value of total blood clearance is equal to hepatic blood flow (90 L/h). This figure illustrates the importance of knowing R_b , the ratio of blood-to-plasma drug concentration, when calculating rates of blood clearance from experimentally determined rates of plasma clearance.

Table 1.3. Physiological data and physiologically based scaling factors (PBSF) for in vitro to in vivo extrapolation (IVIVE)

Physiological parameter	Human	Monkey	Dog	Rat	Mouse
A. Body weight	70 kg	5 kg	13.5 kg	0.3 kg	0.0262 kg
B. Liver weight (g)	1,650	134	480	9.0	1.5
C. Liver blood flow (Q _H) (L/h)	90	15	40.6	1.03	0.157
D. Hematocrit (PCV)	0.44	0.42	0.45	0.43	0.40
E. MPPGL (mg/g liver)	40	NA	55	58	NA
F. HPGL (million cells/g liver)	120	NA	169	127	135
G. PBSF for microsomes (E x B). Units: total mg of microsomal protein per whole liver ¹	66,000	NA	26,400	522	NA
H. PBSF for hepatocytes (F x B). Units: number of million hepatocytes per whole liver ²	198,000	NA	81,120	1143	202.5

NA: Not available

¹ This PBSF is used for studies with microsomes to convert *in vitro* clearance rates (CL_{int}) based on μL/min/mg microsomal protein to *in vivo* hepatic clearance rates. For example, with human liver microsomes:

$$\text{In vivo CL}_{H,int} = \text{In vitro CL}_{int} \times 66,000$$

² This PBSF is used for studies with hepatocytes to convert *in vitro* clearance rates (CL_{int}) based on μL/min/10⁶ hepatocytes to *in vivo* hepatic clearance rates. For example, with human hepatocytes:

$$\text{In vivo CL}_{H,int} = \text{In vitro CL}_{int} \times 198,000$$

Data from: Barter et al., 2007; Barter et al., 2008; Boxenbaum et al., 1980; Brunton et al., 2006; Davies and Morris, 1993; de la Grandmaison et al., 2001; Gerlowski and Jain, 1983; Hakooz et al., 2006; Howgate et al., 2006; Johnson et al., 2005; Naritomi et al., 2001; Price et al., 2003; Smith et al., 2008; Soars et al., 2002; Sohlenius-Sternbeck et al., 2006; Storb et al., 1970; Windberger et al., 2003; Youdim et al., 2008.

There are three major models of hepatic drug clearance (Roberts and Rowland, 1986b; Roberts and Rowland, 1986d; Roberts and Rowland, 1986f; Roberts and Rowland, 1986a; Ching et al., 1989; Ridgway et al., 2003; Roberts, 2010):

1. The well-stirred model (a.k.a. the venous equilibrium model) assumes the drug is mixed infinitely well inside the liver and that the hepatic drug concentration is equal to the outflow drug concentration. In chemical engineering terms, it is analogous to a perfectly mixed reactor.
2. The parallel-tube model (a.k.a. the undistributed sinusoidal perfusion model) views the hepatic sinusoids as a series of parallel tubes that are all identical with respect to blood flow and metabolic activity of the surrounding cells (*i.e.*, all tubes have the same intrinsic clearance capacity). This model assumes the drug is mixed in a highly restricted (infinitesimally small) section of the liver along the sinusoidal flow path from input to output of the liver (which is the extreme opposite of the well-stirred model) and that hepatic drug concentration is equal to the logarithm of the mean of the inflow and outflow drug concentrations. In chemical engineering terms, it is a continuous tubular reactor (a.k.a. a plug-flow reactor).
3. The dispersion model (a.k.a. the convection-dispersion model or the distributed sinusoidal model) also views the hepatic sinusoids as a series of parallel tubes but it differs from the parallel-tube model by assuming that blood flow through each tube and the metabolic activity (intrinsic clearance) of the cells surrounding the tubes are not constant but can vary from one tube to the next. According to the dispersion model, hepatic drug concentration exhibits axial dispersion analogous

to that in a packed-bed chemical reactor. The dispersion model uses a parameter, D_N , to describe the degree of axial mixing of drug in blood within the sinusoids. The average sinusoidal drug concentration lies somewhere between the logarithmic mean of the inflow and outflow drug concentration (the drug concentration for the parallel tube model) and the outflow concentration (the drug concentration for the well-stirred model).

These three models are used for IVIVE, the extrapolation of in vitro measurements of intrinsic hepatic clearance (CL_{int}) to in vivo estimates of hepatic clearance (CL_H). All three models assume that (1) distribution of drug into liver is limited by the rate of liver perfusion and not by diffusion barriers, (2) only unbound drug in blood can enter the liver, and (3) drug-metabolizing enzymes are homogenously distributed throughout the liver (Ito and Houston, 2004). The equations for all three models incorporate Q_H and CL_{int} , which can be adjusted for drug binding, as discussed later in this section. The basic IVIVE equations (without correction for unbound drug in blood or the in vitro test system) for the three models are as follows:

Well-stirred model IVIVE equation:

$$CL_H = \frac{Q_H \times CL_{int}}{Q_H + CL_{int}} \quad \text{Equation 1.16}$$

Parallel-tube model IVIVE equation

$$CL_H = Q_H \times \left(1 - e^{-\frac{CL_{int}}{Q_H}}\right) \quad \text{Equation 1.17}$$

Dispersion model IVIVE equation

$$CL_H = Q_H(1 - F_H) \quad \text{Equation 1.18}$$

where F_H , hepatic availability, is determined from:

$$F_H = \left(\frac{4a}{(1-a)^2 \cdot \exp\left[\frac{a-1}{2D_N}\right] - (1-a)^2 \cdot \exp\left[-\frac{a+1}{2D_N}\right]} \right) \quad \text{Equation 1.19}$$

$$\text{where } a = \left(1 + 4 \frac{CL_{int}}{Q_H} \cdot D_N\right)^{0.5}$$

$D_N = \text{the dispersion number}$

The well-stirred model and the parallel tube model can be viewed as opposite models of hepatic drug disposition. The former regards the liver as a well-stirred compartment; it assumes the concentration of drug in the liver is in equilibrium with that in the emergent blood. The latter regards the liver as a series of parallel tubes with enzymes distributed evenly around the tubes; it assumes the concentration of drug declines along the length of the tube (*i.e.*, there is a sinusoidal concentration gradient from input to output). The dispersion model is intermediate between these two extremes. The dispersion number is a measure of the extent to which drugs (and other solutes) disperse throughout the liver; values of D_N range from 0 to 1. At these two numerical extremes of D_N , the dispersion model becomes the well-stirred model (when $D_N = 1$ and there is complete dispersion) or the parallel tube model (when $D_N = 0$ and there is no dispersion). Experimentally determined values of D_N depend on the solute. A value of 0.17 is commonly used for IVIVE of drug clearance (Roberts and Rowland, 1986b; Roberts and Rowland, 1986d; Naritomi et al., 2001; Ito and Houston, 2004; Chiba et al., 2009).

All three models are widely used in IVIVE. Their relative strengths and weaknesses in terms of their ability to accurately predict *in vivo* hepatic clearance from *in vitro* data are reviewed in Chiba et al. (2009) and Hallifax et al., (2010). Each equation can be (and

usually is) modified to take into account the binding of drugs to blood (f_{uB} , which is often calculated from f_{uP}/R_b) and the binding of drugs to the in vitro incubation test system ($f_{u_{mic}}$ or $f_{u_{hep}}$ depending on whether metabolic clearance in vitro is determined with microsomes or hepatocytes). When only in vitro binding is taken into account, CL_{int} becomes $CL_{u_{int}}$ (i.e., intrinsic clearance based on the unbound fraction of drug), and the IVIVE equation for the well-stirred model becomes:

$$CL_H = \frac{Q_H \cdot \frac{CL_{int}}{f_{u_{inc}}}}{Q_H + \frac{CL_{int}}{f_{u_{inc}}}} = \frac{Q_H \cdot CL_{u_{int}}}{Q_H + CL_{u_{int}}} \quad \text{Equation 1.20}$$

When only binding of drug to blood is taken into account, the IVIVE equation for the well-stirred model becomes:

$$CL_H = \frac{Q_H \cdot f_{uB} \cdot CL_{int}}{Q_H + f_{uB} \cdot CL_{int}} \quad \text{Equation 1.21}$$

When both are taken into account, the IVIVE equation for the well-stirred model becomes:

$$CL_H = \frac{Q_H \cdot f_{uB} \cdot CL_{u_{int}}}{Q_H + f_{uB} \cdot CL_{u_{int}}} \quad \text{Equation 1.22}$$

Through the use of R_b , the blood-to-plasma concentration ratio, and f_{uP} , the unbound fraction of drug in plasma (which is determined experimentally more often than the unbound fraction of drug in whole blood), Equation 1.22 can be modified to calculate the hepatic clearance of drug in plasma ($CL_{H,P}$) (Yang et al., 2007):

$$CL_{H,P} = \frac{Q_H \cdot f_{uP} \cdot CL_{u_{int}}}{Q_H + \frac{f_{uP} \cdot CL_{u_{int}}}{R_b}} \quad \text{Equation 1.23}$$

From Equation 1.24 it is apparent that hepatic clearance in vivo is determined by three factors, namely hepatic blood flow, which is relatively constant, and f_{uB} and $CL_{u_{int}}$, which

vary enormously from one drug to the next. Gillette coined the terms “restrictive clearance” and “nonrestrictive clearance” (Gillette, 1973). Restrictive clearance applies to low-clearance compounds when either the unbound fraction and/or intrinsic clearance is so low that the term $Q_H + f_{UB} \cdot CL_{U_{int}}$ approximates to Q_H and Equation 1.22 simplifies to $CL_H = f_{UB} \cdot CL_{U_{int}}$. Nonrestrictive clearance applies to high-clearance compounds when the unbound fraction and/or intrinsic clearance is so high that the term $Q_H + f_{UB} \cdot CL_{U_{int}}$ approximates to $f_{UB} \cdot CL_{U_{int}}$ and Equation 1.22 simplifies to $CL_H = Q_H$. For such compounds, the intrinsic clearance will be very high and the rate of dissociation of the drug-protein complex must exceed the liver transit time (discussed below). Nonrestricted clearance is also known as flow-limited clearance or flow-limited extraction; it applies to high extraction drugs. Restricted clearance is also known as capacity-limited clearance or capacity-limited extraction; it applies to low extraction drugs.

For hepatically cleared drugs, the extent of hepatic extraction influences the pharmacokinetic consequences of alterations in hepatic clearance, as might occur with drug-drug interactions (DDIs) based on inhibition or induction of drug-metabolizing enzymes. For high extraction (flow-limited) drugs, DDIs mostly affect plasma C_{max} (they inhibit or induce first pass clearance) but not systemic clearance (not plasma half-life). For low extraction (capacity-limited) drugs, DDIs mostly affect systemic clearance (plasma half-life) and not plasma C_{max} . (Gillette, 1973; Kirby and Unadkat, 2010; Rowland and Tozer, 2011).

These pharmacokinetic principles are further illustrated based on a consideration of the impact of plasma protein binding and intrinsic metabolic clearance on hepatic extraction

ratio. Hepatic clearance is related to hepatic blood flow and hepatic extraction ratio as follows:

$$CL_H = Q_H \cdot E_H \quad \text{Equation 1.24}$$

From Equation 1.22 and Equation 1.24, hepatic extraction ratio is given by the following equation:

$$E_H = \frac{f u_B \cdot CL_{u_{int}}}{Q_H + f u_B \cdot CL_{u_{int}}} \quad \text{Equation 1.25}$$

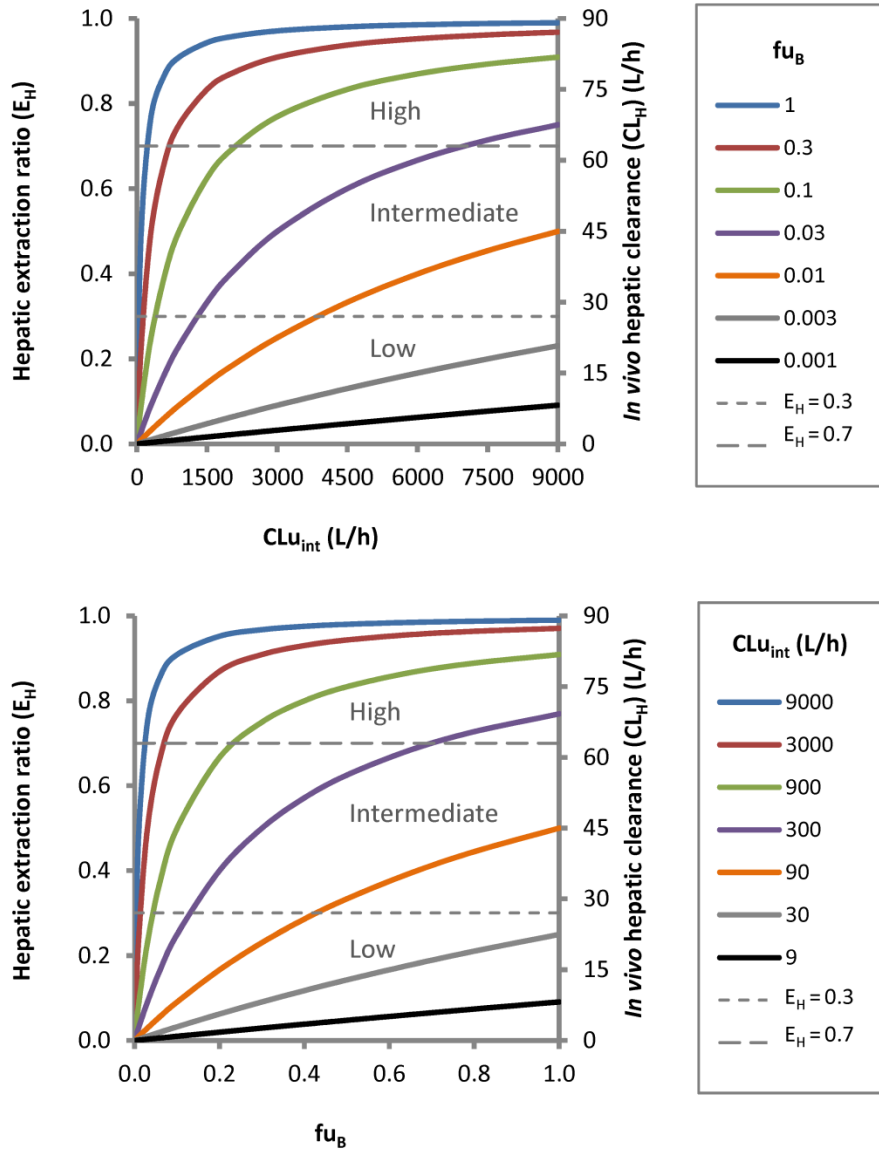


Figure 1.5. The mutual impact of intrinsic clearance (CL_{int}) and the unbound fraction of drug in blood (fu_B) on hepatic extraction ratio (E_H; left axis) and hepatic clearance (CL_H; right axis)

High (E_H > 0.7), intermediate (E_H = 0.3-0.7) and low (E_H < 0.3) refer to the classification of drugs based on hepatic extraction ratio.

Table 1.4. Examples of hepatically cleared drugs classified as having a low, medium or high hepatic extraction ratio based on intravenous dosing

Fraction unbound in blood	Low extraction (E_H <0.3)	Medium extraction (E_H = 0.3 – 0.7)	High extraction (E_H >0.7)
f _{uB} < 0.01 (>99% bound)	Amiodarone Mibefradil Montelukast Rosiglitazone Verlukast	Amlodipine Felodipine Itraconazole Nefazodone Nicardipine	Eltanolone Fluvastatin Maxipost Nisoldipine
f _{uB} = 0.01 – 0.1 (90-99% bound)	Alfentanil Aripiprazole Clozapine Diazepam Diclofenac Erythromycin Gemfibrozil Ibuprofen Lansoprazole Lorazepam Naproxen Oxazepam Pantoprazole Rabeprazole Ritonavir Tacrolimus Temazepam Warfarin Valproic acid	Atomoxetine Carvedilol Chlorpromazine Clomipramine Cyclosporine Ethinylestradiol Fluoxetine Lovastatin acid Midazolam Nifedipine Omeprazole Propafenone Repaglinide Sildenafil Sufentanil Tiprolidine Tolamolol Vardenafil	Buprenorphine Idarubicin Nicardipine Nilvadipine Propofol Trimipramine
f _{uB} = 0.1 – 0.5 (50-90% bound)	Aprepitant Citalopram Chloramphenicol Chlorpheniramine Carbamazepine Dapsone Paclitaxel Pentobarbital Phenytoin Phenobarbital Tolbutamide Triazolam Zolpidem	Bufuralol Desipramine Diltiazem Diphenhydramine Imipramine Lidocaine Mexiletine Nortriptyline Ondansetron Timolol	Alprenolol Butorphanol Cocaine Doxorubicin Indinavir Labetalol Lidocaine Meperidine Nitroglycerin Pentamidine Propoxyphene Propranolol Verapamil
f _{uB} >0.5 (0-50% bound)	Acetaminophen Alprazolam Antipyrine Caffeine Cyclophosphamide Hexobarbital Ifosphamide Metoclopramide Theophylline	Codeine Famotidine Metoprolol Venlafaxine	Flumazenil Ketamine Morphine Nicotine Phenacetin

In each category of hepatic extraction ratio the drugs are organized on the basis of their unbound fraction in blood (f_{uB}). Drugs in bold are borderline; some estimates of in vivo clearance place them in the previous category. Based on hepatic blood flow of 90 L/h, the cut-off extraction ratios of 0.3 and 0.7 correspond to in vivo clearances of 27 and 63 L/h (or 6.4 and 15 mL/min/kg), respectively.

Adapted from Benet and Hoener (2002); Obach et al. (2008); Hallifax et al. (2010), and Rowland and Tozer (2011).

Figure 1.5 shows the relationship between hepatic extraction ratio and $CL_{U_{int}}$ (panel A) and f_{u_B} (panel B) based on Equation 1.25. Values of $CL_{U_{int}}$ ranged from one-tenth to 100 times hepatic blood flow (*i.e.*, from 9 to 9,000 L/h), which are realistic values based on the data for P450-dependent clearance in Table 1.6. Values of f_{u_B} ranged from 1 (no binding to plasma protein) to 0.001 (99.9% binding). Based on an analysis of 222 drugs, Zhang et al. (2012) reported that ~50% of drugs are more than 90% bound to plasma proteins and ~12% are bound 80-90%. Slightly less than 5% of drugs are bound less than 10% to plasma proteins. Accordingly, f_{u_B} values of 0.1 or less are applicable to half the drugs and f_{u_B} values of 0.9 or more are applicable to ~5% of drugs.

The upper panel in Figure 1.5 shows that the impact of changes in hepatic metabolic clearance on hepatic extraction ratio depends on the degree of plasma protein binding. The relationship is almost linear for highly protein-bound drugs ($f_{u_B} < 0.01$); however, as f_{u_B} values increase above 0.01 there is a progressive departure from near-linearity and a progressive move towards a plateau, at which point the hepatic extraction ratio is relatively constant (*i.e.*, roughly equal to hepatic blood flow) over a wide range of $CL_{U_{int}}$ values (from 900 to 9,000 L/h, which is 10 to 100 times hepatic flow).

The lower panel of Figure 1.5 shows that the impact of changes in plasma protein binding on hepatic extraction ratio depends on intrinsic clearance. For low clearance drugs (when $CL_{U_{int}}$ is less than hepatic blood flow [90 L/h]), there is a near-linear relationship between E_H and f_{u_B} ; however, as $CL_{U_{int}}$ values increase and exceed hepatic blood flow there is a progressive departure from near-linearity and a progressive move towards a plateau, at which point the hepatic extraction ratio is relatively constant (*i.e.*, roughly equal to hepatic blood flow) over a wide range of f_{u_B} values (from 0.1 to 1.0). Based on in vitro studies

with perfused rat liver, propranolol (blue), diazepam (green), phenytoin (purple) and tolbutamide (gray) are reasonably well represented by the colored lines in the lower panel of Figure 1.5 (Shand et al., 1976; Schary and Rowland, 1983; Rowland et al., 1984; Jones et al., 1985). For a low extraction drug administered intravenously, a second drug that competes for plasma protein binding (a displacer) can increase tissue uptake and hepatic clearance, which decreases total blood levels with no discernible change in f_{uB} (the increase in unbound fraction is transient). For a high extraction drug administered intravenously, a displacer can potentially increase f_{uB} (with no change in total drug concentration) because the increase in unbound drug does not increase hepatic clearance, which is blood-flow limited (Benet and Hoener, 2002; Rowland and Tozer, 2011).

Hepatically cleared drugs are classified as low extraction ($E_H < 0.3$), medium extraction ($E_H 0.3-0.7$), and high extraction ($E_H > 0.7$). Examples are given in Table 1.4, which shows that in all three categories of hepatic extraction ratio (low, medium and high), there are drugs in all categories of plasma protein binding, from very highly protein-bound drugs ($f_{uB} < 0.01$) to very poorly bound drugs ($f_{uB} > 0.5$). From Table 1.4 and Figure 1.5 it is apparent that categorizing drugs on the basis of hepatic extraction ratio is not based on $CL_{U_{int}}$ alone or f_{uB} alone but is based on a combination of both these parameters. These two parameters are normally determined in separate in vitro experiments. However, a single measurement of in vitro intrinsic clearance in the presence of plasma or serum can potentially provide information on in vivo hepatic extraction ratio.

From Equation 1.24 it is apparent that hepatic clearance is determined by both hepatic blood flow and hepatic extraction ratio. Some drugs alter hepatic blood flow and this can

alter the clearance of intermediate and high extraction drugs. For example, the β -blockers metoprolol and propranolol, which decrease cardiac output and, hence, hepatic blood flow, decrease the hepatic clearance of lidocaine (Conrad et al., 1983).

The binding of drugs to plasma proteins and erythrocytes restricts their hepatic uptake and clearance, for which reason IVIVE is generally based on the unbound drug fraction in blood (f_{uB}), which is determined from Equation 1.15 based on measurements of f_{uP} , the binding of drug to plasma, and R_b , the blood-to-plasma concentration ratio. The restriction on hepatic clearance imposed by the binding of drugs to plasma proteins and erythrocytes can be appreciated from the data in Table 1.6, which estimates the in vivo hepatic clearance of the high-turnover substrates that are commonly used to measure P450 activity in vitro. The estimates of hepatic clearance shown in Table 1.6 are NOT corrected for in vitro binding to microsomes or in vivo binding to blood. In many cases, the estimated in vivo hepatic clearance exceeds hepatic flow (sometimes by two orders of magnitude) and yet many of these drugs are cleared in vivo at rates that are well below hepatic blood flow. Midazolam serves as a good example.

The in vivo parameters for midazolam (Rawden et al., 2005; Hallifax et al., 2010) are as follows:

Blood-to-plasma concentration ratio (R_b) = 0.55

Unbound drug in plasma (f_{uP}) = 0.031

Unbound drug in blood (f_{uB}) = f_{uP}/R_b = 0.0564

Plasma clearance with *iv* dosing (CL_P) = 5.30 – 6.16 mL/min/kg = 22.3 - 25.9 L/h
(average 24.1 L/h)

Blood clearance with *iv* dosing (CL_B) = CL_P/R_b = ~43.8 L/h

The *in vivo* blood clearance of intravenously administered midazolam, which is largely dependent on hepatic metabolism, is ~44 L/h, which is about 50% of hepatic blood flow ($E_H = 0.5$). However, without correction for the binding of midazolam to blood *in vivo* or human liver microsomes *in vitro* ($f_{u_{mic}} = 0.92$ at 0.05 mg protein/mL based on $\log D_{7.4} = 3.9$), the *in vivo* hepatic clearance of midazolam predicted from *in vitro* studies of V_{max}/K_m with human liver microsomes is 2,700 L/h (Table 1.6), which is about 30 times hepatic blood flow. This ~61-fold difference between predicted and observed *in vivo* clearance is largely attributable to the extensive binding (~94.4%) of midazolam to blood ($f_{u_B} = 0.0564$). The actual *in vivo* clearance of midazolam predicted from the V_{max}/K_m data in Table 1.6 and an expanded version of Equation 1.25 is as follows:

$$CL_H = \frac{Q_H \cdot f_{u_B} \cdot \frac{Cl_{int}}{f_{u_{mic}}}}{Q_H + f_{u_B} \cdot \frac{Cl_{int}}{f_{u_{mic}}}} \quad \text{Equation 1.26}$$

$$CL_H = \frac{90 \text{ L/h} \cdot 0.0564 \cdot \frac{2700 \text{ L/h}}{0.92}}{90 \text{ L/h} + 0.0564 \cdot \frac{2700 \text{ L/h}}{0.92}} = \sim 58.3 \text{ L/h}$$

When corrected for both microsomal and blood binding, the *in vivo* hepatic clearance of midazolam predicted from V_{max}/K_m measurements in human liver microsomes (~58 L/h) is slightly greater than the actual *in vivo* blood clearance (~44 L/h). The over-prediction of *in vivo* clearance from *in vitro* data is the exception rather than the rule. In fact, several groups have reported that estimates of drug clearance based on *in vitro* measurements

of V_{\max}/K_m or in vitro half-life systematically underestimate in vivo rates of hepatic clearance in humans, reasons for which are discussed in the next section.

1.7. The underprediction of in vivo hepatic intrinsic clearance (CL_H)

This section examines why measurements of in vitro clearance with human liver microsomes or hepatocytes, when corrected for drug binding to the test system in vitro and to blood in vivo, systematically underpredict in vivo hepatic metabolic clearance (CL_H). Based on a review of several databases, Chiba et al. (2009) reported that, on average, human liver microsomes underpredict in vivo clearance by a factor of 9 and hepatocytes underpredict by a factor of 3-6. However, for high clearance drugs, hepatocytes tend to underpredict to a greater extent than microsomes (Lu et al., 2006; Hallifax et al., 2010).

Several studies have compared predictions of hepatic clearance in vivo from in vitro studies with human liver microsomes and hepatocytes (Hallifax et al., 2005; Riley et al., 2005; Lu et al., 2006; Brown et al., 2007b; Hallifax et al., 2010; Foster et al., 2011). For drugs whose clearance is determined by P450-dependent metabolism, these two in vitro systems would be expected to provide similar estimates of in vivo clearance even if that estimate was an underprediction of in vivo clearance. The agreement between microsomes and hepatocytes is quite good except for drugs with high intrinsic metabolic clearance, in which case hepatocytes underpredict in vivo clearance more so than microsomes. These comparisons are based on experiments with hepatocytes and microsomes prepared from different human livers. Foster et al. (2011) measured the intrinsic clearance of several drugs (all of them cleared predominantly by P450-dependent

metabolism, with the possible exception of diclofenac, which is also directly glucuronidated [Kumar et al. (2002)] in hepatocytes and microsomes prepared from the same four individuals. Intrinsic clearance was measured based on in vitro half-life or V_{max}/K_m for the major metabolite(s) formed by cytochrome P450. Data for just three drugs are shown in Table 1.5 and Figure 1.6. In the case of tolbutamide, an anionic drug metabolized primarily by CYP2C9, human liver microsomes and hepatocytes supported comparable rates of intrinsic clearance (within a factor of three). In the case of bufuralol, a basic drug metabolized primarily by CYP2D6, hepatocytes supported higher rates of clearance than microsomes (by a factor of 3.1 to 12 fold) whereas in the case of midazolam, a neutral drug metabolized by CYP3A4, microsomes supported higher rates of clearance than hepatocytes (by a factor of 5.6 to 41 fold). For drugs with low-to-medium intrinsic clearance (namely tolbutamide, bufuralol, alprenolol and triazolam), clearance in hepatocytes was equal to or greater than clearance in microsomes. In contrast, for drugs with high intrinsic clearance (namely midazolam, nifedipine and diclofenac), clearance in hepatocytes was less than that in microsomes. Foster et al. (2011) observed that, when scaled to whole liver, measurements of intrinsic clearance in hepatocytes over- or underpredicted intrinsic clearance in microsomes by a factor that was dependent on intrinsic clearance: hepatocytes overpredicted microsomal clearance by 1.5 fold for low intrinsic clearance drugs (<40 L/h), underpredicted clearance by 1.5 fold for medium intrinsic clearance drugs (40-400 L/h), and underpredicted clearance by fourfold for high intrinsic clearance drugs (>400 L/h). The authors derived the following equation to relate metabolic CL_{int} determined with microsomes with metabolic CL_{int} determined with hepatocytes.

$$\log CL_{int,hepatocytes} = 0.582 \cdot \log CL_{int,microsomes} + 0.435 \quad \text{Equation 1.27}$$

Table 1.5. Comparison of in vitro intrinsic clearance (based on V_{max}/K_m) by microsomes and hepatocytes prepared from the same four human livers.

Data are adapted from Foster et al. (2011).

Test System	CYP2C9 (Tolbutamide 4'-hydroxylation)				CYP2D6 (Bufuralol 1'-Hydroxylation)				CYP3A4 (Midazolam 1'-hydroxylation)			
	V_{max}	K_m	$CL_{u_{int}}$	Ratio	V_{max}	K_m	$CL_{u_{int}}$	Ratio	V_{max}	K_m	$CL_{u_{int}}$	Ratio
Microsome 0408	14.3	252	5.75	2.6	3.65	14.3	31.6	4.4	48.0	2.87	2190	0.078
Hepatocyte 0408	4.20	46.6	15.2		10.2	9.71	138		15.9	10.1	171	
Microsome 8053	14.9	90.6	15.2	0.55	3.50	6.75	54.2	3.1	66.6	4.80	1860	0.024
Hepatocyte 8053	15.2	129	8.40		9.85	8.15	168		5.19	8.76	44.9	
Microsome 8040	18.1	166	12.8	0.74	1.05	91.1	0.991	12	162	3.54	6090	0.14
Hepatocyte 8040	5.00	67.4	9.41		3.88	36.6	11.6		30.1	4.05	827	
Microsome 8043	9.27	233	3.82	2.7	1.59	10.1	17.6	11	13.6	4.63	403	0.18
Hepatocyte 8043	3.53	65.8	10.3		6.99	6.53	187		4.04	6.44	72.2	

V_{max} values are in units of nmol/min/g liver based on 40 mg microsomal protein/g liver and 120 million hepatocytes/g liver.

K_m values are in units of μ M based on the total concentration of drug.

$CL_{u_{int}}$ values are in units of L/h based on the unbound drug concentration. The published values were in units of mL/min/kg based on V_{max}/K_m values corrected for $f_{u_{mic}}$ or $f_{u_{hep}}$ and based on 21.4 g liver/kg body weight (*i.e.*, 1,500 g liver for 70 kg body weight). They were converted to L/h based on an average body weight of 70 kg. For comparative purposes, hepatic blood flow is 90 L/h.

Ratio calculation: (hepatocyte clearance/microsome clearance)

The overall physiologically based scaling factors (PBSF) were 60,000 mg microsomal protein/liver for microsomes (based on 40 mg microsomal protein/g liver and an average liver weight of 1,500 g) and 180,000 million hepatocytes/liver for hepatocytes (based on 120 million cells/g liver and an average liver weight of 1,500 g). These values differ slightly from those in Table 1.3 (66,000 and 198,000, respectively, which are based on an average liver weight of 1,650 g)

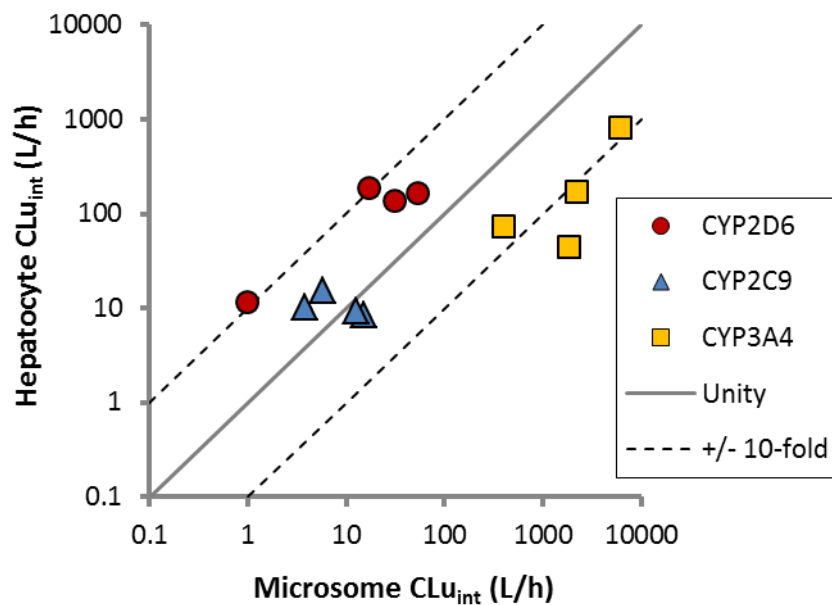


Figure 1.6. Relationship between unbound intrinsic clearance ($CL_{u_{int}}$) in human hepatocytes and microsomes from the same four donors.

The hepatocyte and microsome values of $CL_{u_{int}}$ for CYP2D6 (bufuralol 1'-hydroxylation), CYP2C9 (tolbutamide 4-hydroxylation) and CYP3A4 (midazolam 1'-hydroxylation) are from Table 1.5. Data are adapted from Foster et al. (2011).

For P450-metabolized drugs, greater rates of clearance in hepatocytes compared with microsomes (as observed with the low-clearance drug bufuralol), might reflect the transporter-mediated uptake of drug into hepatocytes, the ability of hepatocytes to further metabolize (*e.g.*, conjugate) metabolites that might otherwise inhibit the metabolism of the parent drug, or the greater stability of P450 enzymes in hepatocytes compared with NADPH-fortified microsomes (Zomorodi et al., 1995; Jones and Houston, 2004). On the other hand, lower rates of clearance in hepatocytes compared with microsomes (as observed with the high clearance drug midazolam) could occur if the uptake of the drug into hepatocytes limited its rate of metabolism by cytochrome P450 (Lu et al., 2006). However, if transporter-mediated uptake into hepatocytes promoted metabolism in the case of bufuralol or if slow hepatocyte uptake restricted metabolism in the case of midazolam, one would expect to see differences in apparent K_m (*i.e.*, a lower K_m for bufuralol metabolism in hepatocytes relative to microsomes and a higher K_m for midazolam metabolism in hepatocytes relative to microsomes). From Table 1.5 it is apparent that such differences in K_m were not observed (even when K_m values are based on the fraction of unbound drug). Based on an analysis of 10 P450 substrates, Brown et al., (2007b) reported that K_m values in microsomes and hepatocytes are similar: on average, unbound K_m values (ranging from 0.5 to 140 μM) were only 50% lower in human hepatocytes compared with human liver microsomes and no K_m value for the same drug differed more than threefold between the two systems. Foster et al. (2011) proposed that the metabolism of midazolam (and other high intrinsic clearance drugs) in hepatocytes is restricted not by uptake but by the availability of cofactor (NADPH), which is present in great excess in microsomal incubations.

Equation 1.27 addresses the difference between the two in vitro test systems but it does not explain the important issue that, even for drugs known to be cleared predominantly by P450-dependent metabolism, studies with human liver microsomes and hepatocytes both systematically underpredict hepatic clearance in vivo (Chiba et al., 2009). Possible sources of error that might lead to a general underprediction of hepatic clearance in vivo are:

1. The mathematical models of hepatic clearance are inadequate;
2. The physiologically based scaling factors are too low;
3. Values of f_{uB} based on in vitro measurements of plasma protein binding (f_{uP}) and the blood-to-plasma concentration ratio R_b) do not reflect the fraction of drug available for hepatic uptake;
4. In vitro values of $CL_{u_{int}}$ are erroneously low due to an overestimation of $f_{u_{mic}}$ or $f_{u_{hep}}$;
5. In vitro values of $CL_{u_{int}}$ are erroneously low because drug-metabolizing enzyme activities in vitro do not reflect those in vivo;
6. The role of hepatic metabolism in hepatic clearance is overestimated because the rate-determining step in hepatic clearance is transporter-mediated hepatic uptake.

Points 1 and 2. There are reports that, for high clearance drugs, the parallel-tube and dispersion models provide improved predictions of in vivo hepatic clearance over the well-stirred model (Ito and Houston, 2004), but the general consensus appears to be that neither the IVIVE models nor the physiologically based scaling factors (PBSF) are largely

responsible for the systematic underprediction of CL_H in vivo (Hallifax et al., 2010). From Equation 1.19, it is apparent that the extrapolation of in vitro CL_{int} to in vivo CL_H is dependent on three variables: hepatic blood flow (Q_H), the fraction of unbound drug in blood (f_{uB}) and $CL_{U,int}$, intrinsic clearance corrected for the in vitro binding of drug to microsomes ($f_{u_{mic}}$) or hepatocytes ($f_{u_{hep}}$). (Equation 1.19 is for the well-stirred model but the following arguments are applicable to the parallel tube and dispersion models of hepatic clearance). Although hepatic blood flow can vary (and can affect the hepatic extraction of high clearance [flow-limited] drugs), there is no reason to suspect that drugs can be delivered to the liver at four to five times greater than 90L/h, the accepted value of Q_H .

Point 3. In the case of f_{uB} , hepatic clearance will be underpredicted if the amount of drug available for hepatic uptake is greater than the unbound fraction in blood. Basing estimates of hepatic clearance on the unbound fraction of drug in blood can, in some cases, lead to underpredictions of in vivo clearance for reasons outlined in the preceding section, where it was noted that the amount of drug available for hepatic uptake can exceed the fraction unbound in blood if the dissociation of the drug from its binding sites, such as albumin, is sufficiently rapid relative to blood transit time through the liver that unbound drug lost to hepatic uptake is replenished (under so-called sink conditions). Baker and Parton (2007) reported that, for most plasma protein-bound drugs, k_{off} is not low enough ($<1 \text{ s}^{-1}$) to limit their hepatic extraction. Chao et al. (2010) suggested that, especially for drugs highly bound to plasma proteins, measurement of k_{off} (the first-order rate of dissociation of the protein-drug complex) would likely provide a better indicator of the amount of drug available for hepatic uptake than measurements of the unbound

fraction of drug in plasma or blood at equilibrium (which is determined by k_{off}/k_{on}). Accordingly, they proposed extrapolating *in vitro* clearance to *in vivo* clearance based on k_{off} and hepatic residence time (t_p) as follows:

$$in\ vivo\ CL = \frac{in\ vitro\ CL_{int}}{1 + \left(\frac{1}{k_{off} \cdot t_p}\right)} \quad \text{Equation 1.28}$$

An alternative to measuring the rate of dissociation of plasma protein-drug complexes (k_{off}) involves performing *in vitro* measurements of intrinsic clearance in the presence of plasma or serum to achieve *in vitro* the same concentration of unbound drug (with the same k_{off} rate) as that present *in vivo* (Skaggs et al., 2006; Lu et al., 2007; Kazmi et al., 2009; Mao et al., 2012). This approach can improve estimates of *in vivo* hepatic clearance, which suggests that, in some cases, an extrapolation of *in vitro* clearance based on f_{uB} does lead to an underestimation of *in vivo* clearance.

Prompted by the possibility that values of f_{uP} underestimate the amount of drug in plasma that is available for hepatic uptake and clearance, Berezhkovskiy (2011) and Poulin et al. (2012) proposed replacing f_{uP} with f_{uP-app} or $f_{u_{liver}}$, respectively, to improve predictions of *in vivo* clearance of those drugs that are highly bound to plasma proteins. The apparent unbound drug concentration in plasma (f_{uP-app}) proposed by Berezhkovskiy is based on a pH difference between plasma (pH 7.4) and intracellular water (pH 7.0), which alters the degree of ionization of basic and acidic drugs. The ratio of the fraction of neutral (unionized) drug in plasma ($f_{n_{plasma}}$) to that in hepatocytes ($f_{n_{liver}}$), termed, F_i , is determined not only by the pH difference between plasma and hepatocytes but also by the pKa values of the ionizable groups on the acidic and basic drugs, as shown below:

$$f_{u_{app}} = f_{u_P} \cdot F_l = f_{u_P} \cdot \frac{f_{plasma}^n}{f_{liver}^n} \quad \text{Equation 1.29}$$

where

$$\text{For acidic drugs: } f^n = \frac{1}{1 + 10^{pH-pKa}} \quad \text{Equation 1.30}$$

$$\text{For basic drugs: } f^n = \frac{1}{1 + 10^{pKa-pH}} \quad \text{Equation 1.31}$$

Poulin et al. (2012) advanced Berezhkovskiy's concept of $f_{u_{P-app}}$ by taking into account not only a difference in pH between plasma and liver but also a difference in the concentration of albumin. PLR, the plasma/liver protein (albumin) ratio, was used with $f_{u_{P-app}}$ to derive $f_{u_{liver}}$ as follows:

$$f_{u_{liver}} = \frac{PLR \cdot f_{u_{P-app}}}{1 + [(PLR - 1) \cdot f_{u_{P-app}}]} \quad \text{Equation 1.32}$$

Poulin et al. (2012) estimated PLR to be 13.3.

Berezhkovskiy (2011) and Poulin et al. (2012) both reported improved predictions of in vivo metabolic clearance based on an analysis of 21 and 25 drugs, respectively. Hallifax and Houston (2012) evaluated these methods with a larger database: 89 drugs tested in human hepatocytes and 64 tested in human liver microsomes (of which 46 were tested in both systems). Based on the conventional f_{u_B} method (Equation 1.22), estimates of in vitro clearance in microsomes and hepatocytes underpredicted in vivo clearance by 4.9- and 3.8-fold, respectively, and clearance of basic drugs was underpredicted to a slightly greater extent than clearance of acidic drugs. Correcting for ionization alone (applying Berezhkovskiy's method) improved predictions of in vivo clearance for basic drugs (4.4

→ 2.0 fold underprediction with hepatocytes and 5.4 → 2.5 fold underprediction with microsomes) but worsened predictions for acidic drugs (3.4 → 8.0 fold underprediction with hepatocytes and 3.7 → 7.3 fold underprediction with microsomes). The worsening of predictions for acidic drugs by considering only the pH differential and drug ionization status (Berezhkovskiy's method) was resolved by also taking into account the plasma-to-liver albumin ratio (Poulin's method). Applying Poulin's method gave good predictions of in vivo clearance of basic drugs (4.4 → 2.0 fold underprediction with hepatocytes and 5.4 → 2.5 fold underprediction with microsomes) due the pH differential/ionization status, and it improved predictions for acidic drugs (5.4 fold underprediction → 1.3 fold overprediction with hepatocytes and 3.4 fold underprediction → 1.3 fold overprediction with microsomes). Berezhkovskiy's method had no impact on predictions of in vivo clearance of neutral drugs whereas Poulin's method improved predictions of in vivo clearance (2.7 fold underprediction → 1.7 fold overprediction with hepatocytes and 5.0 → 1.5 fold underprediction with microsomes).

The method of Poulin et al. (2012) improves predictions of in vivo clearance of basic, acidic and neutral drugs, which suggests differences between intracellular and extracellular pH together with a relatively high concentration of albumin in liver (7.5% of that in plasma based on a PLR of 13.3) are important determinants of in vivo clearance that are not represented in in vitro systems. A pH of 7.0 is the lower limit of reported values of intracellular pH, which range from 7.0 to 7.4 (reviewed in Hallifax and Houston (2012)). As acknowledged by Poulin and colleagues, the PLR value of 13.3 is not based on the intracellular concentration of albumin but based on the concentration of albumin in interstitial space, which was converted to a whole-liver-to-plasma ratio of 13.3 based on

the well-stirred model (which is of questionable relevance to large molecules like albumin). There is uncertainty, therefore, as to whether the intracellular-extracellular pH difference in human liver is as large as 0.4 units and whether a PLR of 13.3 actually represents the ratio of albumin in liver versus plasma. Furthermore, the pH difference and, hence, differences in ionization status become evident only after the drug dissociates from albumin and enters the hepatocyte. The same applies to PLR; whether the concentration of albumin in the interstitial space differs from that in plasma, the drug must dissociate from albumin prior to its uptake into hepatocytes. These parameters, if not physiologically relevant to the hepatic uptake of drugs bound to plasma proteins, will mean the improvements in predicting *in vivo* clearance offered by Equation 1.29, Equation 1.30, Equation 1.31, and Equation 1.32 are akin to an empirical correction factor, such as those proposed by several groups (Chiba et al., 2009; Foster et al., 2011). One reason for questioning the physiological relevance of the assumptions inherent in Equation 1.29, Equation 1.30, Equation 1.31, and Equation 1.32 is that they appear useful for improving predictions of drug clearance in humans but they are not required to accurately predict *in vivo* clearance of drugs in rats, which is discussed under “Points 5 and 6”.

Point 4. Estimates of CL_H *in vivo* would be generally underestimated from measurements of *in vitro* $CL_{U_{int}}$ if the amount of unbound drug ($f_{u_{mic}}$ and $f_{u_{hep}}$) were systematically underestimated. On a case-by-basis, extensive non-specific binding of drugs to the reaction vessel does occur and is not accounted for in calculations of $f_{u_{mic}}$ and $f_{u_{hep}}$, but it would require drugs across all classes and at all concentrations to bind 75-80% to the glass or plastic reaction vessel in order to produce a systematic four- to fivefold underestimation of the concentration of unbound drug *in vitro*, which is not the case.

Points 5 and 6. In 1999, Obach enumerated several assumptions inherent in the use of liver microsomes to measure CL_{int} , one of which was that rates of metabolism and enzyme activities in vitro are truly reflective of those that exist in vivo. In the same paper, Obach also pointed out that “facilitated transport processes that could possibly be responsible for drug uptake or drug efflux from hepatocytes are not accounted for in in vitro studies with microsomes,” which applies equally well to recombinant enzymes and even hepatocytes depending on the experimental design. The following discussion leads to two general conclusions:

First, in the case of neutral and basic drugs, the reported underprediction of in vivo hepatic clearance based on measurements of metabolic $CL_{U_{int}}$ with human liver microsomes or hepatocytes is often due to in vitro enzymes activities being lower than those in vivo.

Second, in the case of acidic and zwitterionic drugs, the underprediction occurs partly because human liver microsomes and hepatocytes have low enzyme activity but, more importantly, because transporter-mediated uptake, not metabolic clearance, is the rate-determining step in hepatic clearance in vivo.

These conclusions are based on studies with liver microsomes and hepatocytes from rats. Ito and Houston (2004) and Jones and Houston (2004) reported some differences between predicted and observed in vivo drug clearance in rats but observed no systematic underprediction based on in vitro studies with rat liver microsomes (52 drugs) or rat hepatocytes (35 drugs) although the latter gave a narrower range of under- and overpredictions. In studies of 200 AstraZeneca drug candidates, Soars et al. (2007, 2009) observed no systematic underprediction of in vivo clearance for neutral and basic drugs

but observed systematic underprediction of acidic and zwitterionic drugs. In the latter case, in vivo clearance was correctly predicted when in vitro clearance was based on rates of hepatocyte uptake by the so-called 'medium-loss' assay. This assay, which can distinguish rates of hepatic uptake from rate of metabolic clearance, is discussed in Chapter 2 and used in Chapter 3.

The finding that in vitro studies with rat liver microsomes and hepatocytes do not systematically underpredict in vivo metabolic clearance of neutral and basic drugs but in vitro studies with the corresponding human systems do suggests that the latter have impaired enzyme activities, which is a distinct possibility because rat microsomes and hepatocytes are prepared from fresh liver that is processed immediately whereas most samples of human liver microsomes and hepatocytes are prepared from donor livers that are removed and perfused with ice-cold medium (such as Belzer UW solution) after up to 30-min cross-clamp time and are processed after many hours (up to 18 h) of transportation at 4°C (Parkinson et al., 2004). Human livers that are not perfused with Belzer UW solution are severely degraded (Parkinson et al., 2004); microsomes from such livers have little or no CYP1, CYP2 or CYP3 activities although they do exhibit CYP4 enzyme activity perhaps because in this family of P450 enzyme the heme moiety is covalently attached to the apocytochrome (Ortiz de Montellano, 2008). The possibility that some studies of in vitro drug metabolism were performed with microsomes from partially degraded human livers is suggested by the finding that in vitro estimates of drug clearance show greater sample-to-sample variation than the inter-individual variation in in vivo clearance, a discordance that is not observed if the in vitro studies are performed

with liver biopsy (fresh) samples from the same study subjects (Thummel et al., 1994a; Thummel et al., 1994b).

Differences in the extent of tissue degradation are probably a major contributor to inter-laboratory differences in CL_{int} values determined with human liver microsomes or hepatocytes (Riley et al., 2005). Such differences can be appreciated from the data for midazolam clearance in Table 1.5 and Table 1.6 and other published values. Based on measurements of V_{max} and K_m with pooled human liver microsomes, CL_{int} for midazolam (based only the 1'-hydroxylation pathway) was determined to be 693 $\mu\text{L}/\text{min}/\text{mg}$ protein (Table 1.6) and, based on f_{mic} of 0.92, $CL_{U_{int}}$ was 753 $\mu\text{L}/\text{min}/\text{mg}$ protein (see the end of the previous section). Based on the data in Table 1.5 for four samples of human liver microsomes (with matching hepatocyte samples), the values of $CL_{U_{int}}$ for midazolam (again based on midazolam 1'-hydroxylation) ranged from 112 to 1,691 $\mu\text{L}/\text{min}/\text{mg}$ protein and averaged 732 $\mu\text{L}/\text{min}/\text{mg}$ protein. (Note: the $CL_{U_{int}}$ values shown in Table 1.5 are scaled values of $CL_{U_{int}}$ so the values were divided by 40 mg microsomal protein/g liver and a liver weight of 1500 g [the same values used by Foster et al. (2011)]). In other words, the data in Table 1.5 and Table 1.6, which were determined with different commercial sources of human liver microsomes, gave comparable values of $CL_{U_{int}}$ for midazolam. As shown at the end of the last section, such values of $CL_{U_{int}}$ (*i.e.*, 753 $\mu\text{L}/\text{min}/\text{mg}$ protein for pooled microsomes and 732 $\mu\text{L}/\text{min}/\text{mg}$ protein for the average of four individual samples) slightly over-predict *in vivo* hepatic clearance. However, in a previous study of midazolam clearance by 9 samples of human liver microsomes (again based on V_{max}/K_m for midazolam 1'-hydroxylation), the same laboratory reported $CL_{U_{int}}$ values ranging from 8.2 to 159 $\mu\text{L}/\text{min}/\text{mg}$ protein (Rawden et al., 2005). The average

value (53 $\mu\text{L}/\text{min}/\text{mg}$ protein) is more than an order of magnitude lower than that reported with microsomal samples obtained from different sources and probably reflects sample degradation prior to tissue processing. It seems reasonable to assume that studies with microsomes and hepatocytes from partially degraded samples of human liver have contributed to the systematic 9-fold underprediction reported for microsomes and the 3- to 6-fold underpredictions reported for hepatocytes (Chiba et al., 2009).

Table 1.6. Estimates of in vivo clearance ($CL_{H,int}$) from in vitro clearance values (CL_{int}) determined from V_{max}/K_m for P450 marker substrates with human liver microsomes and their relationship to hepatic blood flow (Q_H)

Enzyme	Marker substrate and reaction	K_m (μM)	V_{max} (pmol/mg protein/min)	CL_{int} ($\mu L/min/mg$ protein)	$CL_{H,int}$ (whole liver) (L/h)	Fraction of hepatic blood flow ($Q_H = 90$ L/h)
CYP1A2	Phenacetin O-dealkylation	49	1140	23.3	92	1.0
CYP2A6	Coumarin 7-hydroxylation	0.75	1780	2,370	9400	100
CYP2B6	Bupropion hydroxylation	47	1350	28.7	110	1.3
CYP2B6	Efavirenz 8-hydroxylation	4.0	250	62.5	250	2.8
CYP2C8	Amodiaquine N-dealkylation	1.6	4100	2,560	10000	110
	Paclitaxel 6 α -hydroxylation	9.9	650	65.7	260	2.9
CYP2C9	Diclofenac 4'-hydroxylation	6.5	3240	499	2000	22
CYP2C19	S-Mephenytoin 4'-hydroxylation	45	210	4.67	18	0.21
CYP2D6	Dextromethorphan O-demethylation	8.9	297	33.4	130	1.5
CYP2E1	Chlorzoxazone 6-hydroxylation ^a	24	1960	81.7	320	3.6
CYP3A4/5	Testosterone 6 β -hydroxylation ^b	53	5330	101	400	4.4
	Midazolam 1'-hydroxylation	2.8	1940	693	2700	30
	Nifedipine oxidation	9.3	4960	533	2100	23
	Atorvastatin ortho-hydroxylation	42	810	19.3	76	0.85

Human liver microsomes used are a mixed-gender pool of sixteen individual human liver microsomal samples.

^a The values for chlorzoxazone 6-hydroxylation represent the high affinity component only.

^b For testosterone 6 β -hydroxylation, the K_m column represents the S_{50} with a Hill coefficient of 1.4 and the CL_{int} value represents:

$$CL_{max} = \frac{V_{max}}{S_{50}} \cdot \frac{n-1}{n(n-1)^{\frac{1}{n}}}$$

All other values of CL_{int} are based on V_{max}/K_m .

$$CL_{H,int} = CL_{int} \cdot PBSF(66,000) \cdot 60min/h \cdot 10^{-6} L/\mu L$$

Tissue degradation might be part of the reason why, based on the studies reviewed by Chiba et al. (2009), in vitro studies with microsomes underpredict in vivo clearance to a greater extent than hepatocytes. Microsomes can be isolated from extensively degraded livers; viable hepatocytes cannot. Therefore, in vitro studies are more likely to be performed with low quality microsomes than low quality hepatocytes. However, there is another reason microsomes tend to underpredict the clearance of P450-metabolized drug more so than hepatocytes, namely enzyme stability and/or the accumulation of inhibitory metabolites during the in vitro incubation. In studies of in vitro half-life of triazolam, diazepam and clonazepam, Jones and Houston (2004) observed monoexponential loss of all three drugs and all concentrations of rat hepatocytes (0.5×10^6 to 4.0×10^6 cells/mL) but they observed biexponential loss of clonazepam at all concentrations of rat liver microsomes (0.1 - 5.0 mg/mL). When triazolam and diazepam were incubated with rat liver microsomes, monoexponential loss was observed at low protein concentrations (0.1 – 1.0 mg/mL) whereas biexponential loss was observed at high protein concentrations (2 and 5 mg/mL). Jones and Houston (2004) observed greater time-dependent loss of P450 activity from NADPH-fortified microsomes compared with hepatocytes and the rate of loss in microsomes increased with increasing protein concentration (so much so that, after 45 min, microsomes incubated at 5 mg protein/mL had less P450 activity than microsomes incubated at 0.5 mg protein/mL). The marked “spontaneous loss” of P450 activity in microsomes was observed during incubations in the presence of NADPH but in the absence of drug substrate (which was added at different times for a short incubation period to measure P450 activity). P450 activities spontaneously decline over time when human liver microsomes are incubated with NADPH in the absence of a drug substrate.

The loss varies from one P450 enzyme to the next and is slowed by the addition of organic solvent (such as those commonly used to add drug substrates). The differential loss of P450 activities, the greater loss observed with increasing protein concentration and the protective effect of organic solvents on the spontaneous loss of P450 activity over time make it difficult to develop a general formula for correcting in vitro metabolic rates for the spontaneous loss of P450 activity in liver microsomes.

Although P450 enzymes are relatively unstable when microsomes are incubated at 37°C in the presence of NADPH, all P450 activities are remarkably stable (for years) in human liver microsomes stored at -80°C and in cryopreserved hepatocytes stored in liquid nitrogen (Pearce et al., 1996a; Griffin and Houston, 2004; McGinnity et al., 2004). P450 activities in microsomes are stable to repeated cycles of freezing-thawing and hepatocytes can be frozen and thawed through at least two cycles (although cells are lost at each cycle). Consequently, it is possible to prepare large pools of human liver microsomes (from 150 or 200 donors) and large pools of human hepatocytes (from up to 100 donors). Although such pooled samples may have enzyme activities that are lower than the average in vivo activities, the in vitro activities are consistent from batch-to-batch; they are so large that replacing 5 or 10% of donors from one batch to the next has little impact on P450 activities. This consistency is advantageous especially if empirical scaling factors are developed and used to correct a general underprediction of in vivo clearance from in vitro data.

Microsomes from human liver are often prepared from frozen tissue. A human liver typically weighs between one and two kilograms, which is difficult to process all at once. Freezing human liver causes no discernible harm to microsomal membranes but it does

rupture cells and organelles like mitochondria (Parkinson et al., 2004). In contrast to microsomes prepared from fresh liver, microsomes prepared from frozen liver are contaminated with membranes and proteins from other organelles, which is why, for example, liver microsomes from frozen liver have appreciable monoamine oxidase activity, an enzyme located in the outer mitochondria membrane. The additional protein associated with microsomes prepared from frozen liver decreases the specific activity of all microsomal enzyme activities (*i.e.*, all P450, UGT and carboxylesterase activities) by about 30% (Pearce et al., 1996a). Accordingly, an argument could be made that $CL_{U_{int}}$ values or the PBSF value for microsomes (66,000 mg microsomal protein/human liver) should be increased by 1.4 when *in vitro* studies of drug clearance are performed with liver microsomes prepared from frozen human liver. Such considerations are not an issue with hepatocytes, which can only be isolated from fresh (unfrozen) liver.

In the case of intestinal microsomes, the method of tissue processing is critical. Microsomes prepared from intestinal scrapings have negligible P450 activity (less than 5%) compared with microsomes prepared from enterocytes, which can be isolated by incubating intestinal tissue with EDTA-containing buffers (Zhang et al., 1999; Cotreau et al., 2000; Emoto et al., 2000).

In certain cases, such as cytosolic aldehyde oxidase and microsomal UDP-glucuronosyltransferase, there is good evidence that enzyme activities *in vitro* do not reflect those *in vivo*. Human aldehyde oxidase is a cytosolic molybdozyme involved in the oxidative metabolism of numerous heterocyclic aromatic amines (Pryde et al., 2010; Parkinson et al., 2013). Based on an analysis of 11 drugs known to be predominantly cleared *in vivo* by metabolism by aldehyde oxidase, including zaleplon, 6-

deoxypenciclovir, zoniporide, O₆-benzylgaunine, DACA and carbazeran, Zientek et al. (2010) reported that measurements of intrinsic clearance by post-mitochondrial (S9) fraction of human liver underpredicted in vivo clearance by an average of 11 fold (ranging from 0.7 to 52 fold). Predictions based on studies with human liver cytosol were slightly worse; they underpredicted in vivo clearance by ~15 fold; the difference possibly reflecting further loss of aldehyde oxidase activity during the 60-min ultracentrifugation step required to prepare cytosol from S9 fraction.

For drugs that are primarily eliminated by glucuronidation, in vitro studies with rat or human liver microsomes incubated in conventional buffer systems greatly underpredict in vivo clearance (Mistry and Houston, 1987; Boase and Miners, 2002; Soars et al., 2002; Miners et al., 2006; Miners et al., 2010a). Rates of morphine, naloxone and buprenorphine glucuronidation by rat liver and intestinal microsomes follow the same rank order as in vivo rates of glucuronidation but in vitro rates of clearance underpredict in vivo clearance by 18-33 fold (Mistry and Houston, 1987). For 7 drugs whose in vivo glucuronidation accounted for at least 50% of total metabolic clearance, rates of glucuronidation by human liver, intestinal and kidney microsomes collectively underpredicted in vivo clearance by an order of magnitude or more (Boase and Miners, 2002; Soars et al., 2002). In contrast, rates of glucuronidation of the same 7 drugs by fresh or cryopreserved human hepatocytes did not systematically underpredict in vivo clearance by glucuronidation (Soars et al., 2002; Miners et al., 2006).

Regardless of which UGT enzyme is responsible for glucuronidating a drug, in vitro rates of glucuronidation by human liver microsomes increase in the presence of detergents (such as CHAPS or Brij58) or the pore-forming peptide alamethicin because these agents

increase enzyme access to the highly polar cofactor UDP-glucuronic acid (UDP-GlcUA) (Miners et al., 2010a). However, it was recently reported that UDP-GlcUA uptake in HLM is mediated by a specific transporter and this may have an impact on in vitro UGT-mediated clearance (Rowland et al., 2015). In the case of UGT2B7 and UGT1A9, the presence of bovine serum albumin (BSA) increases activity by removing long-chain fatty acids (such as linoleic and arachidonic acid) that are released during the microsomal incubation and which competitively inhibit these two UGT enzymes (but not UGT1A1, UGT1A4 or UGT1A6) (Uchaipichat et al., 2006; Rowland et al., 2007; Rowland et al., 2008a; Rowland et al., 2008c). This so-called “albumin effect” can be accomplished with intestinal fatty acid binding protein (IFABP), which also binds fatty acids that otherwise inhibit certain UGT enzymes (Rowland et al., 2009). For drugs that are glucuronidated by UGT2B7 and, to a lesser extent, by UGT1A9, alamethicin increases their clearance by increasing V_{max} and BSA increases their clearance by lowering K_m . Several groups have improved the prediction of in vivo rates of glucuronidation by conducting studies with human liver, intestinal and kidney microsomes in the presence of both alamethicin and BSA (Kilford et al., 2009; Miners et al., 2010a; Gill et al., 2012; Wattanachai et al., 2012). The benefit of adding BSA to improve the intrinsic clearance of glucuronidated drugs is restricted to certain UGT enzymes (UGT2B7 and UGT1A9) and is restricted to microsomal preparations. Soars et al. (2002) demonstrated that adding BSA to rat hepatocytes does not enhance drug glucuronidation; in fact, it markedly decreases (by an order of magnitude) the glucuronidation of acidic drugs (drugs that bind extensively to albumin).

CYP2C8 and CYP2C9 play a role in the metabolism of fatty acids and their derivatives (Parkinson et al., 2013). It is interesting that the addition of BSA to human liver microsomes lowers the K_m of CYP2C8 for paclitaxel (Wattanachai et al., 2011) and the K_m of CYP2C9 for phenytoin and tolbutamide (Ludden et al., 1997; Carlile et al., 1999; Tang et al., 2002; Rowland et al., 2008a; Kilford et al., 2009). BSA also decreases the K_m of CYP1A2 for phenacetin (Wattanachai et al., 2012). These results suggest that, for certain P450 and UGT enzymes, in vitro clearance by liver microsomes underestimates in vivo clearance because of the presence of inhibitory fatty acids, a phenomenon that appears not to occur in hepatocytes. The possibility that fatty acids competitively inhibit CYP2C9 and CYP2C8 in human liver microsomes is of interest because these enzymes metabolize small and large acidic drugs, respectively; the same drugs that bind extensively to albumin. Inhibition of CYP2C9 and CYP2C8 by fatty acids may be a factor in the general underprediction of in vivo clearance of highly protein-bound drugs although such underprediction would be relevant to microsomes and not hepatocytes.

Loss of enzyme activity during the procurement, shipping and processing of human organs and tissues, the spontaneous loss of microsomal P450 activities during prolonged incubations, the presence of inhibitory fatty acids in microsomal membranes, the contamination of microsomes prepared from frozen livers with proteins from other organelles, and cofactor insufficiency in hepatocytes all appear to play a role in the systematic underprediction of in vivo clearance by human liver microsomes and hepatocytes. However, for some drugs, notably acidic and zwitterionic drugs, systematic underprediction of in vivo clearance stems in large part from the role of drug transporters in hepatic uptake and clearance.

1.8. Mechanisms of P450 and UGT inhibition

The inhibition of P450 and UGT enzymes can be mechanistically divided into two types: reversible inhibition (a.k.a. direct inhibition) or irreversible inhibition (a.k.a. time- or metabolism-dependent inhibition). Generally, only direct inhibition is known to occur with UGT enzymes, whereas both direct, time- or metabolism-dependent inhibition can occur with P450. Reversible or direct inhibition refers to immediate P450 or UGT inhibition; in other words it occurs as soon as the drug binds to the P450 or UGT enzyme (which is on the order of milliseconds) and without the need for biotransformation. For example, quinidine and ketoconazole are direct, reversible inhibitors of CYP2D6 and CYP3A4, respectively (Ching et al., 1995; Boxenbaum, 1999; Ogilvie et al., 2008). Direct inhibition can be further divided into two categories: competition between two drugs that are metabolized by the same enzyme and competition between two drugs only one of which is a substrate for the enzyme. The first scenario is exemplified by the interaction between omeprazole and diazepam, both substrates of CYP2C19. When co-administered, omeprazole decreases the clearance and prolongs the half-life of diazepam due to the competition for metabolism by CYP2C19, which does not occur in CYP2C19 poor metabolizers (PMs) (Andersson et al., 1990; Andersson et al., 1994; Ogilvie et al., 2008). Incidentally, it has been recently discovered that omeprazole is also a metabolism-dependent inhibitor of CYP2C19, and prolonged administration of omeprazole leads to partial inactivation of CYP2C19 (Ogilvie et al., 2011). A good example of the second category of direct inhibition is the interaction between the antitussive agent dextromethorphan and quinidine. Dextromethorphan is metabolized by CYP2D6 to its O-

demethylated metabolite dextrorphan, and this metabolism is impaired in those individuals with a CYP2D6 PM genotype. CYP2D6 extensive-metabolizers (EMs) also have impaired dextromethorphan metabolism when administered quinidine (a 48-fold increase in dextromethorphan AUC), which is a potent inhibitor of CYP2D6 (unbound $K_i < 1$ nM) but is metabolized by CYP3A4 (Nielsen et al., 1999; Margolis and Obach, 2003; Pope et al., 2004; Ogilvie et al., 2008). Direct inhibition of P450 enzymes can occur through four mechanisms: competitive inhibition, noncompetitive inhibition, mixed inhibition and uncompetitive inhibition. Competitive inhibition occurs when an inhibitor and substrate compete for binding to the same active site of an enzyme, which results in no change in the maximal rate of the enzyme (V_{max}) but results in a decrease in the affinity of the substrate towards the enzyme (as reflected in an increase in K_m). Noncompetitive inhibition is when the inhibitor binds to an allosteric site on the enzyme that is not at the substrate active site and results in a decrease in V_{max} and an unaltered K_m . In noncompetitive inhibition the inhibitor binds the enzyme and the enzyme-substrate complex with equal affinity; and it is thought to be a special case of mixed inhibition (Barr and Jones, 2011). Uncompetitive inhibition is characterized by stabilization of the enzyme-substrate complex through binding of an inhibitor either at the substrate active site or at an allosteric site (after binding of the substrate), ultimately resulting in a decrease in V_{max} and an decrease in K_m (this is because binding of the inhibitor to the enzyme-substrate complex, which normally exists in equilibrium with the enzyme and substrate, shifts the equilibrium to replace the inhibited complex, leading to an increase in substrate binding to the enzyme until a new equilibrium is established with enzyme-substrate and enzyme-substrate-inhibitor complexes). Lastly, mixed inhibition (also known as

competitive-noncompetitive inhibition) is characterized by inhibitor binding to the substrate active site as well as an allosteric site on the enzyme, or inhibitor binding to the substrate active site without blocking substrate binding and as a result will cause a decrease in V_{max} and an increase in K_m (Ogilvie et al., 2008). For direct inhibition the kinetics as well as the affinity with which an inhibitor binds to the enzyme is often described by the K_i value (dissociation constant for the enzyme-inhibitor complex) as shown in Figure 1.7.

The second type of P450 inhibition is time-dependent (metabolism-dependent) inhibition that can occur through five mechanisms: (1) slow on-rate inhibition which is a reversible process, meaning inhibition becomes more potent over time without metabolism, an example of which is inhibition of CYP19 (aromatase) by 19-azido-androstenedione (Wright et al., 1991); (2) non-enzymatic conversion of a drug to an inhibitory product that may occur with unstable compounds such as rabeprazole or some acyl glucuronides (Li and Benet, 2003; Li et al., 2004); (3) the conversion of a parent drug to a metabolite that is a more potent direct-acting (reversible) inhibitor than the parent, which occurs for the drug bupropion whose metabolites *erythro*-hydrobupropion and *threo*-hydrobupropion are more potent direct-acting inhibitors of CYP2D6 than bupropion itself (Reese et al., 2008; Parkinson et al., 2010); or (4) the biotransformation of a drug to a metabolite that coordinates with the ferrous heme iron in P450 enzymes (i.e. quasi-irreversible inhibition of CYP3A4 by troleandomycin) or (5) biotransformation to a reactive metabolite that covalently modifies the P450 apoprotein or heme moiety and abolishes enzyme activity (i.e. irreversible inhibition of CYP3A4 by mibefradil) (Ogilvie et al., 2008; Foti et al., 2011). The fourth and fifth mechanisms are common in metabolism-dependent inhibition. In the

literature, the terms time-dependent, metabolism-dependent and mechanism-based inhibition are often used interchangeably. However, there are subtle differences between each of these terms. Time-dependent inhibition (TDI) refers to a decrease in enzymatic activity that increases over time but is not dependent on biotransformation (such that it occurs even in the absence of NADPH). The term metabolism-dependent inhibition (MDI) refers to the NADPH-dependent loss of enzymatic activity over time, and includes inhibition by the formation of more potent direct-acting metabolites, quasi-irreversible inhibition and irreversible inhibition. Lastly, mechanism-based inhibition (MBI) refers strictly to quasi-irreversible and irreversible inhibition of P450 enzymes (Silverman, 1995; Ogilvie et al., 2008). The parameters often generated in these studies are the maximal rate of enzyme inactivation (K_{inact}) and potency of inactivation (K_i) as described in Figure 1.7.

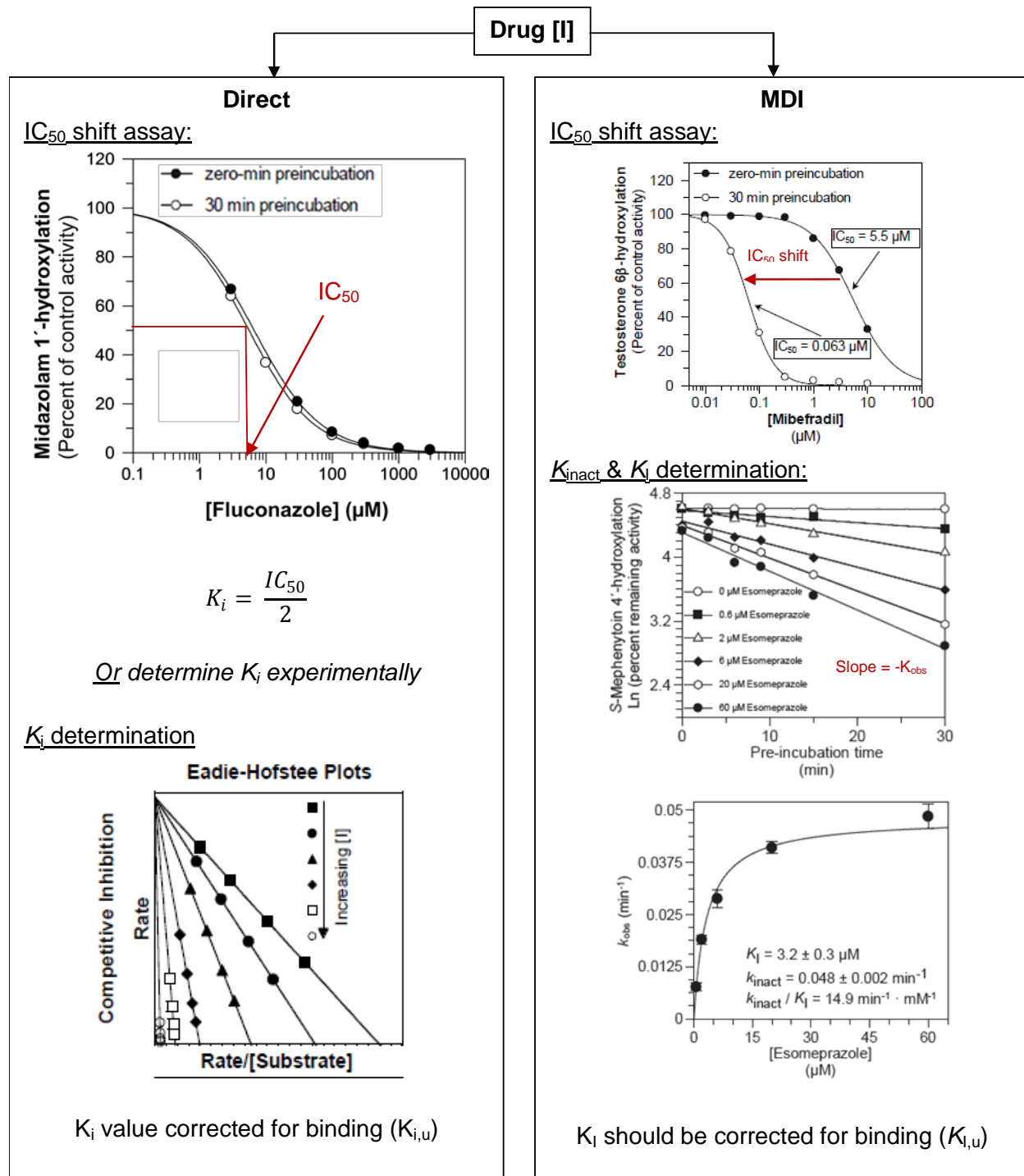


Figure 1.7. Current paradigm for performing in vitro P450 and UGT inhibition studies

The above figure depicts the typical types of experiments performed for the assessment of UGT inhibition (direct inhibition) and P450 inhibition (direct and metabolism-dependent inhibition [MDI]).

1.9. Regulatory perspective on P450 and UGT inhibition

The FDA and EMA have adopted conservative approaches (summarized in Table 1.7) to the interpretation of in vitro P450 and UGT inhibition data because there is typically ambiguity regarding the drug concentration at the P450 or UGT active site and the extent of first-pass drug metabolism (pre-systemic clearance) (Ogilvie et al., 2008; FDA, 2012; EMA, 2013). Furthermore, experimentally determined K_i values for direct inhibition may vary with incubation conditions due to factors such as membrane partitioning of the inhibitor. The FDA basic static model of predicting the potential for drug interactions by a drug from K_i values and some measure of the in vivo concentrations of the drug is as follows (Bjornsson et al., 2003):

$$AUCR = \frac{AUC_i}{AUC_{ui}} = 1 + \frac{[I]}{K_i} \quad \text{Equation 1.33}$$

Where AUCR is the plasma area-under-the-curve (AUC) ratio of AUC_i (the plasma AUC in the presence of inhibitor [the inhibited AUC]) and AUC_{ui} (the plasma AUC in the absence of inhibitor [the uninhibited AUC]), [I] is the mean plasma C_{max} value at steady state for *total* drug (i.e. bound plus unbound) and K_i is the in vitro inhibition constant based on *unbound* drug. As shown in Figure 1.8, the use of the above equation allows for predictions of clinical interactions (the theoretical curve is shown in Figure 1.8) (Ito et al., 2004; Brown et al., 2006; Obach et al., 2006). The FDA criteria for likely clinically significant P450 inhibition is $[I]/K_i > 1.1$ (or $[I]/K_i > 11$ for drugs that are orally dosed CYP3A inhibitors to account for intestinal metabolism; where $[I] = [I]_{\text{gut}} = \text{molar dose}/250 \text{ mL}$ (Zhang et al., 2008)) (FDA, 2012). The EMA guidance recommends cutoff criteria of $[I]/K_i > 0.02$ (or $[I]/K_i > 10$ for orally administered CYP3A4 inhibitors; where $[I] = [I]_{\text{gut}}$ as

described above) where both the parameters [I] and K_i are based on *unbound* concentration of drug (EMA, 2013). Should a drug candidate fail the basic model criteria, both the FDA and EMA recommend the use of mechanistic static models that incorporate parameters such as the effect of direct and metabolism-dependent inhibition, P450 induction, and intestinal and hepatic metabolism to yield a net AUC ratio (AUC_R) which must be within the regulatory range for bioequivalence (80% to 125% of AUC) to avoid a clinical study (Fahmi et al., 2009; FDA, 2012; EMA, 2013). There is precedent in the literature for the use of these models in the prediction of UGT mediated DDIs (Miners et al., 2010g). Other models also exist and have been embraced by the regulatory agencies, such as dynamic modeling and physiologically based pharmacokinetic (PBPK) modeling, however the initial assessment of clinically relevant *in vitro* P450 inhibition by new drug candidates is typically tested with the basic static model as described above. With respect to metabolism-dependent inhibition (MDI) both the FDA and EMA also recommend a basic static model which is as follows (Bjornsson et al., 2003; Grimm et al., 2009):

$$\frac{AUC_i}{AUC_{ui}} = \frac{(K_{obs} + K_{deg})}{K_{deg}} \text{ where } K_{obs} = \frac{K_{inact} \times [I]}{(K_I + [I])} \quad \text{Equation 1.34}$$

With K_{obs} representing the apparent inactivation rate constant, K_{deg} is the apparent first order degradation constant for the given enzyme, K_{inact} is the maximal inactivation rate constant, and K_i representing the apparent inactivation constant (it is important to note that K_i is distinct from K_i with the latter term representing the direct inhibition constant). Contrary to the basic static model for direct inhibition, the FDA recommends using the total (i.e. bound and unbound) values for K_i which was been shown to vary based on nonspecific binding of the drug (Tran et al., 2002; Margolis and Obach, 2003; Parkinson et al., 2011; FDA, 2012). The inhibitor concentration [I] in this case is the total drug

concentration based on the FDA guidance, and the free drug concentration (i.e. unbound) based on the EMA guidance. The basis for these models stems from regulatory agency concern regarding the possibility of in vitro false negatives (see Figure 1.8) from a public safety perspective and has shown this possibility with a review of several new drug applications (NDAs), in some of which the in vitro evaluation grossly under-predicted the in vivo interaction (Davit et al., 1999; Yao et al., 2001; Ogilvie et al., 2006; Ogilvie et al., 2008). Drug candidates examined for their potential to inhibit P450 and UGT enzymes in vitro may inhibit multiple P450/UGT enzymes, and the various models allow for the rank order across different P450/UGT enzymes for the same drug helping to prioritize clinical drug-drug interaction evaluations.

Table 1.7. FDA and EMA models for the prediction of clinically significant P450 and UGT inhibition

Model	FDA	EMA
Basic static (direct)	$1 + \frac{[I]}{K_{i,u}} = R$ <p>[I] = total $C_{max\ ss}$; $K_{i,u}$ = unbound K_i value; R > 1.1</p> <p><u>For CYP3A inhibitors given orally:</u></p> <p>[I] = [I]_{gut} = molar dose/250 mL; R > 11</p>	$1 + \frac{[I]_u}{K_{i,u}} = R$ <p>[I]_u = unbound $C_{max\ ss}$; $K_{i,u}$ = unbound K_i value; R ≥ 0.02</p> <p><u>For CYP3A inhibitors given orally:</u></p> <p>[I] = [I]_{gut} = molar dose/250 mL; R ≥ 10</p>
Basic static (MDI)	$\frac{(K_{obs} + K_{deg})}{K_{deg}} = R$ <p>Where $K_{obs} = \frac{K_{inact} \times [I]}{(K_i + [I])}$</p> <p>$K_{obs}$ = apparent inactivation rate constant</p> <p>K_{deg} = apparent first order degradation constant for a given enzyme</p> <p>K_{inact} = maximal inactivation rate constant</p> <p>K_i = apparent inactivation constant</p> <p>[I] = total $C_{max\ ss}$; R > 1.1</p>	$\frac{(K_{obs} + K_{deg})}{K_{deg}} = R$ <p>Where $K_{obs} = \frac{K_{inact} \times [I]}{(K_i + [I])}$</p> <p>$K_{obs}$ = apparent inactivation rate constant</p> <p>K_{deg} = apparent first order degradation constant for a given enzyme</p> <p>K_{inact} = maximal inactivation rate constant</p> <p>K_i = apparent inactivation constant</p> <p>[I] = unbound $C_{max\ ss}$; R > 1.25</p>
Mechanistic static	$AUCR = \left(\frac{1}{[A_h \times B_h \times C_h] \times f_m \times (1 - f_m)} \right) \times \left(\frac{1}{[A_g \times B_g \times C_g] \times (1 - F_g) + F_g} \right)$ <p>Where</p> $A_h = \frac{K_{deg,h}}{K_{deg,h} + \frac{[I]_h \times K_{inact}}{[I]_h + K_i}} \quad B_h = 1 + \frac{d \times E_{max} \times [I]_h}{[I]_h + EC_{50}} \quad C_h = \frac{1}{1 + \frac{[I]_h}{K_i}}$ <p>A, B, and C denote MDI, induction, and direct inhibition, respectively. The subscript <i>h</i> and <i>g</i> denote hepatic and gut contributions, respectively (note the equations that define A, B, and C are identical for liver and gut). AUC_R is the net AUC ratio. F_g = fraction available after gut metabolism, f_m = fraction of systemic clearance of the substrate mediated by the P450 enzyme that is subject to inhibition/induction.</p> <p>[I]_h = $f_{u,b} \times ([I]_{max,b} + F_a \times K_a \times Dose/Q_h)$; [I]_g = $F_a \times K_a \times Dose/Q_{en}$</p> <p>$F_{u,b}$ is fraction unbound in blood, [I]_{max,b} is maximal total (free and bound) inhibitor at steady state; F_a is fraction absorbed after oral administration; K_a is first order absorption constant, Q_h and Q_{en} are blood flow through the liver and enterocytes, respectively.</p> <p>If $AUC_R > 1.25$ (inhibition) or $AUC_R < 0.8$ (induction)</p>	

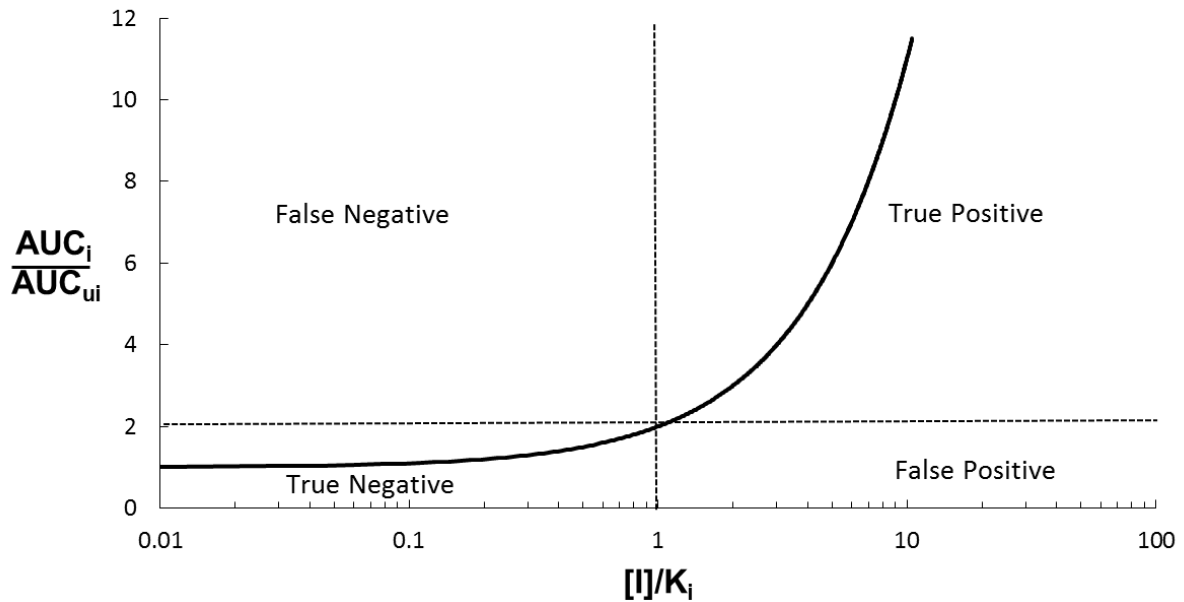


Figure 1.8. Theoretical prediction of drug-drug interactions involving P450 and UGT inhibition on the basis of inhibitory potency

Based on the equation

$$\frac{AUC_i}{AUC_{ui}} = 1 + \frac{[I]}{K_i}$$

Where AUC_i is the inhibited area under the curve (AUC), AUC_{ui} is the uninhibited AUC, $[I]$ is the mean plasma C_{max} value at steady state for total drug (i.e. bound plus unbound) and K_i is the in vitro inhibition constant based on unbound drug.

1.10. Statement of purpose

As described in Chapter 1 (Background and Introduction), the in vitro-to-in vivo (IVIVE) extrapolation of drug clearance and DDI potential are influenced by many factors, including intrinsic factors such as limitations within a given in vitro test system or extrinsic factors such as incubation conditions. In vitro studies with liver microsomes and hepatocytes have both been reported to underpredict the in vivo clearance of drugs (Chiba et al., 2009); however, the underprediction is much greater with high CL_{int} drugs when the in vitro studies are performed with hepatocytes compared with liver microsomes (Lu et al., 2006; Hallifax et al., 2010). Of particular note is the curious case of midazolam, a high CL_{int} substrate of CYP3A4/5, where its clearance is underpredicted by hepatocytes to a greater extent than liver microsomes. Other researchers have proposed possible explanations for this system-dependent clearance that include membrane permeability or cofactor limitations (Lu et al., 2006; Foster et al., 2011). The primary purpose of this research was to elucidate the mechanism underlying the test system-dependent clearance of midazolam and to determine if the restricted clearance of midazolam in hepatocytes versus microsomes was a property of other P450 enzymes and other CYP3A4/5 substrates, particularly other high CL_{int} substrates of CYP3A4/5. I hypothesized that neither membrane permeability nor cofactor availability limited the clearance of midazolam by hepatocytes, but rather an extrinsic factor such as incubation conditions (such as ionic strength and buffer/medium composition) was the underlying cause of the system-dependent clearance of midazolam. During the course of this research, studies with the CYP3A4/5 substrate loratadine identified the ability of hepatocytes to form not just desloratadine but also 3-hydroxydesloratadine. Despite

extensive investigations (Ghosal et al., 2009) the enzyme responsible for converting desloratadine to 3-hydroxydesloratadine, its major metabolite in humans, has not be identified, in part because no in vitro test system has been shown to catalyze this reaction. Having identified the reaction in human hepatocytes for the first time, I conducted a series of experiments that lead to the identification the enzyme responsible for converting desloratadine to 3-hydroxydesloratadine, which involves a highly unusual mechanism.

CHAPTER 2 : MATERIALS AND METHODS

Chemicals and Reagents

1-Aminobenzotriazole, alamethicin, atorvastatin, β -NADPH, chenodeoxycholic acid (CDCA), chlorzoxazone, coumarin, desloratadine, dextromethorphan, estradiol furafylline, gemfibrozil, hecogenin, ketoconazole, morphine, mibefradil, midazolam, 1-naphthol, nicotine, nifedipine, oxazepam, paclitaxel, paroxetine, phencyclidine, propofol, quinidine, repaglinide, saccharic acid 1,4-lactone, saponin, testosterone, tolbutamide, trifluoperazine, verapamil and Waymouth's medium were purchased from Sigma-Aldrich (St. Louis, MO); levomedetomidine was a gift from Orion Corporation (Espoo, Finland); Dulbecco's modified Eagle medium (DMEM) + HEPES was purchased from Gibco (Grand Island, NY); Krebs-Henseleit buffer (KHB) and modified Chee's medium with ITS supplement were prepared in house at XenoTech LLC (Lenexa, KS); cerivastatin, CYP3cide, esomeprazole, and gemfibrozil glucuronide were purchased from Toronto Research Chemicals (Toronto, ON, Canada); montelukast was purchased from Sequoia Research Products (Pangbourne, UK); tienilic acid was purchased from Cypex (Dundee, Scotland, UK); alfentanil, amodiaquine and troleandomycin were purchased from US Pharmacopeia (Rockville, MD); 3-hydroxydesloratadine and clopidogrel glucuronide were purchased from Santa Cruz Biotechnology (Dallas, TX); 3-hydroxydesloratadine glucuronide, 5-hydroxydesloratadine, 6-hydroxydesloratadine were purchased from TLC PharmaChem (Vaughan, ON, Canada); 3-hydroxydesloratadine-d₄ was purchased from Medical Isotopes, Inc. (Pelham, NH). Testosterone 17-O-glucuronide-d₅, oxazepam N-glucuronide-d₅, and prochlorperazine glucuronide were prepared in-house at XenoTech LLC (Lenexa, KS). Morphine 3-glucuronide-d₃ was purchased from Cerilliant (Round Rock, TX). All other deuterated glucuronides were purchased from Toronto Research

Chemicals (Toronto, ON, Canada). The sources of all other reagents have been described previously (Ogilvie et al., 2006; Parkinson et al., 2011; Kazmi et al., 2014a).

Test system

Pooled human liver microsomes (HLM, n = 16 or 200, mixed gender), pooled human liver S9 fraction (HS9, n = 200, mixed gender) and pooled suspended cryopreserved human hepatocytes (CHH, n = 50 or 100, mixed gender) or individual donor CHH (see Table 2.2 for donor information) were prepared from non-transplantable livers and characterized at XenoTech, LLC (Lenexa, KS) as described previously (Pearce et al., 1996c; Parkinson et al., 2004). Hepatocytes from Sprague-Dawley rat (male, n = 4), Beagle dog (male, n = 3), CD1 mouse (male, n = 7), Rhesus monkey (male, n = 3), New Zealand white rabbit (male, n = 3) and Gottingen minipig (male, n = 3) were prepared and characterized at XenoTech, LLC (Lenexa, KS) as described previously. Recombinant enzymes were purchased from Corning (Woburn, MA) or Cypex (Dundee, Scotland, UK).

In vitro hepatocyte clearance determinations

The in vitro hepatic clearance of dextromethorphan and midazolam was assessed with cryopreserved human hepatocytes (CHH) at 1 million cells/mL. Briefly dextromethorphan, midazolam, alfentanil, nifedipine and verapamil were incubated with CHH in 160- μ L incubations at 37°C with 95% humidity and 5% CO₂ in KHB medium at 1 μ M (and plasma C_{max} for dextromethorphan [0.014 μ M] and midazolam [0.34 μ M]) for zero, 10, 20, 30, 60, 90 and 120 min (midazolam and dextromethorphan) or 0, 30, 60, 90, 120, 150, 180 and 240 min (for all other substrates). Reactions were initiated with the addition of CHH. At each time point reactions were quenched with the addition of an equal volume of

acetonitrile containing internal standard (shown in Table 2.3). Precipitated protein was removed by centrifugation (10 min at 920 RCF). The supernatant fraction was analyzed by liquid chromatography tandem mass spectrometry (LC-MS/MS) to monitor dextromethorphan and midazolam disappearance.

In vitro microsome clearance and kinetic determinations

The in vitro clearance of midazolam, dextromethorphan, alfentanil, nifedipine, and verapamil was also assessed in pooled HLM (n = 200) at a protein concentration of 0.33 mg/mL, which is equivalent to the concentration of microsomes in hepatocytes at 1 million cells/mL (Hakooz et al., 2006; Sohlenius-Sternbeck, 2006; Barter et al., 2007). Briefly, 1 μ M midazolam, dextromethorphan, alfentanil, nifedipine or verapamil were incubated for 1-8 min (midazolam), 15-60 min (dextromethorphan), or 5-120 min (all other substrates), respectively, with NADPH-fortified HLM at 37°C in 200- μ L incubation mixtures containing pooled HLM (0.33 mg/mL), potassium phosphate buffer (50 mM, pH 7.4), MgCl₂ (3 mM), EDTA (1 mM, pH 7.4), and an NADPH-generating system (consisting of 1 mM NADP, 5 mM glucose 6-phosphate, and 1 unit/mL glucose-6-phosphate dehydrogenase). Reactions were initiated by the addition of an NADPH-generating system and quenched with the addition of an equal volume of acetonitrile containing the appropriate internal standard, followed by precipitation of protein and LC-MS/MS analysis.

The kinetic parameters, K_m and V_{max} , were determined in HLM (pooled HLM, n = 16) for midazolam 1'-hydroxylation and dextromethorphan O-demethylation. Briefly midazolam (0.5, 1, 2.5, 5, 10, 15, 20, and 40 μ M) and dextromethorphan (0.5, 1, 2.5, 5, 10, 20, 50

and 100 μ M) were incubated for 10 min at 37°C in 200- μ L incubation mixtures containing pooled HLM (0.1 mg/mL), potassium phosphate buffer (50 mM, pH 7.4), MgCl₂ (3 mM), EDTA (1 mM, pH 7.4), and an NADPH-generating system (consisting of 1 mM NADP, 5 mM glucose 6-phosphate, and 1 unit/mL glucose-6-phosphate dehydrogenase). Reactions were initiated by the addition of an NADPH-generating system and terminated by the addition of 200 μ L of acetonitrile containing the appropriate internal standard. Precipitated protein was removed by centrifugation (920 RCF for 10 min at 10°C) followed by LC-MS/MS analysis as described below.

Isolation of microsomes from cryopreserved human hepatocytes and assessment of CYP2D6 and CYP3A4 activity

Microsomes were prepared from pooled cryopreserved human hepatocytes (n = 50) as described previously (Pearce et al., 1996c; Parkinson et al., 2004). Briefly, cryopreserved human hepatocytes were thawed and sonicated for 40 sec with homogenization buffer (50 mM Tris-HCl at pH 7.4 containing 150 mM KCl and 2 mM EDTA). Homogenate was then centrifuged at ~7000g for 20 min at 4°C. The supernatant fraction was subjected to further centrifugation at ~100,000g for 60 min at 4°C. The microsomal pellet was resuspended and washed with buffer (150 mM KCl and 10 mM EDTA at pH 7.4). The washed pellet was then re-isolated by centrifugation at ~100,000g for 60 min at 4°C. The final pellet was resuspended in 250 mM sucrose and protein concentration was determined with a Pierce BCA assay (Pierce Chemical, Rockford, IL). CYP3A4 and CYP2D6 activity in microsomes isolated from pooled hepatocytes was compared with a standard preparation of pooled HLM (both at 0.1 mg/mL) with midazolam and

dextromethorphan at 1 μ M and V_{max} (40 and 75 μ M, respectively). Reactions were initiated by the addition of an NADPH-generating system and terminated by the addition of an equal volume of acetonitrile containing the appropriate internal standard. Precipitated protein was removed by centrifugation (920 RCF for 10 min at 10°C) followed by LC-MS/MS analysis as described below.

In vitro metabolism of midazolam in hepatocytes with membrane permeabilization and cofactor supplementation

The in vitro metabolism of midazolam was assessed with pooled CHH (n = 50) at 1 million cells/mL in KHB. Briefly, midazolam (1 μ M) was incubated for zero, 15, 30, 60, 90 and 120 min at 37°C (95% humidity and 5% CO₂). To determine the effect of cofactor supplementation or membrane permeability on midazolam metabolism, the following treatments were performed: (A) intact cells (control), (B) intact cells + exogenous NADPH (0.1 mM), (C) cells disrupted by sonication for 60 sec, (D) cells sonicated for 60 sec + exogenous NADPH (0.1 mM), (E) cells treated with saponin (0.01 % saponin, w/v) for 5 min, and (F) cells treated with 0.01% saponin for 5 min + exogenous NADPH (0.1 mM). At the end of each incubated time, the reaction was quenched with the addition of an equal volume of acetonitrile containing internal standard (d₄-1'-hydroxymidazolam). Precipitated protein was removed by centrifugation (920 RCF for 10 min at 10°C) followed by LC-MS/MS analysis to determine the rate of midazolam disappearance and the rate of formation of 1'-hydroxymidazolam (the major metabolite formed by CYP3A4/5) as described below.

Whole system and media loss of midazolam in CHH

The contribution of midazolam metabolism and hepatocellular uptake was assessed by comparing the whole system loss of midazolam (which reflects metabolism) versus medium loss (which reflects metabolism and cell uptake) (Soars et al., 2007). Briefly, 1 μM midazolam was incubated with pooled CHH (1 million cells/mL) in KHB at 37°C for zero, 0.5, 1, 2, 4, 6, 10, 15, 30, 45, 60, 90 and 120 min. Reactions were initiated with the addition of CHH. For the assessment of whole system loss, reactions were stopped at each time point with the addition of an equal volume of acetonitrile containing internal standard. For the assessment of medium loss, at the end of each incubation period, samples were transferred to Eppendorf tubes (Fisher Scientific, Pittsburgh, PA) and rapidly centrifuged (5 sec) followed by transfer of the supernatant fraction to an equal volume of stop reagent (acetonitrile containing internal standard). Precipitated protein was removed by centrifugation (920 RCF for 10 min at 10°C) followed by LC-MS/MS analysis.

Assessment of midazolam N-glucuronide as an inhibitor of CYP3A4/5 activity

Midazolam N-glucuronide was evaluated in an IC_{50} shift experiment with and without a preincubation step as described previously (Parkinson et al., 2011). Briefly, midazolam N-glucuronide was incubated at 0.2, 0.6, 2, 6, 20, 60, and 200 μM (for midazolam) or 0.1, 0.3, 1, 3, 10, 30 and 100 μM (for nifedipine) in 200- μL incubation mixtures containing pooled HLM (≤ 0.1 mg/mL), potassium phosphate buffer (50 mM, pH 7.4), MgCl_2 (3 mM), EDTA (1 mM, pH 7.4), an NADPH-generating system (consisting of 1 mM NADP, 5 mM glucose 6-phosphate, and 1 unit/mL glucose-6-phosphate dehydrogenase), for zero or

30 min at 37°C followed by the addition of midazolam (4 µM) or nifedipine (10 µM) and an additional 5 min incubation. An equal volume of acetonitrile containing the appropriate internal standard was added to terminate the reactions, followed by protein precipitation and LC/MS-MS analysis.

The effect of buffer ionic strength and cell culture media on P450 activity in human liver microsomes

CYP1A2 (phenacetin *O*-dealkylation), CYP2A6 (coumarin 7-hydroxylation), CYP2B6 (bupropion hydroxylation), CYP2C8 (amodiaquine *N*-dealkylation), CYP2C9 (diclofenac 4'-hydroxylation), CYP2C19 (*S*-mephenytoin 4'-hydroxylation), CYP2D6 (dextromethorphan *O*-demethylation), CYP2E1 (chlorzoxazone 6-hydroxylation) and CYP3A4/5 activity (midazolam 1'-hydroxylation, midazolam 4-hydroxylation, nifedipine oxidation, alfentanil *N*-dealkylation, verapamil *N*-dealkylation, testosterone 6β-hydroxylation, and atorvastatin ortho-hydroxylation) in human liver microsomes was assessed in 5, 50 and 200 mM potassium phosphate buffer) as well as commonly used cell culture media (KHB, MCM+, Waymouth's, DMEM+HEPES and Williams' E + HEPES) or their salts only versions (see Table 2.1). Briefly, phenacetin (40 µM), coumarin (5 µM), bupropion (50 µM), amodiaquine (7 µM), diclofenac (6 µM), *S*-mephenytoin (40 µM), dextromethorphan (7.5 µM), chlorzoxazone (30 µM), midazolam (4 µM), nifedipine (10 µM), alfentanil (40 µM), verapamil (9 µM), testosterone (70 µM) or atorvastatin (40 µM) was incubated at 37°C for 5 min with 0.1 mg/mL human liver microsomes (n = 200) [or 0.25 mg/mL human liver S9 fraction; n = 200] at three (5, 20 and 200 mM) of concentrations of phosphate buffer (each containing 3 mM MgCl₂ and 1 mM EDTA at pH

7.4) or in different cell culture media. Reactions were initiated with an NADPH regenerating system (5 mM glucose 6-phosphate, 1U/mL glucose 6-phosphate dehydrogenase, and 1 mM NADP) and stopped after 5 min with an equal volume of stop reagent (acetonitrile with internal standard). The samples were processed and analyzed by LC/MS/MS as described previously (Parkinson et al., 2011)

The effect of cell culture media on P450 activity in CHH

CYP1A2 (phenacetin *O*-dealkylation), CYP2B6 (bupropion hydroxylation), CYP2C8 (amodiaquine *N*-dealkylation), CYP2C9 (tolbutamide hydroxylation), CYP2C19 (*S*-mephenytoin 4'-hydroxylation), CYP2D6 (dextromethorphan *O*-demethylation), and CYP3A4/5 activity (midazolam 1'-hydroxylation, midazolam 4-hydroxylation, nifedipine oxidation, alfentanil oxidative *N*-dealkylation, verapamil *N*-dealkylation, testosterone 6 β -hydroxylation and atorvastatin ortho-hydroxylation) in cryopreserved human hepatocytes was assessed in commonly used cell culture media (KHB, MCM+, Waymouth's, DMEM+HEPES and Williams' E + HEPES). Briefly, phenacetin (40 μ M), bupropion (50 μ M), amodiaquine (2 μ M), tolbutamide (150 μ M), *S*-mephenytoin (40 μ M), dextromethorphan (7.5 μ M), midazolam (4 μ M), nifedipine (10 μ M), alfentanil (40 μ M), verapamil (9 μ M), testosterone (70 μ M) or atorvastatin (40 μ M) was incubated at 37°C at 95% relative humidity and 5% CO₂ for 10-60 min with 1 million cells/mL cryopreserved human hepatocytes (n = 50) in different cell culture media. Reactions were initiated in 48 well plates with the addition of hepatocytes (total incubation volume of 160 μ L per well) and stopped with an equal volume of stop reagent (acetonitrile with internal standard).

The samples were processed and analyzed by LC/MS/MS as described previously (Parkinson et al., 2011).

The effect of cell culture media on CHH viability over time

The viability of CHH (1 million cells/mL) in KHB, Waymouth's, MCM+, DMEM + HEPES and Williams' E + HEPES was assessed in 160- μ L incubations at 37°C, 95% humidity and 5% CO₂ on an orbital shaker (~150 rpm) for zero, 30, 60, 120, and 240 min. At each time point, 50 μ L was removed for cell viability assessment by trypan blue exclusion (Life Technologies, Carlsbad, CA) as described previously (Strober, 2001).

The kinetics of midazolam and chlorzoxazone metabolism in HLM with various cell culture media

The kinetic parameters, K_m and V_{max} , were determined in HLM (pooled HLM, n = 200) for midazolam 1'-hydroxylation and chlorzoxazone 6-hydroxylation in the presence of various cell culture media. Briefly midazolam (0.5, 1, 2, 4, 6, 10, 20, and 30 μ M) and chlorzoxazone (5, 10, 20, 30, 60, 100, 150, and 250 μ M) were incubated for 5 min at 37°C in 200- μ L incubation mixtures containing pooled HLM (0.1 mg/mL), potassium phosphate buffer (50 mM, pH 7.4), MgCl₂ (3 mM), EDTA (1 mM, pH 7.4); or cell culture media (KHB, Waymouth's, MCM+, DMEM + HEPES and Williams' E + HEPES), and an NADPH-generating system (consisting of 1 mM NADP, 5 mM glucose 6-phosphate, and 1 unit/mL glucose-6-phosphate dehydrogenase). Reactions were initiated by the addition of an NADPH-generating system and terminated by the addition of 200 μ L of acetonitrile containing the appropriate internal standard. Precipitated protein was removed by

centrifugation (920 RCF for 10 min at 10°C) followed by LC-MS/MS analysis as described below.

The effect of buffer ionic strength and cell culture media on rCYP3A4 and rCYP3A5 activity

Human recombinant CYP3A4 and CYP3A5 Bactosomes[®] (Cypex, Dundee, Scotland, UK) with or without cytochrome b₅ were tested for their ability to form midazolam 1'-hydroxylation and midazolam 4-hydroxylation with different cell culture media. Briefly, 4 µM midazolam was incubated in 200-µL incubation mixtures containing recombinant enzyme (20 pmol/mL), potassium phosphate buffer (50, or 200 mM, pH 7.4), MgCl₂ (3 mM), EDTA (1 mM, pH 7.4); or cell culture media (KHB, Waymouth's, MCM+, DMEM + HEPES or Williams' E + HEPES), an NADPH-generating system (consisting of 1 mM NADP, 5 mM glucose 6-phosphate, and 1 unit/mL glucose-6-phosphate dehydrogenase) for 5 min at 37°C. An equal volume of acetonitrile containing internal standard was added to terminate the reactions, followed by protein precipitation and LC-MS/MS analysis.

The effect of cell culture media on midazolam metabolism by HLM lacking CYP3A5 activity

HLM from an individual lacking CYP3A5 (CYP3A5*3/*3; H0204 prepared at XenoTech, LLC, Lenexa, KS) were tested for their ability to form midazolam 1'-hydroxylation and midazolam 4-hydroxylation with different cell culture media. Briefly, 4 µM midazolam was incubated in 200-µL incubation mixtures containing HLM (0.1 mg/mL), potassium phosphate buffer (50, pH 7.4), MgCl₂ (3 mM), EDTA (1 mM, pH 7.4); or cell culture media

(KHB, Waymouth's, MCM+, DMEM + HEPES or Williams' E + HEPES), an NADPH-generating system (consisting of 1 mM NADP, 5 mM glucose 6-phosphate, and 1 unit/mL glucose-6-phosphate dehydrogenase) for 5 min at 37°C. An equal volume of acetonitrile containing internal standard was added to terminate the reactions, followed by protein precipitation and LC-MS/MS analysis.

Loratadine metabolism in CHH with various cell culture media

The CYP3A4/5 mediated formation of desloratadine from loratadine was assessed with pooled CHH in the presence of various cell culture media. Briefly, 10 µM loratadine was incubated at 37°C at 95% relative humidity and 5% CO₂ for 60 min with pooled CHH (n = 50, 1 million cells/mL) in the presence of KHB, Waymouth's, MCM+, DMEM + HEPES or Williams' E + HEPES cell culture media. Reactions were initiated in 48 well plates with the addition of hepatocytes (total incubation volume of 160 µL per well) and stopped with an equal volume of stop reagent (acetonitrile with internal standard). The samples were processed and analyzed by LC/MS/MS as described below.

In vitro incubations of desloratadine with HLM, HS9 and CHH

Desloratadine was incubated with HLM, HS9 and CHH to determine if any of these in vitro test systems would support the formation of 3-hydroxydesloratadine. Briefly, 1 or 10 µM desloratadine was incubated at 37°C in 200-µL incubation mixtures containing pooled HLM (0.1 or 1 mg/mL) or HS9 (0.5 or 5 mg/mL), potassium phosphate buffer (50 mM, pH 7.4), MgCl₂ (3 mM), EDTA (1 mM, pH 7.4), an NADPH-generating system (consisting of 1 mM NADP, 5 mM glucose 6-phosphate, and 1 unit/mL glucose-6-phosphate dehydrogenase) for zero, 0.5, 1, 2, and 4 h. For assays with pooled CHH (n = 50),

desloratadine incubations were conducted at 37°C with 95% humidity and 5% CO₂ on an orbital shaker (~150 rpm) in 160-µL incubation mixtures containing pooled CHH (1 million cells/mL) and Williams' E media supplemented with 2 mM glutaMAX (Gibco, Grand Island, NY) and 0.1 mM HEPES. Reactions were initiated by the addition of an NADPH-generating system (for HLM and HS9) or hepatocytes (for CHH assays) and terminated by the addition of 200 µL (160 µL for CHH assays) of acetonitrile containing 3-hydroxydesloratadine-d₄ as an internal standard. Precipitated protein was removed by centrifugation (920 RCF for 10 min at 10°C) followed by LC-MS/MS analysis as described below.

***K_m* and *V_{max}* determination of 3-hydroxydesloratadine formation in CHH**

Desloratadine was incubated at 0.1, 0.2, 0.5, 1, 2, 5, 10, 20 and 30 µM in 160-µL incubation mixtures containing pooled CHH (n = 100; 1 million cells/mL) and Williams' E media supplemented with 2 mM glutaMAX (Gibco, Grand Island, NY) and 0.1 mM HEPES. Reactions were initiated with the addition of hepatocytes and conducted for 2 h at 37°C with 95% humidity and 5% CO₂ on an orbital shaker (~150 rpm). An equal volume of acetonitrile containing 3-hydroxydesloratadine-d₄ as an internal standard was added to terminate the reactions, followed by protein precipitation and LC-MS/MS analysis.

Assessment of 3-hydroxydesloratadine formation in animal hepatocytes

Hepatocytes from rat, dog, mouse, monkey, rabbit, minipig and human (n = 100) were assessed for their ability to form 3-hydroxydesloratadine. Briefly, 1 or 10 µM desloratadine was incubated in 160-µL incubation mixtures containing pooled hepatocytes (1 million cells/mL) and Williams' E media supplemented with 2 mM glutaMAX (Gibco, Grand

Island, NY) and 0.1 mM HEPES. Reactions were initiated with the addition of hepatocytes and conducted for 2 h at 37°C with 95% humidity and 5% CO₂ on an orbital shaker (~150 rpm). An equal volume of acetonitrile containing internal standard was added to terminate the reactions, followed by protein precipitation and LC-MS/MS analysis.

Recombinant P450 assessment of 3-hydroxydesloratadine formation

Human recombinant P450 enzymes, namely CYP1A1, CYP1A2, CYP1B1, CYP2A6, CYP2B6, CYP2C8, CYP2C9, CYP2C18, CYP2C19, CYP2D6, CYP2E1, CYP2J2, CYP3A4, CYP3A5, CYP3A7, CYP4A11, and CYP4F2 Bactosomes[®] (Cypex, Dundee, Scotland, UK); and CYP4F3a, CYP4F3b, CYP4F12, FMO1, FMO3 and FMO5 Supersomes[®] (Corning, Woburn, MA) were tested for their ability to form 3-hydroxydesloratadine. Briefly, 1 or 10 µM desloratadine was incubated in 200-µL incubation mixtures containing recombinant enzyme (50 pmol/mL) potassium phosphate buffer (50 mM, pH 7.4), MgCl₂ (3 mM), EDTA (1 mM, pH 7.4), an NADPH-generating system (consisting of 1 mM NADP, 5 mM glucose 6-phosphate, and 1 unit/mL glucose-6-phosphate dehydrogenase) for 1 h at 37°C. An additional time course experiment was conducted with rCYP2C8 (both Bactosomes[®] and Supersomes[®]) at 1, 2, 4 and 6 h. An equal volume of acetonitrile containing internal standard was added to terminate the reactions, followed by protein precipitation and LC-MS/MS analysis.

Chemical inhibition of 3-hydroxydesloratadine formation in CHH

P450 involvement was assessed using a chemical inhibition approach as described previously (Kazmi et al., 2014d). Briefly, pooled CHH (n = 100) at 1 million cells/mL were pre-incubated with P450 inhibitors for 30 min (2 h for the strong CYP2C8 inhibitor panel)

at 37°C on an orbital shaker (~150 rpm) with 95% humidity and 5% CO₂ in 120-µL incubation mixtures containing CHH and Williams' E media supplemented with 2 mM glutaMAX (Gibco, Grand Island, NY) and 0.1 mM HEPES. The chemical P450 inhibitors used were furafylline (10 µM), phencyclidine (10 µM), gemfibrozil (100 µM), gemfibrozil glucuronide (100 µM), montelukast (50 µM), clopidogrel glucuronide (100 µM), repaglinide (100 µM), cerivastatin (100 µM), tienilic acid (20 µM), esomeprazole (10 µM), paroxetine (1 µM), quinidine (5 µM), mibefradil (1 µM), CYP3cide (2.5 µM), troleandomycin (50 µM), ketoconazole (4 µM), and 1-aminobenzotriazole (1 mM). Following pre-incubation, 40 µL of desloratadine dissolved in Williams' E media was added to yield a final concentration of 10 µM and the incubation was continued for 2 h; or, for those samples pre-incubated with CYP2C8 inhibitors, additional incubations with amodiaquine (10 µM) and paclitaxel (10 µM) were conducted for 10 and 30 min respectively. Reactions were terminated by the addition of an equal volume of acetonitrile containing internal standard, followed by protein precipitation and LC-MS/MS analysis.

Correlation analysis of CHH with a range of CYP2C8 activities

Individual donor CHH that were pre-characterized with a range of CYP2C8 activities were assessed for 3-hydroxydesloratadine formation. Briefly, nine individual lots of hepatocytes (Table 2.2) were incubated at 1 million cells/mL with 1 or 10 µM desloratadine, amodiaquine or paclitaxel in 160-µL incubation mixtures containing Williams' E media supplemented with 2 mM glutaMAX (Gibco, Grand Island, NY) and 0.1 mM HEPES. Reactions were initiated by the addition of hepatocytes and conducted for 10 min (amodiaquine), 30 min (paclitaxel) or 2 h (desloratadine) at 37°C with 95% humidity and 5% CO₂ on an orbital shaker (~150 rpm). Reactions were terminated by the

addition of an equal volume of acetonitrile containing internal standard, followed by protein precipitation and LC-MS/MS analysis.

Correlation analysis of individual CHH with UGT2B10 activity

CHH from nine individual donors were assessed for levomedetomidine formation and 3-hydroxydesloratadine formation. Briefly, nine individual lots of hepatocytes (1 million cells/mL; Table 2.2) were incubated with 1 or 10 μ M levomedetomidine or desloratadine 160- μ L incubation mixtures containing Williams' E media supplemented with 2 mM glutaMAX (Gibco) and 0.1 mM HEPES. Reactions were initiated by the addition of hepatocytes and conducted for 30 min (2 h for desloratadine) at 37°C with 95% humidity and 5% CO₂ on an orbital shaker (approximately 150 rpm). Reactions were quenched by the addition of an equal volume of acetonitrile containing internal standard, followed by protein precipitation and LC-MS/MS analysis.

Exogenous cofactor addition with CHH, HLM or HS9

Pooled CHH (n=100; 1 million cells/mL) were treated with 0.01% (w/v) saponin (5 min) or disrupted with a probe sonicator (45 sec at 40-60% amplitude) followed by incubation in 160- μ L incubation mixtures containing 10 μ M desloratadine in Williams' E media supplemented with 2 mM glutaMAX (Gibco, Grand Island, NY) and 0.1 mM HEPES. Incubations were conducted in the presence or absence 0.1 mM NADPH and/or 1 mM UDP-GlcUA and conducted for 2 h at 37°C with 95% humidity and 5% CO₂ on an orbital shaker (~150 rpm). For incubations with pooled subcellular fractions, HLM at 0.1 and 1 mg/mL or HS9 at 0.5 and 5 mg/mL were pretreated for 15 min on ice with 25 μ g/mg alamethicin followed by incubation with or without 1 mM chemical NADPH and/or 10 mM

UDP-GlcUA at 37°C in 200- μ L incubation mixtures containing potassium phosphate buffer (50 mM, pH 7.4), MgCl₂ (3 mM), EDTA (1 mM, pH 7.4) for zero, 1, 2, 4 and 6 h. Other cofactors such as NADH, FAD, AMP and ATP were also tested (each at 1 mM). All reactions were terminated by the addition of an equal volume of acetonitrile containing internal standard, followed by protein precipitation and LC-MS/MS analysis.

Recombinant UGT panel with recombinant CYP2C8

Recombinant human UGT enzymes, namely UGT1A1, UGT1A3, UGT1A4, UGT1A6, UGT1A7, UGT1A8, UGT1A9, UGT1A10, UGT2B4, UGT2B7, UGT2B10, UGT2B15, and UGT2B17 Supersomes[®] (Corning, Woburn, MA) supplemented with recombinant CYP2C8 Supersomes[®] (Corning, Woburn, MA) were evaluated for their ability to form 3-hydroxydesloratadine. Briefly, 0.125 mg/mL recombinant UGT was supplemented with 25 pmol/mL of recombinant CYP2C8, followed by addition of 1 or 10 μ M desloratadine and incubation with 1 mM chemical NADPH and 10 mM UDP-GlcUA at 37°C in 200- μ L incubation mixtures containing potassium phosphate buffer (50 mM, pH 7.4), MgCl₂ (3 mM), EDTA (0.5 or 1 mM, pH 7.4) for 2 h. Reactions were terminated by the addition of an equal volume of acetonitrile containing internal standard, followed by protein precipitation and LC-MS/MS analysis.

In vitro P450 inhibition by desloratadine in human liver microsomes

Desloratadine was evaluated as an inhibitor of P450 enzymes as described previously (Parkinson et al., 2011). Briefly, 10 μ M desloratadine was incubated at 37°C in 200- μ L incubation mixtures containing pooled HLM (\leq 0.1 mg/mL), potassium phosphate buffer (50 mM, pH 7.4), MgCl₂ (3 mM), EDTA (1 mM, pH 7.4), an NADPH-generating system

(consisting of 1 mM NADP, 5 mM glucose 6-phosphate, and 1 unit/mL glucose-6-phosphate dehydrogenase), and a P450 marker substrate at a concentration approximately equal to its K_m . Substrates included phenacetin (CYP1A2; 40 μ M), bupropion (CYP2B6; 50 μ M), paclitaxel (CYP2C8; 5 μ M), diclofenac (CYP2C9; 6 μ M), S-mephenytoin (CYP2C19; 40 μ M), dextromethorphan (CYP2D6; 7.5 μ M), and midazolam (CYP3A4/5, 3 μ M). Prior to marker substrate addition, desloratadine was preincubated for 0 and 30 min with and without NADPH in HLM to assess direct, time-dependent and metabolism-dependent inhibition. Marker reactions were initiated by the addition of an NADPH-generating system and terminated after 5 min by the addition of 200 μ L of acetonitrile containing internal standards. Precipitated protein was removed by centrifugation (920 RCF for 10 min at 10°C) followed by liquid chromatography tandem mass spectrometry (LC-MS/MS) analysis as described below.

In vitro CYP2C8 inhibition by desloratadine in cryopreserved human hepatocytes (CHH)

Desloratadine was evaluated in an IC_{50} shift experiment with and without a preincubation step as described previously with minor modifications (Kazmi et al., 2014a). Briefly, desloratadine was incubated at 0.1, 0.3, 1, 3, 10, 30, and 100 μ M in 100- μ L incubation mixtures containing pooled CHH ($n = 100$; 0.5 million cells/mL), Williams' E media supplemented with 2 mM glutaMAX (Gibco, Grand Island, NY) and 0.1 mM HEPES, and 10 μ M amodiaquine or paclitaxel. Reactions were initiated by the addition of hepatocytes and desloratadine was preincubated with the test system for 0, 30, and 120 min at 37°C with 95% humidity and 5% CO_2 on an orbital shaker (~150 rpm). Following preincubation,

CYP2C8 marker substrates were added and samples were incubated for an additional 10 (amodiaquine) or 30 min (paclitaxel). An equal volume of acetonitrile containing the appropriate internal standard was added to terminate the reactions, followed by protein precipitation and LC/MS-MS analysis.

UGT chemical inhibition of 3-hydroxydesloratadine formation in HLM

UGT1A4 and UGT2B10 involvement in desloratadine metabolism was assessed using a chemical inhibition approach. Briefly, pooled HLMs (n = 200) at 0.1 mg/mL were incubated at 37°C in 200- μ L incubation mixtures containing 1 or 10 μ M desloratadine, 5 μ M levomedetomidine, or 20 μ M trifluoperazine; with 100 μ M hecogenin (UGT1A4 inhibitor), 500 μ M nicotine (UGT2B10 inhibitor) or both hecogenin and nicotine; Tris-HCl (100 mM, pH 7.7), MgCl₂ (10 mM), EDTA (1 mM) D-saccharic acid 1,4-lactone (0.1 mM), UDP-GlcUA (10 mM) and NADPH (1 mM). Reactions were initiated by the addition of an UDP-GlcUA with NADPH and terminated after 5 min (trifluoperazine), 10 min (levomedetomidine) or 2 h (desloratadine) by the addition of 200 μ L of acetonitrile containing internal standards, followed by protein precipitation and LC-MS/MS analysis.

Analytical methods

P450 marker substrates

LC-MS/MS analysis of all P450 marker substrates was conducted as described in Table 2.3 and as described previously (Ogilvie et al., 2006; Paris et al., 2009; Parkinson et al., 2011; Kazmi et al., 2014a).

UGT marker substrates

For UGT analytes, samples were analyzed by LC-MS/MS with LC gradients applied to a Waters Atlantis dC18 column (5 μm , 2.1 x 100 mm). Mobile phases comprised either 0.2% formic acid in water (A) and methanol (B) or 0.1 mM ammonium acetate in 95:5 (v/v) water: methanol (A) and methanol (B). Shimadzu Prominence or Nexera LC systems (Columbia, MD) were interfaced to AB Sciex API3000 triple quadrupole or API4000 or 5500 triple quadrupole linear ion trap mass spectrometers (Foster City, CA) by ESI. The corresponding internal standard compounds, mass spectrometry modes and MRM transitions employed for each specific glucuronide metabolite monitored are shown in Table 2.4.

Desloratadine and its hydroxymetabolites

Samples were analyzed by LC-MS/MS using a method developed in-house. The LC system comprised a Shimadzu SIL-5000 autosampler, two Shimadzu LC-20AD_{VP} pumps and a Shimadzu DGU-20A3 degasser (Shimadzu, Columbia, MD). An LC gradient employing 0.2% formic acid in water (A) and acetonitrile (B) at 0.6 mL min⁻¹ was applied to a Waters XBridge C18 column (5 μm , 4.6 x 100 mm) for separation of desloratadine and its metabolites. The gradient consisted of 10% B for 0.5 min followed by a linear ramp to 95% B at 9.5 min, a 1 min hold at 95% B and then a 2 min re-equilibration period at 10% B.

Analytes were detected with an AB Sciex API4000 QTrap mass spectrometer (AB Sciex, Foster City, CA) using positive mode and electrospray ionization. A multiple reaction monitoring (MRM) information-dependent acquisition (IDA) detection method was developed based on manually derived transitions for known and predicted metabolites of

desloratadine. Twenty-seven MRM transitions with 30 msec dwell times were employed, including 311/259 for desloratadine (5.3 min retention time); 327/275 for 3-hydroxydesloratadine and 331/279 for 3-hydroxydesloratadine-d₄ (5.2 min), 327/275 for 5-hydroxydesloratadine (4.9, 5.0 min) and 327/275 for 6-hydroxydesloratadine (4.7 min); and 503/327 for 3-hydroxydesloratadine glucuronide (5.1 min). Retention times for these 5 analytes were confirmed by comparison with reference standards. The electrospray voltage applied was 4500 V, the collision gas was set to high, the curtain gas was at 30 psi, the source temperature was 600°C, and the collision energy for the MRM scans was 35 eV. The declustering potential applied was 80 V for desloratadine and oxidative metabolite transitions and 30 V for labile conjugated metabolite transitions. The IDA criteria were set to acquire product ion spectra across the *m/z* range 80-700 for a peak exceeding 500 counts in the survey MRM scan. The product ion spectra were used to further confirm detection of the 3-hydroxydesloratadine (characteristic neutral loss of 17 amu) versus the 5- and 6-hydroxydesloratadine metabolites (characteristic neutral loss of 18 amu) as reported by Ramanathan et al. (2000). Where applicable, a calibration curve comprising six concentration levels prepared in duplicate across the range 0.005 – 1 µM was used for 3-hydroxydesloratadine quantitation with quadratic regression and 1/*x*² weighting.

Data analysis

All data processing and statistical analysis were conducted with Microsoft Excel 2010 (Microsoft, Redmond, WA) or SigmaPlot (Systat Software, San Jose, CA). TPSA, logP and logD_{pH 7.4} values were all predicted with MarvinSketch 5.9 (ChemAxon, Cambridge, MA). Non-linear fitting and determination of *K_m* and *V_{max}* were performed with GraFit 7.0.2

(Erithacus Software Ltd., Horley, Surrey, UK). For IC₅₀ shift experiments, the data were processed by non-linear regression with GraFit 7.0.2 using a non-linear regression algorithm based on the following two-parameter sigmoidal-logistic IC₅₀ equation:

$$y = \frac{100\%}{1 + \left(\frac{x}{IC_{50}}\right)^s} \quad \text{Equation 2.1}$$

This equation assumes that y falls with increasing x, and s is the slope factor. Data using equation 1 are both background and range corrected (i.e. lower data limit is 0 and the upper data limit is 100) as percent of control values are utilized.

In vitro intrinsic clearance and In vivo hepatic intrinsic clearance calculations

The in vitro intrinsic clearance (CL_{int}) was calculated based on the experimental elimination rate constant (k_{el}) or K_m and V_{max}. Briefly, the time course elimination of drugs when conforming to first order elimination in vitro (or in plasma) is a process in which a constant fraction of drug is removed per unit time. This fraction corresponds to the elimination rate constant (k_{el}) (units: min⁻¹) and can be calculated from the slope of a semi-log plot of log₁₀ [Drug] versus time. From k_{el}, the half-life (t_{1/2}) (units of time) can be calculated with the following equation:

$$\text{Half life } (t_{1/2}) = \frac{0.693}{k_{el}} \quad \text{Equation 2.2}$$

From both k_{el} and t_{1/2} the in vitro CL_{int} can be calculated based on the following equations:

$$CL_{int} = k_{el} \times \frac{\text{volume of incubation}}{\text{mg microsomes or million cells hepatocytes in the incubation}} \quad \text{Equation 2.3}$$

Or:

$$CL_{int} = \frac{0.693}{t_{1/2}} \times \frac{\text{volume of incubation}}{\text{mg microsomes or million cells hepatocytes in the incubation}} \quad \text{Equation 2.4}$$

An alternative method of calculating CL_{int} involves using the parameters V_{max} and K_m and can be determined according to the following equation:

$$CL_{int} = \frac{V_{max}}{K_m} \quad \text{Equation 2.5}$$

The scaled in vivo hepatic intrinsic metabolic clearance (in vivo $CL_{H,int}$) was determined with physiologically based scaling factors (PBSF) according to the following equation:

$$\begin{aligned} \text{In vivo } CL_{H,int} &= \text{In vitro } CL_{int} \\ &\times \text{PBSF for microsomes or hepatocytes} \end{aligned} \quad \text{Equation 2.6}$$

Where for human liver microsome scaling:

$$\text{In vivo } CL_{H,int} = \frac{V_{max}}{K_m} \times \frac{40 \text{ mg microsomes}}{\text{g liver}} \times \frac{1650 \text{ g}}{\text{liver}} \quad \text{Equation 2.7}$$

For human hepatocyte scaling:

$$\begin{aligned} \text{In vivo } CL_{H,int} &= K_{el} \times \frac{\text{Volume of incubation}}{\text{million cells of hepatocytes in incubation}} \\ &\times \frac{120 \text{ million hepatocytes}}{\text{g liver}} \times \frac{1650 \text{ g}}{\text{liver}} \end{aligned} \quad \text{Equation 2.8}$$

The PBSF for microsomes is thus 66,000 (40 mg microsomes per g liver multiplied by 1650 g liver) whereas for hepatocytes it is 198,000 (120 million hepatocytes per g liver multiplied by 1650 g liver), and is based on liver microsomal content and hepatocellularity as described previously (Hakooz et al., 2006; Sohlenius-Sternbeck, 2006; Barter et al., 2007).

Microsomal binding calculations

Membrane partitioning of drugs to microsomes was calculated by the methods described by Hallifax and Houston, (2006) as shown in Table 1.2.

Ionic strength calculations

Ionic strength (I) is a measure of the concentration of all ions present in a particular solution. The ionic strength of in vitro incubation buffers with varying phosphate concentration or salts only cell culture media was calculated according to the following equation as described previously (IUPAC, 1997).

$$I = \frac{1}{2} \sum_{i=1}^n c_i z_i^2 \quad \text{Equation 2.9}$$

Where c_i is the molar concentration of ion i , z_i is the charge number of that ion and the sum is taken over all the ions in the solution.

Table 2.1. Salt composition and ionic strength of various cell culture media

Salt	Final concentration (mg/mL) ^a				
	KHB	Waymouth's	MCM+	DMEM	Williams' E
Calcium Chloride, 2H ₂ O	0.494	0.12	0.265	0.265	0.265
Magnesium Chloride 6H ₂ O	0.141	0.24			
Potassium Phosphate monobasic	0.16				
Potassium Chloride	0.35	0.15	0.4	0.4	0.4
Sodium Bicarbonate	2.1	2.24	22.01	3.7	2.2
Sodium Chloride	6.9	6	4.5	6.4	6.8
Cupric sulfate 5H ₂ O			0.0003		0.0000001
Ferric nitrate 9H ₂ O			0.0012	0.0001	0.0000001
Magnesium Sulfate (anhydrous)		0.098	0.174	0.098	0.098
Sodium Phosphate monobasic		0.08	0.125	0.109	0.14
Sodium Phosphate dibasic		0.566			
Ionic strength (mM)^b	182	169	361	173	163

^a Final concentrations (mg/mL) are based on the hydrated salt molecular weights.

^b Values were calculated based only on the salt composition of the various media as described in Equation 2.9. The ionic strengths of 5, 50 and 200 mM phosphate buffer were calculated to be 35, 282 and 1108 mM respectively.

Table 2.2. Individual human donor information for CYP2C8 and UGT2B10 correlation analysis.

Xenotech Liver Number	Gender	Age (years)	Ethnicity
H924	M	40	Caucasian
H954	M	55	Caucasian
H1008	M	36	Hispanic
H1039	M	61	African American
H1042	M	51	Caucasian
H1059	F	21	Caucasian
H1086	M	63	Caucasian
H1135	F	54	African American
H1141	F	20	Asian

Table 2.3. Analytical conditions for the measurement of P450 activity in HLM and CHH by LC-MS/MS with electrospray ionization (ESI)

Enzyme	P450 activity	Ionization mode	Mass transition monitored	Internal standard (IS)	IS mass transition monitored
CYP1A2	Phenacetin O-dealkylation	Positive	152 / 110	d ₄ -Acetaminophen	156 / 114
CYP2A6	Coumarin 7-hydroxylation	Negative	161 / 133	d ₅ -7-hydroxycoumarin	166 / 138
CYP2E1	Chlorzoxazone 6-hydroxylation	Negative	184 / 120	d ₂ -6-Hydroxychlorzoxazone	188 / 122
CYP2B6	Bupropion hydroxylation	Positive	256 / 238	d ₆ -Hydroxybupropion	262 / 244
CYP2C8	Amodiaquine N-dealkylation	Positive	328 / 283	d ₅ -N-Desethylamodiaquine	333 / 283
	Paclitaxel 6 α -hydroxylation	Positive	868 / 541	d ₅ -6 α -Hydroxypaclitaxel	873 / 541
CYP2C9	Diclofenac 4'-hydroxylation	Negative	312 / 231	d ₄ -4'-Hydroxydiclofenac	318 / 237
	Tolbutamide 4-hydroxylation	Negative	285 / 186	d ₉ -4-Hydroxytolbutamide	294 / 186
CYP2C19	S-Mephenytoin 4'-hydroxylation	Negative	233 / 190	d ₃ -4'-Hydroxymephenytoin	236 / 193
CYP2D6	Dextromethorphan O-demethylation	Positive	258 / 157	d ₃ -Dextrorphan	261 / 157
CYP3A4	Midazolam 1'-hydroxylation	Positive	342 / 324	d ₄ -1'-Hydroxymidazolam	346 / 203
	Midazolam 4-hydroxylation	Positive	342 / 297		
	Testosterone 6 β -hydroxylation	Positive	305 / 269	d ₃ -6 β -Hydroxytestosterone	308 / 272
	Nifedipine oxidation	Positive	345 / 284	d ₆ -dehydronifedipine	351 / 287
	Alfentanil N-dealkylation	Positive	148 / 92	d ₅ -N-Phenylpropionamide	155 / 99
	Verapamil N-dealkylation	Positive	291 / 151	d ₆ -D617	297 / 151
	Atorvastatin <i>ortho</i> -hydroxylation	Negative	573 / 278	d ₅ - <i>ortho</i> -Hydroxyatorvastatin	578 / 283

Table 2.4. Experimental conditions for measuring UGT activity for enzyme inhibition and metabolism studies in human liver microsomes (HLM) by LC-MS/MS with electrospray ionization (ESI)

Enzyme	Substrate concentration (μM)	HLM (mg/mL)	Incubation time (min)	Ionization mode	Mass transition of metabolite	Metabolite monitored (Internal standard)	IS mass transition
UGT1A1	9	0.1	5	Negative	447 / 271	17 β -Estradiol-3-glucuronide (17 β -Estradiol 3-glucuronide-d ₅)	452 / 276
UGT1A3	20	0.1	10	Negative	567 / 391	Chenodeoxycholic acid 24-O-glucuronide (Chenodeoxycholic acid 24-O-glucuronide-d ₅)	572 / 396
UGT1A4	12	0.1	5	Positive	584 / 408	Trifluoperazine N-glucuronide (Prochlorperazine N-glucuronide)	550 / 374
UGT1A6	1	0.005	5	Negative	319 / 143	1-Naphthol O-glucuronide (1-Naphthol O-glucuronide-d ₇)	326 / 150
UGT1A9	20	0.1	5	Negative	353 / 177	Propofol O-glucuronide (Propofol O-glucuronide-d ₁₇)	370 / 194
UGT2B7	400	0.1	5	Positive	462 / 286	Morphine 3-O-glucuronide (Morphine 3-O-glucuronide-d ₃)	465 / 289
UGT2B10	7	0.1	10	Positive	377 / 201	Levomemetomidine N-glucuronide (1'-Hydroxymetomidolam-d ₄)	347 / 329
UGT2B15	50	0.1	10	Positive	463 / 286	Oxazepam O-glucuronide (Oxazepam O-glucuronide-d ₅)	468 / 291
UGT2B17	5	0.1	10	Positive	465 / 289	Testosterone 17 β -O-glucuronide (Testosterone 17 β -O-glucuronide-d ₅)	470 / 294

CHAPTER 3 : TEST SYSTEM-DEPENDENT DRUG CLEARANCE
PART 1: MIDAZOLAM CLEARANCE IN HUMAN HEPATOCYTES IS
RESTRICTED COMPARED WITH HUMAN LIVER MICROSOMES BUT
NOT BY CELL PERMEABILITY OR COFACTOR AVAILABILITY

ABSTRACT

This study confirms previous reports that the intrinsic metabolic clearance of CYP3A4/5 substrates, especially midazolam, is underpredicted by cryopreserved human hepatocytes compared with human liver microsomes (HLM) and examines previous proposals namely permeability- and cofactor-restricted clearance in hepatocytes, to explain this unexpected system-dependent difference. The clearance of midazolam (high CL_{int} CYP3A4/5 substrate) was compared with the clearance of dextromethorphan (low CL_{int} CYP2D6 substrate) in pooled CHH (1 million cells/mL) and a physiologically equivalent concentration of pooled HLM (0.33 mg/mL), based on hepatic scaling factors. Dextromethorphan CL_{int} was similar between test systems (within 2-fold); however, midazolam CL_{int} in CHH was approximately one tenth that in HLM. Sonication or saponin treatment of CHH (to increase membrane permeability) with and without the addition of exogenous NADPH (removal of cofactor availability as a variable) had no effect on midazolam metabolism. When midazolam was incubated with CHH, the rate of substrate loss from the medium greatly exceeded that from the whole system, suggesting the uptake of midazolam is considerably faster than its metabolism. CYP3A4/5 activity in microsomes prepared from the pooled CHH was comparable to that in pooled HLM. These results suggest that neither membrane permeability nor cofactor availability limits midazolam clearance in CHH. When the clearance of other CYP3A4/5 substrates, namely alfentanil, nifedipine and verapamil, was assessed in CHH (1 million cells/mL) and HLM (0.33 mg/mL), estimates of hepatic intrinsic metabolic clearance ($CL_{H,int}$) with HLM were 2.6- to 3.7-fold greater than those estimated with CHH compared with a ~9-fold difference

for midazolam. This suggests that the system-dependent clearance of midazolam is more pronounced than that of other CYP3A4/5 substrates.

INTRODUCTION

The in vitro to in vivo extrapolation (IVIVE) of drug clearance involves the determination of intrinsic clearance in vitro (CL_{int}), based on in vitro measurements of V_{max}/K_m or half-life ($t_{1/2}$) in human liver microsomes (HLM) or cryopreserved human hepatocytes (CHH), which are then scaled to predict hepatic clearance in vivo ($CL_{H,int}$) (Obach, 1999; Griffin and Houston, 2004; Jones and Houston, 2004). This is common practice in the pharmaceutical industry because CL_{int} values can be used, for example, to assess whether metabolism represents a major pathway of clearance in vivo and whether an investigational drug is a candidate for once-a-day dosing. Assessing the rank order of in vitro CL_{int} values for drug candidates is also useful for evaluating species or gender differences in metabolic clearance. Although in vitro values of CL_{int} often underpredict in vivo values of $CL_{H,int}$, especially with human-derived test systems, the values of CL_{int} determined with HLM would be expected to match those determined in CHH for drugs predominantly cleared by cytochrome P450 enzymes (P450). However, in the case of drugs rapidly cleared by CYP3A4/5, there are reports showing that CL_{int} values determined in microsomes are much greater than those determined in hepatocytes whereas the opposite has been observed with drugs that are slowly cleared by CYP2D6 (Lu et al., 2006; Brown et al., 2007b; Hallifax et al., 2010). These test system-dependent differences in drug clearance raise the possibility that HLM and CHH differ in their capacity to support the metabolism of drugs whose clearance is largely dependent on metabolism by P450 enzymes.

Previous investigators have proposed that the lower clearance of midazolam (and other high clearance drugs metabolized by CYP3A4) in hepatocytes compared with

microsomes may be due a limitation imposed by membrane permeability or the availability of cofactor (NADPH), two factors that would restrict midazolam clearance by CHH but not by HLM (Lu et al., 2006; Foster et al., 2011). Lu and colleagues (2006) examined the impact of membrane partitioning and membrane permeability by assessing the CL_{int} of 7-ethoxycoumarin, phenacetin, propranolol, and midazolam in rat and human liver microsomes as well as hepatocytes. They surmised that higher rates of clearance in microsomes than hepatocytes was due to system-dependent differences in the fraction of unbound drug and/or because the rate of uptake of drug into hepatocytes limited the rate of metabolism, which was consistent with the observation that discrepancies in CL_{int} between CHH and HLM tends to be a feature of high clearance drugs. Without correction for membrane partitioning, which lowers the fraction of unbound drug immediately available for metabolism, midazolam clearance in rat microsomes was shown to be 40-fold greater than that in rat hepatocytes; however, after correcting for the fraction of unbound drug in both microsomes and hepatocytes the difference in midazolam CL_{int} was reduced to approximately 4 fold. In the case of human microsomes and hepatocytes, correcting for membrane partitioning reduced the difference in CL_{int} to 3.5 fold; however, the CL_{int} of midazolam in human hepatocytes was found to be much lower than that in rat hepatocytes.

Foster and colleagues (2011) compared the CL_{int} of seven P450 substrates with a wide range of clearance values in HLM and CHH prepared from the same liver donor in an attempt to exclude donor variability bias. They found that for the high clearance substrates midazolam, nifedipine and diclofenac there was a 4-fold underprediction of CL_{int} by hepatocytes versus microsomes. However, in contrast to Lu et al., (2006), they concluded

that membrane permeability did not account for the relatively low rate of midazolam clearance in CHH because they observed no difference between HLM and CHH in the K_m for midazolam clearance or metabolite formation. Had membrane permeability impeded the cellular uptake of midazolam, the intracellular concentration of midazolam in CHH would be lower than that in HLM, which would have increased the apparent K_m , but this was not observed. Foster et al., (2011) noted that, as the value of CL_{int} increased, K_m remained unchanged but the maximal rate of drug metabolism (i.e., V_{max}) by CHH progressively declined relative to V_{max} by HLM; accordingly, they proposed that a factor other than membrane permeability limited the rate of CYP-dependent drug metabolism in hepatocytes. They postulated that cofactor (NADPH) availability might be such a factor.

In the present study I examined the clearance of the CYP3A4/5 substrate midazolam (high intrinsic clearance) and the CYP2D6 substrate dextromethorphan (low intrinsic clearance) in HLM and CHH and confirmed previous reports that midazolam clearance in hepatocytes is considerably lower than in HLM. Experiments were then undertaken to assess whether other substrates of CYP3A4/5 exhibited the same test system-dependent clearance and to examine whether membrane permeability or cofactor availability account for the relatively low rate of clearance of midazolam in CHH.

RESULTS

3.1. Comparison of midazolam and dextromethorphan clearance in HLM and CHH.

To compare the in vitro clearance of CYP2D6 and CYP3A4/5 substrates, dextromethorphan and midazolam were incubated at 1 μM and plasma C_{max} (0.014 μM and 0.34 μM , respectively) with pooled CHH ($n = 50$) at 1 million cells/mL for up to 120 min, as described in *Chapter 2*. The results are shown in Figure 3.1, and demonstrate first-order elimination of both midazolam and dextromethorphan over time with a half-life of 75 and 56 min respectively at 1 μM ; or 63 and 81 min at plasma C_{max} , respectively. The clearance of both substrates (1 μM) was also assessed in pooled HLM ($n=200$) at a protein concentration of 0.33 mg/mL, which is equivalent to the concentration of microsomal protein in hepatocytes at 1 million cells/mL (Hakooz et al., 2006; Sohlenius-Sternbeck, 2006; Barter et al., 2007). In HLM, the half-life of midazolam was 8.5 min whereas the half-life of dextromethorphan was 85 min, as shown in Figure 3.2. The kinetics of dextromethorphan and 1'-hydroxymidazolam formation by HLM (0.1 mg/mL) were assessed as described in *Chapter 2*. As shown in Figure 3.3, V_{max} and K_{m} for CYP2D6 were 276 pmol/mg/min and 9.5 μM dextromethorphan, respectively, whereas V_{max} and K_{m} for CYP3A4 were 1290 pmol/mg/min and 2.4 μM midazolam, respectively.

Because CHH and HLM were incubated at physiologically equivalent concentrations, the half-life of a drug metabolized primarily by P450 would be the same in the absence of test system-dependent factors. As shown in Figure 3.1 and Figure 3.2, the half-life of dextromethorphan in CHH (56-81 min) was comparable to that in HLM (85 min). However,

the half-life of midazolam in CHH (63-75 min) was less than one-tenth the half-life in HLM (8.5 min). In vitro values of CL_{int} (based on in vitro half-life or V_{max}/K_m) were extrapolated to in vivo values of hepatic intrinsic metabolic clearance ($CL_{H,int}$) based on physiologically based scaling factors (PBSF; described in the Discussion section), and the results are summarized in Table 3.1. With dextromethorphan, the value of $CL_{H,int}$ determined with microsomes (97.8 to 115 L/h) was comparable to that determined with hepatocytes (102 to 147 L/h). In contrast, with midazolam, the value of $CL_{H,int}$ determined with microsomes (978 to 2130 L/h) was 7.6- to 19.2-fold (approximately an order of magnitude) greater than that determined with hepatocytes (110 to 129 L/h). These results confirmed previous reports of system-dependent clearance of midazolam (Lu et al., 2006; Foster et al., 2011).

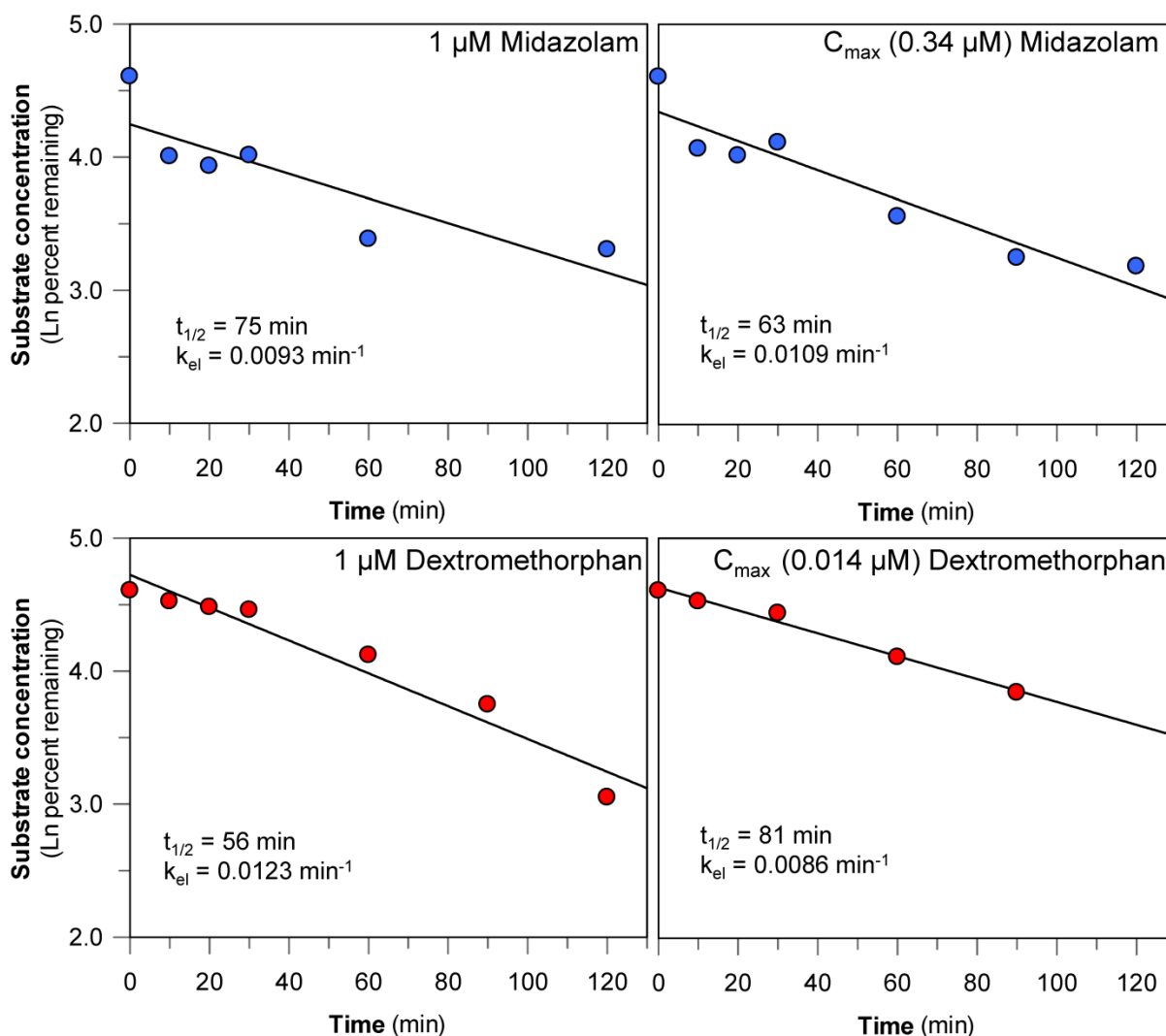


Figure 3.1. The in vitro clearance of midazolam (top) and dextromethorphan (bottom) at 1 μM and plasma C_{max} in cryopreserved human hepatocytes (CHH)

Pooled CHH (1 million cells/mL) were incubated with midazolam (colored blue) or dextromethorphan (colored red) at 1 μM or at their plasma C_{max} concentrations (0.34 and 0.0014 μM, respectively) for up to 120 min. Disappearance of substrate was measured by LC-MS/MS. In vitro half-life and the first-order elimination rate constant (k_{el}) were calculated as described in *Chapter 2*.

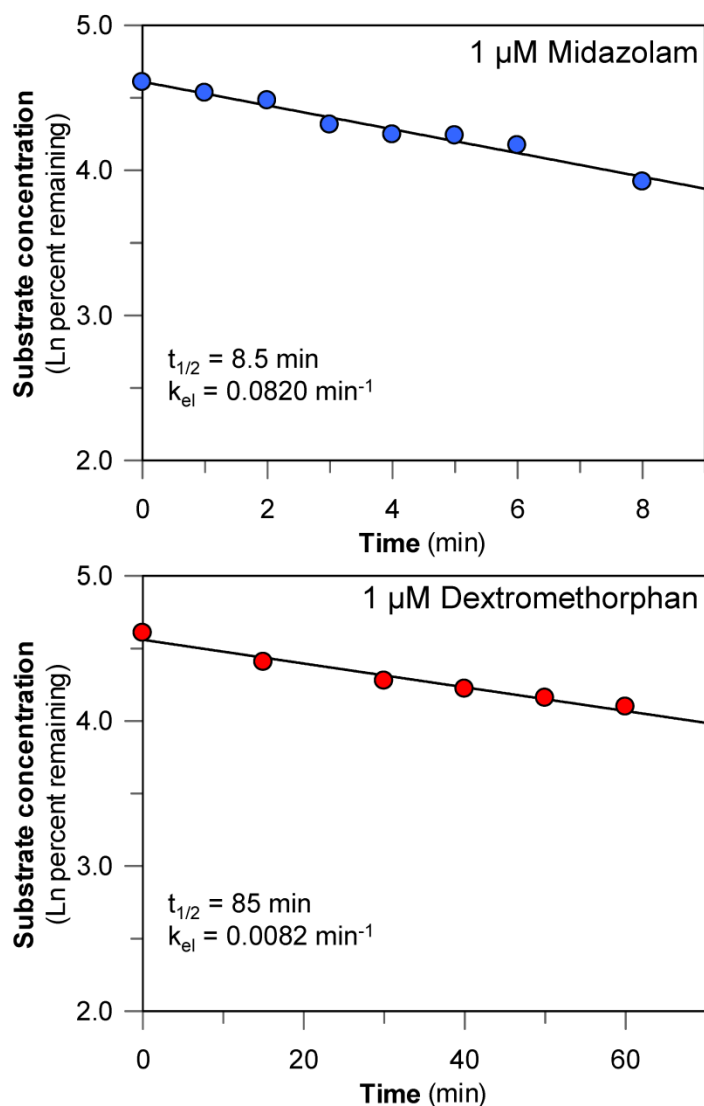


Figure 3.2. The in vitro clearance of midazolam (top) and dextromethorphan (bottom) at 1 μ M in pooled human liver microsomes

As described in *Chapter 2*, 1 μ M midazolam and 1 μ M dextromethorphan were incubated with pooled human liver microsomes at 0.33 mg/mL, a protein concentration equivalent to the microsomal content of human hepatocytes at 1 million cells/mL. Incubations were conducted for up to 8 min (midazolam) or 60 min (dextromethorphan). Disappearance of substrate was measured by LC-MS/MS. In vitro half-life and the first-order elimination rate constant (k_{el}) were calculated as described in *Chapter 2*.

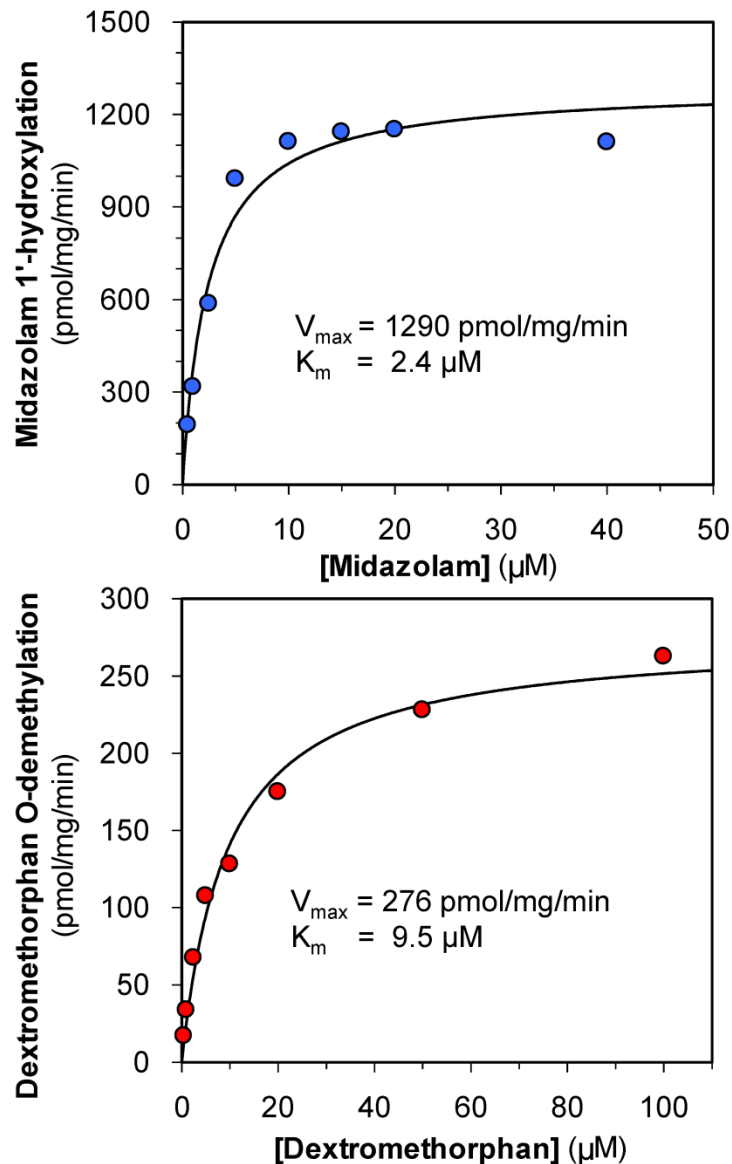


Figure 3.3. Kinetics of 1'-hydroxymidazolam (CYP3A4/5) formation (top) and dextromethorphan (CYP2D6) formation (bottom) pooled human liver microsomes

The K_m and V_{max} of 1'-hydroxymidazolam and dextromethorphan formation were determined by incubating pooled human liver microsomes (0.1 mg/mL) with eight concentrations of midazolam (0.5 to 40 μM) or dextromethorphan (0.5 to 100 μM) for 10 min, as described in *Chapter 2*.

Table 3.1. Summary of scaled values of in vivo hepatic intrinsic clearance ($CL_{H,int}$) from values of in vitro intrinsic clearance (CL_{int}) determined with cryopreserved human hepatocytes and human liver microsomes

Substrate	Cryopreserved human hepatocytes					
	In vitro half-life (substrate disappearance) with [S] = 1 μ M and 1 x 10 ⁶ cells/mL			In vitro half-life (substrate disappearance) with [S] = plasma C_{max} and 1 x 10 ⁶ cells/mL		
	$t_{1/2}$ (min)	k_{el} (min ⁻¹)	$CL_{H,int}^a$	$t_{1/2}$ (min)	k_{el} (min ⁻¹)	$CL_{H,int}^a$
Dextromethorphan	56	0.01234	147 L/h	81	0.00859	102 L/h
Midazolam	75	0.00928	110 L/h	63	0.01092	129 L/h
Substrate	Human liver microsomes					
	In vitro half-life (substrate disappearance) with [S] = 1 μ M and HLM at 0.33 mg/mL			V_{max} and K_m of 1'-hydroxymidazolam formation by HLM at 0.1 mg/mL		
	$t_{1/2}$ (min)	k_{el} (min ⁻¹)	$CL_{H,int}^b$	V_{max} (pmol/mg/min)	K_m (μ M)	$CL_{H,int}^c$
Dextromethorphan	85	0.0082	97.8 L/h	276	9.5	115 L/h
Midazolam	8.5	0.0820	978 L/h	1290	2.4	2130 L/h

^a Hepatocyte $CL_{H,int}$ based on in vitro half-life (substrate disappearance) was calculated as follows: $k_{el} \times \text{volume of incubation/million cells per incubation} \times 198,000 \text{ PBSF}$. Units were converted to L/h.

^b Microsomal $CL_{H,int}$ based on in vitro half-life (substrate disappearance) was calculated as follows: $k_{el} \times \text{volume of incubation/mg protein per incubation} \times 66,000 \text{ PBSF}$. Units were converted to L/h.

^c Microsomal $CL_{H,int}$ based on the kinetics of 1'-hydroxymidazolam formation was calculated as follows: $V_{max}/K_m \times 66,000 \text{ PBSF}$. Units were converted to L/h.

Note: $CL_{H,int}$ values were not corrected for substrate binding to microsomes or hepatocytes.

3.2. Assessment of CYP3A4/5 activity in microsomes prepared from CHH compared with a standard preparation of HLM.

To determine whether the difference in midazolam metabolic clearance between HLM and CHH could be attributed to low CYP3A4/5 activity in CHH, microsomes were isolated from pooled CHH (n = 50) and both CYP2D6 and CYP3A4/5 activity was compared with that in a standard preparation of pooled HLM (n = 200) (i.e., microsomes prepared directly from human liver). In each case the microsomes were incubated at 0.1 mg/mL with 1 μ M substrate or a substrate concentration equal to roughly 10 times K_m (so-called V_{max} conditions), as described in *Chapter 2*. As shown in Table 3.2, microsomes isolated from pooled CHH metabolized both dextromethorphan (CYP2D6) and midazolam (CYP3A4/5) at rates comparable (within 20%) to the standard preparation of pooled HLM. These results established that the test system-dependent difference in midazolam metabolism could not simply be ascribed to an abnormally low activity of CYP3A4/5 in the pooled CHH.

Table 3.2. Comparison of metabolic rates between microsomes isolated from cryopreserved human hepatocytes and a standard preparation of pooled human liver microsomes with two concentrations of midazolam (CYP3A4/5) and dextromethorphan (CYP2D6)

Test system	Rate (pmol/mg/min)			
	Midazolam 1'-hydroxylation		Dextromethorphan O-demethylation	
	1 μ M	40 μ M	1 μ M	75 μ M
Pooled HLM (n = 200)	263	1132	45	259
HLM isolated from CHH (n =50)	206	893	46	220

3.3. Determining the effect of membrane permeabilization and cofactor supplementation on midazolam metabolism in CHH.

To assess the impact of membrane permeability cofactor availability on midazolam metabolism in CHH, the plasma membrane of intact cells was disrupted by sonication or treatment with the membrane-permeabilizing agent saponin with and without the addition of exogenous NADPH. Six different treatment groups were assessed: intact hepatocytes with and without NADPH, sonicated hepatocytes with and without NADPH, and saponin-treated hepatocytes with and without NADPH, as described in *Chapter 2*. The results are shown in Figure 3.4. Sonication or treatment of hepatocytes with saponin had little or no effect (<20%) on the rate of disappearance of midazolam or the rate of formation of 1'-hydroxymidazolam. Likewise, the addition of NADPH to intact hepatocytes or hepatocytes permeabilized by sonication or saponin treatment failed to stimulate the metabolism of midazolam. These results suggest that neither membrane permeability nor cofactor availability limits the rate of metabolism of midazolam by human hepatocytes.

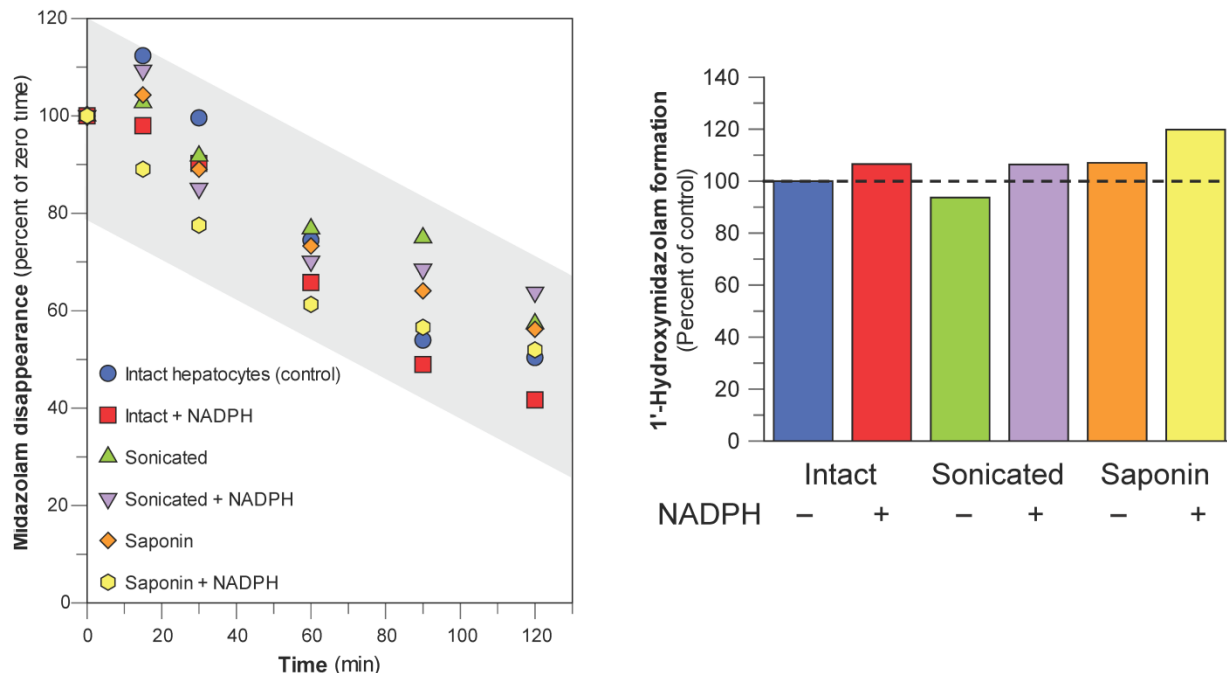


Figure 3.4. The effects of membrane permeabilization by sonication or saponin treatment and cofactor supplementation on the in vitro metabolism of midazolam in cryopreserved human hepatocytes

Cryopreserved human hepatocytes (CHH) at 1 million cells/mL were either sonicated or treated with saponin (0.01% w/v) followed by the addition of 0.1 mM NADPH to select treatment groups and then incubation with 1 μ M midazolam for up to 120 min. The disappearance of midazolam and formation of 1'-hydroxymidazolam were determined as described in *Chapter 2*. Representative data for 1'-hydroxymidazolam formation at t = 60 min are shown in the right-hand figure.

3.4. Assessment of midazolam uptake into CHH.

To further assess whether midazolam clearance in human hepatocytes is restricted by membrane permeability, the combined rate of hepatocellular uptake and metabolism (i.e., the rate of disappearance of midazolam from the cell culture medium) was compared with the rate of metabolism of midazolam (i.e., the rate of disappearance of midazolam from the whole system). Medium loss and whole-system loss of midazolam (1 μ M) were assessed with CHH at 1 million cells/mL for up to 120 min, as described in *Chapter 2*. In the whole-system loss assay (cells + medium), drug loss can occur only by metabolism; whereas in the medium-loss assay the disappearance of drug from the cell culture medium can occur by both metabolism and cellular uptake (which represents membrane partitioning of the drug into the plasma membrane, passive diffusion into hepatocytes and/or transporter-mediated uptake). As shown in Figure 3.5, the results indicate that there is an initial, rapid uptake of midazolam into CHH. Approximately 45% of midazolam disappeared from the medium within the first 10 min (due to uptake and metabolism), at which point less than 10% of midazolam was lost from the whole system (due to metabolism). These results suggest that the rate of midazolam uptake into hepatocytes greatly exceeded its rate of metabolism, which provides additional evidence that membrane permeability does not restrict the metabolic clearance of midazolam by human hepatocytes.

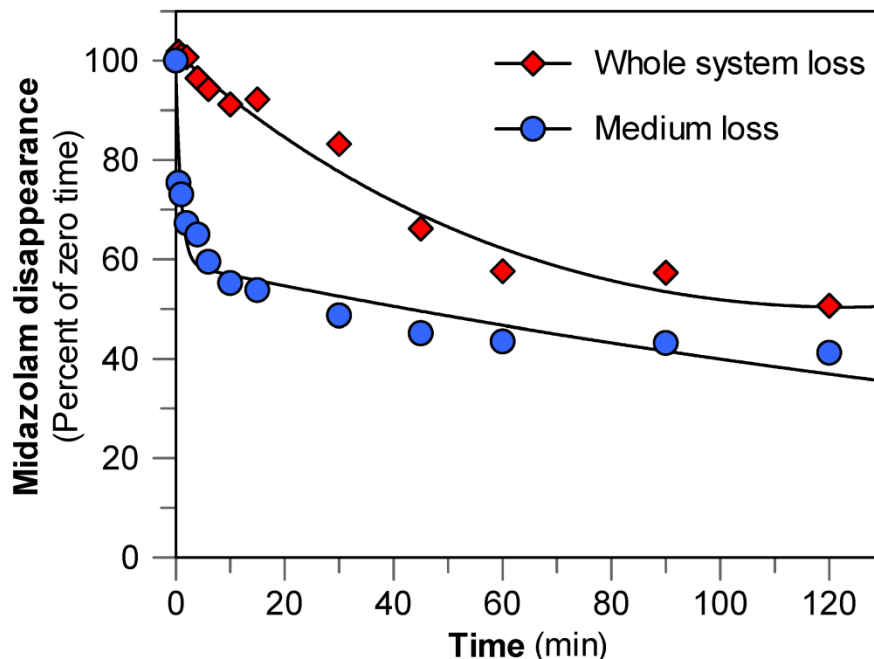


Figure 3.5. The contribution of metabolism and uptake as determined by whole-system loss versus medium loss of midazolam (1 μM) in cryopreserved human hepatocytes (1 million cells/mL)

As described in the *Chapter 2*, midazolam (1 μM) was incubated with pooled CHHs (1 million cells/mL) for zero, 0.5, 1, 2, 4, 6, 10, 15, 30, 45, 60, 90 and 120 min. Whole-system loss of midazolam was assessed by the addition of stop reagent to each incubation sample (cells + medium) whereas medium loss was assessed by transferring an aliquot of cell-free medium to the stop reagent. Disappearance of midazolam was measured by LC-MS/MS, as described in *Chapter 2*.

3.5. Clearance of four CYP3A4/5 substrates in HLM and CHH.

The in vitro clearance of midazolam, alfentanil, nifedipine and verapamil was evaluated in HLM and CHH at physiologically equivalent concentrations of 0.33 mg protein/mL and 1 million cells/mL, respectively. The final concentration of each substrate was 1 μ M. The half-life of each drug was based on the rate of substrate loss (the initial loss conforming to first-order elimination), which was measured at multiple time points for up to 120 min with HLM and up to 240 min with CHH (see Figure 3.6). In vitro intrinsic metabolic clearance (CL_{int}) and scaled in vivo intrinsic hepatic clearance ($CL_{H,int}$) were estimated from in vitro half-life, as described in *Chapter 2*.

As shown in Table 3.4, the in vivo hepatic intrinsic metabolic clearance ($CL_{H,int}$) of alfentanil, nifedipine and verapamil estimated with HLM were 2.6- to 3.7-fold greater than those estimated with CHH. In contrast, midazolam $CL_{H,int}$ estimated with HLM was \sim 9 times greater than that estimated with CHH. These results suggest that the system-dependent clearance of midazolam is more pronounced than that of other CYP3A4/5 substrates.

It is particularly noteworthy that, in the case of alfentanil, nifedipine and verapamil, rates of in vivo clearance predicted with HLM closely predicted their observed rates of blood clearance, but was underestimated by CHH by \sim 2-fold (Table 3.5). Likewise, blood clearance of midazolam was also accurately predicted based on in vitro experiments with HLM but was underestimated with CHH approximately 5-fold. These results establish that the system-dependent clearance of midazolam is not because HLM metabolize

midazolam at an unusually high rate but because CHH metabolize midazolam at an unusually low rate.

Table 3.3. Characteristics of the four CYP3A4/5 substrates used in measurements of intrinsic metabolic clearance in human liver microsomes and cryopreserved human hepatocytes

Characteristic	Midazolam	Alfentanil	Nifedipine	Verapamil
MW	326	417	346	455
LogP ¹	3.93	2.81	2.97	5.04
Total polar surface area (TPSA) (Å ²) ²	25	81	110	64
Basic pKa ²	–	7.5	–	9.0
Major species at pH 7.4	Neutral	Cation	Neutral	Cation
P_{app} (A to B) in MDCK cells (nm/s) ³	369	376	389	318
P_{app} (A to B) in Caco-2 cells (nm/s) ³	324	293	235	138
Efflux ratio in MDCK or Caco-2 ³	<2	<2	<2	<2
Contribution of CYP3A enzymes to clearance in HLM ⁴	CYP3A	92	ND	95
	CYP3A4	43		81
	CYP3A5	49		41
Plasma clearance (IV dosing) (L/h) ^{2,3}	22.3 – 25.9	16.4 – 17.6	30.7 – 31.7	49.1 – 75.6
R_b (blood-to-plasma ratio) ³	0.55	0.63	0.67	0.89
Plasma protein binding (f_{uP}) ³	0.031	0.086	0.044	0.093
Blood binding (f_{uB}) ⁵	0.0564	0.1365	0.0657	0.1045
Blood clearance (L/h) ⁶	40.5 – 47.0	26.0 – 27.9	45.8 – 47.3	55.2 – 84.9
Extraction ratio ⁷	0.45 - 0.52	0.29 - 0.31	0.51 - 0.53	0.61 - 0.94
Extraction classification (Low \leq 0.3, high \geq 0.7)	Intermediate	Low	Intermediate	High

¹ LogP values for midazolam and nifedipine are from Obach et al. (2008). LogP value for alfentanil and verapamil were estimated with commercial software available at: <http://www.chemaxon.com>

² Values are from Obach et al.(2008)

³ Values are from Gertz et al. (2010)

⁴ Estimates of the contribution of CYP3A enzymes to drug clearance in HLM are from Table 1 in Tseng et al. (2014) and are based on studies of in vitro half-life with HLM (from CYP3A4 and CYP3A5 extensive metabolizers) in the presence of ketoconazole (an inhibitor of both CYP3A4 and CYP3A5) or CYP3cide (a selective CYP3A4 inhibitor). ND: Not determined.

⁵ Fraction of unbound drug in blood (f_{uB}) = f_{uP}/R_b .

⁶ Blood clearance = plasma clearance/ R_b .

⁷ Extraction ratio = blood clearance/hepatic blood flow (Q_H), where Q_H = 90 L/h.

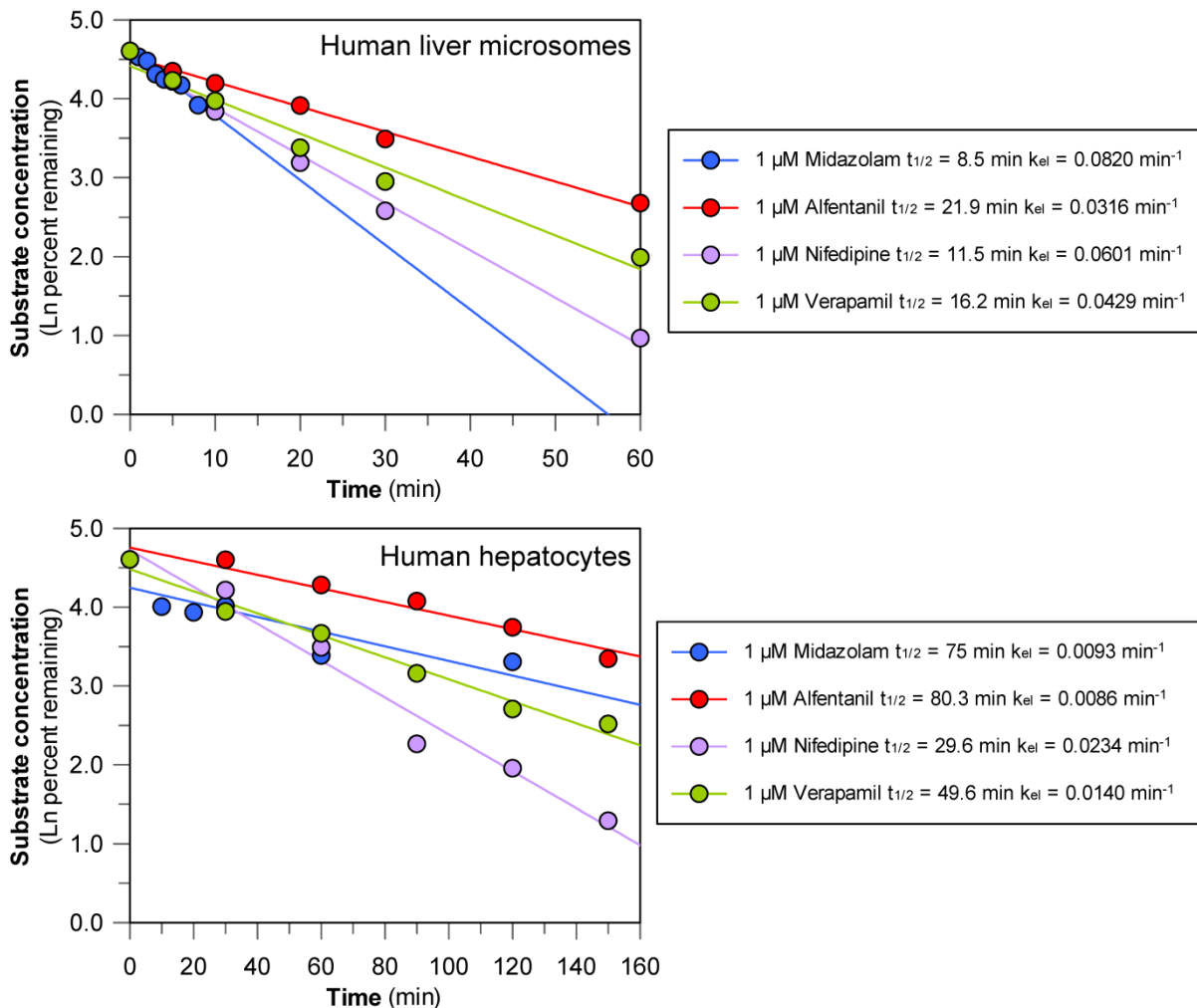


Figure 3.6. The in vitro clearance of the CYP3A4/5 substrates midazolam, alfentanil, nifedipine and verapamil at 1 μM in human liver microsomes (top) and cryopreserved human hepatocytes (bottom)

Pooled cryopreserved human hepatocytes (CHH, 1 million cells/mL) or pooled human liver microsomes (HLM, 0.33 mg/mL) were incubated with midazolam (colored blue), alfentanil (colored red), nifedipine (colored purple) or verapamil (colored green) at 1 μM for up to 120 min (HLM) or 240 min (CHH). Disappearance of substrate was measured by LC-MS/MS. In vitro half-life and the first-order elimination rate constant (k_{el}) were calculated as described in *Chapter 2*.

Table 3.4. Estimates of intrinsic clearance of four CYP3A4/5 substrates by human liver microsomes (HLM) and cryopreserved human hepatocytes (CHH) based on in vitro half-life.

Drug	Half-life (min)	CL _{int} (μL/min/mg protein or million cells)	CL _{H,int} (L/h)	CL _{H,int} corrected for fu _{inc} (L/h)	Predicted hepatic clearance (CL _H) ¹ (L/h)	Hepatic intrinsic clearance (CL _{H,int}) ratio
HLM (0.33 mg/mL in 50 mM phosphate buffer)						HLM/CHH
Midazolam	8.5	247	978	1553	44.4	8.9
Alfentanil	21.9	96	380	432	35.6	3.7
Nifedipine	11.5	183	723	851	34.5	2.6
Verapamil	16.2	130	513	2445	66.6	3.1
CHH (1 million cells/mL in KHB medium)						CHH/HLM
Midazolam	75	9.2	110	174	8.9	0.11
Alfentanil	80.3	8.6	103	117	13.5	0.27
Nifedipine	29.6	23.4	278	327	17.3	0.38
Verapamil	49.6	14.0	166	791	43.1	0.32

Microsomal CL_{H,int} based on in vitro half-life (substrate disappearance) was calculated as follows: $k_{el} \times \text{volume of incubation/mg protein per incubation} \times 66,000 \text{ PBSF}$. Units were converted to L/h.

Hepatocyte CL_{H,int} based on in vitro half-life (substrate disappearance) was calculated as follows: $k_{el} \times \text{volume of incubation/million cells per incubation} \times 198,000 \text{ PBSF}$. Units were converted to L/h.

fu_{inc} was calculated according to Hallifax and Houston, (2006) as shown in Table 1.2 based on values from Table 3.3

¹ Predicted hepatic clearance (CL_H) is CL_{H,int} corrected for both fu_{inc} and fu_B. based on Equation 1.8 and Equation 1.26.

In vivo and physicochemical parameters of all drugs are from Table 3.3.

Table 3.5. Observed blood clearance of four CYP3A4/5 substrates following intravenous administration and blood clearance predicted from in vitro half-lived in human liver microsomes (HLM) and cryopreserved human hepatocytes (CHH)

Drug	Blood clearance (observed) (L/h)	Blood clearance (CL_H predicted with HLM) (L/h)	Blood clearance (CL_H predicted with CHH) (L/h)
Midazolam	40.5 – 47.0	44.4	8.9
Alfentanil	26.0 – 27.9	35.6	13.5
Nifedipine	45.8 – 47.3	34.5	17.5
Verapamil	55.2 – 84.9	66.6	43.1

Predicted CL_H values were calculated based on Equation 1.14 and Equation 1.26 respectively.

Observed blood clearance values of all drugs are from Table 3.3.

3.6. Assessment of midazolam N-glucuronide as an inhibitor of CYP3A4/5 activity

One notable difference between CHH and HLM is that hepatocytes convert midazolam to an N-glucuronide whereas microsomes supplement with only NADPH do not. To examine the possibility that midazolam N-glucuronide inhibits the CYP3A4/5-dependent metabolism of midazolam, midazolam N-glucuronide (0.1–200 μM) was incubated with HLM (≤ 0.1 mg/mL) with and without a 30-min preincubation step in the presence of NADPH. CYP3A4/5 activity was measured based on the rate of midazolam 1'-hydroxylation, midazolam 4-hydroxylation and nifedipine oxidation (with each substrate at a final concentration roughly equal to K_m), as described in *Chapter 2*. As shown in Figure 3.7, midazolam N-glucuronide did not inhibit midazolam nor nifedipine metabolism. Preincubating midazolam N-glucuronide for 30 min with HLM in the presence of NADPH appeared to increase the rate of midazolam 1'- and 4-hydroxylation but this probably an experimental artifact caused by an increase in midazolam concentration due to hydrolysis of midazolam N-glucuronide. These results suggest that midazolam N-glucuronide does not inhibit CYP3A4/5 activity; hence, formation of midazolam N-glucuronide is unlikely to account for the low rate of clearance of midazolam in CHH.

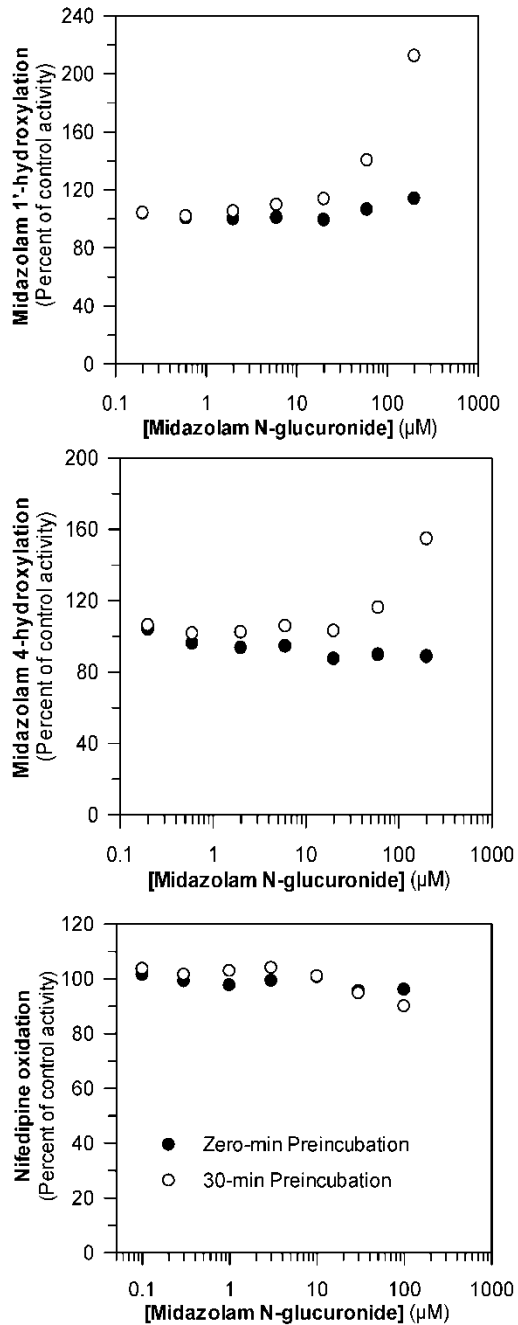


Figure 3.7. Evaluation of midazolam N-glucuronide as an inhibitor of CYP3A4/5 activity toward midazolam 1'-hydroxylation (top), midazolam 4-hydroxylation (middle) and nifedipine oxidation (bottom) in human liver microsomes (HLM)

As described in *Chapter 2* the inhibition of CYP3A4/5 as measured by midazolam 1'-hydroxylation (top), midazolam 4-hydroxylation (middle) and nifedipine oxidation (bottom) was performed with 0.1-200 µM midazolam N-glucuronide in HLM (≤ 0.1 mg/mL).

Midazolam N-glucuronide was preincubated with HLM for 0 and 30 min, after which CYP3A4/5 activity was measured with 5-min incubation with midazolam (4 μ M) or nifedipine (10 μ M).

DISCUSSION

In the pharmaceutical industry HLM and CHH are commonly used to measure the *in vitro* metabolic intrinsic clearance (CL_{int}) of new drug candidates in order to identify candidates with favorable pharmacokinetic properties such as once-a-day dosing and low oral dose. Physiologically based scaling factors (PBSF) can be used to extrapolate *in vitro* values of CL_{int} to *in vivo* estimates of intrinsic hepatic metabolic clearance ($CL_{H,int}$). However, based on a review of several databases, Chiba *et al.* (2009) reported that, on average, HLM underpredict *in vivo* clearance by a factor of 9 and CHHs underpredict by a factor of 3 to 6. The greater underprediction of *in vivo* clearance by HLM can be attributed, at least in part, to the fact that, in contrast to hepatocytes, microsomes support a limited range of metabolic pathways either because a particular drug-metabolizing enzyme is expressed in another subcellular fraction (e.g., cytosolic sulfotransferases) or because the microsomes are supplemented with NADPH (to support CYP and FMO enzymes) but not, for example, with UDP-glucuronic acid (to support glucuronidation). However, for high intrinsic clearance drugs that are predominantly metabolized by cytochrome P450, hepatocytes underpredict *in vivo* clearance to a greater extent than microsomes (Lu *et al.*, 2006; Hallifax *et al.*, 2010).

Several studies have compared predictions of hepatic clearance *in vivo* from *in vitro* studies with HLM and CHH (Hallifax *et al.*, 2005; Riley *et al.*, 2005; Lu *et al.*, 2006; Brown *et al.*, 2007b; Hallifax *et al.*, 2010; Foster *et al.*, 2011). For drugs whose clearance is determined by CYP-dependent metabolism, these two *in vitro* systems would be expected to provide similar estimates of *in vivo* metabolic clearance even if that estimate were an

under- or over-prediction. The agreement between microsomes and hepatocytes is quite good except for drugs with high intrinsic metabolic clearance, in which case hepatocytes underpredict in vivo clearance to a greater extent than microsomes (Foster et al., 2011). In the case of midazolam, a comparison of metabolic clearance by microsomes and hepatocytes prepared from the same livers revealed that microsomes support higher rates of clearance than hepatocytes by a factor of 5.6 to 41 fold (Foster et al., 2011). In the present study, I sought to determine the underlying reason why high clearance drugs like midazolam are metabolized relatively slowly in hepatocytes compared with microsomes. I initially tested two previously proposed explanations, namely that membrane permeability (Lu et al., 2006) or cofactor availability (Foster et al., 2011) restricts the metabolic clearance of midazolam in hepatocytes.

The results summarized in Table 3.1 confirmed previous reports of system-dependent clearance of midazolam, a high clearance drug, but not dextromethorphan, a low clearance drug. In microsomal incubations at 0.33 mg/mL or hepatocyte incubations at 1 million cells/mL, which contain equivalent amounts of microsomal protein, the half-life of dextromethorphan in CHH was comparable (within a factor of 2) to that in HLM. In contrast, the half-life of midazolam in CHHs was approximately one-tenth that in HLM. Values of in vitro CL_{int} were extrapolated to in vivo values of $CL_{H,int}$ based on PBSFs of 66,000 mg microsomal protein/liver for HLM and 198,000 million cells/liver for CHH. These values are based on the amount of microsomal protein per gram of liver (MPPGL; 40 mg/g liver) and liver hepatocellularity (120 million cells/g liver) and an average human liver weight of 1,650 g, as described previously (Hakooz et al., 2006; Sohlenius-

Sternbeck, 2006; Barter et al., 2007). The threefold difference in PBSF is the basis for equating HLM at 0.33 mg protein/mL with CHH at 1 million cells/mL.

Between test systems, dextromethorphan CL_{int} was similar in hepatocytes (at 1 μ M and C_{max}) and microsomes, which is consistent with previous findings (Brown et al., 2007b) whereas midazolam CL_{int} in HLMs was approximately an order of magnitude greater than in CHH, as previously reported (Lu et al., 2006; Foster et al., 2011). To exclude the possibility that the pooled CHH used in these experiments had abnormally low CYP3A4/5 activity, microsomes were prepared from the CHH and shown to have CYP3A4/5 activity comparable to that in pooled HLM prepared directly from human liver, as shown in Table 3.2.

Previous reports have proposed that the difference in microsomal and hepatocyte clearance of midazolam may be explained by limitations on midazolam clearance imposed by membrane permeability or cofactor availability in hepatocytes (Lu et al., 2006; Foster et al., 2011). To investigate these possibilities, the metabolic clearance of midazolam was measured in CHH that were permeabilized by sonication or saponin treatment with and without supplementation with NADPH. If membrane permeability were rate limiting, sonication or saponin treatment would be expected to increase the rate of midazolam metabolism, but no such increase was observed, as shown in Figure 3.4. Furthermore, permeabilization plus NADPH supplementation did not increase the rate of midazolam metabolism. These results suggest that neither membrane permeability nor cofactor availability accounts for the relatively low rate of midazolam metabolism by CHH.

The inability of additional exogenous NADPH to influence the metabolism of midazolam is consistent with the abundance of NADPH cofactor in hepatocytes, which has been suggested to reach cytosolic concentrations of at least 100 μM based on data from rat livers (Lowry et al., 1961; Veech et al., 1969; Reiss et al., 1984). The K_m value for NADPH with P450 oxidoreductase (NADPH-cytochrome c reductase) is approximately 5 μM (Sem and Kasper, 1993), suggesting that even at 50 μM NADPH (10x K_m) all of P450-oxidoreductase present in the hepatocyte would support near maximal rates of P450 metabolism. This value (50 μM NADPH) is half the lowest estimate of hepatic NADPH levels (and one-tenth the highest estimate) (Lowry et al., 1961; Veech et al., 1969; Reiss et al., 1984). Therefore, unless NADPH production is severely compromised in isolated hepatocytes, they should contain sufficient NADPH to support near maximal rates of P450 metabolism. The possibility that membrane permeability restricts midazolam clearance in CHH was also investigated in a whole-system loss versus medium loss experiment with CHH. As shown in Figure 3.5, the rate of loss of midazolam from the cell culture medium (due to a combination of uptake and metabolism) greatly exceeded the rate of whole-system loss (due to metabolism alone), suggesting that membrane permeability does not restrict the metabolic clearance of midazolam by CHHs. These results are consistent with observations by Foster and colleagues (2011) that membrane permeability did not account for the relatively low rate of midazolam clearance in CHH because no difference between HLM and CHH in the K_m for midazolam clearance or metabolite formation was seen. However, membrane permeability may play a role in the restricted clearance between in vitro test systems of some other high CL_{int} CYP3A4/5 substrates. For example, simvastatin, saquinivir and tacrolimus have been shown to have much higher CL_{int} values

in HLM than midazolam (2.5- to 22-fold higher) (Tseng et al., 2014), but have lower passive permeability based on their calculated topological polar surface area values (TPSA = 70-178 Å² versus 30 Å² for midazolam). Polar surface area has been previously shown to be a good measure of the passive permeability of a compound, with high rates of passive diffusion shown to occur at low TPSA (<60 Å²) and low rates of passive diffusion shown to occur at TPSA values above 75 Å² (Palm et al., 1997; Smith and Dalvie, 2012). Based on these parameters, the rate of clearance of simvastatin, saquinivir and tacrolimus would be expected to be limited by membrane permeability in CHH, a factor that is not predicted or experimentally evident with midazolam.

In contrast to the situation with midazolam, the clearance of alfentanil, nifedipine and verapamil by HLM was up to 3.7-fold greater than that by CHH. In the case of the CYP3A4/5 substrates, rates of in vivo clearance predicted with HLM accurately predicted their observed rates of blood clearance; however, CHH underestimated in vivo clearance by ~2-fold (Table 3.5). Likewise, blood clearance of midazolam was accurately predicted based on in vitro experiments with HLM but was underestimated with CHH (approximately 5-fold). These results establish that the system-dependent clearance of midazolam is not because HLM metabolize midazolam at an unusually high rate but because CHH metabolize midazolam at an unusually low rate. There is nothing obvious that distinguishes alfentanil, nifedipine and verapamil from midazolam, as summarized in Table 3.3. All four drugs have a relatively high logP and low TPSA, such that they are predicted to cross biological membranes with a high rate of passive diffusion, which is supported by their high rates of permeation across monolayers of MDCK and Caco-2 cells

(Table 3.3). In HLM from CYP3A4 and CYP3A5 extensive metabolizers (i.e., liver microsomes prepared from donors with a *1/*1 genotype for both enzymes), CYP3A5 contributes significantly to the metabolism of midazolam, but the same is true of verapamil and, to a lesser extent, nifedipine (Tseng et al. (2014) and Table 3.3).

In hepatocytes, midazolam is also converted to an N-glucuronide (Hyland et al., 2009), which raises the possibility that the system-dependent clearance of midazolam involves inhibition of midazolam hydroxylation by midazolam N-glucuronide, which would form in CHH but not in HLM (at least not in the absence of UDPGA). The results presented in Figure 3.7 tested this possibility, and no inhibition of midazolam hydroxylation or nifedipine oxidation was observed by midazolam N-glucuronide in HLM, suggesting that formation of midazolam N-glucuronide does account for the relatively low rate of midazolam clearance in hepatocytes. The results presented in Figure 3.4 and Table 3.5 lend further support to this interpretation. When CHH were permeabilized by sonication or saponin treatment, which releases UDPGA and inhibits glucuronidation, there was no increase in midazolam hydroxylation even when the permeabilized hepatocytes were supplemented with NADPH. Furthermore, N-glucuronidation of midazolam occurs in hepatocytes in vitro and in vivo; hence, if midazolam N-glucuronide impeded the clearance of midazolam in CHH in vitro it would be expected to have the same effect in vivo (Table 3.5).

The results of this study raise several questions. When comparing HLM and CHH, system-dependent clearance was observed with midazolam but not dextromethorphan. Is this because midazolam is a high clearance drug whereas dextromethorphan is a low

clearance drug, or is it because midazolam is a CYP3A4/5 substrate whereas dextromethorphan is a CYP2D6 substrate? The clearance of 3 other CYP3A4/5 substrates, namely alfentanil, nifedipine and verapamil, was also found to be test system dependent, with CHH underpredicting in vivo clearance up to 3.7-fold compared to HLM. However the clearance of midazolam was underpredicted by CHH ~9-fold in comparison to HLM. These results suggest some other factor, such as test system incubation conditions, may be involved in the pronounced system-dependent clearance of midazolam. These questions are addressed in Chapter 4.

CHAPTER 4 : TEST SYSTEM-DEPENDENT DRUG CLEARANCE
PART 2: THE EFFECT OF BUFFER IONIC STRENGTH AND VARIOUS
CELL CULTURE MEDIA ON THE IN VITRO METABOLISM OF
CYTOCHROME P450 SUBSTRATES IN HUMAN LIVER MICROSOMES
AND CRYOPRESERVED HUMAN HEPATOCYTES

ABSTRACT

In the previous chapter, I verified previous reports that the intrinsic metabolic clearance of midazolam by cryopreserved human hepatocytes (CHH) is nearly an order of magnitude less than midazolam clearance by human liver microsomes (HLM). This discrepancy could not be explained by membrane permeability- or cofactor-restricted clearance of midazolam in CHH. Three other CYP3A4/5 substrates also exhibited system-dependent clearance but not to the same extent as midazolam. The present study examined in vitro factors that might account for system-dependent clearance of midazolam. Buffer ionic strength and cell culture media were examined for their effects on P450 enzymes in HLM, human S9 fraction (HS9) and CHH, including their effects on multiple CYP3A4/5 substrates. CYP3A4/5 and CYP2E1 activities were found to increase with increasing buffer ionic strength in HLM, whereas other P450 activities peaked at 50 mM phosphate. Midazolam metabolism in HLM and HS9 was markedly reduced in the presence of certain cell culture media, namely, Waymouth's, MCM+ and DMEM, but this effect was not observed with other substrates of CYP3A4/5, nor was it observed to the same extent in CHH. Kinetic analysis of CYP3A4/5 activity in HLM incubated in the complete versions and salt-only versions of cell culture media suggested the presence of inhibitory components especially in MCM+, which increased the K_m for midazolam hydroxylation by 50 fold. None of the cell culture media examined improved the prediction of midazolam clearance in CHH; hence, none solved the problem of system-dependent clearance. Overall, this study was unable to solve or provide a mechanistic basis for the system-dependent clearance of midazolam; however, this study provided further insight

into the effects of in vitro incubation conditions on P450 activity and supported recommendations for improvements in the design of in vitro studies of drug clearance.

INTRODUCTION

Human liver microsomes (HLM) and cryopreserved human hepatocytes (CHH) are the two in vitro test systems most commonly used in the pharmaceutical industry for predicting drug clearance in vivo. Both of these test systems have been shown to underpredict in vivo clearance: microsomes by a factor of 9 and hepatocytes by a factor of 3 to 6 depending on the database (Chiba et al., 2009). Although there is a systematic underprediction with both test systems, it is reasonable to assume that, in the case of drugs whose primary route of clearance involves P450-mediated metabolism, both microsomes and hepatocytes should provide similar predictions of in vivo clearance. This is the case for most drugs, with the notable exception of certain high intrinsic clearance (CL_{int}) drugs like midazolam, where hepatocytes underpredict in vivo clearance to a greater extent than liver microsomes (Hallifax et al., 2005; Lu et al., 2006; Foster et al., 2011). In Chapter 3, I examined the clearance of midazolam, a high intrinsic clearance drug metabolized predominantly by CYP3A4 and CYP3A5 (Tseng et al., 2014), in HLM at 0.33 mg protein/mL and CHH at 1 million cells/mL, which are physiologically equivalent concentrations based on the content of microsomes in human liver (40 mg microsomal protein/g liver) and the cellularity of human liver (120 million cells/g liver) (Hakooz et al., 2006; Sohlenius-Sternbeck, 2006; Barter et al., 2007). When corrected for the unbound fraction of drug in the test system ($f_{u,inc}$) and extrapolated to in vivo clearance based on physiologically based scaling factors (PBSF), intrinsic hepatic metabolic clearance in vivo ($CL_{H,int}$) was estimated to be 978 L/h based on the half-life of midazolam in HLM and only 110 L/h based on the half-life of midazolam in CHH (both determined at 1 μ M midazolam). The values of $CL_{H,int}$, which differ by 8.9 fold, assume that hepatic clearance in vivo is

not restricted by hepatic blood flow or binding to plasma protein. When hepatic blood flow ($Q_H = 90$ L/h) and binding of midazolam to blood ($f_{u,B} = 0.0564$) are taken into consideration, HLM and CHH predict *in vivo* rates of hepatic clearance (CL_H) of 44.4 and 8.9 L/h. Blood clearance of intravenously administered midazolam is approximately 44 L/h (40.5 to 47.0 L/h); hence, HLM accurately predicted the actual *in vivo* clearance of midazolam whereas CHH underpredicted *in vivo* clearance by almost a factor of 5.

Midazolam is the most commonly used *in vitro* and *in vivo* probe of CYP3A4/5 activity. Accordingly, it is somewhat surprising that the marked difference in midazolam clearance between HLM and CHH has received relatively little attention, with the notable exception of studies published by Lu et al. (2006) and Foster et al. (2011). Furthermore, based on the large number of drugs whose clearance is determined by CYP3A4 (second to no other CYP enzyme), the system-dependent clearance of midazolam has potential implications for numerous other drugs. It is possible that system-dependent clearance (i.e., lower-than-expected clearance in CHH compared with HLM) is a characteristic of midazolam that is more pronounced than other CYP3A4/5 substrates. It was shown in Chapter 3 that three other CYP3A4/5 substrates, namely alfentanil, nifedipine and verapamil, also exhibited system-dependent intrinsic clearance (up to 3.7-fold) but not to the same extent as midazolam (~9 fold), and once again HLM accurately predicted the hepatic clearance (CL_H) of these three CYP3A4/5 substrates, whereas CHH underpredicted CL_H by approximately a factor of 2. In some respects, this makes the system-dependent clearance of midazolam all the more intriguing because it suggests there may be a particularly pronounced impairment of midazolam clearance by CHH.

In the present study, various in vitro incubation conditions were examined for their effects on CYP activity in HLM and CHH in an attempt to identify the basis for the system-dependent metabolism of midazolam. The effects of buffer ionic strength on the activities of a panel of P450 enzymes, namely CYP1A2, CYP2A6, CYP2B6, CYP2C8, CYP2C9, CYP2C19, CYP2D6, CYP2E1, and CYP3A4/5 (with multiple substrates), were examined in HLM and HS9 (hepatic post-mitochondrial supernatant fraction containing microsomes and cytosol). The effects of five common cell culture media (KHB, Waymouth's, MCM+, DMEM, and Williams' E) on P450 activities in CHH and HLM were also examined. The aim of the media studies in CHH was to identify a cell culture medium that preferentially increases the rate of metabolism of midazolam over that of other CYP3A4/5 substrates. The aim of the media studies in HLM was to investigate the possibility that cell culture media contain a substance that preferentially inhibits the metabolism of midazolam over other CYP3A4/5 substrates.

RESULTS

4.1. Effects of buffer ionic strength and pH on midazolam 1'-hydroxylation by HLM

HLM are typically incubated in phosphate buffer (generally 50 or 100 mM phosphate at pH 7.4) whereas CHH are always incubated in cell culture medium. Having determined that neither membrane permeability nor cofactor availability restricts the metabolic clearance of midazolam in CHH (Chapter 3), experiments were conducted to examine the effect of buffer ionic strength on CYP3A4/5 midazolam activity in HLM. As described in *Chapter 2*, phosphate buffers of varying ionic strength (at pH 7.4) were incubated with NADPH-fortified HLM (0.1 mg/mL) containing 1 μ M midazolam. Formation of 1'-hydroxymidazolam was measured after 5 min. The results are shown in Figure 4.1. Increasing the concentration of phosphate buffer from 10 to 200 mM caused a progressive increase in the rate of midazolam metabolism.

To assess whether the effect of phosphate concentration on CYP3A4/5 activity was due to ionic strength and not phosphate ion itself, HLM (0.1 mg/mL) were incubated in 10 mM phosphate buffer (pH 7.4) containing 50 to 500 mM potassium chloride. As shown in Figure 4.1, CYP3A4/5 activity was stimulated by potassium chloride at concentrations up to 300 mM. Interestingly, 300 mM potassium chloride stimulated midazolam 1'-hydroxylation (261% increase) more than midazolam 4-hydroxylation (167% increase).

To assess the effect of pH on the rate of metabolism of midazolam (1 μ M), HLM were incubated in three concentrations of phosphate buffer (10, 50 and 200 mM) at six pH

values ranging from 6.8 to 8.0. Formation of 1'-hydroxymidazolam was measured after 5 min. The results are shown in Figure 4.1. The highest rate of midazolam metabolism at 10, 50 and 200 mM phosphate was observed at pH 8.0, 7.4 and 7.2, respectively, but the effects of pH were relatively minor.

The results suggest that the common practice of incubating HLM in high ionic strength buffer is partly responsible for the relatively high rate of midazolam metabolism by HLM compared with hepatocytes.

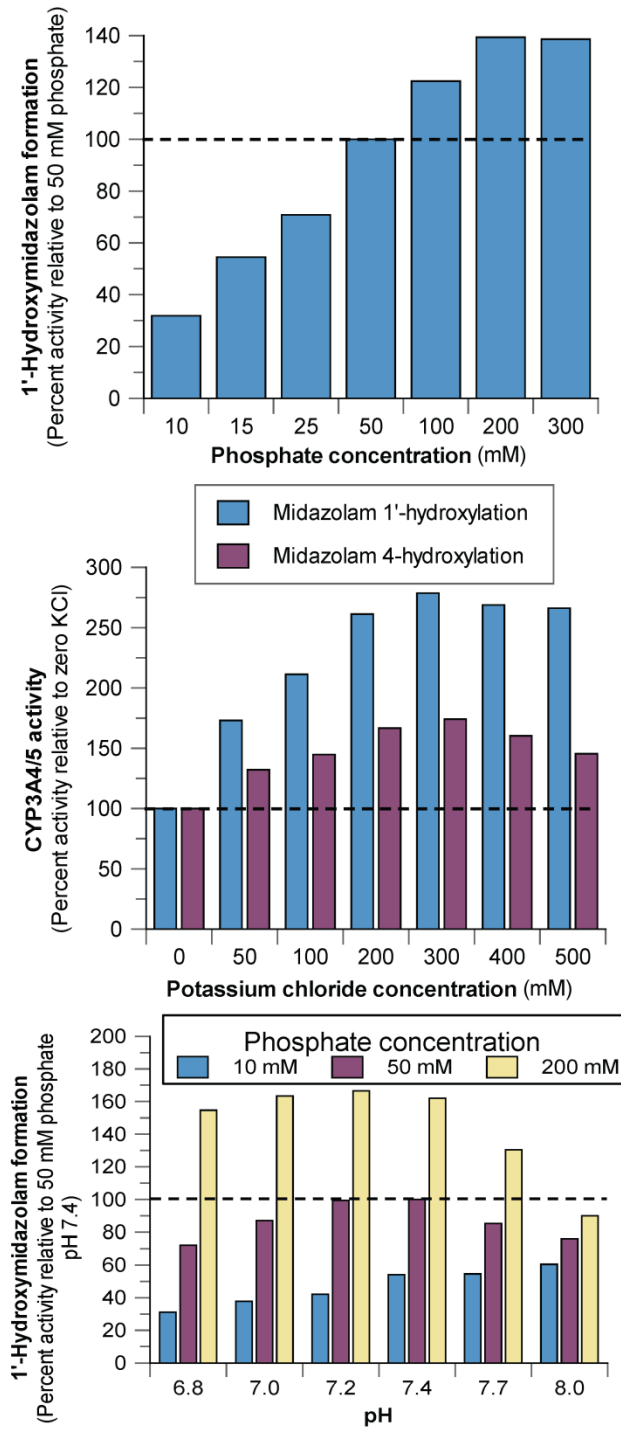


Figure 4.1. The effect of phosphate buffer (top), potassium chloride (middle) and pH (bottom) on midazolam hydroxylation in human liver microsomes (HLM)

The formation of 1'-hydroxymidazolam was assessed in pooled HLM (0.1 mg/mL) incubated in various concentrations of potassium phosphate buffer (10-300 mM phosphate, pH 7.4; top panel). Furthermore, the formation of 1'-hydroxymidazolam and 4-hydroxymidazolam was assessed in HLM (0.1 mg/mL) incubated in various concentrations of potassium chloride (0-500 mM, middle panel) containing 10 mM phosphate. The rate of formation of 1'-hydroxymidazolam was determined in HLM (0.1 mg/mL) incubated in three concentrations of phosphate (10, colored blue; 50, colored purple; and 200 mM, colored yellow) at six pH values (bottom panel). The final concentration of midazolam was 1 μ M and the incubation time was 5 min. Formation of 1'-hydroxymidazolam was measured by LC-MS/MS, as described in *Chapter 2*. The rate of formation of 1'-hydroxymidazolam in 50 mM phosphate buffer at pH 7.4 (standard buffer conditions) was set to 100%.

4.2. Effects of buffer ionic strength and cell culture media on various P450 activities in HLM

HLM (0.1 mg/mL) were incubated in three concentrations of phosphate buffer (5, 50 and 200 mM, all at pH 7.4) or one of five cell culture media, namely KHB, Waymouth's, MCM+, DMEM and Williams' E, designated A-E, respectively. Based on their salt composition, four of these media (KHB, Waymouth's, DMEM and Williams' E) have similar ionic strengths (163-182 mM) whereas MCM+ has a twofold higher ionic strength (361 mM), as shown in Table 4.3 and Table 2.1 in *Chapter 2*. The activities of CYP1A2 (40 μ M phenacetin), CYP2A6 (5 μ M coumarin), CYP2B6 (50 μ M bupropion), CYP2C8 (7 μ M amodiaquine), CYP2C9 (6 μ M diclofenac), CYP2C19 (40 μ M S-mephenytoin), CYP2D6 (7.5 μ M dextromethorphan), CYP2E1 (30 μ M chlorzoxazone) and CYP3A4/5 (4 μ M midazolam) were determined with the P450-selective substrates listed in parentheses, as described in *Chapter 2*. The substrate concentration was equal to K_m except for the high turnover substrates coumarin and amodiaquine, where the concentration of substrate was 5-10 times K_m in order to measure metabolite formation under initial rate conditions.

As shown in Figure 4.2, when HLM were incubated in phosphate buffer and various cell culture media, the CYP enzymes could be divided into three groups (A-C). Group A enzymes included CYP1A2, CYP2A6, CYP2B6, CYP2C8, CYP2C19 and CYP2D6; their activity was highest in 50 mM phosphate buffer and it was higher in Waymouth's, MCM+ and DMEM compared with KHB or Williams' E (i.e., in the order they are shown in Figure 4.2, the media show a bell-shaped curve). Group B enzymes included CYP3A4/5 and CYP2E1; their activity was highest in 200 mM phosphate buffer and it was higher in KHB

and Williams E' compared with Waymouth's, MCM+ and DMEM (i.e., in the order they are shown in Figure 4.2, the media show an inverse bell-shaped curve). CYP2C9 (Group C) had the highest activity in 50 mM phosphate buffer (like the Group A enzymes) but showed slightly lower activity in KHB and Williams' E compared with Waymouth's, MCM+ and DMEM (like the Group B enzymes).

If the various effects of cell culture media on P450 activity were due to differences in ionic strength then MCM+, which has twice the ionic strength of the other four media and exceeds that of 50 mM phosphate, would be expected to support the highest activity of CYP3A4/5 and CYP2E1, the two enzymes whose activity increased when the concentration of phosphate buffer was increased from 50 mM to 200 mM. However, MCM+ supported the lowest (or close to the lowest) activity of CYP3A4/5 and CYP2E1.

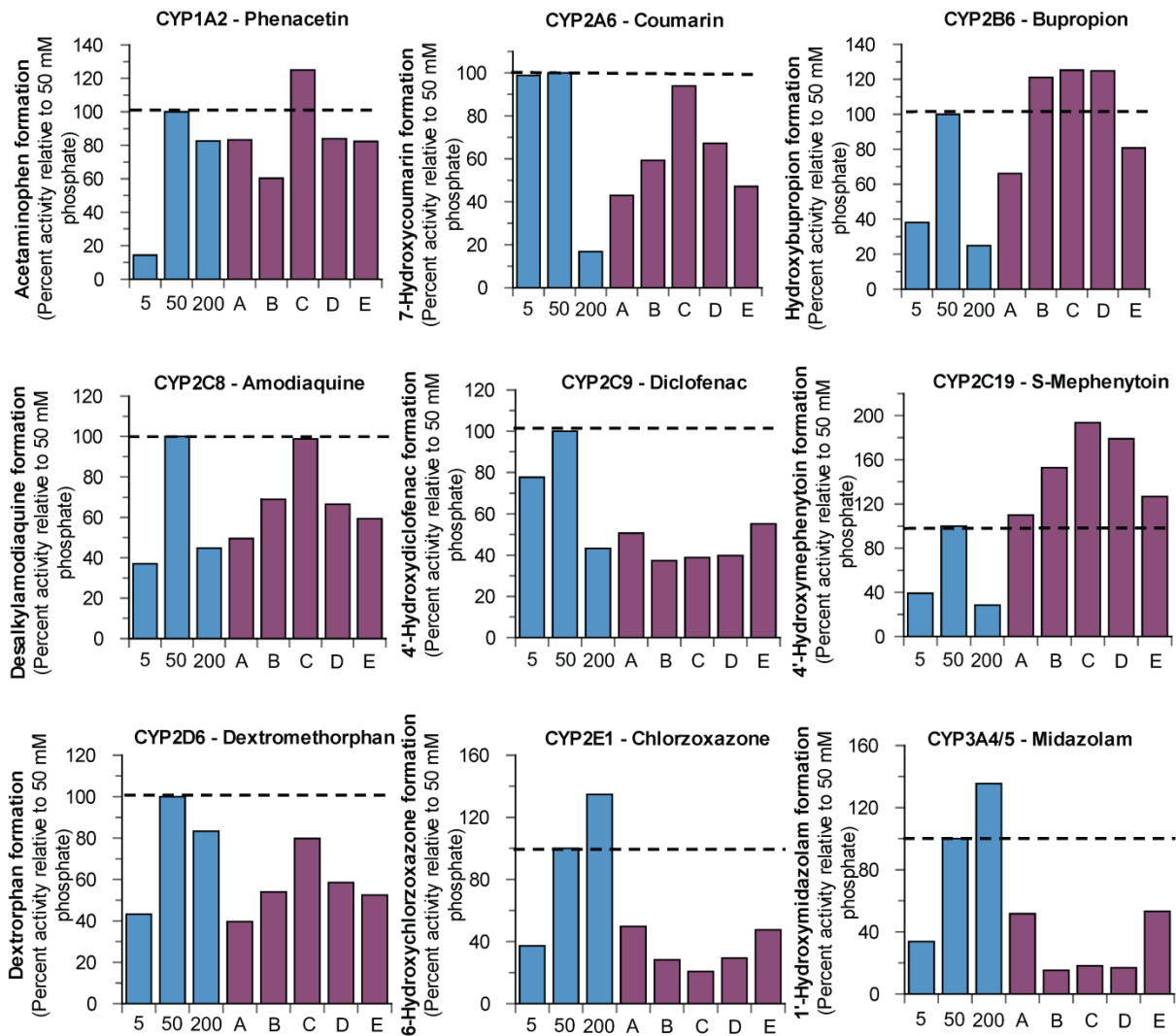


Figure 4.2. The effect of different concentrations of phosphate buffer (5-200 mM, pH 7.4) and five cell culture media on CYP enzyme activity in human liver microsomes.

The activities of nine P450 enzymes were assessed in pooled HLM (0.1 mg/mL) with marker substrates for CYP1A2 (phenacetin, 40 μ M), CYP2A6 (coumarin, 5 μ M), CYP2B6 (bupropion, 50 μ M), CYP2C8 (amodiaquine, 7 μ M), CYP2C9 (diclofenac, 6 μ M), CYP2C19 (S-mephenytoin, 40 μ M), CYP2D6 (dextromethorphan, 7.5 μ M), CYP2E1 (chlorzoxazone, 30 μ M), and CYP3A4/5 (midazolam, 4 μ M); with 5, 50, and 200 mM phosphate buffer, pH 7.4 or with KHB (A), Waymouth's (B), MCM+ (C), DMEM (D), and Williams' E (E) cell culture media. P450 activities are phenacetin O-dealkylation

(CYP1A2), coumarin 7-hydroxylation (CYP2A6), bupropion hydroxylation (CYP2B6), amodiaquine N-dealkylation (CYP2C8), diclofenac 4'-hydroxylation (CYP2C9), S-mephenytoin 4'-hydroxylation (CYP2C19), dextromethorphan O-demethylation (CYP2D6) and midazolam 1'-hydroxylation (CYP3A4), which were measured as described in *Chapter 2*. P450 activity in 50 mM phosphate buffer (standard incubation conditions) was set to 100%.

4.3. Effects of various cell culture media on P450 activities in CHH.

The effects of various cell culture media on P450 activity were assessed in pooled CHH (n = 50) at 1 million cells/mL. Metabolite formation from CYP-selective substrates was measured at 10, 30 and 60 min, as described in *Chapter 2*. The results for the 30-min time point are shown in Figure 4.3. Williams' E supported slightly higher rates of midazolam 1'-hydroxylation than KHB (the medium used to measure midazolam clearance in CHH in Chapter 3). However, the increase was too small to correct the large underprediction of midazolam clearance in CHH. The other media (Waymouth's, MCM+ and DMEM) supported lower rates of midazolam 1'-hydroxylation than KHB, suggesting these media only amplify the system-dependent clearance of midazolam. The effects of media on CYP3A4/5 activity in CHH (which showed an inverse bell-shaped curve based on their order in Figure 4.3) resembled their effects on CYP3A4/5 activity in HLM (Figure 4.2), albeit to a lesser extent.

There were no marked effects of cell culture media on the activity of CYP1A2, CYP2B6, CYP2C8, and CYP2D6 in CHH. In contrast to their activity in HLM, the activity of these enzymes in CHH was not notably higher in Waymouth's, MCM+ and DMEM compared with KHB and Williams' E (i.e., there was no bell-shaped curve). MCM+ did support the highest activity of CYP2C19 in both HLM and CHH, but this was the exception rather than the rule.

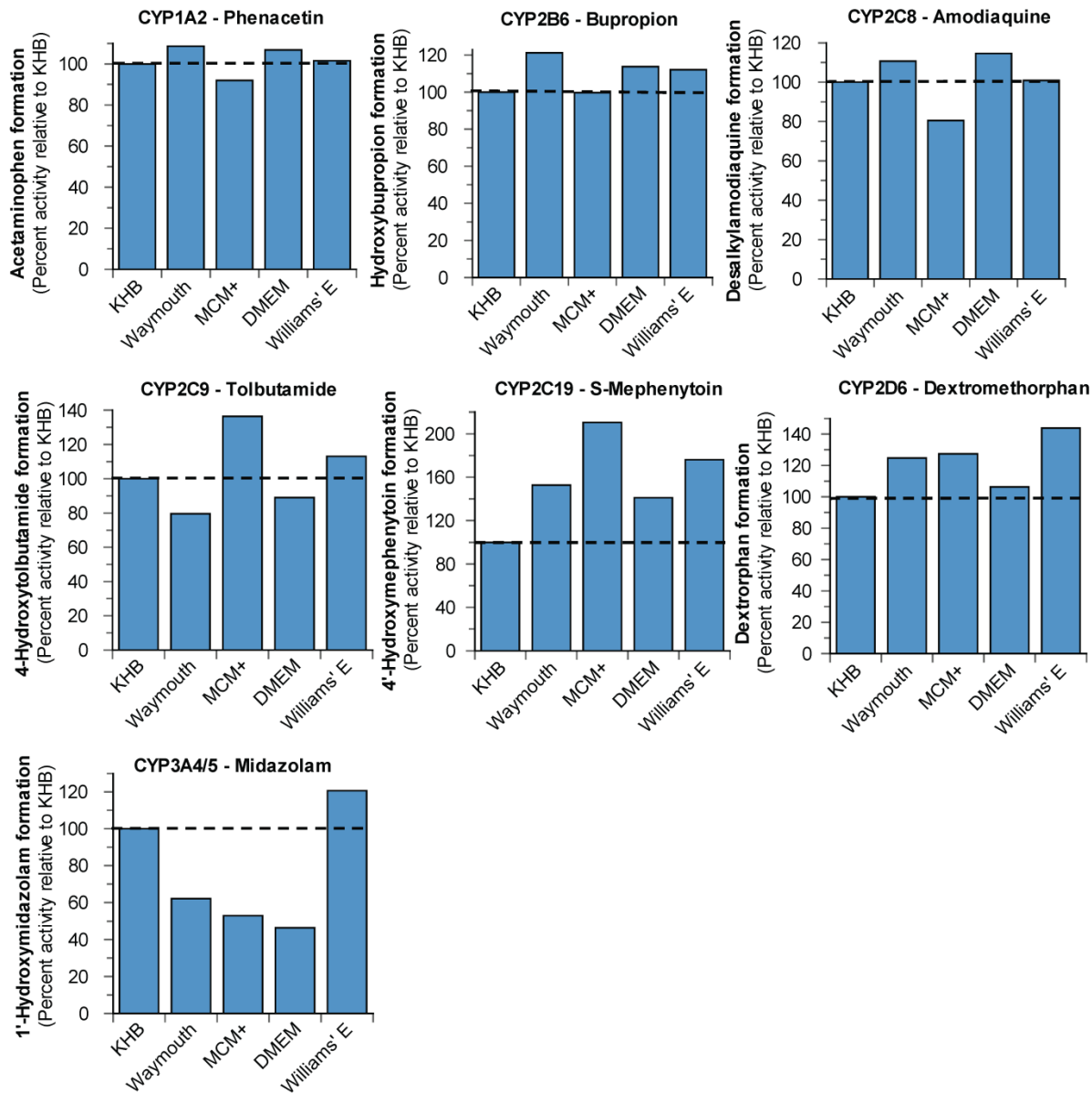


Figure 4.3. The effect of various media on multiple P450 activities in human hepatocytes over time

Seven P450 activities, namely CYP1A2 (phenacetin, 40 μ M), CYP2B6 (bupropion, 50 μ M), CYP2C8 (amodiaquine, 2 μ M), CYP2C9 (tolbutamide, 150 μ M), CYP2C19 (S-mephenytoin, 40 μ M), CYP2D6 (dextromethorphan, 7.5 μ M), and CYP3A4/5 (midazolam, 4 μ M) were assessed with CHH (1 million cells/mL) with five common cell culture media for 30 min as described in *Chapter 2*. The activity in KHB medium was set to 100%.

4.4. Effects of buffer ionic strength and cell culture media on the metabolism of multiple CYP3A4/5 substrates in HLM and HS9

To determine whether the effect of buffer ionic strength and cell culture media on the metabolism of midazolam by HLM occurred with other CYP3A4/5 substrates, HLM (0.1 mg/mL) and HS9 (0.25 mg/mL) were incubated with three concentrations of phosphate buffer (5, 50 and 200 mM) or one of five cell culture media, and one of six CYP3A4/5 substrates, namely midazolam, nifedipine, alfentanil, verapamil, testosterone and atorvastatin. Rates of midazolam 1'- and 4-hydroxylation, nifedipine oxidation, alfentanil N-dealkylation, verapamil N-dealkylation, testosterone 6 β -hydroxylation, and atorvastatin ortho-hydroxylation were measured as described in *Chapter 2*.

As shown in Figure 4.4, the activity of CYP3A4/5 in both HLM and HS9 increased toward all six substrates when the concentration of phosphate buffer was increased up to 200 mM. The degree of activation observed when the concentration of phosphate buffer was increased from 50 mM to 200 mM varied from one substrate to the next (from 37% to 172%), and this effect was observed in both HLM and HS9 (to roughly the same extent). In contrast to midazolam, the five other CYP3A4/5 substrates (nifedipine, alfentanil, verapamil, testosterone and atorvastatin) were all metabolized by HLM and HS9 to a similar extent in all five media (within a factor of ~2 of the rate supported by 50 mM phosphate buffer). Two media, namely KHB and Williams' E (media B and E), also supported the 1'- and 4-hydroxylation of midazolam by HLM and HS9 at rates within a factor of ~2 of that supported by 50 mM phosphate buffer. In contrast, midazolam metabolism was greatly reduced (~90%) when HLM and HS9 were incubated in

Waymouth's, MCM+ and DMEM (media B, C and D) compared with that in 50 mM phosphate buffer. These results suggest that cell culture media affect the metabolism of midazolam by HLM and HS9 differently than the other five CYP3A4/5 substrates examined. This raises the possibility that cell culture media contain one or more substances capable of selectively impairing the metabolism of midazolam.

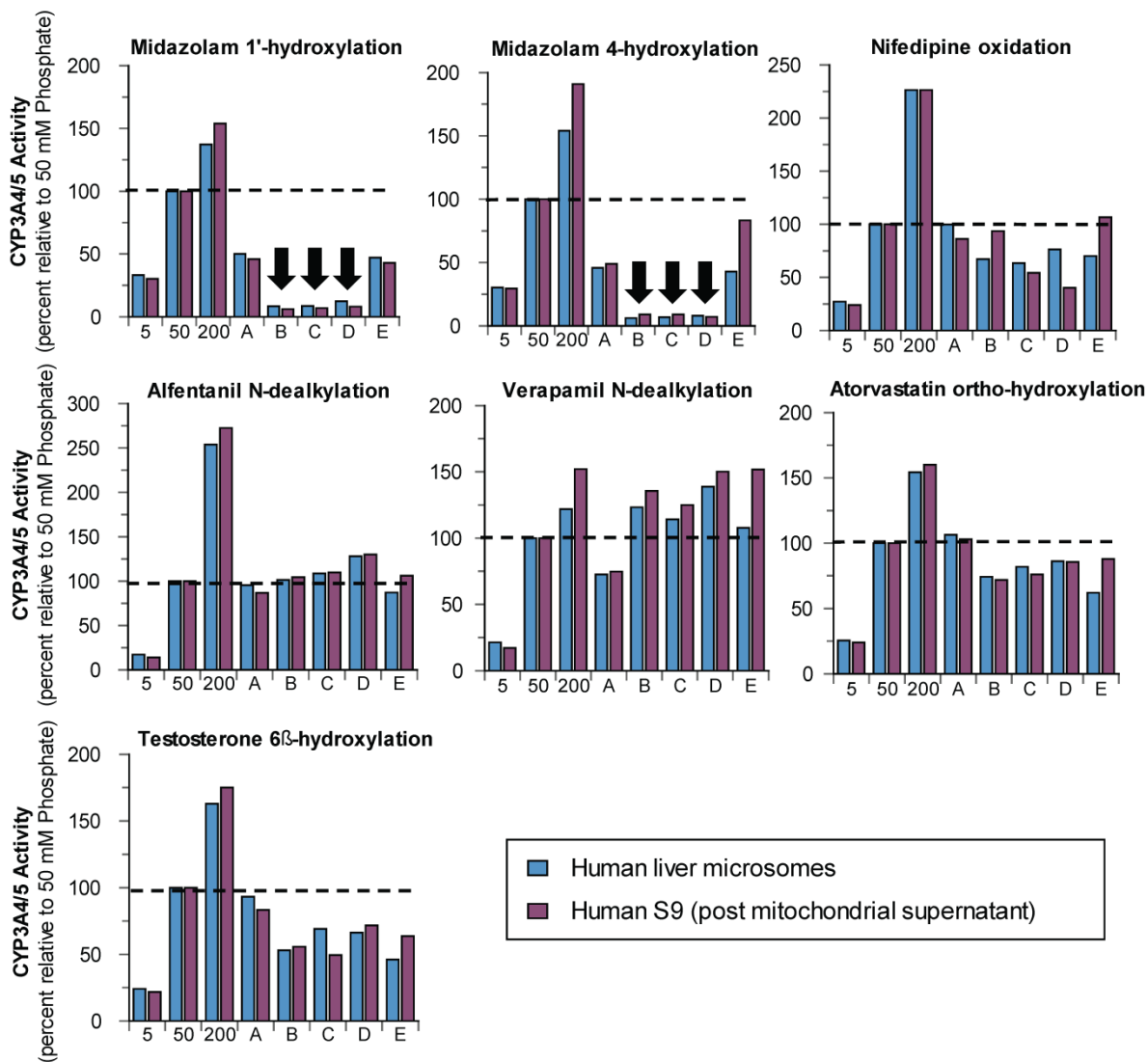


Figure 4.4. The effect of phosphate buffer concentration (5-200 mM, pH 7.4 and cell culture media on the metabolism of six CYP3A4/5 substrates by human liver microsomes (top) and human S9 fraction (bottom).

Six CYP3A4/5 marker substrates, namely, midazolam (4 μ M), nifedipine (10 μ M), alfentanil (40 μ M), verapamil (9 μ M), testosterone (70 μ M) and atorvastatin (40 μ M) were incubated with pooled human liver microsomes (0.1 mg/mL) or pooled human S9 fraction (0.25 mg/mL) with 5, 50 and 200 mM phosphate buffer (pH 7.4) or one of five cell culture media, namely KHB (A), Waymouth's (B), MCM+ (C), DMEM (D) and Williams' E (E). Rates of midazolam 1'- and 4-hydroxylation, nifedipine oxidation, alfentanil N-

dealkylation, verapamil N-dealkylation, testosterone 6 β -hydroxylation, and atorvastatin ortho-hydroxylation were measured as described in *Chapter 2*. Downward arrows highlight the low rate of midazolam metabolism when HLM or HS9 was incubated in Waymouth's, MCM+ or DMEM (media B, C and D). Rates of metabolism in 50 mM phosphate buffer (standard incubation conditions) were set to 100%.

4.5. Effects of various cell culture media on the metabolism of multiple CYP3A4/5 substrates in CHH.

To determine the effect of various cell culture media on CYP3A4/5 activity towards multiple substrates in hepatocytes, pooled CHH (1 million cells/mL) were incubated in five different media and with six different substrates, namely midazolam, nifedipine, alfentanil, verapamil, testosterone and atorvastatin. Measurements of CYP3A4/5 activity were based on rates of by midazolam 1'-hydroxylation, nifedipine oxidation, alfentanil N-dealkylation, verapamil N-dealkylation, testosterone 6 β -hydroxylation, and atorvastatin ortho-hydroxylation, as described in *Chapter 2*. The results are shown in Figure 4.5. For all six substrates there were negligible differences (<10%) between KHB and Williams' E media. These two media supported the highest rates of metabolism of midazolam and nifedipine. Waymouth's medium supported the highest rate of alfentanil metabolism; DMEM supported the highest rate of verapamil metabolism and MCM+ supported the highest rates of testosterone and atorvastatin. The results suggest that cell culture media can affect CYP3A4/5 activity in CHH in a substrate-dependent manner.

Cell viability was monitored at various times over a 240-min incubation of CHH in each of the five cell culture media, as described in *Chapter 2*. As shown in Table 4.1, KHB supported the highest initial cell viability, but had the lowest overall hepatocyte viability at the end of the 4-h incubation (68%). Williams' E medium supported the highest overall viability (79% at 4 h). These results suggest that differences in cell viability are not a major contributor to medium-dependent differences in CYP3A4/5 activity in CHH.

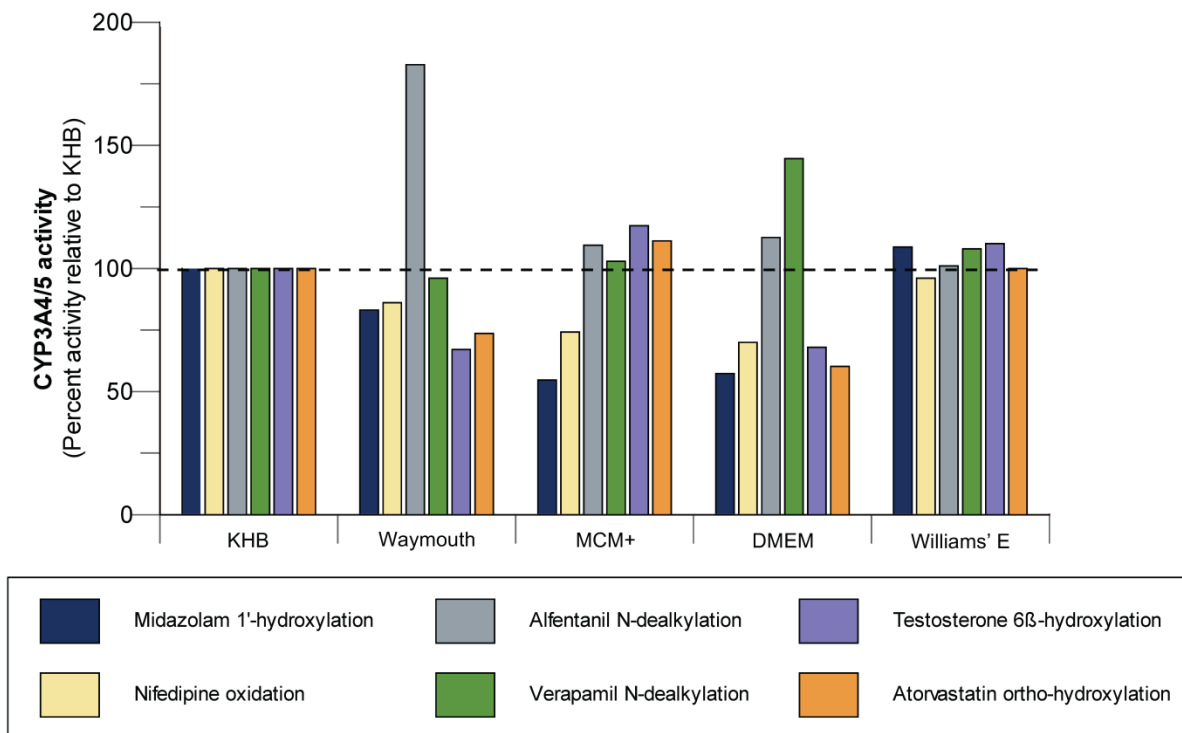


Figure 4.5. The effect of cell culture media on the metabolism of six CYP3A4/5 substrates in cryopreserved human hepatocytes.

The rate of metabolism of six CYP3A4/5 marker substrates, namely, midazolam (4 μM), nifedipine (10 μM), alfentanil (40 μM), verapamil (9 μM), testosterone (70 μM) and atorvastatin (40 μM), was assessed in pooled cryopreserved human hepatocytes (1 million cells/mL) suspended in one of five different cell culture media (KHB, Waymouth's, MCM, DMEM and Williams' E) and incubated for 30 min, as described in *Chapter 2*. Rates of metabolism were based on measurements of midazolam 1'-hydroxylation, nifedipine oxidation, alfentanil N-dealkylation, verapamil N-dealkylation, testosterone 6 β -hydroxylation, and atorvastatin ortho-hydroxylation. Rates of metabolism in KHB medium were set to 100%.

Table 4.1. The effect of various cell culture media on the viability of pooled cryopreserved human hepatocytes (1 million cells/mL) over a 240-min incubation period

Incubation time (min)	Average Viability (%)				
	KHB	Waymouth's	MCM+	DMEM	Williams' E
0	84.1	76.3	77.7	82.5	77.2
30	71.4	83.6	80.8	69.0	88.8
60	65.0	77.1	70.1	74.8	80.0
120	64.5	68.3	68.4	78.3	76.1
240	52.6	Not determined	71.4	62.1	72.7
Overall Average	67.5	76.3	73.7	73.3	79.0

4.6. Effects of cell culture media on the kinetics of midazolam and chlorzoxazone metabolism in HLM

When HLM were used to examine the effects of ionic strength and cell culture media on CYP activity (Section 4.1), the various CYP enzymes examined could be divided into three groups (A-C). The Group B enzymes, namely CYP2E1 and CYP3A4/5, were distinguished by their high activity in 200 mM phosphate buffer and their low activity in Waymouth's, MCM+ and DMEM media (relative to KHB and Williams' E media), as shown in Figure 4.2. Experiments were conducted to determine how cell culture media influence the kinetics of midazolam and chlorzoxazone metabolism by HLM. K_m and V_{max} were determined by incubating HLM (0.1 mg/mL) with 5-30 μ M midazolam or 5-250 μ M chlorzoxazone for 5 min, as described in *Chapter 2*. The kinetic plots are shown in Figure 4.6 and the results are summarized in Table 4.2 and Figure 4.7.

The results in Figure 4.7 show the effects of each cell culture medium on V_{max} , K_m and clearance (determined from V_{max}/K_m) in comparison with values determined when HLM were incubated in 50 mM phosphate buffer (standard incubation conditions). Based on their effects on CYP3A4/5 activity, the cell culture media could be divided in two groups. The first group, namely KHB, Waymouth's, and DMEM, caused a relatively *modest increase* in K_m and a *modest decrease* in V_{max} . The second group, namely MCM+ and Williams' E medium, caused a *marked increase* in K_m and a *modest increase* in V_{max} . Compared with 50 mM phosphate buffer, all cell culture media decreased the intrinsic clearance (CL_{int}) of midazolam. Similar but not identical results were observed with CYP2E1. For example, the same two buffers (MCM+ and Williams' E) that caused the

largest increase in the K_m of CYP3A4/5 also caused the largest increase in K_m of CYP2E1. For both CYP3A4/5 and CYP2E1, the effects of MCM+ and Williams' E on clearance were more pronounced than those of KHB, Waymouth's and DMEM.

The marked increase in K_m for midazolam hydroxylation observed with MCM+ and Williams' E suggest these media contain a substance that competitively inhibits CYP3A4/5 activity in HLM. These two media increased K_m and decreased midazolam clearance (V_{max}/K_m) to a greater extent than KHB, Waymouth's or DMEM; however, these latter three media also decreased midazolam CL_{int} by a factor of 3 to 5. The decreases in midazolam CL_{int} observed with all five media might be a consequence of their relatively low ionic strength (with the exception of MCM+) or it might be due to presence of inhibitory substances. These possibilities were examined by comparing each medium with its salt-only version on CYP3A4/5 activity in HLM, as described in the following section.

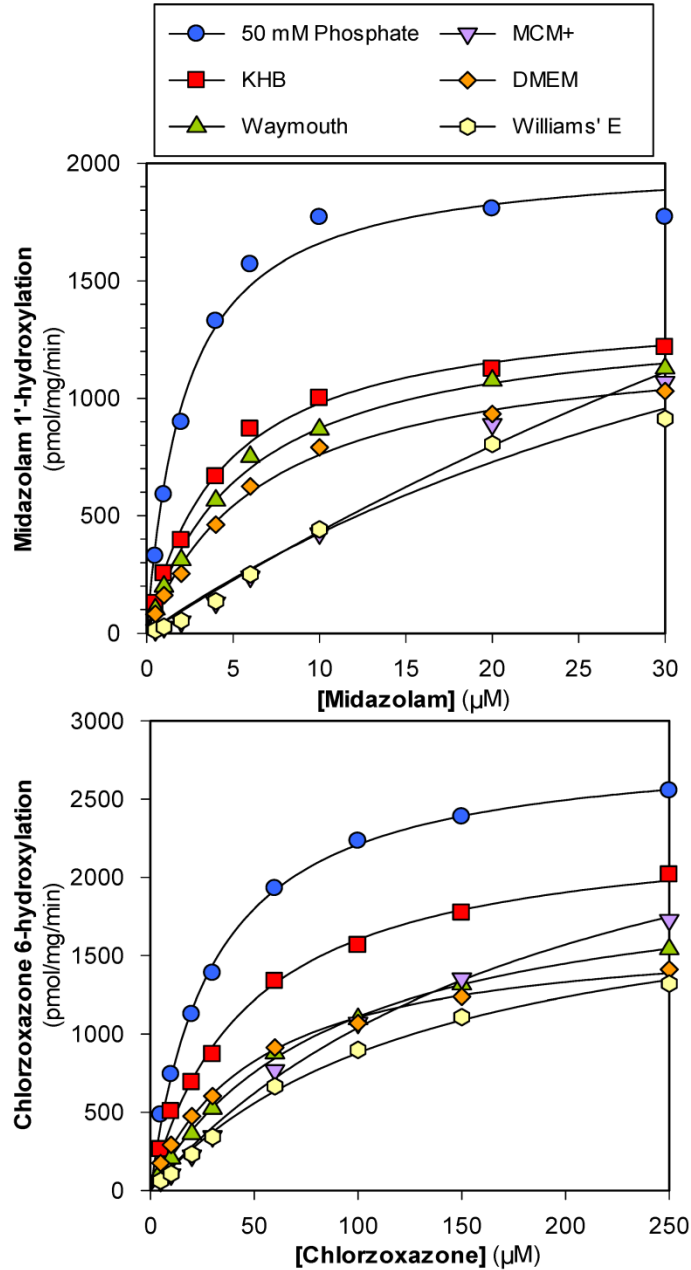


Figure 4.6. Kinetics of midazolam 1'-hydroxylation (CYP3A4/5; top) and chlorzoxazone 6-hydroxylation (CYP2E1; bottom) by pooled human liver microsomes incubated in 50 mM phosphate buffer or various cell culture media

The K_m and V_{max} of 1'-hydroxymidazolam and 6-hydroxychlorzoxazone formation were determined in incubations with pooled HLM (0.1 mg/mL) and eight concentrations of midazolam (0.5-30 µM) or chlorzoxazone (5-250 µM) for 5 min in the presence of KHB,

Waymouth's, MCM+, DMEM, or Williams' E cell culture medium as described in *Chapter 2*.

Table 4.2. Summary of kinetic constants (K_m and V_{max}) and scaled values of hepatic clearance (CL_{int}) based on V_{max}/K_m for midazolam and chlorzoxazone metabolism by human liver microsomes incubated in 50 mM phosphate buffer or various cell culture media

Buffer or Media	Midazolam 1'-hydroxylation			Chlorzoxazone 6-hydroxylation		
	V_{max} (pmol/mg/min)	K_m (μ M)	CL_{int} (L/h)	V_{max} (pmol/mg/min)	K_m (μ M)	CL_{int} (L/h)
50 mM potassium phosphate, pH 7.4	2020	2.2	3640	2860	30	378
KHB	1400	4.4	1260	2350	47	198
Waymouth's	1470	5.7	1020	2090	89	93
MCM+	5240	111	186	3200	208	61
DMEM	1270	6.7	750	1670	51	130
Williams' E	2570	51	199	2080	137	60

Microsomal CL_{int} was calculated as follows: $V_{max}/K_m \times 66,000$ PBSF. Units were converted to L/h

Note: All CL_{int} vales have not been corrected for binding

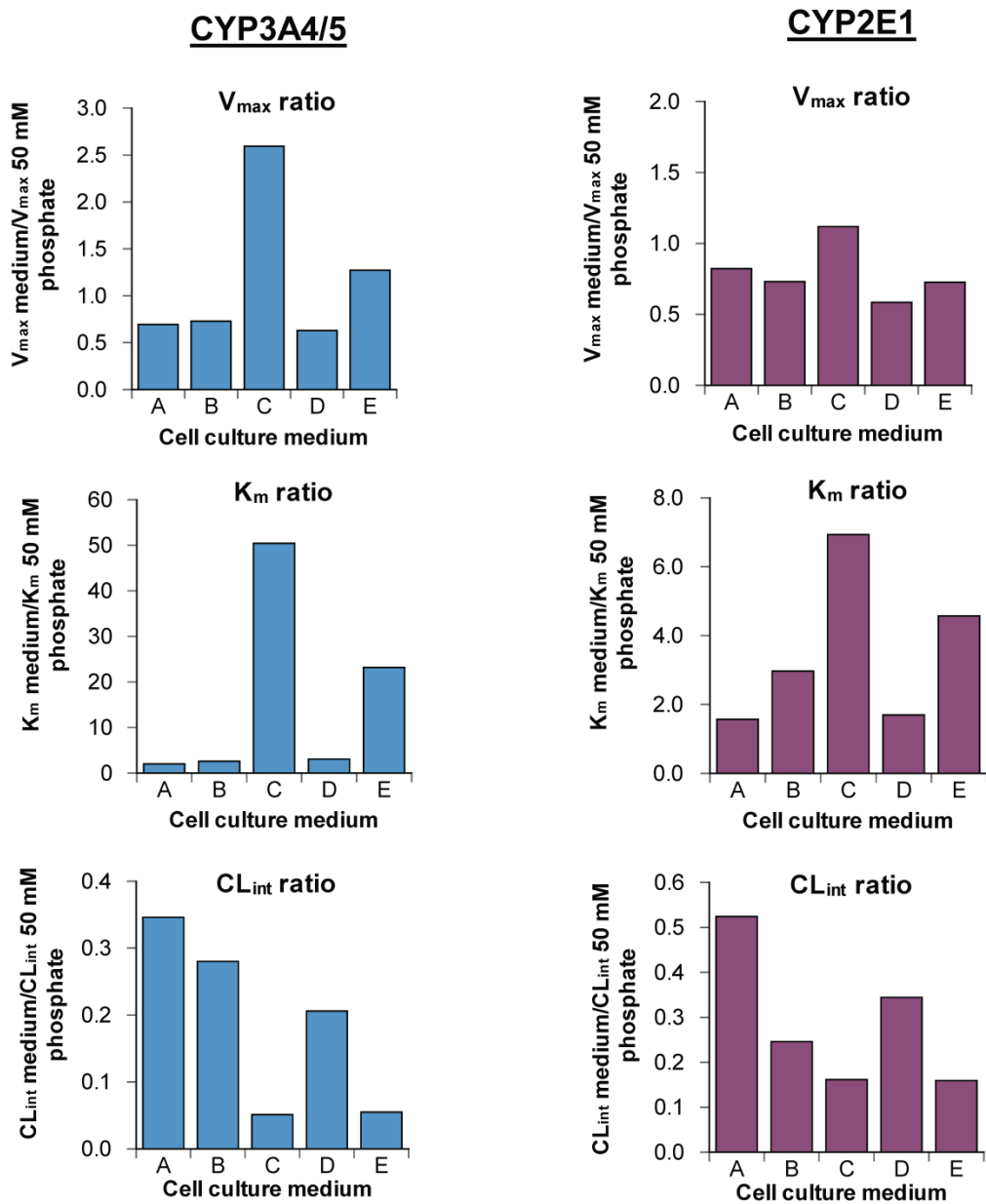


Figure 4.7. Effects of cell culture media on the kinetics of midazolam 1'-hydroxylation and chlorzoxazone hydroxylation in human liver microsomes: Ratio of V_{max}, K_m and CL_{int} (V_{max}/K_m) values in media and those determined in 50 mM phosphate buffer.

Values of V_{max}, K_m and CL_{int} (V_{max}/K_m) are presented in Table 4.2. The cell culture media were KHB (A), Waymouth's (B), MCM+ (C), DMEM (D) and Williams' E (E).

4.7. Evaluating cell culture media for the presence of CYP3A4/5 modulators

To evaluate whether the decrease in midazolam clearance (V_{max}/K_m) observed when HLM were incubated in cell culture media is attributable to an effect of ionic strength or the presence of a CYP3A4/5 inhibitor, each cell culture medium was compared with its 'salt-only' version for its effects on the metabolism of six CYP3A4/5 substrates by HLM. The salt-only version of each medium was a solution containing only the inorganic salts present in each cell culture medium (at matching concentrations), as shown in Table 4.3 and Table 2.1 in Chapter 2.

The differences between a complete medium and its salt-only version were both substrate and medium dependent, as shown in Figure 4.8. In the case of nifedipine, alfentanil and verapamil metabolism, there were only small differences between the complete and salt-only versions of each medium. In the case of midazolam, the relatively low rates of 1'- and 4-hydroxylation in Waymouth's, MCM+ and DMEM all increased when HLM were incubated in the salt-only versions of these media, suggesting that the complete versions of these media contain an inhibitor of midazolam metabolism. Based on this interpretation, the complete version of Williams' E medium may also contain an inhibitor because the rate of midazolam 1'- and 4-hydroxylation was higher in the salt-only version of Williams' E medium. In the case of atorvastatin and testosterone, the salt-free versions of MCM+ and/or DMEM supported *lower* rates of metabolism than the corresponding complete versions.

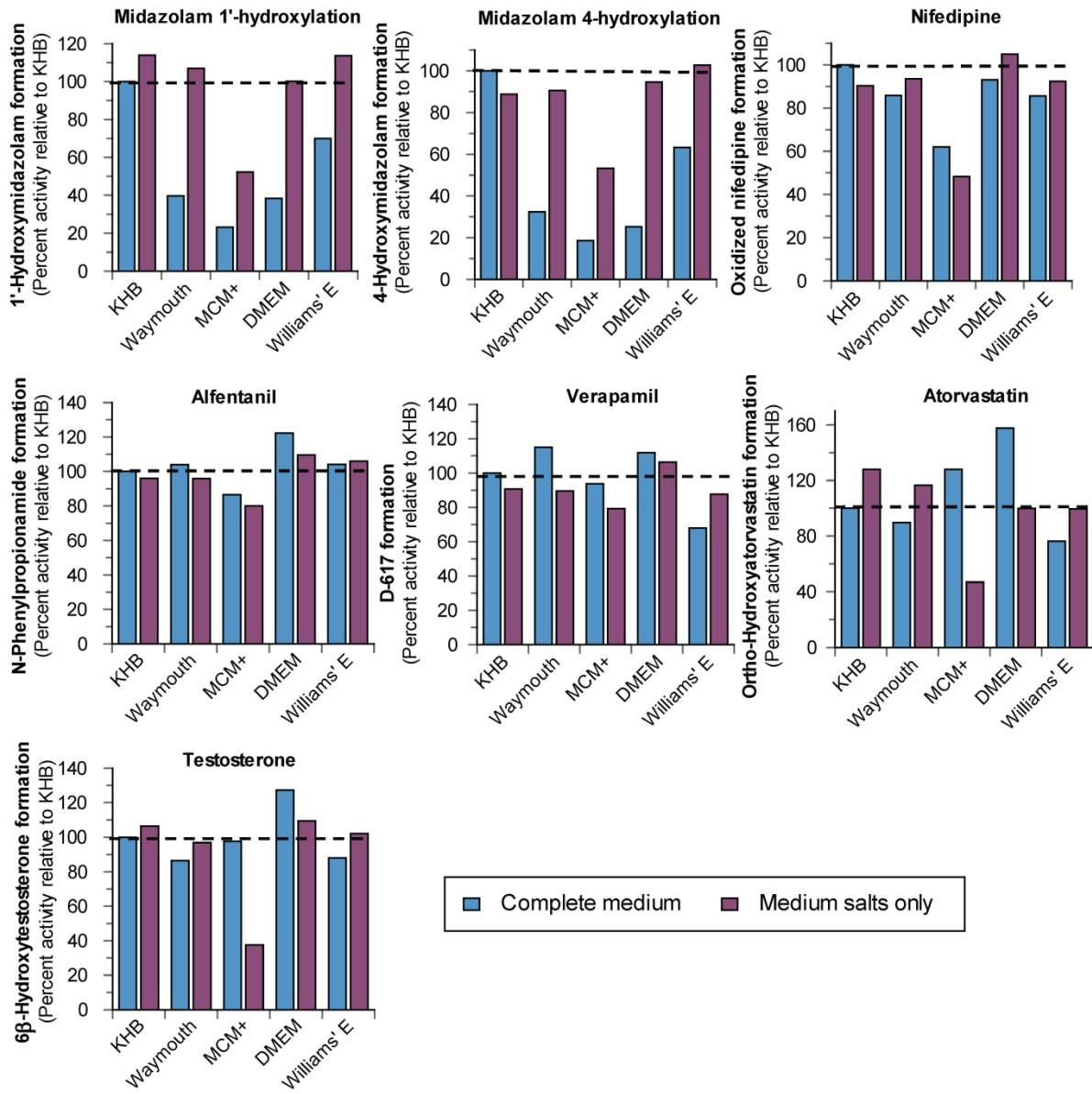


Figure 4.8. The effect of complete versions or salt-only versions of cell culture media on the metabolism of six CYP3A4/5 substrates by human liver microsomes

Rates of metabolite formation from six CYP3A4/5 marker substrates, namely, midazolam (4 μ M), nifedipine (10 μ M), alfentanil (40 μ M), verapamil (9 μ M), atorvastatin(40 μ M), and testosterone (70 μ M), were measured in in pooled human liver microsomes (0.1 mg/mL) incubated in the complete version (blue) and five salt-only version (purple) of five cell culture media, as described in *Chapter 2*. Rates of metabolism in complete KHB medium were set to 100%.

Table 4.3. Ion concentration and ionic strength of cell culture medium composed of salts only

Component	Units	Concentration				
		KHB	Waymouth's	MCM+	DMEM	Williams' E
Cations						
Sodium	mM	144	140	341	155	145
Potassium		5.84	2.59	5.33	5.33	5.33
Magnesium		0.695	2.00	1.45	0.814	0.811
Calcium		3.36	0.816	1.80	1.80	1.80
Iron (ferric)	μM			3	0.2	0.00025
Copper (cupric)				1.2		0.00040
Anions						
Phosphate	mM	4.67	5.30	1.04	0.908	1.17
Chloride		132	107	86.5	119	126
Bicarbonate		25	26.7	262	44.0	26.2
Sulfate			0.814	1.45	0.814	0.811
Nitrate	μM			8.9	0.7	0.00074
Ionic strength^a	mM	182	169	361	173	163

^a Values were calculated based only on the salt composition of the various media as described in Equation 2.9. The ionic strengths of 5, 50 and 200 mM phosphate buffer were calculated to be 35, 282 and 1108 mM respectively.

4.8. Effects of buffer ionic strength and cell culture media on midazolam metabolism by HLM, rCYP3A4 and rCYP3A5 with and without cytochrome b₅.

When HLM were used to examine the effects of ionic strength and cell culture media on CYP activity (Section 4.1), the various CYP enzymes examined could be divided into three groups (A-C). The Group B enzymes, namely CYP2E1 and CYP3A4/5, were distinguished by their high activity in 200 mM phosphate buffer and their low activity in Waymouth's, MCM+ and DMEM media (relative to KHB and Williams' E media), as shown in Figure 4.2. It is interesting to note that CYP2E1, CYP3A4 and CYP3A5 are the three enzymes most affected by cytochrome b₅ (Parkinson et al., 2013). Accordingly, buffer ionic strength and cell culture media were examined for their effects on midazolam 1'- and 4-hydroxylation by recombinant CYP3A4 and CYP3A5 with and without cytochrome b₅. The results are shown in Figure 4.9.

When the recombinant enzymes were expressed without cytochrome b₅, the effects of cell culture media on midazolam 1'- and 4-hydroxylation by both CYP3A4 and CYP3A5 closely resembled their effects on midazolam metabolism by HLM (i.e., relatively low activity was observed with Waymouth's, MCM+ and DMEM). When the recombinant enzymes were expressed with cytochrome b₅, low rates of midazolam hydroxylation were observed with MCM+ and DMEM but not with Waymouth's (relative to KHB and Williams' E). In other words, co-expression with cytochrome b₅ altered the effect of Waymouth's medium on midazolam hydroxylation by both CYP3A4 and CYP3A5.

In HLM, 200 mM phosphate buffer supported higher rates of midazolam 1'- and 4-hydroxylation compared with 50 mM phosphate buffer (Figure 4.9). The same effect was observed with recombinant CYP3A5 with or without cytochrome b₅. However, in the case of recombinant CYP3A4, increasing the concentration of phosphate buffer to 200 mM increased the 4-hydroxylation but not the 1'-hydroxylation of midazolam regardless of whether CYP3A4 was co-expressed with cytochrome b₅.

Overall, the results suggest that the effects of ionic strength and cell culture media on midazolam metabolism by HLM are attributable to effects on CYP3A4 and CYP3A5 that occur independently of cytochrome b₅.

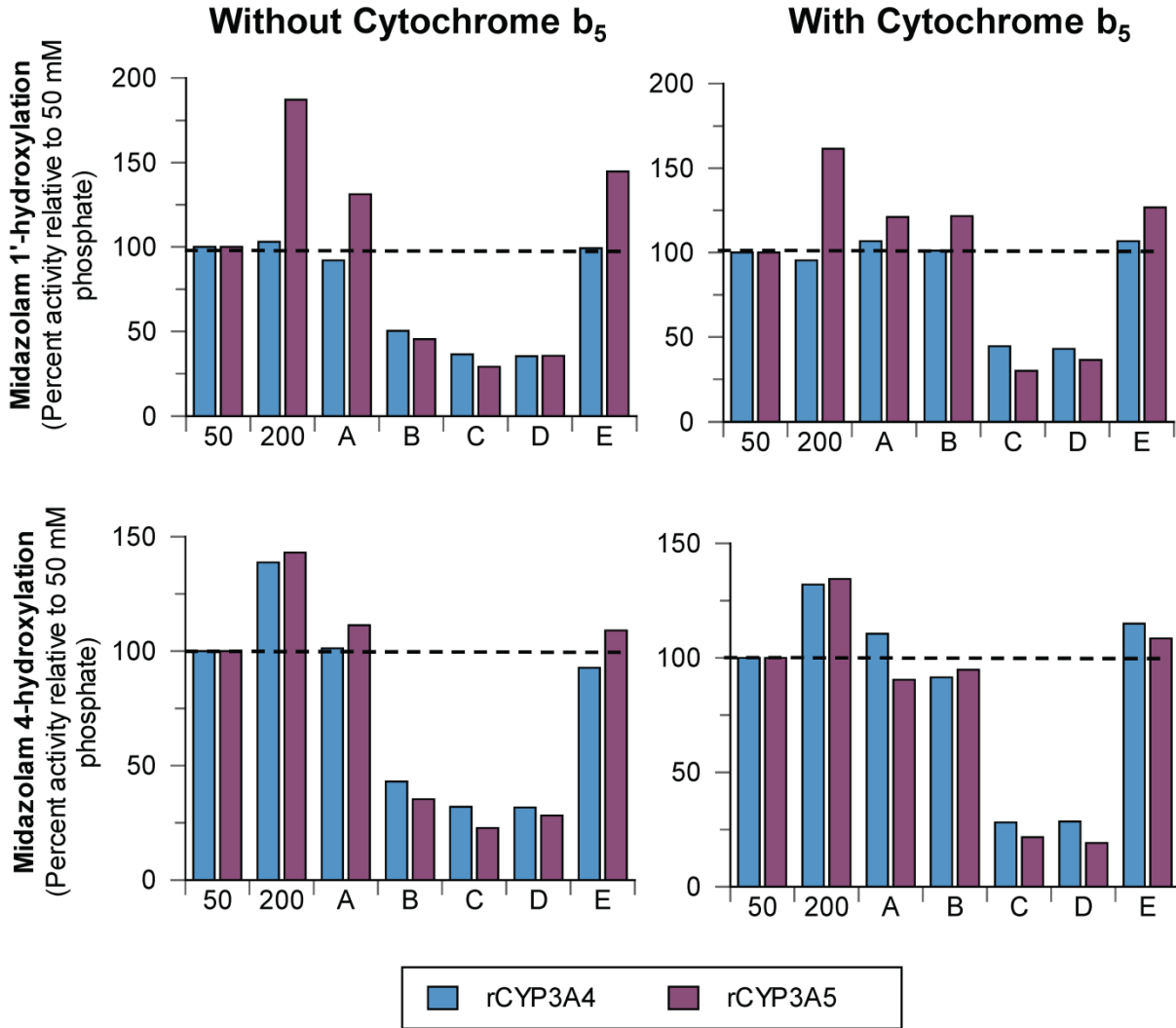


Figure 4.9. The effect of buffer ionic strength and various media on CYP3A4/5 midazolam metabolism in HLM, rCYP3A4 and rCYP3A5

Midazolam 1'- and 4-hydroxylation were measured with recombinant CYP3A4 and CYP3A5 (20 pmol/mL) in the absence and presence of cytochrome b₅ in 50 and 200 mM phosphate buffer (pH 7.4) or in one of five cell culture media, namely KHB (A), Waymouth's (B), MCM+ (C), DMEM (D) and Williams' E (E), as described in the *Chapter 2*. The activity in 50 mM phosphate buffer (standard incubation conditions) was set to 100%.

4.9. Effects of cell culture media on midazolam hydroxylation by HLM lacking CYP3A5

The five cell culture media were examined for their effects on 1'- and 4-hydroxylation of midazolam by HLM lacking CYP3A5 (i.e., liver microsomes prepared from donors genotyped for CYP3A5*3/*3), as described in *Chapter 2*. As shown in Figure 4.10, MCM+, DMEM and, to a lesser extent, Waymouth's all decreased midazolam hydroxylation relative to KHB and Williams' E. The effects of cell culture media on midazolam hydroxylation by HLM lacking CYP3A5 resembled their effects on midazolam hydroxylation by pooled HLM (pool of 200) (Figure 4.2)

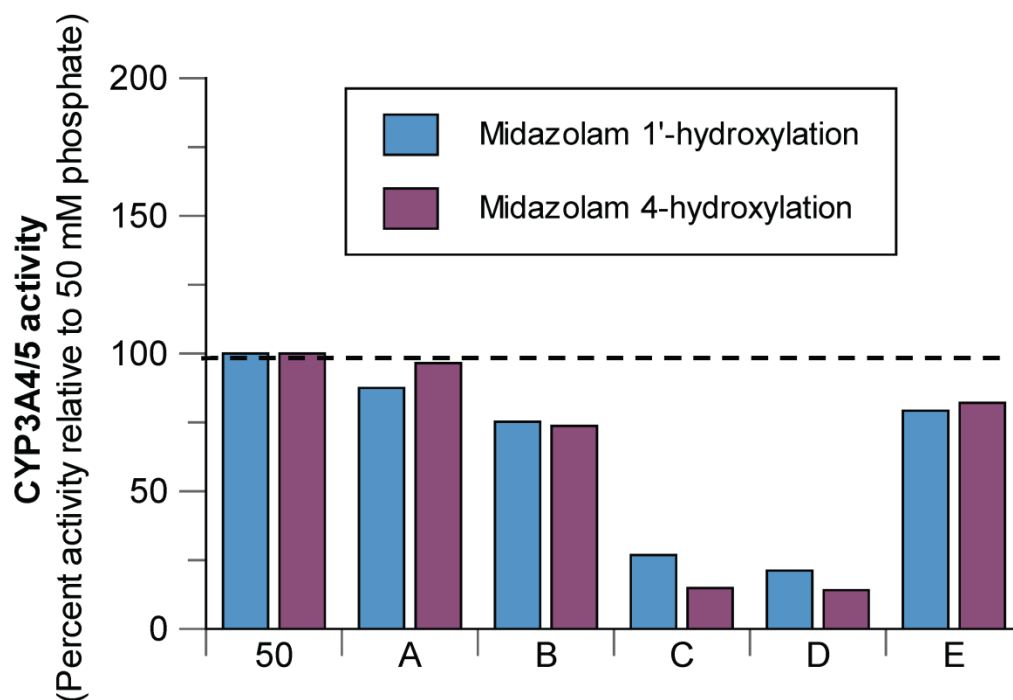


Figure 4.10. Effects of cell culture media on midazolam hydroxylation by human liver microsomes lacking CYP3A5.

The 1'- and 4-hydroxylation of midazolam (4 μ M) by human liver microsomes lacking CYP3A5 (microsomes prepared from a CYP3A5 \ast 3/ \ast 3 individual) was determined after a 5-min incubation in 50 mM phosphate buffer or one of five cell culture media, namely KHB (A), Waymouth's (B), MCM+ (C), DMEM (D) and Williams' E (E), as described in *Chapter 2*. Rates of midazolam hydroxylation in media are relative to those in 50 mM phosphate buffer (standard incubation conditions).

4.10. Detection of 3-hydroxydesloratadine during the assessment of cell culture media on loratadine metabolism in CHH.

In an effort to identify other substrates of CYP3A4/5 that resembled midazolam in terms of its response to various cell culture media, loratadine was incubated with CHH (1 million cells/mL) in KHB, Waymouth's, MCM+, DMEM and Williams' E, as described in *Chapter 2*. As shown in Figure 4.11, the rate of formation of desloratadine from loratadine by CHH (a reaction predominantly catalyzed by CYP3A4/5) was not greatly affected by any of the cell culture media examined. In this respect, loratadine differed from midazolam and resembled nifedipine, alfentanil, verapamil, testosterone and atorvastatin (as shown in Figure 4.5). However, in addition to forming desloratadine (the major metabolite of loratadine), CHH also formed 3-hydroxydesloratadine, which was unexpected because the formation of 3-hydroxydesloratadine is undetectable when desloratadine is incubated with HLM or recombinant CYP enzymes (Ghosal et al., 2009). Accordingly, the enzyme responsible for forming 3-hydroxydesloratadine has never been identified even though this is the major circulating metabolite of desloratadine in humans. The effects of cell culture media on the formation of 3-hydroxydesloratadine by CHH were the opposite of their effects on midazolam hydroxylation; the highest rates of 3-hydroxydesloratadine formation were supported by Waymouth's, MCM+ and DMEM (the three media supporting the lowest rates of midazolam hydroxylation). These results suggest that CHH may be an appropriate in vitro test system to study the enzymology of 3-hydroxydesloratadine formation. Such studies are described in Chapter 5.

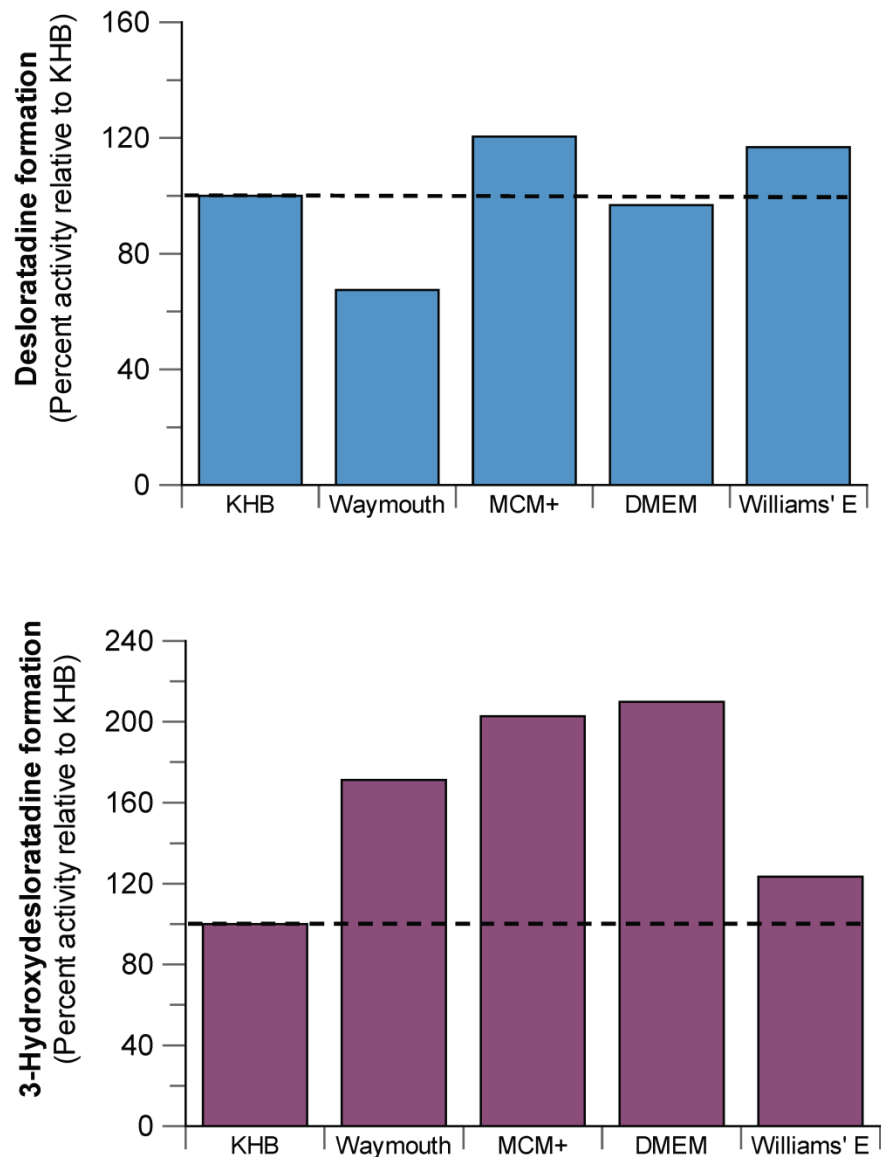


Figure 4.11. The effect of various cell culture media on desloratadine (top) and 3-hydroxydesloratadine (bottom) formation from loratadine in cryopreserved human hepatocytes

The metabolism of loratadine (10 μ M) by cryopreserved human hepatocytes (1 million cells/mL) was assessed in the presence of five cell culture media (KHB, Waymouth's, MCM+, DMEM and Williams' E), as described in Chapter 2. Formation of desloratadine (colored blue) and 3-hydroxydesloratadine (colored purple) was measured after 60 min by LC-MS/MS, as described in *Chapter 2*. Rates of metabolite formation in KHB medium were set to 100%.

DISCUSSION

In the preceding chapter I verified previous reports that the intrinsic metabolic clearance of midazolam by human hepatocytes is almost an order of magnitude less than midazolam clearance by liver microsomes (Lu et al., 2006; Foster et al., 2011). The relatively low clearance of midazolam in CHH, which underpredicts the in vivo hepatic clearance of midazolam, could not be explained by membrane- or cofactor-restricted midazolam metabolism in hepatocytes. The system-dependent clearance of midazolam was observed to a lesser degree with alfentanil, nifedipine and verapamil (Chapter 3). With these three CYP3A4/5 substrates, HLM accurately predicted in vivo blood clearance (CL_H), whereas CHH underpredicted CL_H by approximately 2 fold. In contrast, midazolam blood clearance was accurately predicted by HLM but underestimated by CHH approximately 5 fold. The present study examined in vitro factors that might account for the particularly pronounced system-dependent clearance of midazolam. Buffer ionic strength and cell culture media were examined for their effects on multiple P450 enzymes in HLM, HS9, recombinant enzymes, and CHH and were examined for their effects on multiple substrates for CYP3A4/5

The rate of midazolam hydroxylation by HLM or HS9 increased when the concentration of phosphate buffer was increased from 50 mM to 200 mM (Figure 4.2). This is an unusual feature of CYP3A4/5 (CYP2E1 was the only other enzyme examined that exhibited this property) but not an unusual feature of midazolam. The rates of metabolism of five other CYP3A4/5 substrates all increased when the concentration of phosphate buffer was increased from 50 mM to 200 mM (Figure 4.4). In contrast, with the exception of CYP2E1, the activity of all other CYP enzymes examined, namely CYP1A2, 2A6, 2B6, 2C8, 2C9,

2C19 and 2D6, decreased when the concentration of phosphate buffer increased from 50 to 200 mM (Figure 4.2). Several previous reports have described the effects of buffer ionic strength on P450 enzymes in vitro. Gemzik et al. (1990) observed that, in microsomes prepared from phenobarbital-induced rats, specific pathways of testosterone hydroxylation decreased with buffers of increasing ionic strength for CYP2A1 (6 α - and 7 α -hydroxylation), CYP2B1/2 (16 β -hydroxylation), and CYP2C2C11 (16 α -hydroxylation); whereas an increase in testosterone hydroxylation was observed with CYP3A1/2 (1 β -, 2 β -, 6 β - and 15 β -hydroxylation). Reports of the effects of ionic strength on human P450 enzymes (namely, CYP1A1, CYP1A2, CYP3A4, CYP2C8, CYP2C9, CYP2D6, CYP2E1, and CYP3A4) are generally consistent with those shown in Figure 4.1 and Figure 4.2 (Yamazaki et al., 1997; Maenpaa et al., 1998; Traylor et al., 2011; Kudo et al., 2014).

CYP3A4, CYP3A5 and CYP2E1, the enzymes stimulated by high ionic strength, are unusual inasmuch as their activity is influenced by cytochrome b₅ more so than other P450 enzymes in HLM (Parkinson et al., 2013). However, the stimulatory effect of high ionic strength on CYP3A4/5 activity occurs independently of cytochrome b₅ based on the finding that 200 mM phosphate buffer stimulated midazolam hydroxylation by recombinant CYP3A4 and CYP3A5 in the absence and presence cytochrome b₅ (Figure 4.9). CYP3A4, CYP3A5 and CYP2E1 are also unusual because they have a tendency to oligomerize (Davydov et al., 2015). Interestingly, α -naphthoflavone stimulates the activity of CYP3A4 only when the enzyme is in an oligomeric state (Davydov et al., 2013). It is possible that high ionic strength promotes the dissociation of oligomeric forms of CYP3A4, CYP3A5 and CYP2E1 and thereby facilitates their ability to bind substrate and/or associate with NADPH-cytochrome P450 reductase.

The effects of cell culture media on P450 activity in HLM was both CYP- and substrate-dependent. For simplicity, only KHB and MCM+ will be discussed here, although in general (but with exceptions) Williams' E resembled KHB whereas Waymouth's and DMEM resembled MCM+. KHB supported higher rates of metabolism by CYP3A4/5 (with midazolam), CYP2E1 and CYP2C9 than MCM+, whereas the converse was observed with CYP1A2, 2A6, 2B6, 2C8, 2C19 and 2D6. Although MCM+ supported markedly lower rates of midazolam 1'- and 4-hydroxylation compared with KHB (in HLM and HS9), the difference between these two media was considerably less with other CYP3A4/5 substrates (alfentanil, nifedipine, testosterone and atorvastatin) and, in the case of verapamil, MCM+ supported slightly higher rates of metabolism compared with KHB. These results suggest that cell culture media can affect CYP3A4/5 activity in HLM and HS9 in a substrate-dependent manner and demonstrate that various media reduce the rate of metabolism of midazolam to a greater extent than other CYP3A4/5 substrates. An assessment of the effects of cell culture media on midazolam metabolism with HLM from an individual lacking CYP3A5 (CYP3A5*3/*3) also yielded results similar to those obtained with pooled HLM (Figure 4.10). These results combined with the results from studies with rCYP3A4 and rCYP3A5 (Figure 4.9) suggest buffer conditions and cell culture media have similar effects on both the CYP3A4- and CYP3A5-dependent hydroxylation of midazolam.

The effects of cell culture media on the kinetics of midazolam 1'-hydroxylation by HLM were surprisingly complex and varied. Compared with 50 mM phosphate buffer (standard incubation conditions), KHB caused a small increase in K_m (from 2.2 to 4.4 μM) and decreased V_{max} by a factor of ~ 3 (Table 4.2). In contrast, MCM+ caused a 50-fold increase

in K_m . Unexpectedly, MCM+ actually increased V_{max} by 2.6 fold. In terms of their effects on the kinetics of midazolam 1'-hydroxylation by HLM, Waymouth's and DMEM resembled KHB (they caused relatively small increases in K_m and V_{max}) whereas Williams' E resembled MCM+ (both caused large increases in K_m and a small increase in V_{max}). All media decreased the intrinsic clearance of midazolam by HLM (based on V_{max}/K_m) (Table 4.2 and Figure 4.7).

One of the aims of this study was to identify a cell culture medium that supported higher rates of midazolam clearance in CHH to correct for the underprediction observed with KHB. When CHH were incubated in KHB medium, estimates of the in vivo intrinsic hepatic clearance of midazolam were roughly an order of magnitude lower than estimates of CL_{int} with HLM (Chapter 3). Compared with KHB, Williams' E and Waymouth's supported comparable rates (within 20%) of midazolam metabolism in CHH whereas MCM+ and DMEM supported lower rates (40-45% lower). The ~45% decrease in midazolam metabolism caused by incubating CHH in MCM+ compared with KHB was not observed with alfentanil, verapamil, testosterone or atorvastatin, although MCM+ decreased nifedipine metabolism by 26%. Compared with KHB, DMEM also decreased the rate of metabolism of midazolam, nifedipine, testosterone and atorvastatin (by 32-43%), but slightly stimulated the metabolism of alfentanil (13%) and verapamil (45%) (Figure 4.5). Therefore, the effects of cell culture media on CYP3A4/5 activity in CHH are substrate dependent, as was observed in HLM and HS9. In terms of supporting the metabolism of midazolam in CHH, none of the media examined was superior to KHB and some were inferior; accordingly, CHH underpredicted the clearance of midazolam regardless of which cell culture medium was used.

The effects of MCM+ on CYP3A4/5 activity in HLM are particularly noteworthy in terms of the possible presence of an inhibitory substance. This medium has roughly twice the ionic strength of the other four media. The salt-only version of this medium (with an ionic strength of 361 mM) would be expected to support CYP3A4/5 activity to the same extent as – or to an even greater extent than – 50 mM phosphate buffer (which has an ionic strength of 282 mM). However, when HLM were incubated in the salt-only version of MCM+, the rates of metabolism of midazolam, nifedipine, atorvastatin and testosterone were at least 40% lower than those supported by all of the other salt-only media, which had ionic strengths ranging from 163 to 182 mM. This finding, coupled with the observation that MCM+ caused a 50-fold increase in the K_m for midazolam 1'-hydroxylation, suggest that the salt-only and complete versions of MCM+ both contain one or more substances that inhibit CYP3A4/5 in a substrate-dependent manner; they inhibit the metabolism of midazolam, nifedipine, atorvastatin and testosterone more than they inhibit the metabolism of alfentanil and verapamil.

Certain cell culture media contain components that have been reported to inhibit P450, such as menadione in Williams' E and dexamethasone in MCM+; likewise, divalent cations such as Cu^{2+} (present in Williams' E and MCM+) and Ca^{2+} (present in all media examined) have been shown to inhibit P450 and/or NADPH-cytochrome P450 reductase activity (Tamura et al., 1988; Floreani and Carpenedo, 1990; Gentile et al., 1996; Kim et al., 2002). However, media components that inhibit CYP activity in HLM may not do so in CHHs due to binding, restricted uptake, efflux or metabolism of these components in intact hepatocytes. Overall, the studies of the effects of cell culture media on P450 activities in HLM produced several interesting and unexpected findings but none pointed

to the possibility that all five of the cell culture media examined (all of which underpredict the clearance of midazolam – but not the clearance of other CYP3A4/5 substrates – in CHH) contain a component or components that selectively impair the metabolism of midazolam in CHH.

The results of this study do not provide a mechanistic rationale for the system-dependent clearance of midazolam shown in the previous chapter and described previously by other researchers (Lu et al., 2006; Foster et al., 2011). The marked system-dependent clearance of midazolam (microsomal $CL_{H,int} = \sim 10x$ hepatocyte $CL_{H,int}$) was observed to a lesser extent with other high clearance drugs, namely alfentanil, nifedipine and verapamil (microsomal $CL_{H,int} < 4x$ hepatocyte $CL_{H,int}$), suggesting that system-dependent clearance is more pronounced with midazolam than with other CYP3A4/5 substrates.

Although I have been unable to explain the system-dependent clearance of midazolam, the results of the studies presented here and in the preceding chapter have excluded certain possible explanations (such as restrictive membrane permeability and cofactor availability) and, perhaps more importantly, point to possible improvements in the design of in vitro studies of drug clearance, which continue to play an important role in drug candidate selection. In the present study, the predicted intrinsic hepatic clearance of alfentanil, nifedipine and verapamil based on half-life in HLM was up to 3.7-fold greater than estimates of $CL_{H,int}$ in CHH. In these studies, HLM were incubated in 50 mM potassium phosphate buffer (together with other components, namely $MgCl_2$, EDTA and NADPH). This concentration of phosphate buffer supports near-optimum activity of most CYP enzymes (Figure 4.2). Incubating HLM in 100 mM phosphate buffer (as is commonly done) increases the activity of CYP3A4/5 (and CYP2E1) but decreases the activity of the

other drug-metabolizing P450 enzymes in HLM. Therefore, I recommend researchers use 50 mM phosphate buffer for studies of drug clearance by HLM.

Compared with midazolam, alfentanil, nifedipine or verapamil exhibited modest system-dependent clearance when CHH were incubated in KHB medium (Figure 4.5). In general, KHB and Williams' E supported the highest (or close to the highest) activity of most CYP enzymes in CHH, especially CYP3A4/5 activity, as shown in Figure 4.3. However, as shown in Table 4.1, the viability of human hepatocytes after a 4-h incubation was highest with Williams' E and lowest with KHB. Therefore, KHB is not suitable to support long-term incubations of hepatocytes whereas Williams' E medium can and this has implications for its use in long-term metabolism studies. There have been several reports on the use of extended hepatocyte incubations (the so-called hepatocyte-relay method, see Figure 4.12) for assessing the in vitro half-life of low clearance drugs (Di et al., 2012; Di et al., 2013). With the knowledge that Williams' E supports CYP3A4/5 activity and cell viability better than any of the four other media examined, I recommend that researchers use this medium for both short-term and long-term incubations of suspended human hepatocytes because even modest increases in the activity of CYP3A4/5 can have a profound impact on assay performance.

In an effort to identify a substrate of CYP3A4/5 with the same system-dependent characteristics as midazolam, I tested loratadine, which is converted to desloratadine primarily by CYP3A4/5 (Yumibe et al., 1995; Yumibe et al., 1996). All five media supported similar rates of loratadine metabolism. In this regard, loratadine did not resemble midazolam but resembled the other six CYP3A4/5 substrates examined in this study. However, the study of loratadine metabolism by CHH lead to the detection

3-hydroxydesloratadine, which was unexpected because no previous in vitro test system or non-clinical species has been shown to support the formation of 3-hydroxydesloratadine (Ramanathan et al., 2006; Ghosal et al., 2009). Accordingly the enzyme responsible for forming 3-hydroxydesloratadine, which the major circulating metabolite of desloratadine, has remained unknown despite the fact this was a post-marketing commitment imposed by the FDA on the manufacturer, Schering Plough (Schering-Plough, 2001). The observation that CHH can form 3-hydroxydesloratadine provided an opportunity to investigate the enzymology of its formation. These studies are described in Chapter 5.

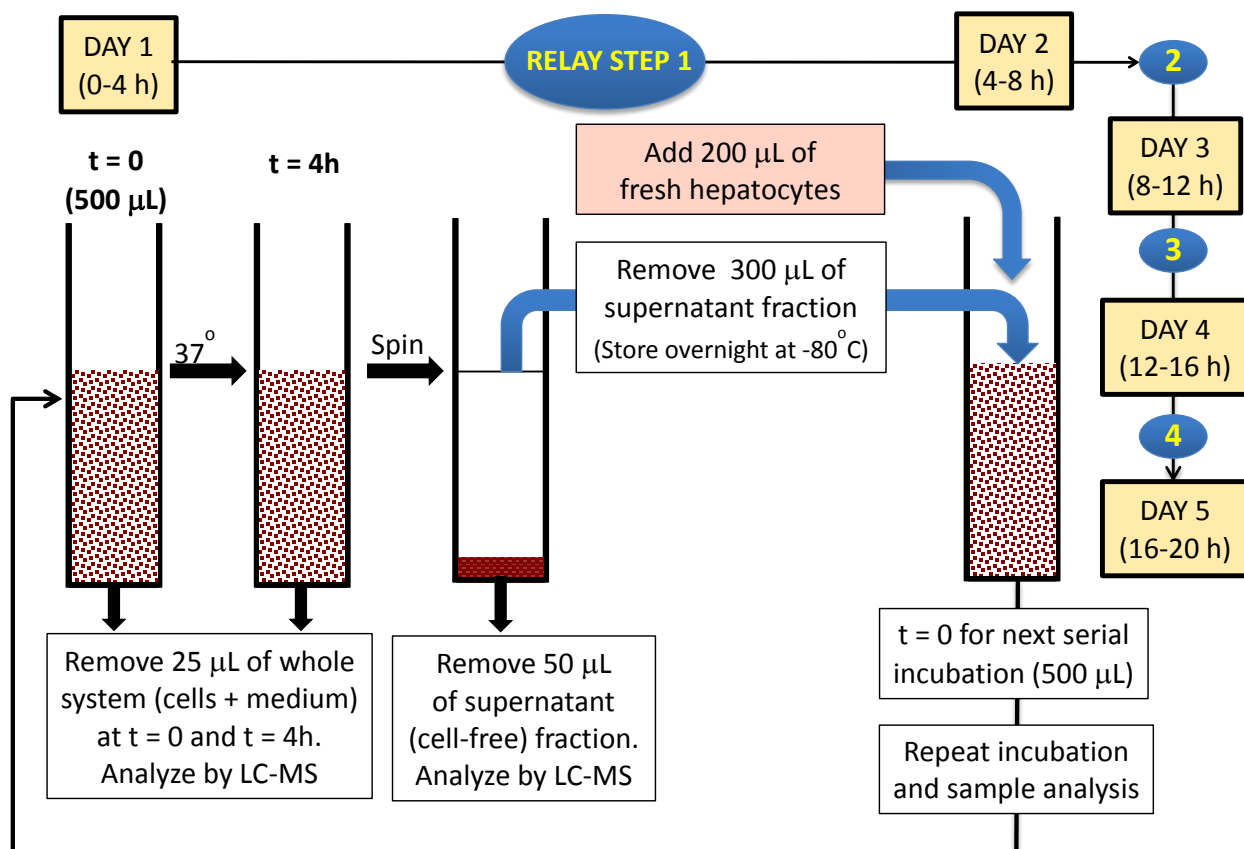


Figure 4.12. Schematic representation of the hepatocyte relay method to measure the in vitro half-life of metabolically stable drugs

The method depicted in the schematic has been previously described by Di et al., (2012, 2013).

**CHAPTER 5 : A LONG-STANDING MYSTERY SOLVED: THE
FORMATION OF 3-HYDROXYDESLORATADINE IS CATALYZED BY
CYP2C8 BUT PRIOR GLUCURONIDATION OF DESLORATADINE BY
UGT2B10 IS AN OBLIGATORY REQUIREMENT**

This section is a reprint of the following manuscript:

Kazmi F, Barbara JE, Yerino P, and Parkinson A. (2015) A Long-Standing
Mystery Solved: The Formation of 3-Hydroxydesloratadine is Catalyzed by
CYP2C8 but Prior Glucuronidation of Desloratadine by UGT2B10 is an
Obligatory Requirement, *Drug Metab Dispos*, **43**:523-533.

Reprinted with permission of the American Society for Pharmacology and Experimental
Therapeutics. All rights reserved. Copyright © 2015 by the American Society for
Pharmacology and Experimental Therapeutics.

ABSTRACT

Desloratadine (Clarinet[®]), the major active metabolite of loratadine (Claritin[®]), is a non-sedating long-lasting antihistamine widely used for the treatment of allergic rhinitis and chronic idiopathic urticaria. For over 20 years, it has remained a mystery as to which enzymes are responsible for the formation of 3-hydroxydesloratadine, the major active human metabolite, largely due to the inability of any in vitro system tested thus far to generate this metabolite. In this study, I demonstrated that cryopreserved human hepatocytes (CHH) form 3-hydroxydesloratadine and its corresponding O-glucuronide. CHHs catalyzed the formation of 3-hydroxydesloratadine with a K_m of 1.6 μ M and V_{max} of 1.3 pmol/min/million cells. Chemical inhibition of cytochrome P450 (CYP) enzymes in CHH demonstrated that gemfibrozil glucuronide (CYP2C8 inhibitor) and 1-aminobenzotriazole (general P450 inhibitor) inhibited 3-hydroxydesloratadine formation by 91% and 98%, respectively. Other inhibitors of CYP2C8 (gemfibrozil, montelukast, clopidogrel glucuronide, repaglinide and cerivastatin) also caused extensive inhibition of 3-hydroxydesloratadine formation (73-100%). Assessment of desloratadine, amodiaquine and paclitaxel metabolism by a panel of individual CHHs demonstrated that CYP2C8 marker activity robustly correlated with 3-hydroxydesloratadine formation (r^2 of 0.70-0.90). Detailed mechanistic studies with sonicated or saponin-treated CHHs, human liver microsomes and S9 fractions showed that both NADPH and UDP-glucuronic acid are both required for 3-hydroxydesloratadine formation, and studies with recombinant UGT and CYP enzymes implicated the specific involvement of UGT2B10 in addition to CYP2C8. Overall, my results demonstrate for the first time that desloratadine

glucuronidation by UGT2B10, followed by CYP2C8 oxidation and a de-conjugation event are responsible for the formation of 3-hydroxydesloratadine.

INTRODUCTION

Desloratadine (Clarinet[®]) is a second generation, non-sedating selective H₁-receptor histamine antagonist with long-acting activity widely used for the treatment of seasonal allergic rhinitis and chronic idiopathic urticaria. Desloratadine is also the major active metabolite of the antihistamine loratadine (Claritin[®]) and has a half-life of 21-27 h with moderate plasma protein binding (82-87%) permitting once-daily dosing (Henz, 2001; Molimard et al., 2004; Devillier et al., 2008). The major in vivo human active metabolite of desloratadine is 3-hydroxydesloratadine which is subsequently glucuronidated to 3-hydroxydesloratadine O-glucuronide. Both are excreted in roughly equal amounts in urine and feces (Ramanathan et al., 2007).

Furthermore, 3-hydroxydesloratadine and its glucuronide were found to be major metabolites in humans, but only trace levels were detectable in nonclinical species such as mice, rats and monkeys (Ramanathan et al., 2006), leading to the concern that nonclinical species may not have been adequately exposed to these metabolites in safety studies.

The conversion of loratadine to desloratadine (a dealkylation reaction leading to loss of a descarboethoxyl moiety) was previously shown to be catalyzed by CYP3A4 and, to a lesser extent, by CYP2D6 (Yumibe et al., 1995; Yumibe et al., 1996; Dridi and Marquet, 2013) However, the enzymology surrounding the conversion of desloratadine to 3-hydroxydesloratadine has remained a mystery both prior to and since its approval by the FDA in 2001 (Schering-Plough, 2001). Ghosal and colleagues (2009) examined the metabolism of loratadine and further characterized the in vitro enzymology of the

metabolites using pooled human liver microsomes (HLM) and recombinant P450 enzymes (rCYPs), demonstrating that desloratadine, 5-hydroxydesloratadine and 6-hydroxydesloratadine formation could be mediated by CYP3A4, CYP2D6 and CYP2C19. However, they were unable to detect 3-hydroxydesloratadine in either in vitro test system and therefore were unable to identify which enzyme or enzymes were involved in its formation. However, the subsequent conjugation of 3-hydroxydesloratadine to 3-hydroxydesloratadine-*O*-glucuronide was previously shown to be catalyzed in vitro by recombinant UGT1A1, UGT1A3 and UGT2B15 (Ghosal et al., 2004).

Clinical pharmacology and safety studies demonstrated that some individuals have a phenotypic polymorphism in the metabolism of desloratadine with greatly reduced formation of 3-hydroxydesloratadine, resulting in a 3-hydroxydesloratadine to desloratadine exposure ratio of <0.1 or a desloratadine half-life of >50 h (Prenner et al., 2006). These poor metabolizers (PMs) of desloratadine were found to have a general population frequency of 6% and were most frequent in African American (17%) compared with Caucasian (2%), Native American (8%), Hispanic (2%) and Jordanian populations (3%) (Prenner et al., 2006; Hakooz and Salem, 2012). Exposure to desloratadine in PMs resulted in a 6-fold increase in desloratadine AUC compared with extensive metabolizers (EMs), leaving the FDA unable to rule out an increased risk of adverse events in PMs (Schering-Plough, 2001). Because the enzymology of 3-hydroxydesloratadine formation has not been elucidated, the genetic basis for the PM phenotype has not been determined.

In the present study, I sought to identify the enzyme or enzymes responsible for the formation of 3-hydroxydesloratadine by identifying an in vitro test system capable of

generating the metabolite. In this report, I demonstrate that 3-hydroxydesloratadine can be formed in cryopreserved human hepatocytes. Using reaction phenotyping approaches (correlation analysis, chemical inhibition and studies with recombinant enzymes), I elucidated the main human metabolic enzymes responsible for converting desloratadine to 3-hydroxydesloratadine. I established that the 3-hydroxylation of desloratadine is catalyzed by CYP2C8, but the reaction is unusual because the prior glucuronidation of desloratadine by UGT2B10 is an obligatory step in the reaction.

RESULTS

5.1. Determination of an in vitro test system capable of producing 3-hydroxydesloratadine.

To determine whether 3-hydroxydesloratadine could be formed in any conventional in vitro test system, desloratadine (1 and 10 μM) was incubated with HLM (0.1 and 1 mg/mL), HS9 (0.5 and 5 mg/mL) and CHH (1 million cells/mL) in a time course experiment up to 4 h as described in *Chapter 2*. The results for 3-hydroxydesloratadine formation with 1 μM desloratadine are shown in Figure 5.1 (10 μM desloratadine data were similar and not shown). 3-Hydroxydesloratadine formation was not observed in any HLM or HS9 sample, consistent with previous reports (Ghosal et al., 2009). However, 3-hydroxydesloratadine was detected in CHH as early as 30 min, with linear metabolite formation up to 4 h. Furthermore, 3-hydroxydesloratadine glucuronide was also detected in CHH as early as 1 h with 10 μM desloratadine, but only at 4 h with 1 μM desloratadine. Additional expected hydroxydesloratadine metabolites such as 5- and 6-hydroxydesloratadine were detected in all three test systems.

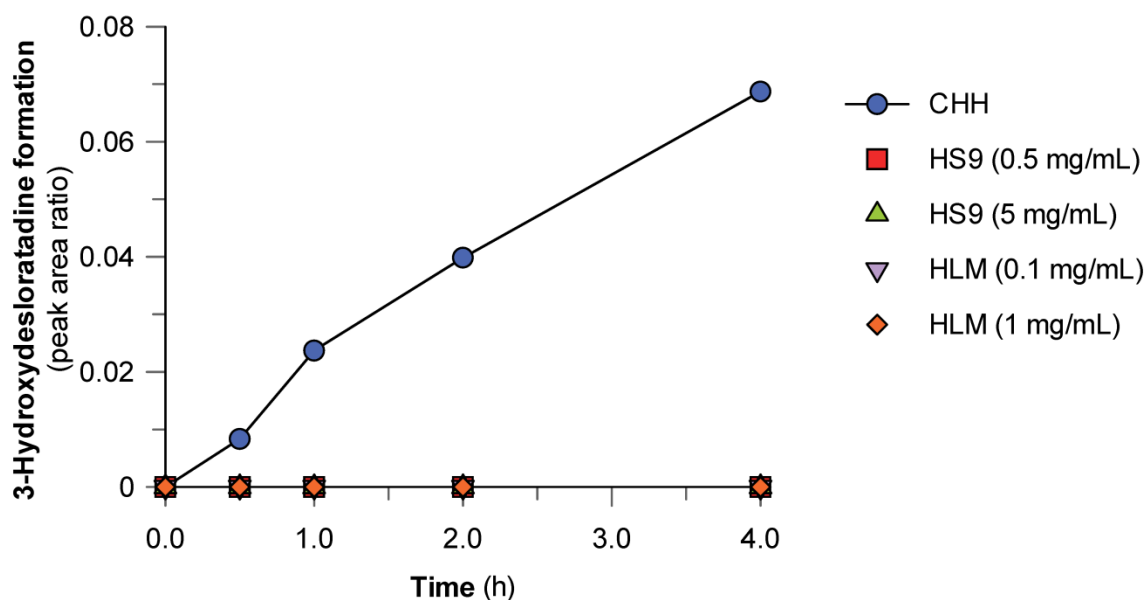


Figure 5.1. The formation of 3-hydroxydesloratadine over time in cryopreserved human hepatocytes (CHH), human liver microsomes (HLM) and human S9 fraction (HS9).

The time course of formation of 3-hydroxydesloratadine was assessed in hepatocytes (1 million cells/mL), liver microsomes (0.1 and 1 mg/mL) and liver S9 (0.5 and 5 mg/mL) with 1 μ M desloratadine for up to 4h.

5.2. Assessment of the kinetics of 3-hydroxydesloratadine formation.

Having established that CHH were the only test system capable of forming 3-hydroxydesloratadine I sought to determine the K_m and V_{max} of 3-hydroxydesloratadine formation from desloratadine. Linearity of 3-hydroxydesloratadine formation was established beyond 2 h. Desloratadine was incubated at nine concentrations with pooled CHH (1 million cells/mL) for 2 h as described in *Chapter 2*. As shown in Figure 5.2, 3-hydroxydesloratadine formation followed Michaelis-Menten kinetics, with K_m and V_{max} values of 1.6 μM and 1.3 pmol/min/million cells, respectively.

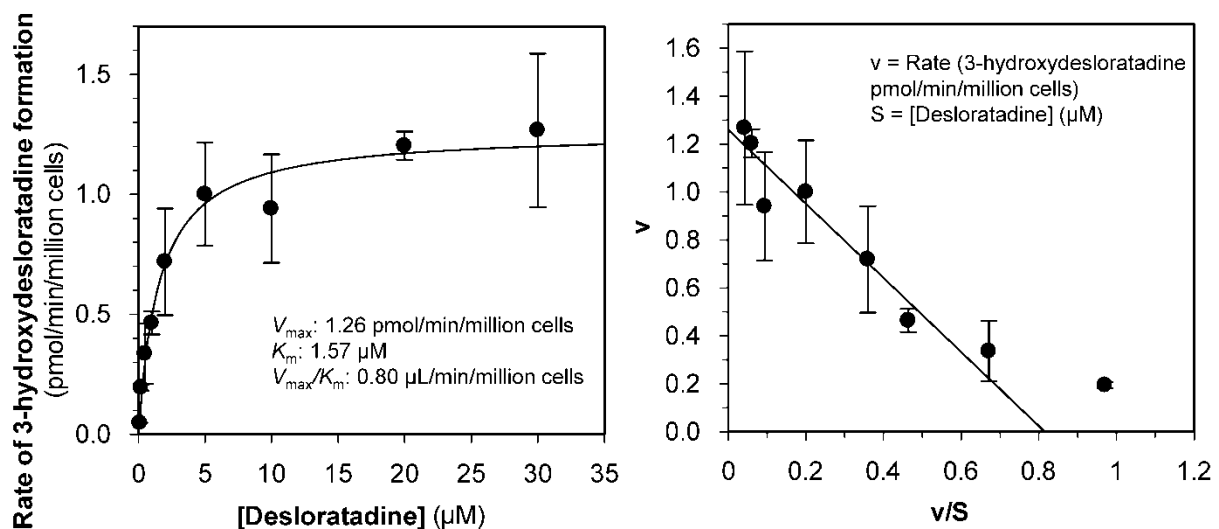


Figure 5.2. Determination of the enzyme kinetics for the formation of 3-hydroxydesloratadine from desloratadine in cryopreserved human hepatocytes (CHH).

As described in *Chapter 2*, the kinetics for the formation of 3-hydroxydesloratadine were determined in CHH (1 million cells/mL) with 0.1, 0.2, 0.5, 1, 2, 5, 10, 20 and 30 μM desloratadine incubated for 2 h. The left panel represents rate versus substrate concentration, and the right panel represents the Eadie-Hofstee plot.

5.3. Assessment of the species specificity of 3-hydroxydesloratadine formation.

I evaluated whether 3-hydroxydesloratadine could be formed by hepatocytes from different species. Mouse, rat, rabbit, dog, minipig, monkey and human hepatocytes (1 million cells/mL) were incubated with 1 or 10 μM desloratadine for 2 h as described in *Chapter 2*. The results for 3-hydroxydesloratadine formation (Figure 5.3) showed that at 1 μM desloratadine, rabbit and human hepatocytes formed similar amounts of 3-hydroxydesloratadine, whereas dog hepatocytes formed one third as much and monkey hepatocytes formed only a trace amount. In contrast, no 3-hydroxydesloratadine was detected in incubations of 1 μM desloratadine with mouse, rat or minipig hepatocytes. At 10 μM desloratadine, only rabbit and human hepatocytes formed 3-hydroxydesloratadine, with rabbit forming three times as much 3-hydroxydesloratadine as human hepatocytes. No 3-hydroxydesloratadine formation was observed in incubations of 10 μM desloratadine with mouse, rat, dog, minipig or monkey hepatocytes. Formation of both 5- and 6-hydroxydesloratadine in each species was determined simultaneously (shown in Figure 5.4), with all animal species forming higher levels of these metabolites than human hepatocytes. Rabbit hepatocytes formed the greatest amount of 5-hydroxydesloratadine, while rabbit and minipig hepatocytes formed the greatest amounts of 6-hydroxydesloratadine.

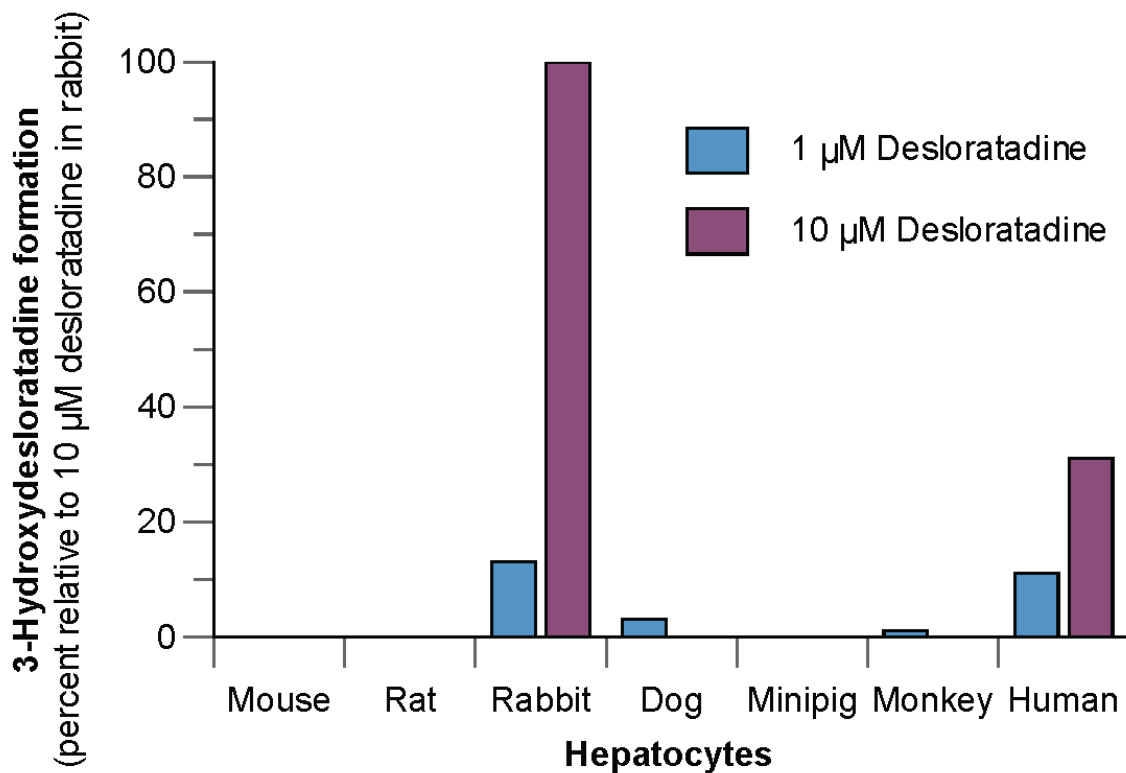


Figure 5.3. Formation of 3-hydroxydesloratadine in pooled cryopreserved mouse, rat, rabbit, dog, minipig, monkey and human hepatocytes.

Hepatocytes were incubated at 1 million cells/mL with 1 or 10 μM desloratadine for 2 h. Data are represented as the percent of 3 hydroxydesloratadine formation relative to the maximum amount formed.

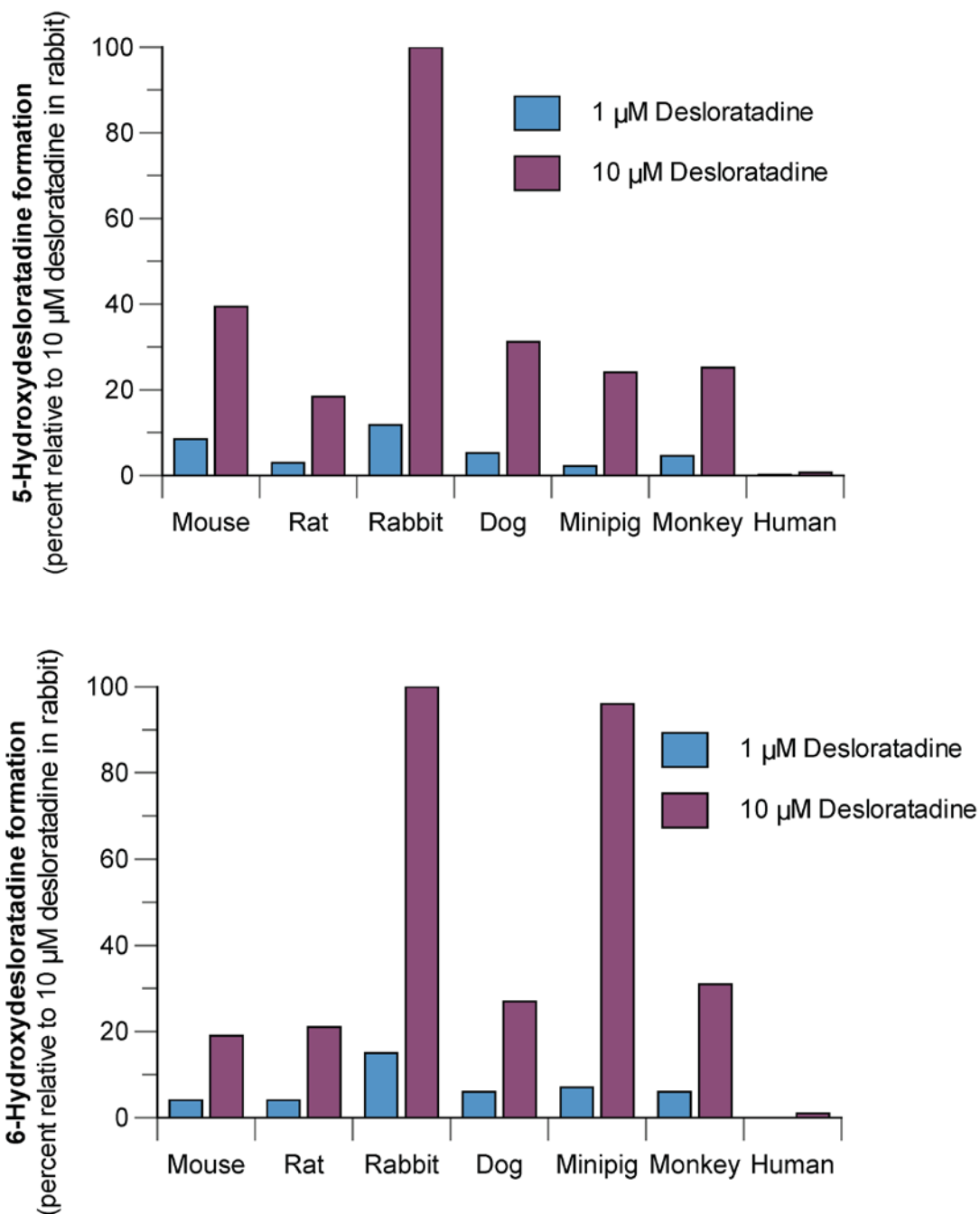


Figure 5.4. Formation of 5- and 6-hydroxydesloratadine in hepatocytes from mouse, rat, rabbit, dog, minipig, monkey and human.

Pooled hepatocytes from mouse, rat, rabbit, dog, minipig, monkey and human were incubated at 1 million cells/mL with 1 or 10 μ M desloratadine for 2 h. Analysis of 5- and 6-hydroxydesloratadine was conducted as described in Chapter 2.

5.4. Identification of the enzyme responsible for 3-hydroxydesloratadine formation using recombinant enzymes.

To determine which specific drug-metabolizing enzymes were responsible for the formation of 3-hydroxydesloratadine, recombinant P450 and FMO enzymes (50 pmol/mL) were incubated with 1 and 10 μ M desloratadine and incubated for 1 h as described in *Chapter 2*. The data are summarized in Table 5.1. No 3-hydroxydesloratadine was detected in any recombinant P450 or FMO enzyme sample tested, consistent with previously reported findings (Ghosal et al., 2009). Both 5- and 6-hydroxydesloratadine were readily formed by CYP1A1, CYP2D6 and CYP3A4, with trace metabolite formation observed for several other P450 enzymes (Table 5.1). A time course experiment for up to 6 h with recombinant CYP2C8 also failed to generate any 3-hydroxydesloratadine (data not shown).

Table 5.1. Chemical inhibition and formation of 3-hydroxydesloratadine in cryopreserved human hepatocytes (CHH) and recombinant enzymes

Enzyme	Inhibitor	Inhibition of 3-OH formation (%)	Recombinant enzyme activity		
			3-OH	5-OH ^a	6-OH ^a
CYP	1-Aminobenzotriazole	98	NA		
CYP1A1	NA	NA	None	Yes	Yes
CYP1A2	Furafylline	0		None ^b	None ^c
CYP1B1	NA	NA			
CYP2A6					
CYP2B6	Phencyclidine	13.3			
CYP2C8	Gemfibrozil glucuronide	91.3-100			
	Gemfibrozil	100			
	Montelukast	100			
	Clopidogrel glucuronide	78.9			
	Repaglinide	73.3			
	Cerivastatin	84.6			
CYP2C9	Tienilic acid	0		Yes	Yes
CYP2C18	NA	NA		None ^b	None ^c
CYP2C19	Esomeprazole	22.5			
CYP2D6	Paroxetine, Quinidine	0		Yes	Yes
CYP2E1	NA	NA		None ^b	None ^c
CYP2J2					
CYP3A4/5	Mibefradil	0		Yes (CYP3A4)	Yes (CYP3A4)
	CYP3cide	0			
	Troleandomycin	0			
	Ketoconazole	27.0			
CYP3A7	NA	NA	None ^b	None ^c	
CYP4A11					
CYP4F2					
CYP4F3a					
CYP4F3b					
CYP4F12					
FMO1					
FMO3					
FMO5					

^a Data from 10 µM desloratadine experiments

^b Trace levels detected for CYP1A2, CYP1B1, CYP2B6, CYP2C8, CYP2C18, CYP2C19, CYP2J2, CYP3A5 and CYP3A7 with 1 µM desloratadine.

^c Trace levels detected for CYP1A2, CYP1B1, CYP2B6, CYP2C8, CYP2C18, CYP2J2 and CYP3A7 with 1 µM desloratadine.

3-OH: 3-hydroxydesloratadine; 5-OH: 5-hydroxydesloratadine; 6-OH: 6-hydroxydesloratadine; NA: Not applicable

5.5. Identification of the enzyme responsible for 3-hydroxydesloratadine formation using chemical inhibitors.

Since a recombinant P450/FMO enzyme approach was unable to identify any enzyme capable of forming 3-hydroxydesloratadine, I evaluated the effects of P450-selective inhibitors on the formation of 3-hydroxydesloratadine by CHH. Initially, a panel of chemical inhibitors specific to different CYP enzymes was used (as summarized in Table 5.1), namely, furafylline (CYP1A2); phencyclidine (CYP2B6); gemfibrozil glucuronide (CYP2C8); tienilic acid (CYP2C9); esomeprazole (CYP2C19); paroxetine and quinidine (CYP2D6); mibefradil, CYP3cide, troleandomycin and ketoconazole (CYP3A4/5); in addition to the non-specific P450 inhibitor 1-aminobenzotriazole (1-ABT). Desloratadine (10 μ M) was incubated with CHH for 2 h following pre-incubation of the hepatocytes with each individual chemical inhibitor as described in *Chapter 2*. As shown in Figure 5.5A and Table 5.1, the formation of 3-hydroxydesloratadine by CHH was extensively inhibited by gemfibrozil glucuronide (91.3% inhibition) and 1-ABT (97.8% inhibition). Furthermore, formation of 3-hydroxydesloratadine-*O*-glucuronide was inhibited completely by the CYP2C8 inhibitor gemfibrozil glucuronide and the nonspecific inhibitor 1-ABT, whereas the formation of 5- and 6-hydroxydesloratadine was primarily inhibited by inhibitors of CYP3A4/5 and 1-ABT (see Figure 5.6). To further explore the involvement of CYP2C8 in 3-hydroxydesloratadine formation, the panel of CYP2C8 inhibitors was extended to include montelukast, repaglinide, cerivastatin, clopidogrel glucuronide, gemfibrozil and its acyl glucuronide. As shown in Figure 5.5B, the formation of 3-hydroxydesloratadine by CHH was completely inhibited by montelukast, gemfibrozil, and gemfibrozil glucuronide; and extensively inhibited by clopidogrel glucuronide (78.9%), repaglinide (73.3%) and

cerivastatin (84.6%). In addition to examining their effects on 3-hydroxydesloratadine formation, the CYP2C8 inhibitors were also examined for their effects on two CYP2C8 marker reactions in CHH, namely amodiaquine N-dealkylation and paclitaxel 6 α -hydroxylation. As expected, inhibition of amodiaquine and paclitaxel metabolism by the panel of CYP2C8 inhibitors correlated well each other and with the degree of inhibition of 3-hydroxydesloratadine formation.

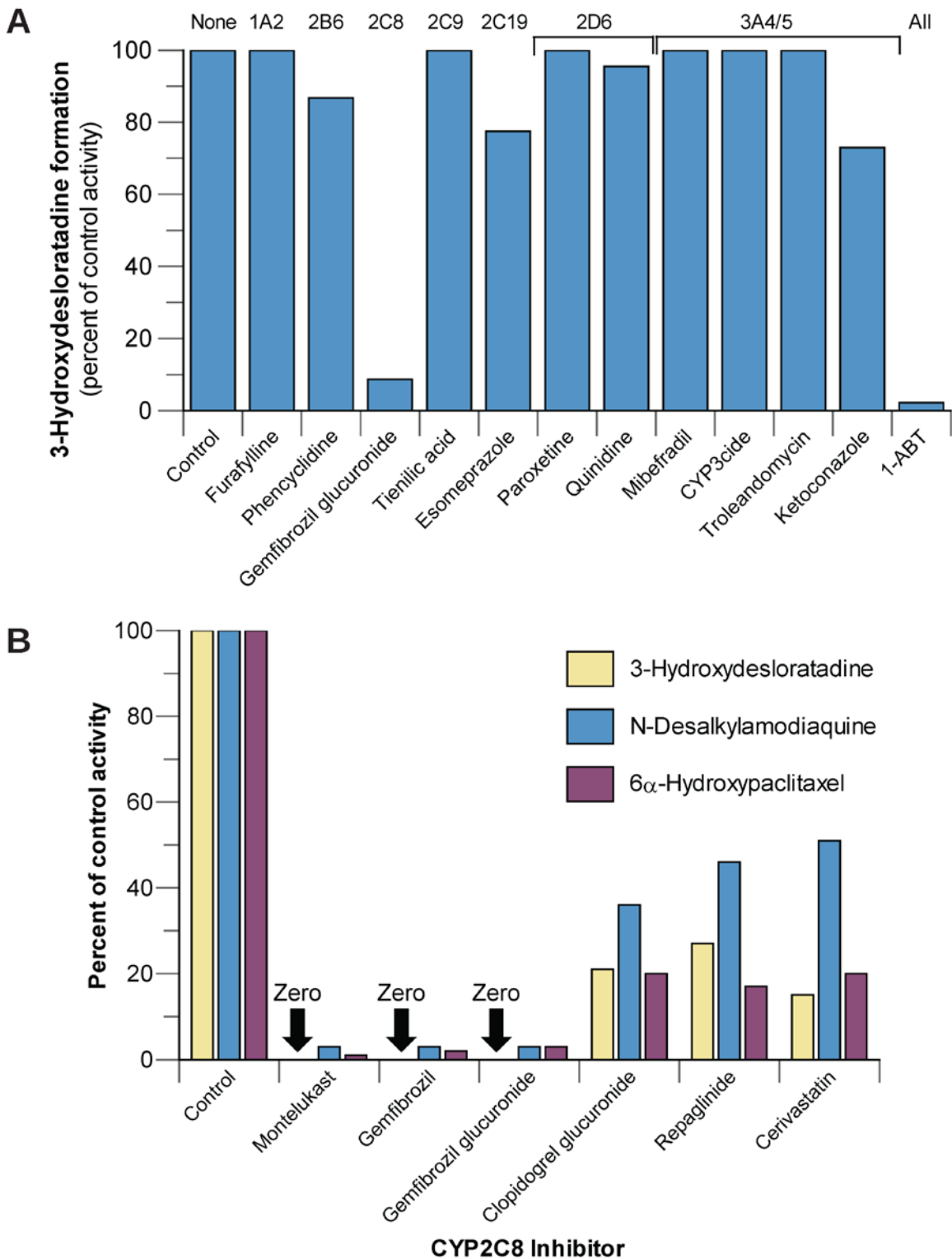


Figure 5.5. Effect of specific P450 chemical inhibitors on formation of 3-hydroxydesloratadine in pooled cryopreserved human hepatocytes (CHH).

As shown in panel A, chemical inhibitors towards specific P450 enzymes, namely furafylline (10 μ M; CYP1A2), phencyclidine (10 μ M; CYP2B6), gemfibrozil glucuronide (100 μ M; CYP2C8), tienilic acid (20 μ M, CYP2C9), esomeprazole (10 μ M; CYP2C19); paroxetine (1 μ M; CYP2D6); quinidine (5 μ M; CYP2D6), mibefradil (1 μ M; CYP3A4/5), CYP3c4e (2.5 μ M; CYP3A4/5), troleandomycin (50 μ M; CYP3A4/5), ketoconazole (4 μ M, CYP3A4/5), and 1 aminobenzotriazole (1 mM; general CYP inhibitor) were incubated with CHH (1 million cells/mL) for 30 min, prior to incubation with 10 μ M desloratadine for 2 h and analysis by LC-MS/MS as described in Chapter 2. Subsequently, multiple inhibitors of CYP2C8 (shown in panel B) were examined for their ability to inhibit 3-hydrodesloratadine formation, amodiaquine N-dealkylation and paclitaxel 6 α -hydroxylation in CHH; namely montelukast (50 μ M), gemfibrozil (100 μ M), gemfibrozil glucuronide (100 μ M), clopidogrel glucuronide (100 μ M), repaglinide (100 μ M) and cerivastatin (100 μ M) as described in *Chapter 2*.

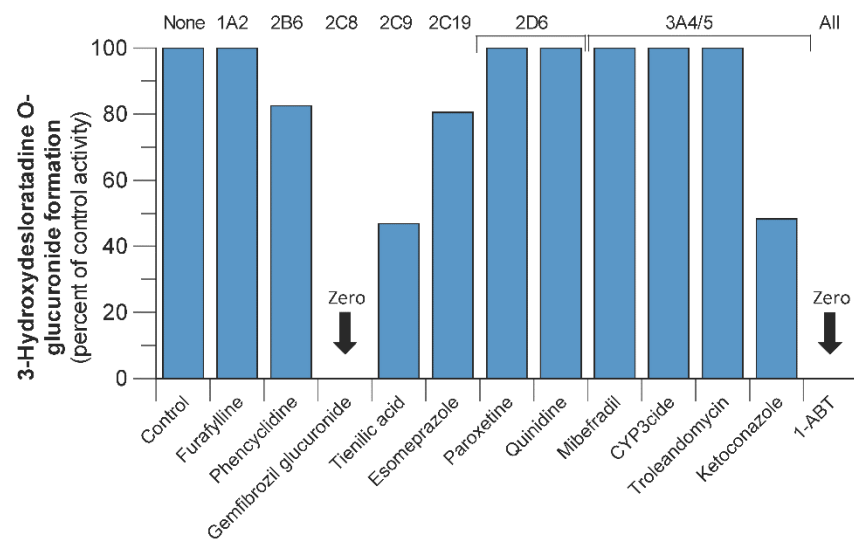
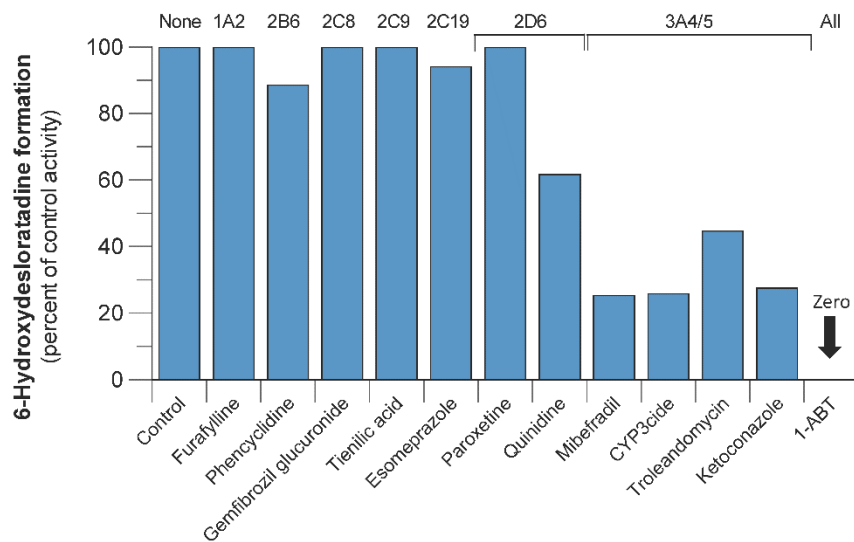
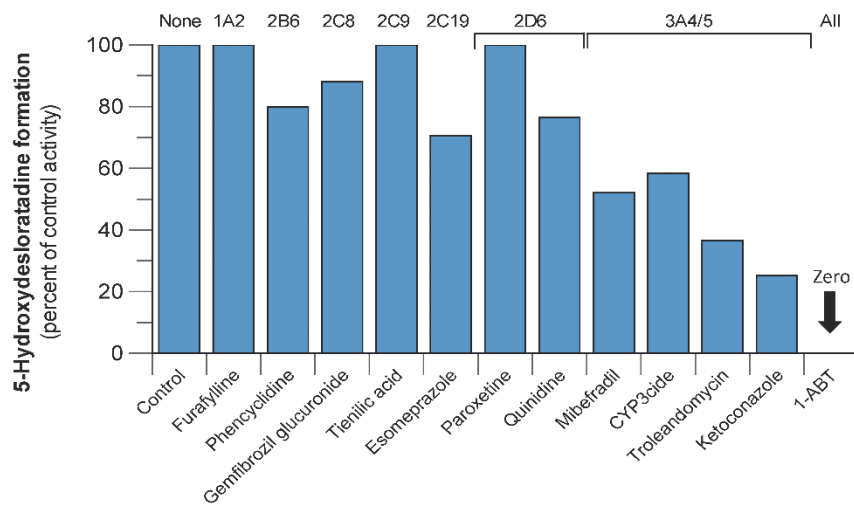


Figure 5.6. The effect of various P450 chemical inhibitors on 5-hydroxydesloratadine, 6-hydroxydesloratadine and 3-hydroxydesloratadine O-glucuronide formation in cryopreserved human hepatocytes (CHH).

Various P450 chemical inhibitors were incubated with CHH (1 million cells/mL) for 30 min prior to the addition of 10 μ M desloratadine followed by incubation for 2 h and analysis of 5-, 6-hydroxydesloratadine, and 3-hydroxydesloratadine O-glucuronide was conducted as described in *Chapter 2*.

5.6. Correlation of 3-hydroxydesloratadine formation with known CYP2C8 activities.

Hepatocytes from nine individual human donors with a range of CYP2C8 activity towards amodiaquine and paclitaxel; and levomedetomidine activity (UGT2B10) were assessed for their ability to form 3-hydroxydesloratadine, as described in *Chapter 2*. As shown in Figure 5.7, the sample-to-sample variation in the 3-hydroxylation of desloratadine (1 and 10 μM) correlated well with the 6 α -hydroxylation of paclitaxel (1 and 10 μM), r^2 values of 0.84 and 0.90 (at 1 and 10 μM) and with the N-dealkylation of amodiaquine, with r^2 values of 0.84 and 0.70 (at 1 and 10 μM). When CYP2C8 activity was correlated to both UGT2B10 activity and 3-hydroxydesloratadine formation at 1 μM substrate concentrations, r^2 values of 0.75 (with amodiaquine) and 0.73 (with paclitaxel) were obtained (Figure 5.8). As expected, amodiaquine and paclitaxel activities highly correlated with each other, with r^2 values of 0.77 and 0.80 (at 1 and 10 μM), as shown in Figure 5.9.

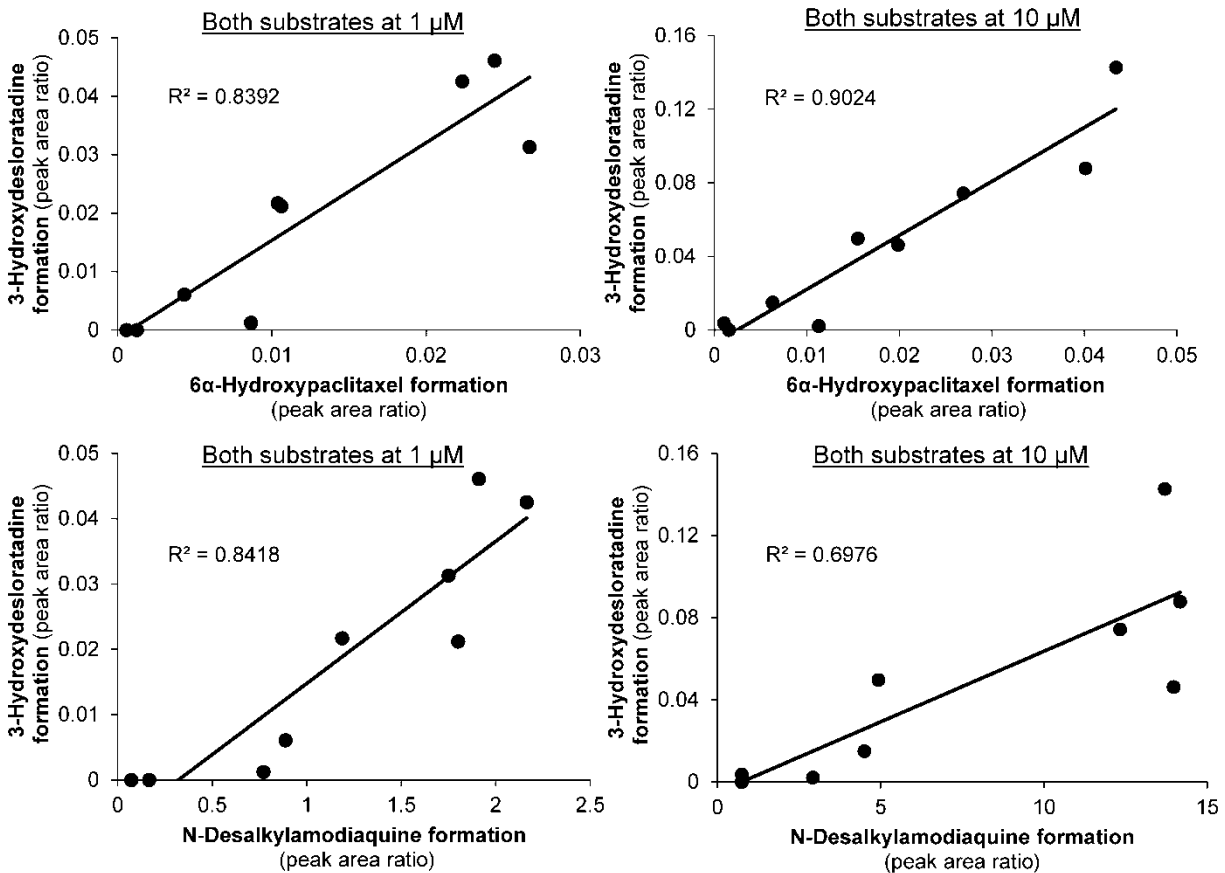


Figure 5.7. Correlation between CYP2C8 activity and 3-hydroxydesloratadine formation in individual donor cryopreserved human hepatocytes (CHH)

As described in *Chapter 2*, individual donor CHH from nine donors with varying CYP2C8 activity were incubated (1 million cells/mL) with 1 or 10 μM amodiaquine, paclitaxel, and desloratadine for 10 min, 30 min and 2 h respectively.

All substrates at 1 μ M

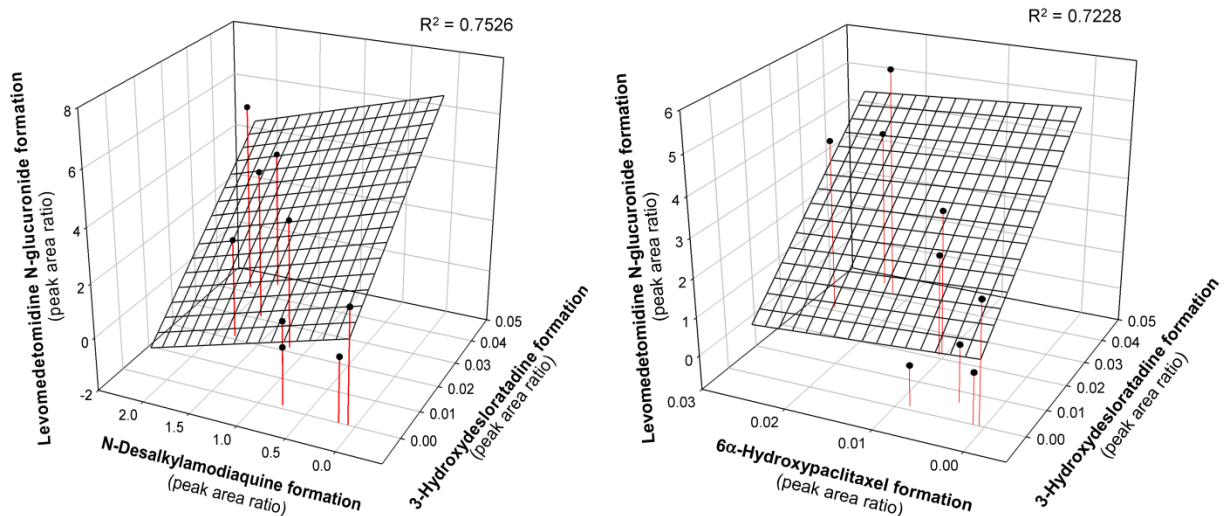


Figure 5.8. Correlation between CYP2C8 activity, UGT2B10 activity and 3-hydroxydesloratadine formation in individual donor cryopreserved human hepatocytes (CHH)

Individual donor CHH from nine donors were assessed for CYP2C8 activity (1 μ M amodiaquine, left panel; or 1 μ M paclitaxel, right panel) incubated for 10 min, UGT2B10 activity (1 μ M levomedetomidine) incubated for 30 min, and 3-hydroxydesloratadine formation (1 μ M desloratadine) in incubated for 2h with 1 million cells/mL as described in the *Chapter 2*.

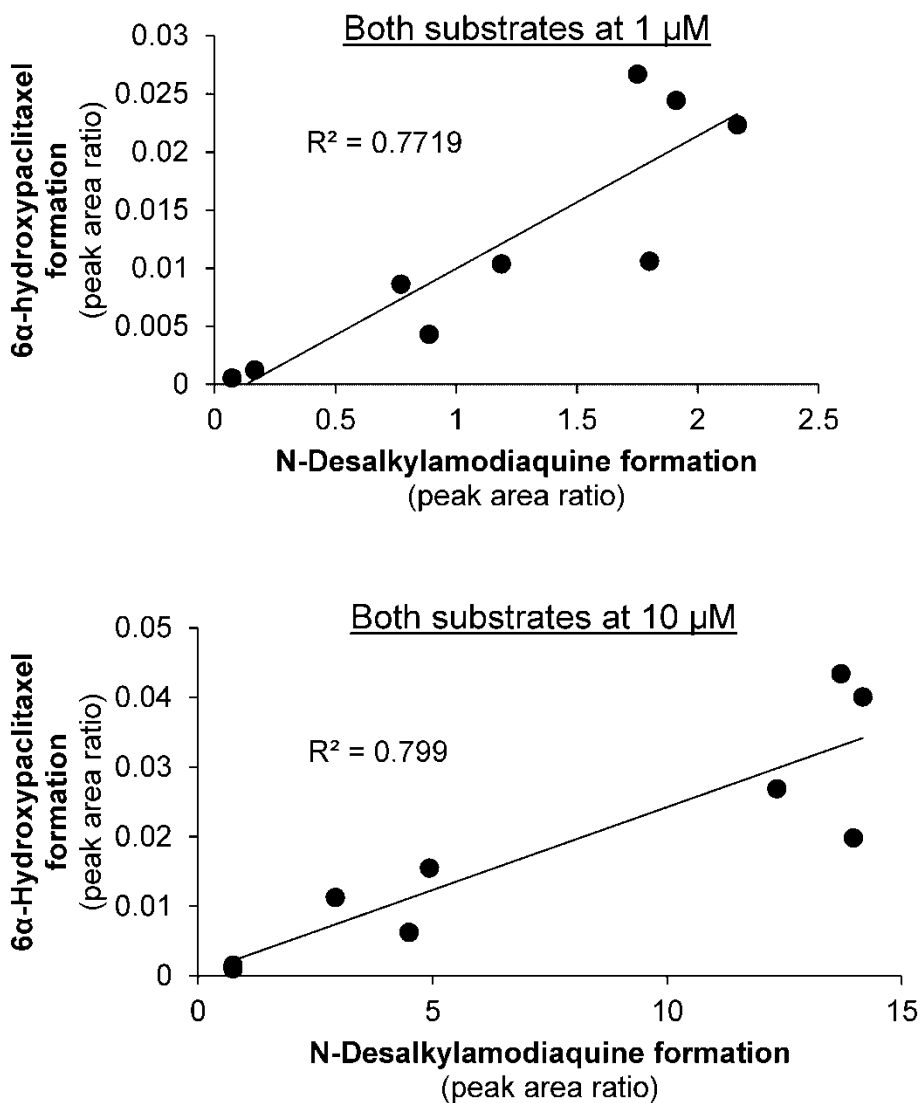


Figure 5.9. Correlation of N-desalkylamodiaquine formation with 6α-hydroxypaclitaxel formation in a panel of individual donor cryopreserved human hepatocytes (CHH).

Individual donor CHH were assessed for CYP2C8 activity with 1 and 10 μM paclitaxel and amodiaquine as described in *Chapter 2*.

5.7. Determining the reason why 3-hydroxydesloratadine forms in hepatocytes but not in subcellular fractions.

As a first approach to understand why CYP2C8 in CHH could convert desloratadine to 3-hydroxydesloratadine whereas HLM, HS9 and recombinant P450 could not, I examined the role of cell integrity and various cofactors involved in xenobiotic metabolism. As described in *Chapter 2*, CHH were treated with 0.01% saponin (to permeabilize the plasma membrane) or sonication (to completely disrupt the plasma membrane) in media supplemented with 10 μ M desloratadine and various cofactors, NADPH, NADH, FAD, AMP, ATP, and UDP-GlcUA. As shown in Figure 5.10A, when intact CHH were treated with 0.01% saponin, the formation of 3-hydroxydesloratadine was reduced by 90%. Addition of exogenous NADPH did not change the rate of 3-hydroxydesloratadine formation; however addition of UDP-GlcUA and NADPH + UDP-GlcUA partially restored 3-hydroxydesloratadine formation to 22% and 37% of that observed in intact CHH, respectively. Similarly, when CHH were probe sonicated, 3-hydroxydesloratadine formation was almost completely eliminated with only 2.5% activity remaining. Addition of exogenous NADPH here also did not alter the level of 3-hydroxydesloratadine formation; however addition of UDP-GlcUA and NADPH + UDP-GlcUA again partially restored 3-hydroxydesloratadine formation to 15% and 34% of that observed in intact CHH, respectively. To ascertain whether a similar combination of cofactors could confer desloratadine 3-hydroxylase activity on subcellular fractions, HLM (0.1 and 1 mg/mL) and HS9 (0.5 and 5 mg/mL) were incubated with 10 μ M desloratadine for up to 6 h with NADPH and/or UDP-GlcUA, as described in *Chapter 2*. With either of these subcellular fractions, only the addition of a combination of NADPH + UDP-GlcUA resulted in

3-hydroxydesloratadine formation; addition of NADPH alone or UDP-GlcUA alone did not. Representative data from 1 mg/mL HLM and 5 mg/mL S9 are shown in Figure 5.10B (0.1 mg/mL HLM and 0.5 mg/mL HS9 data were similar and are shown in Figure 5.11). The addition of several other cofactors (NADH, FAD, AMP and ATP) had no effect on the formation of 3-hydroxydesloratadine in sonicated or permeabilized CHH or in HLM or HS9 (data not shown).

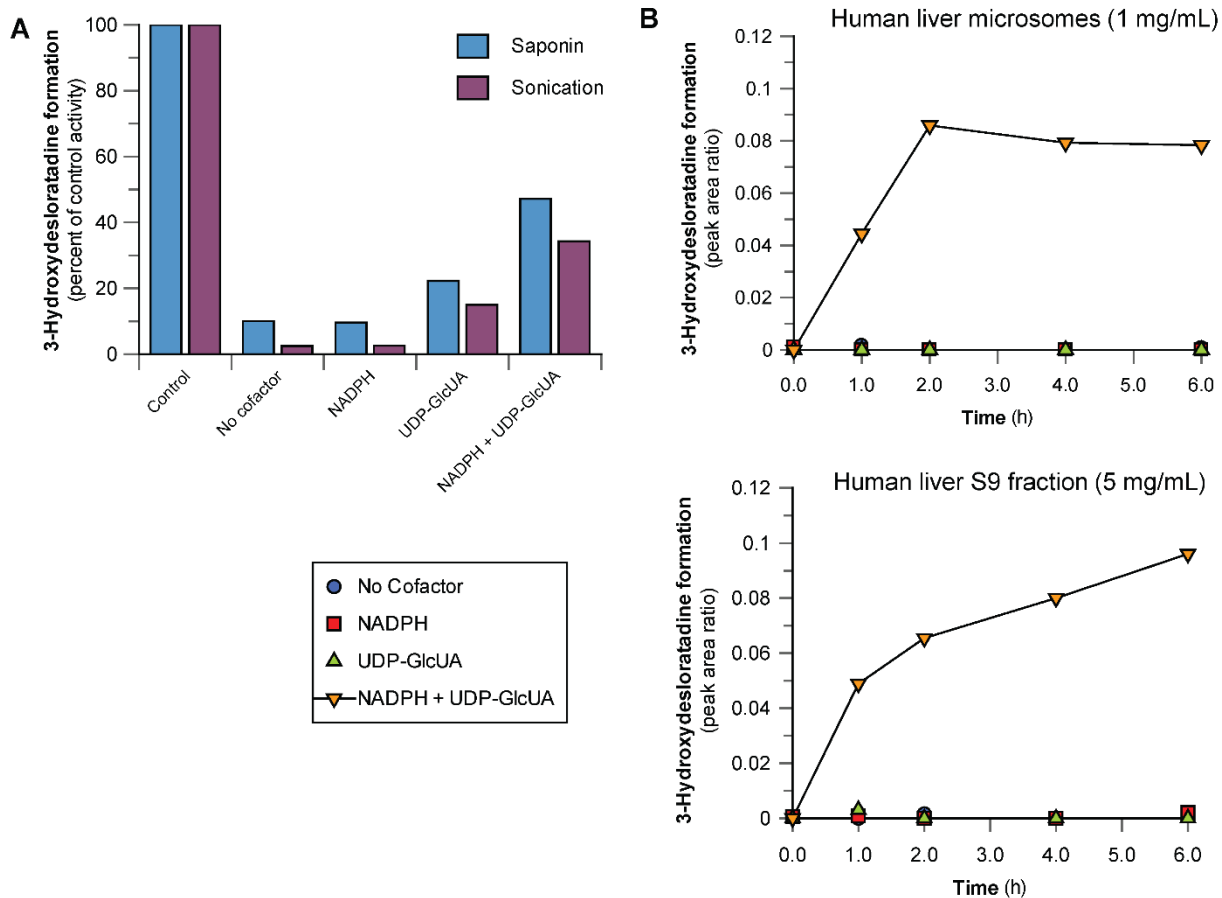


Figure 5.10. Formation of 3-hydroxydesloratadine in saponin treated or sonicated cryopreserved human hepatocytes (CHH) followed by addition of NADPH and/or UDP-GlcUA.

As shown in panel A, CHH (1 million cells/mL) were either pre-treated with 0.01% saponin or probe sonicated followed by addition of 0.1 mM NADPH and/or 1 mM UDPGA and incubation with 10 μ M desloratadine for 2 h. Panel B shows the formation of 3-hydroxydesloratadine in subcellular fractions, namely human liver microsomes (HLM; 1 mg/mL) and human S9 fraction (HS9; 5 mg/mL) as assessed over 6 h with or without 1 mM NADPH and/or 10 mM UDP-GlcUA.

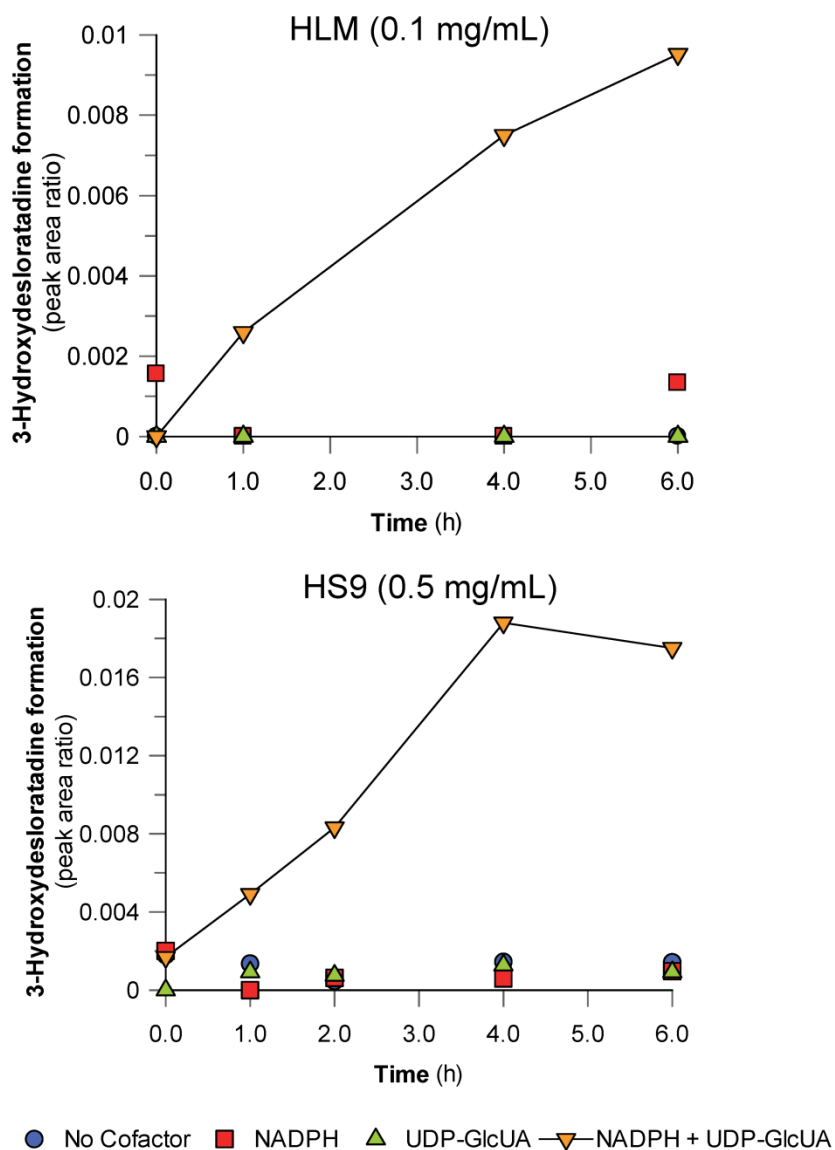


Figure 5.11. Time course of 3-hydroxydesloratadine formation in HLM (0.1 mg/mL) and HS9 (1 mg/mL) with or without NADPH and/or UDP-GlcUA.

HLM (0.1 mg/mL) and HS9 (0.5 mg/mL) were incubated with 10 μ M in a time course up to 6 h with and without the addition of NADPH and/or UDP-GlcUA, as described in *Chapter 2*.

5.8. Identification of the UGT enzymes involved in 3-hydroxydesloratadine formation.

Having established that a combination of both UDP-GlcUA and NADPH was necessary to support 3-hydroxydesloratadine formation by disrupted CHH or subcellular fractions, I sought to determine the specific UGT enzyme involved in 3-hydroxydesloratadine formation. As described in the *Chapter 2*, a panel of 13 recombinant UGT enzymes (at 0.125 mg/mL each) supplemented with recombinant CYP2C8 (25 pmol/mL) was incubated for 2 h with 1 or 10 μ M desloratadine in the presence of both NADPH with UDP-GlcUA. As shown in Figure 5.12, 3-hydroxydesloratadine was formed by a combination of UGT2B10 and CYP2C8. Formation of 3-hydroxydesloratadine was not observed when CYP2C8 was incubated with any other recombinant UGT enzyme.

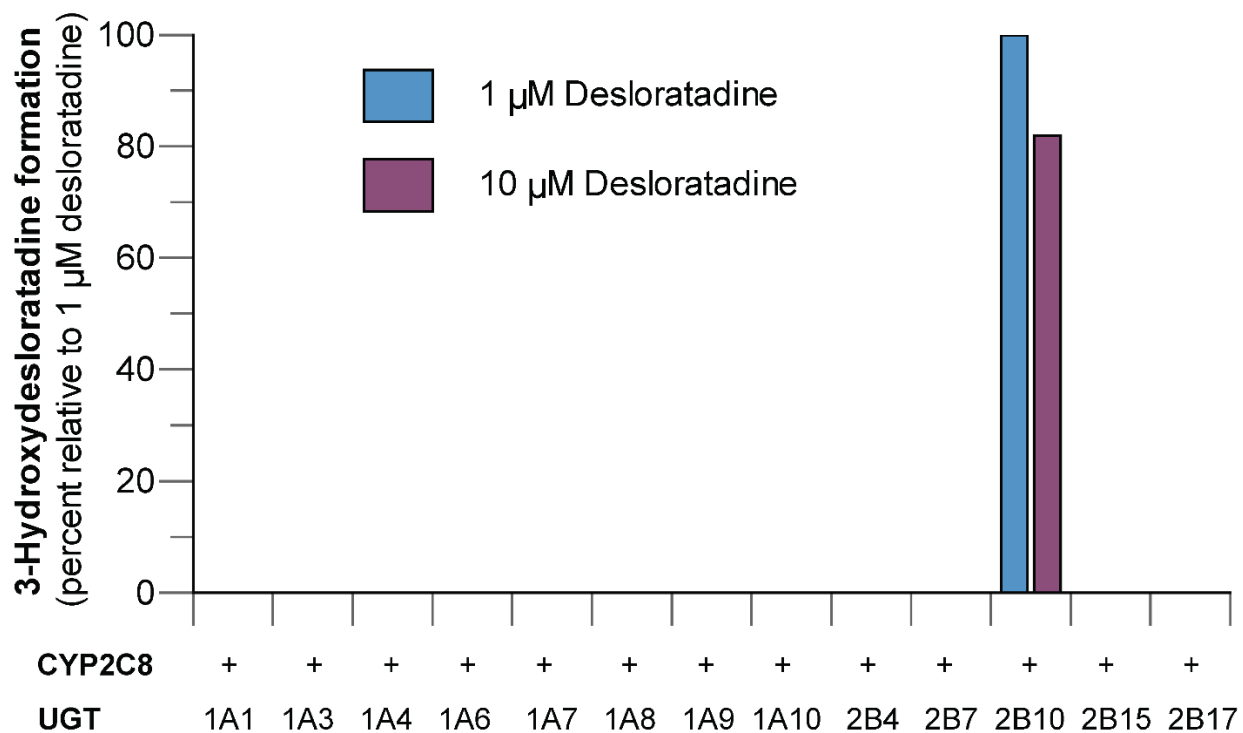


Figure 5.12. Assessment of 3-hydroxydesloratadine formation with a panel of recombinant UGT enzymes supplemented with recombinant CYP2C8.

Thirteen recombinant UGT enzymes (at 0.125 mg/mL) were assessed for their ability to form 3-hydroxydesloratadine when supplemented with recombinant CYP2C8 (25 pmol/mL) and 1 mM NADPH with 10 mM UDP-GlcUA, followed by a 2 h incubation with 1 or 10 μ M desloratadine.

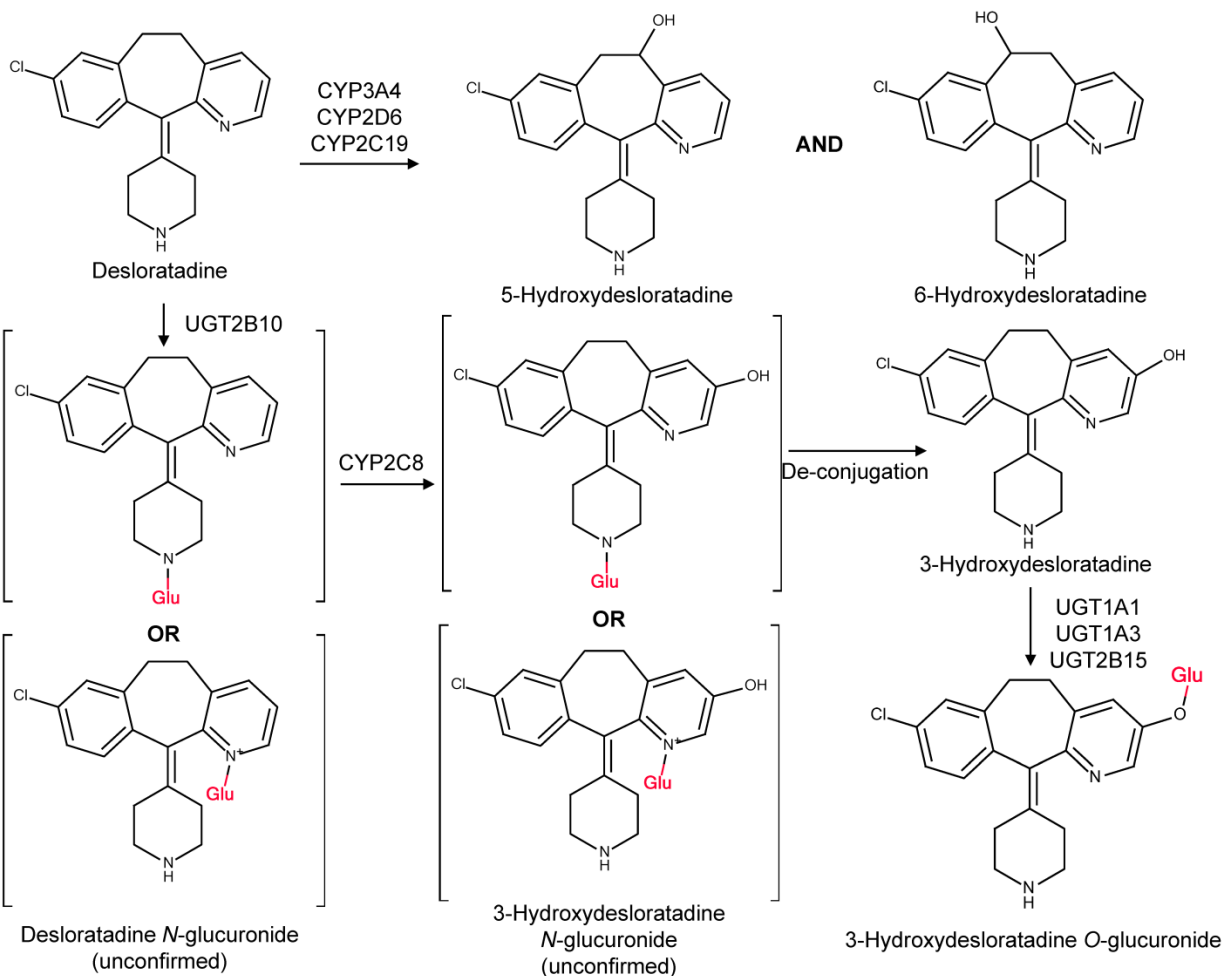


Figure 5.13. Proposed metabolic scheme for the formation of 3-hydroxydesloratadine and its glucuronide in human hepatocytes and liver subcellular fractions.

The proposed metabolic pathway for desloratadine metabolism based on this study. The conversion of 3-hydroxydesloratadine to 3-hydroxydesloratadine glucuronide was previously described by Ghosal et al. (2004).

DISCUSSION

Loratadine (Claritin[®]), first introduced to the U.S. market in 1993, is metabolized primarily by CYP3A4 and CYP2D6 to its pharmacologically active major metabolite desloratadine (Yumibe et al., 1995; Yumibe et al., 1996; Dridi and Marquet, 2013). As a drug in its own right, desloratadine (Clarinet[®] in the US, Aeries[®] in Europe) received FDA approval in 2001. It has long been known that the major circulating metabolite of desloratadine in humans is 3-hydroxydesloratadine, formed by hydroxylation of the pyridine ring (Schering-Plough, 2001). However, as acknowledged in the package insert, the enzyme or enzymes responsible for forming 3-hydroxydesloratadine was unknown when desloratadine was approved by the FDA in 2001 and has remained unknown since that time. Although presumably formed by P450, conventional in vitro test systems do not convert desloratadine to the 3-hydroxy metabolite (Ghosal et al., 2009). In the present study, I confirmed that human liver microsomes (HLM), human S9 fraction (HS9) and recombinant human P450 enzymes all failed to convert desloratadine to 3-hydroxydesloratadine but I demonstrated for the first time that cryopreserved human hepatocytes (CHH) are capable of forming the 3-hydroxy metabolite (Figure 5.1 and Table 5.1). In vitro formation of this previously elusive metabolite allowed us to investigate the enzymology surrounding its formation. The formation of 3-hydroxydesloratadine by CHH conformed to simple Michaelis-Menten kinetics with a V_{max} of 1.26 pmol/min/million cells and a K_m of 1.57 μ M (Figure 5.2), which is consistent with the reported plasma C_{max} of desloratadine in humans (1.3 μ M) (Schering-Plough, 2001). These results strongly suggest that hepatic metabolism is responsible for the formation of 3-hydroxydesloratadine and are consistent with the urinary and biliary excretion of this

metabolite (and its *O*-glucuronide) in humans (Ramanathan et al., 2006; Ramanathan et al., 2007). Data on the metabolism of desloratadine in nonclinical species are limited, with 5- and 6-hydroxydesloratadine reported as the major excreted metabolites in mouse, rat and monkey. In contrast to the situation in humans, 3-hydroxydesloratadine was found to be a minor or trace plasma, urinary and fecal metabolite in nonclinical species (Ramanathan et al., 2005; Ramanathan et al., 2006). In my assessment of desloratadine metabolism in hepatocytes from different species (Figure 5.3), 3-hydroxydesloratadine was observed at low levels in mouse, rat and monkey hepatocytes, consistent with previously reported *in vivo* findings (Ramanathan et al., 2006). However, rabbit, dog and human were able to form the 3-hydroxy metabolite in incubations at a pharmacologically relevant concentration (1 μ M desloratadine), whereas only rabbit and human formed it at the high concentration (10 μ M desloratadine). It is unclear whether rabbits were evaluated as nonclinical metabolism species during desloratadine development; however, my data suggest they may be appropriate species to model 3-hydroxydesloratadine exposure. Formation of 5- and 6-hydroxydesloratadine was faster in hepatocytes from all nonclinical species tested compared with human hepatocytes (Figure 5.4), consistent with the *in vivo* data (Ramanathan et al., 2005; Ramanathan et al., 2006). In the present study, formation of 5- and 6-hydroxydesloratadine was primarily mediated by recombinant CYP1A1, CYP2D6 and CYP3A4, confirming previously reported findings (Ghosal et al., 2009). Chemical inhibition experiments in CHH confirmed the involvement of CYP3A4 in 5-hydroxydesloratadine formation, and likewise confirmed involvement of both CYP2D6 and CYP3A4 in 6-hydroxydesloratadine formation (Table 5.1 and Figure 5.6).

The non-specific inhibitor 1-ABT markedly inhibited (98%) the formation of 3-hydroxydesloratadine by CHH, confirming expectations that this reaction is catalyzed by P450 (Figure 5.5A). Marked inhibition (91%) was also observed with gemfibrozil glucuronide (Figure 5.5A). Gemfibrozil glucuronide is an irreversible (mechanism-based) inhibitor of CYP2C8 and is widely used as an in vitro diagnostic inhibitor of this enzyme (Ogilvie et al., 2006; Parkinson et al., 2011; Kazmi et al., 2014d). To confirm CYP2C8 involvement in 3-hydroxydesloratadine formation, a panel of known CYP2C8 inhibitors or substrates (competitive inhibitors) was evaluated (Figure 5.5B), namely, montelukast, repaglinide, cerivastatin, clopidogrel glucuronide, and both gemfibrozil and gemfibrozil glucuronide (Bidstrup et al., 2003; Walsky et al., 2005; Ogilvie et al., 2006; Tornio et al., 2014). Strong inhibition of 3-hydroxydesloratadine formation was observed with all CYP2C8 inhibitors and correlated well with the degree of inhibition in the metabolism of two CYP2C8 substrates (paclitaxel and amodiaquine), supporting CYP2C8 as the P450 enzyme responsible for 3-hydroxydesloratadine formation. A comparison of CYP2C8 activity in nine individual samples of human hepatocytes demonstrated high correlation ($r^2 = 0.7-0.9$) between 3-hydroxydesloratadine formation and both amodiaquine N-dealkylation and paclitaxel 6 α -hydroxylation (Figure 5.7).

The results presented so far seem paradoxical. They raise the question: If CYP2C8 is the major enzyme responsible for converting desloratadine to 3-hydroxydesloratadine in human hepatocytes, based on chemical inhibition and correlation analysis, why is no 3-hydroxydesloratadine formed by HLM, HS9 or recombinant CYP2C8? I hypothesized that perhaps cellular integrity or the presence of specific cofactors was critical for

3-hydroxydesloratadine formation. In support of this possibility, I found that permeabilizing the plasma membrane of hepatocytes with saponin or completely disrupting the membrane by sonication greatly reduced 3-hydroxydesloratadine formation (Figure 5.10A). Addition of various cofactors to permeabilized/sonicated hepatocytes revealed that formation of 3-hydroxydesloratadine could be partially restored by the addition of both NADPH and UDP-GlcUA. Modest recovery was also observed in permeabilized/sonicated hepatocytes supplemented with only UDP-GlcUA presumably because there was sufficient endogenous NADPH to support some 3-hydroxy metabolite formation. Subsequent experiments with HLM and HS9 (Figure 5.10B and Figure 5.11) confirmed the requirement of both NADPH and UDP-GlcUA for the formation of 3-hydroxydesloratadine.

These results suggested that, in addition to oxidation by CYP2C8, glucuronidation plays a key role in the formation of 3-hydroxydesloratadine. To explore this possibility further, desloratadine was incubated with recombinant CYP2C8 in the absence or presence of a panel of recombinant UGT enzymes (with NADPH and UDP-GlcUA as cofactors). In the absence of any UGT enzyme, CYP2C8 did not form 3-hydroxydesloratadine but did so in the presence of UGT2B10 (Figure 5.12). These results suggest that desloratadine is glucuronidated by UGT2B10 and that desloratadine glucuronide, not desloratadine itself, is the substrate that undergoes 3-hydroxylation by CYP2C8. Furthermore, the results suggest that the glucuronide moiety introduced by UGT2B10 is cleaved during or shortly after metabolism by CYP2C8. When the sample to sample variation of CYP2C8 activities

were correlated to UGT2B10 activity and 3-hydroxydesloratadine formation, good correlation was achieved, with $r^2 = 0.73-0.75$ (Figure 5.8).

A proposed metabolic scheme for 3-hydroxydesloratadine formation is shown in Figure 5.13. The first step is proposed as formation of desloratadine *N*-glucuronide by UGT2B10, followed by hydroxylation to 3-hydroxydesloratadine *N*-glucuronide by CYP2C8, with subsequent de-conjugation to 3-hydroxydesloratadine. Efforts to isolate and characterize the proposed intermediary metabolites are currently underway. An *N*-glucuronide is proposed as the initial metabolite because there are no hydroxyl or thiol groups available for direct conjugation. UGT2B10 is one of two enzymes, the other being UGT1A4, renowned for their ability to catalyze the *N*-glucuronidation of drugs, with UGT2B10 being a high affinity/low capacity enzyme UGT1A4 being a low affinity/high capacity enzyme (Zhou et al., 2010; Parkinson et al., 2013). Ketotifen, a structural analog of desloratadine, is known to be *N*-glucuronidated at the piperidine ring to a quaternary *N*-glucuronide by UGT2B10 and UGT1A4. Furthermore, *N*-glucuronidation of ketotifen is a prominent reaction in rabbits and humans, the two species whose hepatocytes catalyzed the highest rate of formation of 3-hydroxydesloratadine (Kato et al., 2013; Bolleddula et al., 2014). It has been previously reported that rabbits may be a particularly useful species for nonclinical studies of drugs that undergo *N*-glucuronidation in humans (Chiu and Huskey, 1998). However, *N*-glucuronidation by UGT2B10 on the pyridine moiety of desloratadine cannot be ruled out and has been shown to occur in the case of nicotine and cotinine glucuronidation (Murphy et al., 2014).

The ability of CYP2C8 to metabolize a glucuronide conjugate is well established (Parkinson et al., 2013). For example, whereas the 4'-hydroxylation of diclofenac (parent drug) is catalyzed by CYP2C9, the 4'-hydroxylation of diclofenac acyl glucuronide is catalyzed by CYP2C8 (Kumar et al., 2002). This same pattern, where the aglycone (typically a small acidic substrate) is not metabolized by CYP2C8 (and in some cases is metabolized by CYP2C9) whereas the glucuronide metabolite (a large acidic substrate) is metabolized by CYP2C8, has been reported for estradiol 17-O- β -glucuronide and the acyl glucuronide conjugates of naproxen, the PPAR α agonist MRL-C, and gemfibrozil (Delaforge et al., 2005; Kochansky et al., 2005; Ogilvie et al., 2006; Parkinson et al., 2013). In the case of gemfibrozil, the CYP2C8-mediated hydroxylation of its 1-O- β -glucuronide forms a benzyl radical intermediate that causes irreversible inhibition of CYP2C8 (Ogilvie et al., 2006; Baer et al., 2009).

The conversion of desloratadine by UGT2B10 to an *N*-glucuronide that is subsequently hydroxylated by CYP2C8 is consistent with the known properties of these enzymes. Nevertheless, the formation of 3-hydroxydesloratadine is unusual because no 3-hydroxylation is detectable in the absence of glucuronidation and because the *N*-glucuronide is cleaved during or shortly after CYP2C8-dependent hydroxylation. Interestingly, while 3-hydroxydesloratadine is produced from an *N*-glucuronide (formed by UGT2B10 and cleaved following hydroxylation by CYP2C8), 3-hydroxydesloratadine itself is subsequently converted to an *O*-glucuronide (at the 3-hydroxy position) by UGT1A1, UGT1A3 and UGT2B15 (Ghosal et al., 2004).

It is unclear whether there is any potential for drug-drug interactions (DDIs) with desloratadine as it has a large therapeutic safety margin. As a perpetrator, desloratadine has been shown not to be an inhibitor of CYP1A2, CYP2C9, CYP2C19, CYP2D6 or CYP3A4 (Barecki et al., 2001). However, to my knowledge, inhibition of CYP2C8 and UGT2B10 has not been evaluated, so it is unclear whether desloratadine could cause any clinically-relevant interactions with substrates of these enzymes. A recent clinical study examining the effect of desloratadine on montelukast serum levels found no significant difference in montelukast serum levels in fixed-dose combination with desloratadine (Cingi et al., 2013). All other relevant studies have examined the pharmacodynamic/pharmacokinetic interaction potential of desloratadine with CYP2D6 and CYP3A4 substrates, and desloratadine was found to have limited potential for DDI (Gupta et al., 2001; Banfield et al., 2002a; Banfield et al., 2002b; Gupta et al., 2004). With respect to special populations, patients with moderate hepatic impairment have been shown to have elevated levels of desloratadine (2.4-fold increase in AUC); however it has been reported that 3-hydroxydesloratadine exposure was similar between hepatically-impaired and normal patients (Gupta et al., 2007).

The pharmacogenetic basis for the 3-hydroxydesloratadine poor metabolizer (PM) phenotype has remained a mystery. It has been reported that the polymorphism surrounding 3-hydroxydesloratadine formation occurs in approximately 6% of the general population and at a frequency of 17% in African Americans, with PMs having approximately 6-fold greater systemic exposure than extensive metabolizers (EMs) (Prenner et al., 2006). My results suggest that CYP2C8 and/or UGT2B10 polymorphism

may be responsible for the poor metabolizer phenotype. A large number of CYP2C8 genetic polymorphisms have been identified, with CYP2C8*2, CYP2C8*3, CYP2C8*4, CYP2C8*8 and CYP2C8*14 alleles shown to have decreased functional activity (Dai et al., 2001; Bahadur et al., 2002; Hichiya et al., 2005; Gao et al., 2010; Hanioka et al., 2010; Jiang et al., 2011). However, little is currently known about UGT2B10 polymorphisms, although the UGT2B10*2 allele has been shown to correspond to a functional decrease in nicotine and cotinine glucuronide formation (Chen et al., 2007). Further studies will be necessary to establish whether genetic polymorphisms of CYP2C8 and/or UGT2B10 can account for the desloratadine PM phenotype.

In summary, the following evidence suggests that the conversion of desloratadine to 3-hydroxydesloratadine is mediated by CYP2C8 in conjunction with UGT2B10:

1. The formation of 3-hydroxydesloratadine by human hepatocytes is inhibited by reversible and irreversible inhibitors of CYP2C8;
2. In human hepatocytes, the sample to sample variation in 3-hydroxydesloratadine formation correlates with CYP2C8 activity towards amodiaquine and paclitaxel;
3. Human liver microsomes and S9 fraction do not form 3-hydroxydesloratadine unless supplemented with both NADPH and UDP-GlcUA;
4. Recombinant CYP2C8 does not form 3-hydroxydesloratadine unless co-incubated with recombinant UGT2B10 and both NADPH and UDP-GlcUA;
5. No other pair of recombinant CYP and UGT enzyme converted desloratadine to 3-hydroxydesloratadine.

I were unable to detect either desloratadine *N*-glucuronide (formed by UGT2B10) or 3-hydroxydesloratadine *N*-glucuronide (the initial metabolite formed by CYP2C8). These glucuronides appear to be very unstable, which is a characteristic of certain other *N*-glucuronides (Ciotti et al., 1999). Despite this limitation, the identification of CYP2C8 in combination with UGT2B10 in the formation of 3-hydroxydesloratadine contributes to our understanding of the long-standing mystery surrounding the enzymology of 3-hydroxydesloratadine formation in humans, providing a pathway for future investigation of the genetic basis for the desloratadine poor metabolizer phenotype.

**CHAPTER 6 : FURTHER CHARACTERIZATION OF THE METABOLISM
OF DESLORATADINE AND ITS CYTOCHROME P450 AND UDP-
GLUCURONOSYLTRANSFERASE (UGT) INHIBITON POTENTIAL:
IDENTIFICATION OF DESLORATADINE AS A SELECTIVE UGT2B10
INHIBITOR**

ABSTRACT

Desloratadine (Clarinet[®]), the major active metabolite of loratadine (Claritin[®]), is a non-sedating antihistamine used for the treatment of seasonal allergies and hives. In the preceding chapter I reported that the formation of 3-hydroxydesloratadine, the major human metabolite of desloratadine, involves three sequential reactions, namely *N*-glucuronidation by UGT2B10 followed by 3-hydroxylation by CYP2C8 followed by deconjugation (rapid, non-enzymatic hydrolysis of the *N*-glucuronide). In this chapter I assessed the perpetrator potential of desloratadine based on in vitro studies of its inhibitory effects cytochrome P450 (CYP) and UDP-glucuronosyltransferase (UGT) enzymes in human liver microsomes (HLM). Desloratadine (10 μ M) caused no inhibition (<15%) of CYP1A2, CYP2C8, CYP2C9, and CYP2C19 and weak inhibition (32-48%) of CYP2B6, CYP2D6 and CYP3A4/5. In cryopreserved human hepatocytes (CHH), which can form the CYP2C8 substrate desloratadine *N*-glucuronide, desloratadine did not inhibit the CYP2C8-dependent metabolism of paclitaxel or amodiaquine. Assessment of UGT inhibition identified desloratadine as a potent and selective inhibitor of UGT2B10 (IC_{50} value of 1.6 μ M). Chemical inhibition of UGT enzymes in HLM demonstrated that nicotine (UGT2B10 inhibitor) but not hecogenin (UGT1A4 inhibitor) completely inhibited the conversion of desloratadine (1 μ M) to 3-hydroxydesloratadine in HLM fortified with both NADPH and UDP-glucuronic acid. Overall, the results of this study confirm the role of UGT2B10 in 3-hydroxydesloratadine formation and identify desloratadine as a selective in vitro inhibitor of UGT2B10.

INTRODUCTION

Desloratadine (Clarinet[®]), is a long lasting, non-sedating, second-generation, selective H₁-receptor histamine antagonist commonly used for the treatment of seasonal allergies (allergic rhinitis) and chronic hives (chronic idiopathic urticaria) (Geha and Meltzer, 2001; Henz, 2001). Desloratadine is a major and pharmacologically active metabolite of the antihistamine loratadine (Claritin[®]) and is formed primarily by CYP3A4 and to a lesser extent by CYP2D6 (Yumibe et al., 1995; Yumibe et al., 1996; Dridi and Marquet, 2013). In 2001, desloratadine was approved as a drug in its own right; however, at the time of its approval, the enzymology surrounding its metabolism was unknown (Schering-Plough, 2001). In humans, desloratadine is converted to 3-hydroxydesloratadine (by hydroxylation of the pyridine ring) followed by O-glucuronidation to 3-hydroxydesloratadine O-glucuronide. Both 3-hydroxydesloratadine and its glucuronide conjugate are major in vivo metabolites excreted in approximately equal amounts in urine and feces (Ramanathan et al., 2007). Conventional in vitro systems such as recombinant P450 enzymes, human liver microsomes (HLM) and human liver S9 fractions do not convert desloratadine to 3-hydroxydesloratadine; hence, its enzymology and basis for certain individuals being identified as poor metabolizers of desloratadine have remained a mystery for many years (Ghosal et al., 2009). In Chapter 5, I demonstrated that cryopreserved human hepatocytes (CHH) can form 3-hydroxydesloratadine, as can HLM provided they are supplemented with both NADPH and UDP-glucuronic acid (UDP-GlcUA). As shown in Figure 6.1, formation of 3-hydroxydesloratadine involves three sequential reactions: (1) *N*-glucuronidation of desloratadine by UGT2B10; (2) 3-hydroxylation of desloratadine *N*-glucuronide by CYP2C8, and (3) de-conjugation of 3-

hydroxydesloratadine *N*-glucuronide (rapid non-enzymatic hydrolysis of the glucuronide. The *N*-glucuronide of desloratadine is highly unstable (both before and after 3-hydroxylation by CYP2C8). I was unable to detect desloratadine *N*-glucuronide or 3-hydroxydesloratadine *N*-glucuronide by LC-MS/MS in the studies described in Chapter 5. Instability is a characteristic property of certain *N*-glucuronides (Ciotti et al., 1999).

The draft FDA guidance (FDA, 2012) and final EMA guidelines (EMA, 2013) on drug-drug interactions (DDIs) both recommend that the perpetrator potential of investigational drugs be assessed by evaluating their ability to inhibit CYP and UGT enzymes. These regulatory agencies further require that, in the case of CYP enzymes, all investigational drugs be evaluated for their ability to cause time-dependent or metabolism-dependent inhibition (Grimm et al., 2009). The panel of enzymes recommended for testing and the types of inhibition to be evaluated have expanded since the FDA issued its first *Guidance for Industry* on drug interactions (FDA, 1997). Desloratadine was evaluated for its ability to inhibit CYP enzymes shortly after the FDA issued its first drug interaction guidance (Barecki et al., 2001). This study evaluated desloratadine and 3-hydroxydesloratadine as reversible inhibitors of CYP1A2, CYP2C9, CYP2C19, CYP2D6 and CYP3A4 but it did not evaluate the potential for irreversible (time-dependent) inhibition, nor did it evaluate inhibition of CYP2B6 or CYP2C8 (all of which were not recommended by the FDA at the time the study was performed). Furthermore, desloratadine was not evaluated as an inhibitor of UGT enzymes. In view of the role of CYP2C8 and UGT2B10 in the metabolism of desloratadine, it was of interest to evaluate desloratadine as a reversible and irreversible inhibitor of the 7 P450 enzymes currently recommended by testing by the FDA (namely, CYP1A2, 2B6, 2C8, 2C9, 2C19, 2D6 and 3A4/5) and as a reversible inhibitor of

multiple UGT enzymes in HLM (namely, UGT1A1, 1A3, 1A4, 1A6, 1A9, 2B7, 2B10, 2B15 and 2B17). In addition, because the *N*-glucuronide metabolites of desloratadine are highly unstable, I conducted additional (indirect) studies to evaluate whether the *N*-glucuronidation of desloratadine is dependent largely or solely on UGT2B10.

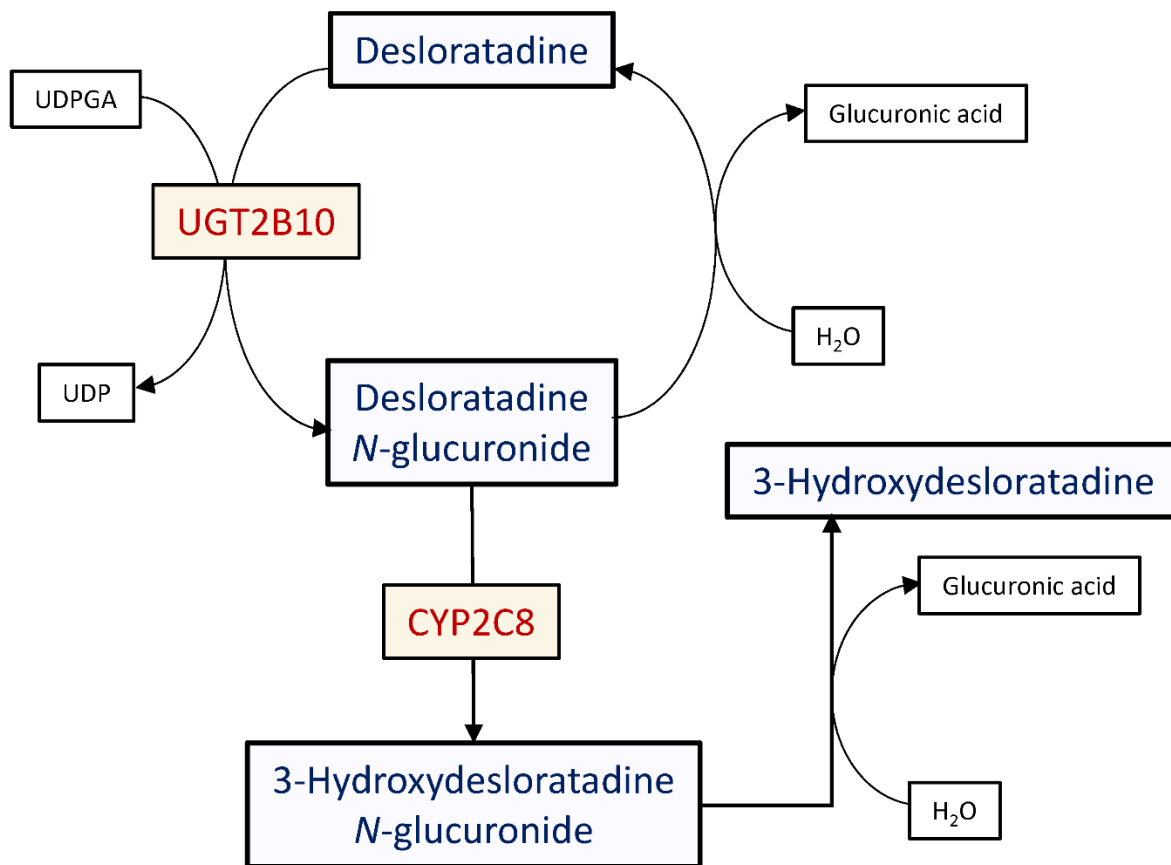


Figure 6.1. The metabolic scheme for the conversion of desloratadine to 3-hydroxydesloratadine

Desloratadine is converted to its corresponding *N*-glucuronide followed by hydroxylation and de-conjugation to 3-hydroxydesloratadine as described in Chapter 5.

RESULTS

6.1. Assessment of desloratadine as an inhibitor of seven P450 enzymes.

To evaluate desloratadine as an inhibitor of P450 enzymes in vitro, desloratadine (10 μ M) was incubated with HLM (\leq 0.1 mg/mL) with and without a 30-min preincubation step in the presence or absence of NADPH. P450 activity was measured with CYP-selective substrates (at a final concentration roughly equal to K_m), as described in *Chapter 2*. As shown in Figure 6.2 and Table 6.1, desloratadine did not inhibit (<15%) CYP1A2, CYP2C8, CYP2C9, or CYP2C19 but caused partial inhibition of CYP2B6 (48%), CYP2D6 (32%) and CYP3A4/5 (44%). Preincubating desloratadine for 30 min with HLM in the absence or presence of NADPH caused little or no increase in P450 inhibition (i.e., there was no evidence of time-dependent or metabolism-dependent inhibition).

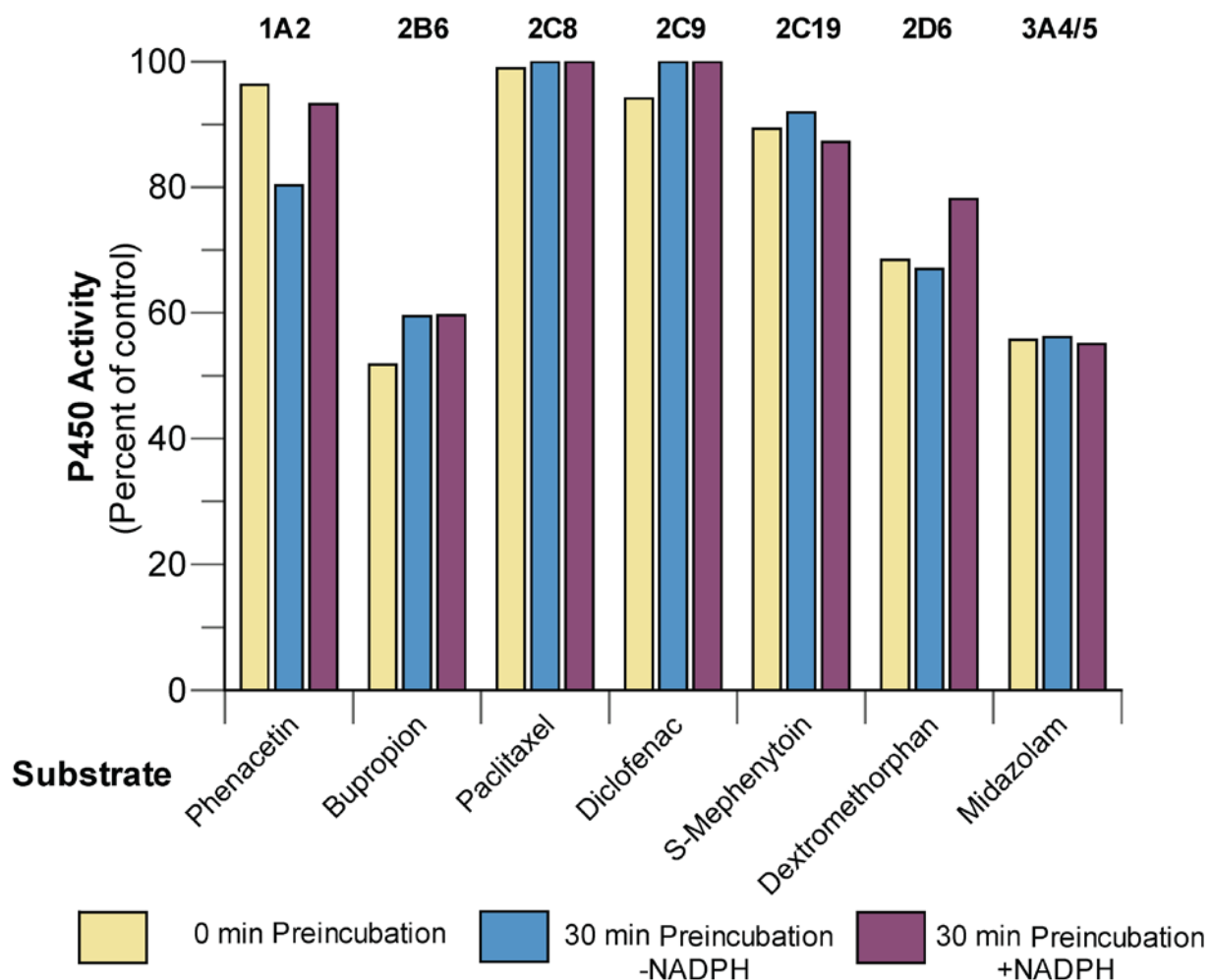


Figure 6.2. Assessment of the inhibition of P450 enzymes by desloratadine.

The P450 inhibition potential of desloratadine (10 μM) was assessed in HLM (≤ 0.1 mg/mL) with and without a 30-min preincubation step in the presence or absence of NADPH, followed by a 5-min incubation with a CYP-selective marker substrate (at a concentration approximately equal to its K_m) as indicated in the figure. Details of the experimental procedures are described in *Chapter 2*.

Table 6.1. Assessment of desloratadine as an inhibitor of P450 and UGT enzymes in pooled human liver microsomes (HLM)

Enzyme	Substrate (concentration)	Inhibition with 10 µM Desloratadine (% activity remaining)			
		Direct inhibition (Zero-min Preincubation)	TDI (30 min preincubation –NADPH)	MDI (30 min preincubation +NADPH)	Barecki et al., 2001 ^a
CYP1A2	Phenacetin (40 µM)	96.3	80.3	93.2	110 ^b
CYP2B6	Bupropion (50 µM)	51.8	59.5	59.6	ND
CYP2C8	Paclitaxel (5 µM)	98.9	117	100	
CYP2C9	Diclofenac (6 µM)	94.1	103	106	106
CYP2C19	S-Mephenytoin (40 µM)	89.3	91.9	87.2	112
CYP2D6	Dextromethorphan (7.5 µM)	68.4	67.0	78.1	86.3
CYP3A4/5	Midazolam (3 µM)	55.7	56.1	55.0	84.0 ^c , 80.0 ^d
UGT1A1	17β-Estradiol (9 µM)	89.7	Not applicable		
UGT1A3	CDCA ^e (20 µM)	92.1			
UGT1A4	Trifluoperazine (12 µM)	88.3			
UGT1A6	1-Naphthol (1 µM)	94.4			
UGT1A9	Propofol (20 µM)	103			
UGT2B7	Morphine (400 µM)	91.2			
UGT2B10	Levomedetomidine (7 µM)	21.6			
UGT2B15	Oxazepam (50 µM)	92.4			
UGT2B17	Testosterone (5 µM)	75.7			

^a Only direct inhibition (0 min preincubation) was evaluated.

^b Substrate used was 7-ethoxyresorufin

^c Substrate used was dextromethorphan

^d Substrate used was testosterone

CDCA: chenodeoxycholic acid; NA: not applicable; ND: no data

6.2. Assessment of desloratadine as an inhibitor of CYP2C8 in human hepatocytes.

As shown in the preceding section (Figure 6.2 and Table 6.1), desloratadine did not inhibit CYP2C8. This enzyme does not metabolize desloratadine but it does metabolize desloratadine *N*-glucuronide. Unfortunately, this *N*-glucuronide is too unstable to perform direct tests of its inhibitory potential. Therefore, desloratadine was evaluated as an inhibitor of CYP2C8 in CHH, which can convert desloratadine to its *N*-glucuronide. In this assay, desloratadine (0.1–100 μM) was incubated with CHH (0.5 million cells/mL) for up to 2 h, after which the activity of CYP2C8 was measured with paclitaxel (10 μM) and amodiaquine (10 μM), as described in *Chapter 2*. As shown in Figure 6.3 and Table 6.1, desloratadine was not a direct or time-dependent inhibitor of CYP2C8 in CHH (IC_{50} values >100 μM).

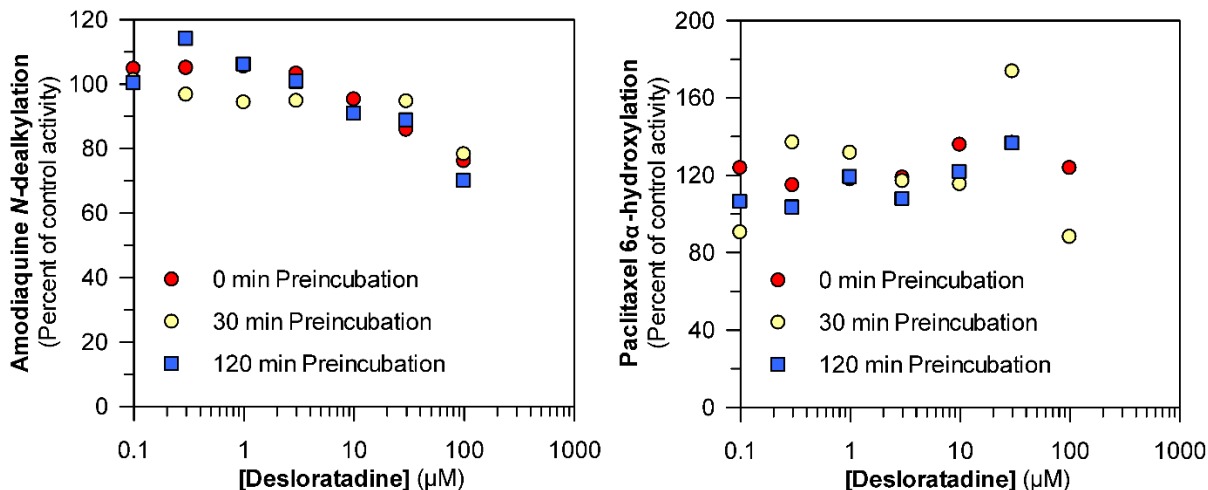


Figure 6.3. Evaluation of desloratadine as an inhibitor of CYP2C8 activity toward amodiaquine (left) and paclitaxel (right) in cryopreserved human hepatocytes

As described in *Chapter 2*, the inhibition of CYP2C8, as measured by amodiaquine N-dealkylation (left panel) and paclitaxel 6α-hydroxylation (right panel), was performed with 0.1, 0.3, 1, 3, 10, 30, and 100 µM desloratadine in cryopreserved human hepatocytes (0.5 million cells/mL). Desloratadine was preincubated with CHH for 0, 30 and 120 min, after which CYP2C8 activity was measured with a 10-min incubation with amodiaquine (10 µM) or 30-min incubation time with paclitaxel (10 µM).

6.3. Assessment of desloratadine as an inhibitor of nine UGT enzymes.

Desloratadine was evaluated as an inhibitor of nine UGT enzymes in HLM (≤ 0.1 mg/mL) as described in Table 2.4 and *Chapter 2*. As shown in Table 6.1 and Figure 6.4, desloratadine (10 μ M) caused no inhibition ($<15\%$) of UGT1A1, UGT1A3, UGT1A4, UGT1A6, UGT1A9, UGT2B7, or UGT2B15 and caused weak inhibition of UGT2B17 (24%). In contrast, UGT2B10 activity, as measured by levomedetomidine *N*-glucuronidation, was strongly inhibited (78%) by desloratadine. The UGT2B10 inhibition assay was repeated with a wide range of concentrations of desloratadine (0.1-100 μ M), which established that desloratadine inhibited UGT2B10 with an IC_{50} of 1.6 μ M, as shown in Figure 6.5.

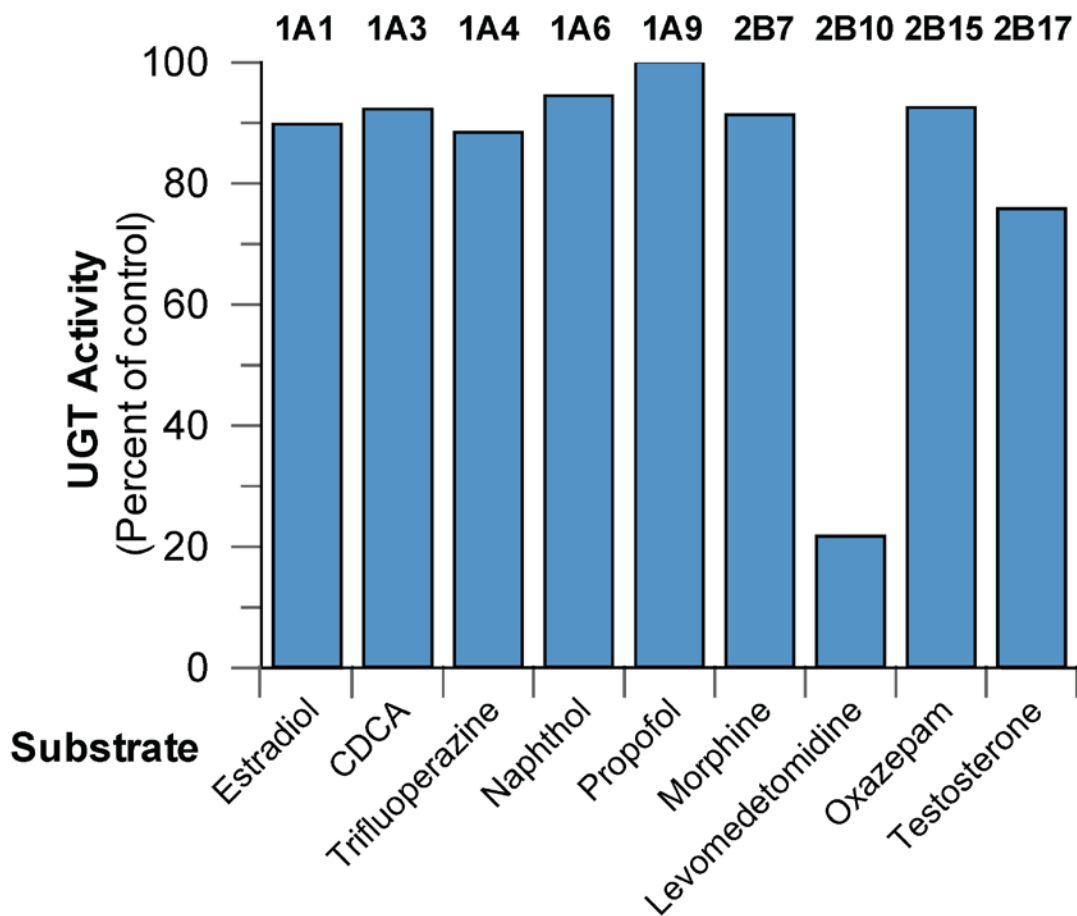


Figure 6.4. Evaluation of desloratadine (10 μ M) as an inhibitor of UGT enzymes in human liver microsomes

The UGT inhibition potential of desloratadine (10 μ M) was assessed in HLM (\leq 0.1 mg/mL) with UDP-GlcUA and the UGT-selective substrates identified in the figure (at a final concentration approximately equal to its K_m). The incubation time was 5 or 10 min. Experimental details are described in *Chapter 2*.

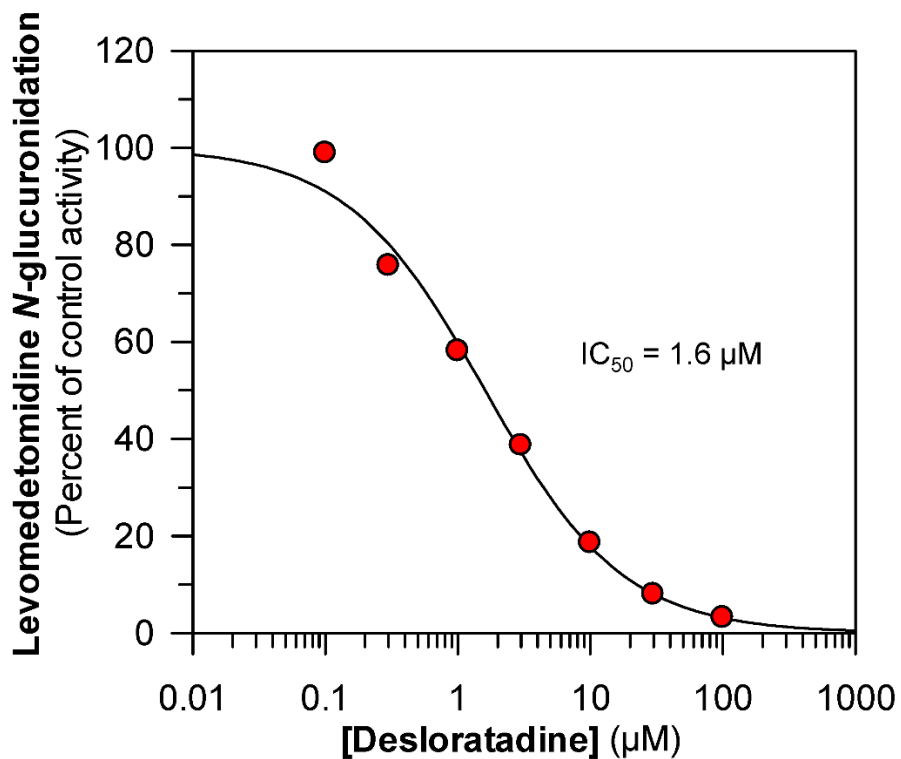


Figure 6.5. IC₅₀ determination of the UGT2B10 inhibition potential by desloratadine in HLM

Desloratadine (0.1, 0.3, 1, 3, 10, 30, and 100 µM) was evaluated as an inhibitor of UGT2B10 (levomedetomidine *N*-glucuronidation) in HLM (0.1 mg/mL). The substrate concentration was 7 µM and the incubation time was 10 min, as described in *Chapter 2*.

6.4. Further characterization of the UGT enzymes involved in 3-hydroxydesloratadine formation.

I previously identified recombinant UGT2B10 as the only UGT enzyme capable of supporting the CYP2C8-dependent formation of 3-hydroxydesloratadine in Chapter 5. However, this assessment was based on studies with a panel of recombinant UGT enzymes (each of which was co-incubated with recombinant CYP2C8). Although these studies implicated UGT2B10 in the formation of 3-hydroxydesloratadine they do not exclude the possibility that HLM contain other UGT enzymes that contribute to this reaction. UGT2B10 is one of two enzymes renowned for its ability to form *N*-glucuronides; the other is UGT1A4 (Parkinson et al., 2013). To evaluate the role of UGT2B10 and UGT1A4 in the formation of 3-hydroxydesloratadine, inhibitors either UGT1A4 (hecogenin; 100 μ M) or UGT2B10 (nicotine; 500 μ M) were added separately or in combination to HLM (0.1 mg/mL) in the presence of NADPH and UDP-GlcUA, followed by assessment of 3-hydroxydesloratadine formation and/or measurement of UGT1A4 activity (trifluoperazine *N*-glucuronidation) and UGT2B10 activity (levomedetomidine *N*-glucuronidation), as described in *Chapter 2*. As shown in Figure 6.6, trifluoperazine *N*-glucuronidation was inhibited only by the UGT1A4 inhibitor hecogenin whereas levomedetomidine *N*-glucuronidation was inhibited only by the UGT2B10 inhibitor nicotine. When NADPH- and UDP-GlcUA-fortified HLM were incubated with 10 μ M desloratadine, hecogenin did not inhibit 3-hydroxydesloratadine formation whereas nicotine and a combination of hecogenin and nicotine caused moderate inhibition of 45% and 35% respectively. When the concentration of desloratadine was lowered to 1 μ M, complete inhibition of 3-hydroxydesloratadine formation was observed with nicotine and

hecogenin + nicotine, whereas hecogenin caused no inhibition of 3-hydroxydesloratadine formation. These results suggest that UGT2B10 is the only UGT enzyme in HLM capable of catalyzing the *N*-glucuronidation of desloratadine.

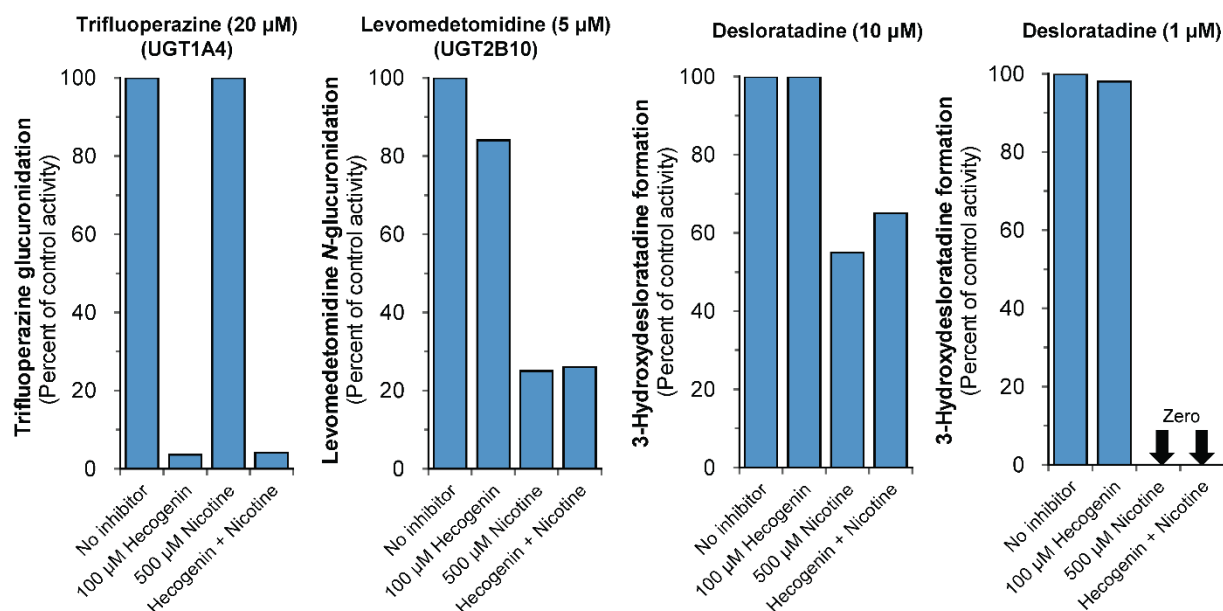


Figure 6.6. The effect of the UGT1A4 inhibitor hecogenin and the UGT2B10 inhibitor nicotine on the formation of 3-hydroxydesloratadine by NADPH- and UDP-GlcUA-fortified human liver microsomes (HLM)

Inhibitors of UGT1A4 (hecogenin; 100 μM) and UGT2B10 (nicotine; 500 μM) or the combination of both were examined for their ability to inhibit the conversion of desloratadine (1 and 10 μM) to 3-hydroxydesloratadine by human liver microsomes (0.1 mg/mL) supplemented with NADPH and UDP-GlcUA. The activity of UGT1A4 and UGT2B10 were measured as trifluoperazine *N*-glucuronidation and levomedetomidine *N*-glucuronidation, respectively. Experimental details are described in *Chapter 2*.

DISCUSSION

Desloratadine (marketed as Clarinex[®] in the US and Aeries[®] in Europe) received FDA approval in 2001 for the treatment of allergic rhinitis and chronic idiopathic urticaria (Geha and Meltzer, 2001; Henz, 2001). The major human circulating metabolite of desloratadine is 3-hydroxydesloratadine, a metabolite whose enzymology remained a mystery for over 20 years due, in large part, to the inability of conventional in vitro test systems, such as subcellular fractions, to form 3-hydroxydesloratadine (Ghosal et al., 2009). As described in Chapters 4 and 5, I demonstrated that CHH are capable of forming 3-hydroxydesloratadine, with a K_m of 1.6 μ M. Studies with P450 inhibitors in CHH and comparisons of the sample-to-sample variation in 3-hydroxydesloratadine formation with the variation in P450 activities in CHH (correlation analysis) implicated CYP2C8 in the conversion of desloratadine to 3-hydroxydesloratadine (Chapter 5). These findings in CHH made the inability of HLM to form 3-desloratadine all the more puzzling because HLM contain functional CYP2C8. Furthermore, recombinant CYP2C8 was also incapable of converting desloratadine to 3-hydroxydesloratadine despite catalyzing high rates of metabolism of substrates like paclitaxel and amodiaquine. The seemingly paradoxical findings were resolved with the discovery that the substrate for CYP2C8 is not desloratadine itself but its *N*-glucuronide, as shown in Figure 6.1. When individual recombinant UGT enzymes were co-incubated with recombinant CYP2C8, it was found that UGT2B10 was the only UGT enzyme capable of supporting the CYP2C8-dependent conversion of desloratadine to 3-hydroxydesloratadine (Chapter 5).

The studies in Chapter 5 advanced our understanding of the victim potential of desloratadine. Based on these studies, it is now known, for example, that drugs that alter

the activity of UGT2B10 and CYP2C8 are factors that likely impact the disposition of desloratadine. Furthermore, genetic polymorphisms (loss-of-function allelic variants) of UGT2B10 and/or CYP2C8 are candidates for explaining why a small percentage of human subjects are poor metabolizers of desloratadine (Prenner et al., 2006).

In the present study, I examined the perpetrator potential of desloratadine based on its ability to inhibit P450 and UGT enzymes in HLM. The direct but not time- or metabolism-dependent P450 inhibition potential of desloratadine was previously evaluated by Barecki and colleagues (2001). Since this study was published, subsequent regulatory guidelines expanded the panel of CYP enzymes recommended for testing (CYP2B6 and CYP2C8 were added) and they recommended an evaluation of both reversible and irreversible inhibition of P450 enzymes (FDA, 2012; EMA, 2013). Inhibition of CYP2B6 or CYP2C8 is the basis for certain clinically relevant DDIs, such as the mechanism-based inactivation of CYP2B6 by clopidogrel and ticlopidine leading to clinical interactions with bupropion, efavirenz and ketamine (Richter et al., 2004; Turpeinen et al., 2005; Peltoniemi et al., 2011; Jiang et al., 2013). Likewise, the mechanism-based inactivation of CYP2C8 by gemfibrozil glucuronide or clopidogrel glucuronide leads to a clinical interaction with cerivastatin that resulted in the withdrawal of cerivastatin from the market (Backman et al., 2002; Ogilvie et al., 2006; Tornio et al., 2014).

In the present study, the inhibition of seven P450 enzymes, namely CYP1A2, CYP2B6, CYP2C8, CYP2C9, CYP2C19, CYP2D6 and CYP3A4/5, was evaluated with a single concentration of desloratadine (10 μ M; approximately 10 times C_{max}) at low HLM concentrations (\leq 0.1 mg/mL) with a short probe-substrate incubation time (5 min) and included an assessment of reversible inhibition (no preincubation, time-dependent

inhibition (30-min pre-incubation of desloratadine and HLM without NADPH) and metabolism-dependent inhibition (30-min pre-incubation of desloratadine and HLM with NADPH). There was no evidence that desloratadine caused significant time- or metabolism-dependent inhibition of any of the CYP enzymes examined, but it did cause reversible inhibition of certain enzymes. Consistent with the data reported by Barecki and colleagues (2001), the results of this study (Figure 6.2 and Table 6.1) showed that desloratadine is not an inhibitor of CYP1A2, CYP2C9, and CYP2C19; but is a moderate inhibitor of CYP2D6 and CYP3A4/5. The slightly greater degree of CYP2D6 and CYP3A4 inhibition observed in the current study (32% and 44%, respectively) compared with the Barecki study (14% and 16-20%, respectively) can reasonably be differences in experimental design. Barecki et al. (2001) used relatively high protein concentrations (up to 10 times those used in the current study), which would have lowered the unbound concentration of desloratadine to a greater extent. In addition to inhibiting CYP2D6 and CYP3A4/5, desloratadine also inhibited CYP2B6 (~48%).

The ability of desloratadine to inhibit CYP2C8 was evaluated in HLM and CHH. Hepatocytes were used to evaluate the possibility that CYP2C8 could be inhibited by desloratadine *N*-glucuronide. No inhibition of CYP2C8 was observed in either HLM or CHH (Table 6.1, Figure 6.2 and Figure 6.3). These results are consistent with a clinical report demonstrating no effect of desloratadine on serum levels of the CYP2C8 substrate montelukast (Cingi et al., 2013). Few clinical studies have been performed to evaluate desloratadine as an inhibitor of CYP2D6 or CYP3A4. Desloratadine does not affect the pharmacokinetics of fluoxetine or azithromycin to a clinically significant extent (Gupta et al., 2001; Gupta et al., 2004). The previously reported requirement of UDP-GlcUA in

3-hydroxydesloratadine formation led us to investigate the perpetrator potential of desloratadine towards UGT1A1, UGT1A3, UGT1A4, UGT1A6, UGT1A9, UGT2B7, UGT2B10, UGT2B15 and UGT2B17. Desloratadine was identified as a potent and selective inhibitor of UGT2B10 (Figure 6.4), consistent with its involvement in 3-hydroxydesloratadine formation. Desloratadine inhibited UGT2B10 with an IC_{50} of 1.6 μ M (Figure 6.5), which is comparable to the reported clinical plasma C_{max} value of 1.3 μ M (Schering-Plough, 2001).

In accordance with regulatory guidelines (FDA, 2012), the potential clinical relevance of P450 inhibition in vitro can be evaluated based on the $[I]/K_i$ ratio, (where $[I]$ is the total unbound plasma C_{max} concentration and K_i is the unbound inhibition constant) and is used for in vitro to in vivo extrapolation (IVIVE) to predict the fold change in AUC of a victim drug (where $AUC \text{ with inhibitor} / AUC \text{ without inhibitor} = 1 + [I]/K_i$) (Ito et al., 1998). When the substrate concentration is equal to K_m , the K_i value can be estimated from the IC_{50} value using the Cheng-Prusoff equation, where $K_i = IC_{50}/2$ for competitive inhibition (Cheng and Prusoff, 1973; Haupt et al., 2011). This same approach has also been applied for the prediction of UGT mediated DDIs (Williams et al., 2004; Miners et al., 2010g). The $f_{u,inc}$ for desloratadine would be 0.84 based on a logP value of 4 (from www.drugbank.ca) using the equation from Hallifax et al., (2006). Using this approach, the unbound K_i value is 0.67 μ M therefore desloratadine is predicted to cause a 2.9-fold increase in the plasma AUC of a drug that is cleared exclusively by UGT2B10. To my knowledge, there is no known drug exclusively cleared through UGT2B10. Many drugs that are substrates of UGT enzymes are commonly cleared through other pathways, and many substrates of UGT2B10 are also *N*-glucuronidated by UGT1A4. Nevertheless, the discovery that

desloratadine is a selective UGT2B10 inhibitor is important for in vitro UGT reaction phenotyping studies; it can be used as a chemical inhibitor to determine the fraction of a drug metabolized through UGT2B10.

Both UGT1A4 and UGT2B10 are well known for their ability to *N*-glucuronidate drugs such as amitriptyline, imipramine, ketotifen, pizotifen, olanzapine, diphenhydramine, tamoxifen, ketoconazole and midazolam (Kato et al., 2013). In Chapter 5, I determined that recombinant UGT2B10 was the only UGT enzyme capable of supporting the CYP2C8-dependent conversion of desloratadine. This finding does not establish that UGT2B10 is the only enzyme in HLM capable of supporting this reaction. It is possible, for example, that in a more complete test system such as HLM, UGT1A4 may play a role in addition to UGT2B10. To evaluate this possibility, I performed a chemical inhibition study using the UGT1A4 inhibitor hecogenin and the UGT2B10 inhibitor nicotine (alone or in combination) with HLM (supplemented with both UDP-GlcUA and NADPH) and examined the formation of 3-hydroxydesloratadine as well as the activity UGT1A4 (with trifluoperazine) and UGT2B10 (with levomedetomidine) (Figure 6.6). The formation of 3-hydroxydesloratadine was inhibited by the CYP2B10 inhibitor nicotine but not by the UGT1A4 inhibitor hecogenin, confirming that UGT2B10 is solely responsible for the formation of 3-hydroxydesloratadine, consistent with the results of my previous study with recombinant enzyme results (Kazmi et al., 2015).

Desloratadine *N*-glucuronide is so unstable that efforts to detect its formation by LC-MS/MS were unsuccessful. In an effort to find evidence for desloratadine glucuronidation, I attempted to use an indirect measure of glucuronidation by measuring formation of UDP, a byproduct of UGT reactions, as shown in Figure 6.1. Unfortunately, I was unsuccessful

in developing an LC-MS/MS method for UDP. I also attempted to measure desloratadine glucuronidation indirectly by incubating desloratadine (as well as the UGT2B10 substrate levomedetomidine) for up to 4 hours with HLM or rUGT2B10 + rUGT1A6 and a low concentration of UDP-GlcUA (30 μ M) followed by the addition of an excess (500 μ M) of 1-naphthol (a UGT1A6 substrate that is rapidly glucuronidated) for 10 min to consume any remaining UDP-GlcUA. The amount of 1-naphthol glucuronide should have provided an indirect measure of the amount of UDP-GlcUA remaining; however, there was no discernible difference between control (no drug), desloratadine or levomedetomidine incubations.

In conclusion, desloratadine was identified as a potent and selective inhibitor of UGT2B10, the enzyme implicated in the *N*-glucuronidation of desloratadine. Desloratadine was a weak reversible inhibitor P450 enzymes and showed no significant time- or metabolism-dependent inhibition of any of the CYP enzymes examined. Because of the instability of desloratadine *N*-glucuronide, desloratadine is unsuitable as a probe substrate for UGT2B10. However, as an inhibitor of UGT2B10, desloratadine can be used as part of standard in vitro chemical inhibition studies for the reaction phenotyping of UGT substrates, allowing for the determination of fractional metabolism by UGT2B10. These findings contribute to our understanding of the role of UGT enzymes in drug clearance and provide greater insight into the potential for desloratadine mediated DDIs.

CHAPTER 7 : CONCLUSIONS AND FUTURE DIRECTIONS

7.1. Summary and overall conclusions

Before I was born, the metabolism of debrisoquine and the duration of its hypotensive effect in humans were shown to be under the control of a single recessive gene, which was subsequently identified as CYP2D6 (Mahgoub et al., 1977; Idle et al., 1978). In 1990 Monahan et al. published the first paper describing elevated levels of terfenadine and torsade de pointes (a risk factor for ventricular arrhythmia) following the coadministration of terfenadine with the CYP3A4/5 inhibitor ketoconazole (Monahan et al., 1990). Since these seminal findings, the activity of all P450 enzymes involved in drug metabolism have been shown to vary enormously from one individual to the next due to intrinsic factors, such as genetic polymorphisms (as in the case of CYP2D6) or extrinsic factors, such as concomitant drug therapy (as in the case of CYP3A4/5). Accordingly, identifying the drug-metabolizing enzymes and drug transporters that determine the disposition of a drug candidate is indispensable to the drug development process; one that is required by regulatory agencies such as the FDA and EMA to ensure the safety and well-being of patients. Over the last 50 years, there have been considerable advances in the in vitro test systems used to assess drug disposition, from the early days of animal liver microsomal samples to the current availability of large pools (n=200) of human liver microsomes (HLM), large pools (n=50 or 100) of cryopreserved human hepatocytes (CHH) and recombinant enzymes, as well as the identification of enzyme-specific substrates and inhibitors that can be used in vitro and, in many cases, in vivo. The large pools of HLM and CHH eliminate the large sample-to-sample in enzyme activity that complicated early studies of in vitro drug metabolism, although this wide variation is the basis for the technique known as correlation analysis, which is one of the so-called

reaction phenotyping methods for identifying which CYP enzyme is primarily responsible for metabolizing a drug candidate. These current in vitro test systems are important mainstays for the assessment of drug disposition and the data generated with these assays is widely used by pharmaceutical companies and regulatory agencies to make risk assessments of new drug candidates.

Although considerable advances have been made with the quality of HLM and CHH, certain key differences remain that are inherent to each test system. CHH for instance are an intact cellular test system with the ability to perform Phase I and Phase II metabolism with a full complement of enzymatic cofactors, as well as transport processes of drugs (such as drug uptake). HLM on the other hand are isolated endoplasmic reticulum and their ability to metabolize drugs is not restricted by drug permeability, although the range of metabolic reactions that can be assessed is limited (typically P450, FMO, UGT and carboxylesterase) and requires the addition of exogenous cofactor. Regardless of the advantages or limitations of each system, both in vitro test systems are widely employed by the pharmaceutical industry for the in vitro to in vivo extrapolation (IVIVE) of drug metabolic clearance, which plays an important role in the process of identifying drug candidates with favorable pharmacokinetic properties, such as low dose and once-a-day dosing. As described in previous chapters (Chapter 1, 3 and 4), both HLM and CHH generally underpredict the in vivo clearance of drugs (Chiba et al., 2009); however, this underprediction is much greater in CHH with high intrinsic clearance drugs (CL_{int}) than in HLM (Lu et al., 2006; Hallifax et al., 2010). The case of midazolam, a high CL_{int} substrate of CYP3A4/5, is of particular importance because midazolam is widely used as an in vitro and in vivo CYP3A4/5 probe in the assessment of drug-drug

interactions (DDIs). Therefore, the initial focus of my dissertation research was to determine the mechanism by which midazolam clearance is restricted in hepatocytes compared with microsomes. Other investigators had proposed that midazolam clearance is restricted in CHH by permeability or cofactor availability (Lu et al., 2006; Foster et al., 2011). However the results presented in Chapter 3 demonstrated that neither membrane permeability nor intracellular cofactor availability was a likely explanation for the system-dependent clearance of midazolam, based on the following observations:

1. Permeabilizing CHH by sonication or the pore-forming agent saponin did not increase the rate of midazolam metabolism even when the permeabilized hepatocytes were supplemented with NADPH;
2. The rate of uptake of midazolam by CHH greatly exceeded the rate of metabolism of midazolam;
3. Microsomes isolated from the pooled CHH had comparable CYP3A4/5 activity towards midazolam as microsomes prepared directly from human liver (indicating the pooled CHH used in these studies did not contain abnormally low CYP3A4/5 activity).

In an effort to determine if the system-dependent clearance midazolam was unique or a property of other CYP3A4/5 substrates with similar physicochemical properties, the clearance of alfentanil, nifedipine and verapamil was assessed in HLM and CHH. System-dependent clearance was observed with these other CYP3A4/5 substrates, although when estimates of hepatic clearance based on in vitro clearance were compared with experimentally determined values of blood clearance in vivo the difference was much less than that of midazolam (~2-fold for alfentanil, nifedipine and verapamil versus 5-fold for

midazolam). These results suggested that the underprediction of midazolam clearance was more pronounced than that of other substrates of CYP3A4/5.

Having established in Chapter 3 that a factor other than permeability or cofactor availability is responsible for the system-dependent clearance of midazolam, I examined the impact of in vitro incubation conditions on P450 activity, namely the ionic strength of the incubation buffer and the effect of cell culture media. These studies are described in Chapter 4. There was precedent for this investigation, as previous researchers had shown that P450 reactions were in some cases highly dependent on buffer ionic strength (Gemzik et al., 1990; Yamazaki et al., 1997; Maenpaa et al., 1998). The effects of cell culture media on the clearance of substrates was a novel aspect of this research as I sought to identify a cell culture medium capable of increasing midazolam clearance in CHH to that of HLM. The results showed that in HLM, P450 activities generally peaked at 50 mM phosphate buffer, with the exceptions of CYP3A4/5 and CYP2E1 where the enzymatic activities were found to increase with increasing buffer ionic strength. However, in HLM in the presence of cell culture media, namely, Waymouth's, MCM+ and DMEM, the metabolism of midazolam (CYP3A4/5) and chlorzoxazone (CYP2E1) were markedly reduced. This finding was interesting because CYP3A4/5 and CYP2E1 share other properties that distinguish them from other P450 enzymes; for example, CYP3A4, CYP3A5 and CYP2E1 form oligomers (homodimers through hexamers) and their activities are stimulated by cytochrome b_5 (even heme-depleted cytochrome b_5) (Parkinson et al., 2013; Davydov et al., 2015). The effects of cell culture media on midazolam clearance in CHH had a similar but less pronounced effect to that of HLM. Another interesting finding was that the reduction of midazolam clearance by certain cell culture media in both HLM

and CHH was not observed to the same extent as other substrates of CYP3A4/5. When the kinetics of midazolam metabolism were assessed in HLM, both MCM+ and Williams' E medium caused a marked increase in K_m compared to 50 mM phosphate buffer, suggesting the presence of inhibitory substances in these media. Complete versions and salt-only versions of each medium were examined for their effects on CYP3A4/5 activity in HLM towards different substrates. Midazolam metabolism was increased in the salt-only media, lending further evidence for the presence of an inhibitory substance in the cell culture media examined. The effects of the salt-only media varied from one CYP3A4/5 substrate to the other, with little or no changes observed for some substrates and inverse changes (relative to midazolam) observed for others. This suggests that the inhibitory effect of cell culture media is relatively specific to midazolam metabolism. This was an unexpected finding because CYP3A4/5 is known to contain two overlapping substrate binding pockets, a so-called benzodiazepine-binding site and a steroid-binding site (Parkinson et al., 2013), and many of the substrates evaluated in this study are considered, like midazolam, to bind to the benzodiazepine binding site (such as nifedipine, alfentanil and verapamil). The effect of an inhibitor on midazolam metabolism would therefore be expected to have a similar effect on the metabolism of other substrates of the same binding site, an effect that was not observed in my research.

Overall, I was unable to find a cell culture media that increased midazolam metabolism in CHH; however, my findings have implications on the conduct of in vitro metabolism studies. First, many researchers use buffers of varying ionic strength (typically up to 100 mM phosphate) in studies with HLM. The studies described in Chapter 4 suggest that 50 mM phosphate is the optimum concentration because it supports maximal activity of most

P450 activities and, although submaximal for CYP3A4/5, it accurately predicts the in vivo clearance of CYP3A4/5 drugs like midazolam, alfentanil, nifedipine and verapamil. Second, Williams' E medium was found to support CYP3A4/5 activity in CHH to similar levels as KHB medium (the medium used in Chapter 3). This is important, because KHB medium is not suitable for prolonged incubations of CHH; however, Williams' E is suitable, suggesting that Williams' E medium should be used for long-term metabolism studies in CHH, such as the hepatocyte relay-method for measuring the half-life of metabolically stable drugs described by Di et al., (2012, 2013). Even modest changes in the activity of CYP3A4/5 can have profound effects on the metabolism of low clearance drugs over long term incubations, and having a medium that maintains CYP3A4/5 activities over time is beneficial.

The focus of my dissertation research shifted when attempting to find a substrate of CYP3A4/5 with the same system-dependent clearance characteristics as midazolam. I tested loratadine, which is metabolized primarily by CYP3A4/5 to desloratadine, in CHH with varying cell culture media and found that loratadine metabolism resembled the other CYP3A4/5 substrates that were examined. However, the metabolite 3-hydroxydesloratadine was also detected in these incubations, which was unexpected because no prior in vitro test system or non-clinical species had been shown to support its formation (Ramanathan et al., 2006; Ghosal et al., 2009). 3-Hydroxydesloratadine is the major circulating human metabolite of desloratadine, and the enzymology of its formation, prior to this study, was unknown, despite a post-marketing commitment imposed by the FDA on the manufacturer, Schering-Plough (Schering-Plough, 2001). This finding was also interesting from the perspective of system-dependent clearance,

because the metabolism of desloratadine to 3-hydroxydesloratadine was found to occur only in CHH, and not HLM, suggesting that desloratadine was a drug metabolized more readily in CHH than HLM; a finding opposite to that of midazolam.

The studies outlined in Chapter 5 were designed to identify the enzyme or enzymes responsible for forming 3-hydroxydesloratadine. Using a panel of CYP-selective inhibitors, I was able to determine that CYP2C8 was involved in the formation of 3-hydroxydesloratadine in CHH. This finding was unusual for two reasons. First, CYP2C8 activity is well represented in HLM, and therefore HLM should be capable of forming 3-hydroxydesloratadine when in fact they are not. Second, desloratadine is a basic drug and CYP2C8 tends to metabolize acidic drugs. This led me to investigate what factors were promoting 3-hydroxydesloratadine formation in CHH and conversely preventing its formation in HLM. When CHH were sonicated or permeabilized with saponin, they lost the ability to form 3-hydroxydesloratadine even when supplemented with NADPH. However, when sonicated/saponin-treated hepatocytes were supplemented with both NADPH (to support P450 activity) and UDP-GlcUA (to support UGT activity) their ability to form 3-hydroxydesloratadine was partially restored. This suggested glucuronidation of desloratadine was involved in the formation of 3-hydroxydesloratadine by CYP2C8. This possibility was confirmed when I demonstrated that recombinant CYP2C8 could form 3-hydroxydesloratadine when co-incubated with recombinant UGT2B10. Only recombinant UGT2B10 supported the CYP2C8-dependent formation of 3-hydroxydesloratadine. This finding was consistent with the known properties of UGT2B10 and CYP2C8. The only glucuronidation reaction that can occur with desloratadine is *N*-glucuronidation (which could occur at one of two nitrogen atoms in

desloratadine). Interestingly, UGT2B10 is one of the few human UGT enzymes capable of catalyzing the *N*-glucuronidation of drugs (the other notable enzyme is UGT1A4). Once converted to an *N*-glucuronide, desloratadine is transformed into a large acidic compound and, as such, the type of substrate typically metabolized by CYP2C8 (Parkinson et al., 2013). When the sample-to-sample variation in 3-hydroxydesloratadine formation by CHH was examined, a high correlation was observed with both CYP2C8 and UGT2B10 activity. Unfortunately, the *N*-glucuronide of desloratadine was too unstable to characterize by mass spectrometry. Nevertheless, the results presented in Chapter 5 strongly suggest that desloratadine *N*-glucuronide is an obligatory intermediate in the conversion of desloratadine to 3-hydroxydesloratadine.

Having solved the enzymology of 3-hydroxydesloratadine formation in Chapter 5, the studies in Chapter 6 examined the perpetrator potential of desloratadine; i.e., its ability to cause DDIs by inhibiting P450 or UGT enzymes *in vitro*. Desloratadine was found to be a selective inhibitor of UGT2B10, consistent with the role of this UGT in the formation of 3-hydroxydesloratadine. Further characterization of the formation of 3-hydroxydesloratadine in NADPH- and UDP-GlcUA-fortified HLM with selective inhibitors of UGT2B10 and UGT1A4 confirmed that indeed UGT2B10 is the solely responsible for supporting the CYP2C8-dependent formation of 3-hydroxydesloratadine. Desloratadine was a weak inhibitor of certain P450 enzymes in HLM (namely, CYP2B6, CYP2D6 and CYP3A4) but, based on criteria proposed by the FDA, the inhibition was too weak to be clinically significant. Desloratadine did not inhibit CYP2C8 in HLM or CHH, suggesting that desloratadine will not cause clinically significant inhibition of CYP2C8.

The research presented in Chapter 5 and Chapter 6 solved the mystery surrounding the enzymology of formation of 3-hydroxydesloratadine. Given that a segment of the population are poor metabolizers (PMs) of desloratadine with greatly reduced 3-hydroxydesloratadine formation (Prenner et al., 2006), the research presented in this dissertation now provides a pathway for the investigation of the genetic basis of the PM phenotype. Based on my findings, I anticipate that the FDA label for desloratadine will likely be changed to indicate the enzymology of 3-hydroxydesloratadine formation. Furthermore, there are limited selective in vitro chemical inhibitors for use in reaction phenotyping studies of UGT enzymes with new drug candidates (Miners et al., 2010a). The identification of desloratadine as a selective inhibitor of UGT2B10 serves to advance this field of research. In the future, desloratadine can be used in vitro studies to delineate the contribution of UGT1A4 and UGT2B10 to the *N*-glucuronidation of new drug candidates.

7.2. Future directions

The research outlined in this dissertation did establish that the system-dependent clearance of midazolam, which is much greater in HLM than CHH, was more pronounced than that of other CYP3A4/5 substrates. Although I was unable to find a cell culture medium that increased the metabolism of midazolam in CHH to compensate for the system-dependent difference, I did establish that other incubation conditions, such as buffer ionic strength, can play a role in midazolam clearance. In the future, the following four studies might help to explain the system-dependent clearance of midazolam. First, cryopreserved rat and human hepatocytes could be compared with freshly isolated rat and human hepatocytes for their ability to metabolize midazolam. A comparison of midazolam clearance in rat liver microsomes and freshly isolated rat hepatocytes revealed no system-dependent clearance (Jones and Houston, 2004). This raises the possibility that the process of cryopreservation impairs midazolam clearance by human hepatocytes. In itself, this finding would not establish the mechanism underlying the system-dependent clearance of midazolam but it would identify the issue as an *in vitro* artifact.

Second, a wide variety of media (more than the five examined in my dissertation) could be screened in the hope of identifying a medium that supported much higher rates of midazolam clearance by CHH.

Third, endogenous factors could be investigated as a cause of the underprediction of midazolam clearance by CHH. It is possible, for example, that high concentrations of ammonia in CHH impede the metabolic clearance of midazolam. In 1998, Maenpaa et al.

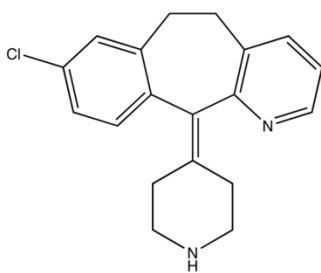
identified ammonia present in glucose 6-phosphate dehydrogenase solutions (used as a component of the NADPH-generating system) inhibits the metabolism of midazolam by HLM (Maenpaa et al., 1998). Ammonia is formed during the metabolism of amino acids (which are present in certain cell culture media at super-physiological concentrations). The intracellular concentration of ammonia in hepatocytes can reach millimolar levels through pH partitioning (Remesy et al., 1986). Therefore, in CHH, it is possible that ammonia is acting as an endogenous inhibitor of midazolam clearance. To assess this, it would be interesting to add ammonium chloride (at hepatocyte concentrations) to HLM and evaluate midazolam metabolism under those conditions. However, the research in Chapter 3 may argue against ammonia as an inhibitor, because when CHH were sonicated or treated with saponin, any endogenous ammonia should have been released from the hepatocytes and diluted approximately 100 fold in the incubation matrix (at 1 million cells/mL hepatocytes are roughly 1% of the incubation volume). No changes in midazolam metabolism were observed in permeabilized CHH, Nevertheless, evaluating of ammonia content of CHH (and freshly isolated hepatocytes) and evaluating the effects of ammonium chloride on midazolam clearance in CHH may be interesting avenues to pursue in the future.

Fourth, while suspended CHH are often used for metabolic clearance determinations, there are other hepatocyte based models used for other applications. These include hepatocyte co-culture systems, 3D-hepatocyte systems such as spheroids, and microfluidic systems that include media flow (Godoy et al., 2013). These models offer improvements in hepatocyte longevity and function, and it would be interesting to

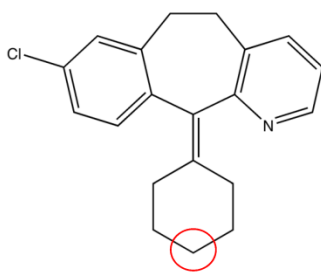
determine if midazolam clearance in these hepatocyte models is improved over suspended CHH.

With respect to the studies on desloratadine metabolism, indirect evidence was presented that desloratadine *N*-glucuronide is an obligatory intermediate in the formation of 3-hydroxydesloratadine by CYP2C8. The evidence was necessarily indirect because desloratadine *N*-glucuronide was too unstable to characterize by mass spectrometry. Accordingly, no experiments with synthetic desloratadine *N*-glucuronide were attempted. However, two studies could be conducted in the future to ascertain which of the two possible *N*-glucuronides of desloratadine is metabolized by CYP2C8 to 3-hydroxydesloratadine. First, an attempt could be made to synthesize both *N*-glucuronides (the tertiary *N*-glucuronide formed by glucuronidation of the piperidine ring and the quaternary ammonium glucuronide formed by glucuronidation of the pyridine ring). If one of these *N*-glucuronides is stable and one is not, the former can be evaluated as a substrate for CYP2C8 and, if no 3-hydroxydesloratadine is formed, then the latter can be assumed to be the unstable *N*-glucuronide that is metabolized by CYP2C8 to 3-hydroxydesloratadine. A second approach is to synthesize the 4 analogs of desloratadine shown in Figure 7.1. Analogs 1A and 2A lack the piperidine and pyridine nitrogen atom, respectively. I predict that CHH will convert only one of these analogs to a 3-hydroxylated metabolite, which will identify the site of *N*-glucuronidation. The analogs 1B and 2B are desloratadine derivatives containing a stable cyclohexyl-carboxylic acid moiety (a glucuronide mimetic). I predict that only one of these will be metabolized by recombinant CYP2C8 (or HLM) to a 3-hydroxy metabolite. Both approaches will potentially provide additional support for the role of *N*-glucuronidation in the formation of 3-

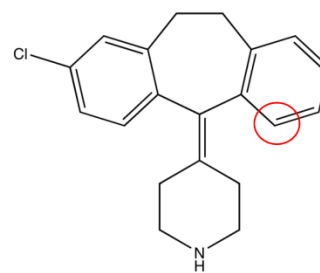
hydroxydesloratadine and will provisionally identify which of the two possible *N*-glucuronides of desloratadine is formed by UGT2B10.



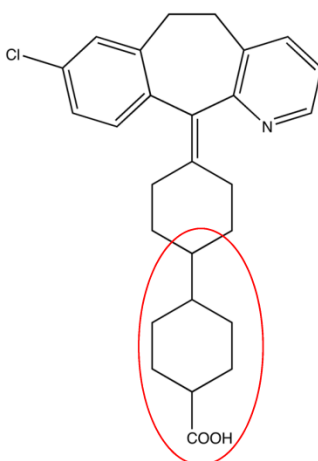
Desloratadine



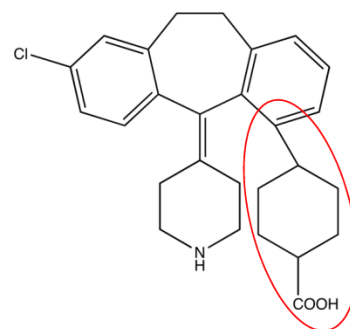
Analog 1A



Analog 2A



Analog 1B



Analog 2B

Figure 7.1. Analogs of desloratadine to investigate the site of N-glucuronidation that supports the CYP2C8-dependent formation of 3-hydroxydesloratadine

Only a limited number of clinical DDI studies have been conducted with desloratadine either as the victim or perpetrator drug. Studies in Chapter 6 predicted that desloratadine will not cause clinically relevant inhibition of any of the major drug-metabolizing P450 enzymes in HLM. Although desloratadine caused weak inhibition of CYP2D6 and CYP3A4, clinical studies established that desloratadine does not inhibit these enzymes in the clinic (reviewed in Chapter 6). In the future, it would be of interest to ascertain whether, as predicted, desloratadine does not cause clinically relevant inhibition of the metabolism of a sensitive in vivo probe substrate of CYP2C8, such as repaglinide. If, in the future, a drug is identified whose clearance is largely dependent on metabolism by UGT2B10, it would be interest to investigate whether desloratadine can inhibit its metabolism in a clinical DDI study. However, it was recently shown that UGT2B10 genotype plays a key role in nicotine *N*-glucuronidation (Berg et al., 2010). Therefore, it would be interesting in the future to evaluate whether desloratadine can lower blood and urinary levels of nicotine *N*-glucuronide in cigarette smokers.

Based on the research in this dissertation, a clinical interaction study of desloratadine with a strong inhibitor of UGT2B10 or CYP2C8 would provide in vivo confirmation of my in vitro findings. While no clinically significant UGT2B10 inhibitors have been identified, gemfibrozil and clopidogrel (through conversion to their acyl glucuronide) are clinically significant, irreversible inhibition of CYP2C8 (Backman et al., 2002; Ogilvie et al., 2006; Tornio et al., 2014). Therefore, in the future, it would be interesting to evaluate the pharmacokinetics of desloratadine in healthy subjects before and after treatment with gemfibrozil (to inhibit CYP2C8). I predict that gemfibrozil will inhibit the metabolic clearance and increase systemic exposure (plasma AUC) of desloratadine.

Poor metabolizers of desloratadine have been identified, as described in Chapter 5. The studies described in my dissertation suggest the PM phenotype is due to genetic polymorphisms (loss-of-function alleles) of CYP2C8 and/or UGT2B10. This prediction could be tested in vitro and in vivo. In the future, it would be interesting to genotype a wide panel of CHH from individual donors to determine their CYP2C8 and UGT2B10 allele status and examine the effects of these allelic variants on the conversion of desloratadine to 3-hydroxydesloratadine. A similar study could be conducted in individuals who, on the basis of prior genotyping analysis, could be categorized as poor metabolizers with respect to CYP2C8 or UGT2B10. For example, it would be interesting to evaluate the pharmacokinetics of desloratadine in those individuals identified as poor metabolizers of nicotine *N*-glucuronidation and shown to have loss-of-function alleles of UGT2B10. Likewise, it would be interesting to evaluate the pharmacokinetics of desloratadine in individuals previously identified as poor metabolizers of repaglinide due to loss-of-function alleles of CYP2C8. Alternatively, the pharmacokinetics of desloratadine could be assessed in a large population to identify poor metabolizers who could then be genotyped for CYP2C8 and UGT2B10. Such studies would establish whether, as predicted based on my dissertation research, genetic polymorphisms of CYP2C8 and UGT2B10 are the basis for poor metabolizers of desloratadine.

7.3. Final thoughts

Despite over 50 years of research on P450 enzymes since their discovery by Omura and Sato (1964), it is astonishing that we are still learning more about the fundamental properties of these enzymes. The research presented in this dissertation helps our understanding of the clearance of different drugs by P450 under various in vitro conditions and adds further perspective on the curious case of the system-dependent clearance of midazolam. The ultimate goal of the pharmaceutical industry is to have predictive in vitro models to expedite drug development and ultimately ensure patient safety. My dissertation research furthers our advancement towards that goal, as we attempted to gain a mechanistic understanding of the system-dependent clearance of midazolam, the most commonly used CYP3A4/5 probe in in vitro studies.

My successful characterization of the enzymology of desloratadine metabolism to 3-hydroxydesloratadine has a direct impact on the users of loratadine and desloratadine, as this research can now be used to update the labels of these drugs and provide a foundation for the investigation of the desloratadine poor metabolizer phenotype. The research in this dissertation also provides pharmaceutical researchers with a better understanding of nuances of the currently and widely used in vitro systems and provides recommendations for in vitro incubation conditions as well as a new selective UGT2B10 inhibitor to use in drug metabolism studies.

REFERENCES

- Andersson T, Cederberg C, Edvardsson G, Heggelund A, and Lundborg P (1990) Effect of omeprazole treatment on diazepam plasma levels in slow versus normal rapid metabolizers of omeprazole. *Clin Pharmacol Ther* **47**:79-85.
- Andersson T, Miners JO, Veronese ME, and Birkett DJ (1994) Diazepam metabolism by human liver microsomes is mediated by both S-mephenytoin hydroxylase and CYP3A isoforms. *Br J Clin Pharmacol* **38**:131-137.
- Aquilante CL, Kosmiski LA, Bourne DW, Bushman LR, Daily EB, Hammond KP, Hopley CW, Kadam RS, Kanack AT, Kompella UB, Le M, Predhomme JA, Rower JE, and Sidhom MS (2013) Impact of the CYP2C8 *3 polymorphism on the drug-drug interaction between gemfibrozil and pioglitazone. *Br J Clin Pharmacol* **75**:217-226.
- Austin RP, Barton P, Cockcroft SL, Wenlock MC, and Riley RJ (2002) The influence of nonspecific microsomal binding on apparent intrinsic clearance, and its prediction from physicochemical properties. *Drug Metab Dispos* **30**:1497-1503.
- Austin RP, Barton P, Mohamed S, and Riley RJ (2005) The binding of drugs to hepatocytes and its relationship to physicochemical properties. *Drug Metab Dispos* **33**:419-425.

Backman JT, Kyrklund C, Neuvonen M, and Neuvonen PJ (2002) Gemfibrozil greatly increases plasma concentrations of cerivastatin. *Clin Pharmacol Ther* **72**:685-691.

Baer BR, DeLisle RK, and Allen A (2009) Benzylic oxidation of gemfibrozil-1-O-beta-glucuronide by P450 2C8 leads to heme alkylation and irreversible inhibition. *Chem Res Toxicol* **22**:1298-1309.

Bahadur N, Leathart JB, Mutch E, Steimel-Crespi D, Dunn SA, Gilissen R, Houdt JV, Hendrickx J, Mannens G, Bohets H, Williams FM, Armstrong M, Crespi CL, and Daly AK (2002) CYP2C8 polymorphisms in Caucasians and their relationship with paclitaxel 6alpha-hydroxylase activity in human liver microsomes. *Biochem Pharmacol* **64**:1579-1589.

Baker M and Parton T (2007) Kinetic determinants of hepatic clearance: plasma protein binding and hepatic uptake. *Xenobiotica* **37**:1110-1134.

Banfield C, Herron J, Keung A, Padhi D, and Affrime M (2002a) Desloratadine has no clinically relevant electrocardiographic or pharmacodynamic interactions with ketoconazole. *Clin Pharmacokinet* **41 Suppl 1**:37-44.

Banfield C, Hunt T, Reyderman L, Statkevich P, Padhi D, and Affrime M (2002b) Lack of clinically relevant interaction between desloratadine and erythromycin. *Clin Pharmacokinet* **41 Suppl 1**:29-35.

- Barecki ME, Casciano CN, Johnson WW, and Clement RP (2001) In vitro characterization of the inhibition profile of loratadine, desloratadine, and 3-OH-desloratadine for five human cytochrome P-450 enzymes. *Drug Metab Dispos* **29**:1173-1175.
- Barr JT and Jones JP (2011) Inhibition of human liver aldehyde oxidase: implications for potential drug-drug interactions. *Drug Metab Dispos* **39**:2381-2386.
- Barter ZE, Bayliss MK, Beaune PH, Boobis AR, Carlile DJ, Edwards RJ, Houston JB, Lake BG, Lipscomb JC, Pelkonen OR, Tucker GT, and Rostami-Hodjegan A (2007) Scaling factors for the extrapolation of in vivo metabolic drug clearance from in vitro data: reaching a consensus on values of human microsomal protein and hepatocellularity per gram of liver. *Curr Drug Metab* **8**:33-45.
- Barter ZE, Chowdry JE, Harlow JR, Snawder JE, Lipscomb JC, and Rostami-Hodjegan A (2008) Covariation of human microsomal protein per gram of liver with age: absence of influence of operator and sample storage may justify interlaboratory data pooling. *Drug Metab Dispos* **36**:2405-2409.
- Beasley CM, Jr., Masica DN, Heiligenstein JH, Wheadon DE, and Zerbe RL (1993) Possible monoamine oxidase inhibitor-serotonin uptake inhibitor interaction: fluoxetine clinical data and preclinical findings. *J Clin Psychopharmacol* **13**:312-320.

Benet LZ and Hoener B-A (2002) Changes in plasma protein binding have little clinical relevance. *Clin Pharmacol Ther* **71**:115-121.

Berezhkovskiy LM (2011) The corrected traditional equations for calculation of hepatic clearance that account for the difference in drug ionization in extracellular and intracellular tissue water and the corresponding corrected PBPK equation. *J Pharm Sci* **100**:1167-1183.

Berg JZ, von Weymarn LB, Thompson EA, Wickham KM, Weisensel NA, Hatsukami DK, and Murphy SE (2010) UGT2B10 genotype influences nicotine glucuronidation, oxidation, and consumption. *Cancer Epidemiol Biomarkers Prev* **19**:1423-1431.

Bidstrup TB, Bjornsdottir I, Sidelmann UG, Thomsen MS, and Hansen KT (2003) CYP2C8 and CYP3A4 are the principal enzymes involved in the human in vitro biotransformation of the insulin secretagogue repaglinide. *Br J Clin Pharmacol* **56**:305-314.

Bjornsson TD, Callaghan JT, Einolf HJ, Fischer V, Gan L, Grimm S, Kao J, King SP, Miwa G, Ni L, Kumar G, McLeod J, Obach SR, Roberts S, Roe A, Shah A, Snikeris F, Sullivan JT, Tweedie D, Vega JM, Walsh J, and Wirghton SA (2003) The conduct of in vitro and in vivo drug-drug interaction studies: a PhRMA perspective. *J Clin Pharmacol* **43**:443-469.

- Boase S and Miners JO (2002) In vitro-in vivo correlations for drugs eliminated by glucuronidation: investigations with the model substrate zidovudine. *Br J Clin Pharmacol* **54**:493-503.
- Bolleddula J, DeMent K, Driscoll JP, Worboys P, Brassil PJ, and Bourdet DL (2014) Biotransformation and bioactivation reactions of alicyclic amines in drug molecules. *Drug Metab Rev* **46**:379-419.
- Boxenbaum H (1980) Interspecies variation in liver weight, hepatic blood flow, and antipyrine intrinsic clearance: extrapolation of data to benzodiazepines and phenytoin. *J Pharmacokinet Biopharm* **8**:165-176.
- Boxenbaum H (1999) Cytochrome P450 3A4 in vivo ketoconazole competitive inhibition: determination of K_i and dangers associated with high clearance drugs in general. *J Pharm Pharm Sci* **2**:47-52.
- Brown HS, Chadwick A, and Houston JB (2007a) Use of isolated hepatocyte preparations for cytochrome P450 inhibition studies: comparison with microsomes for K_i determination. *Drug Metab Dispos* **35**:2119-2126.
- Brown HS, Galetin A, Hallifax D, and Houston JB (2006) Prediction of in vivo drug-drug interactions from in vitro data : factors affecting prototypic drug-drug interactions involving CYP2C9, CYP2D6 and CYP3A4. *Clin Pharmacokinet* **45**:1035-1050.

Brown HS, Griffin M, and Houston JB (2007b) Evaluation of cryopreserved human hepatocytes as an alternative in vitro system to microsomes for the prediction of metabolic clearance. *Drug Metab Dispos* **35**:293-301.

Brunton LL, Lazo JS, and Parker KL (2006) *Goodman & Gilman's The Pharmacological Basis of Therapeutics*. McGraw-Hill, New York, NY.

Carlile DJ, Hakooz N, Bayliss MK, and Houston JB (1999) Microsomal prediction of in vivo clearance of CYP2C9 substrates in humans. *Br J Clin Pharmacol* **47**:625-635.

Cascorbi I (2012) Drug interactions-principles, examples and clinical consequences. *Dtsch Arztebl Int* **109**:546-555.

Catella-Lawson F, Reilly MP, Kapoor SC, Cucchiara AJ, DeMarco S, Tournier B, Vyas SN, and FitzGerald GA (2001) Cyclooxygenase inhibitors and the antiplatelet effects of aspirin. *N Engl J Med* **345**:1809-1817.

Chao P, Uss AS, and Cheng KC (2010) Use of intrinsic clearance for prediction of human hepatic clearance. *Expert Opin Drug Metab Toxicol* **6**:189-198.

Chen G, Blevins-Primeau AS, Dellinger RW, Muscat JE, and Lazarus P (2007) Glucuronidation of nicotine and cotinine by UGT2B10: loss of function by the UGT2B10 codon 67 (Asp>Tyr) polymorphism. *Cancer Res* **67**:9024-9029.

Cheng Y and Prusoff WH (1973) Relationship between the inhibition constant (K_1) and the concentration of inhibitor which causes 50 per cent inhibition (I_{50}) of an enzymatic reaction. *Biochem Pharmacol* **22**:3099-3108.

Chiba M, Ishii Y, and Sugiyama Y (2009) Prediction of hepatic clearance in human from in vitro data for successful drug development. *AAPS J* **11**:262-276.

Ching MS, Blake CL, Ghabrial H, Ellis SW, Lennard MS, Tucker GT, and Smallwood RA (1995) Potent inhibition of yeast-expressed CYP2D6 by dihydroquinidine, quinidine, and its metabolites. *Biochem Pharmacol* **50**:833-837.

Ching MS, Morgan DJ, and Smallwood RA (1989) Models of hepatic elimination: implications from studies of the simultaneous elimination of taurocholate and diazepam by isolated rat liver under varying conditions of binding. *J Pharmacol Exp Ther* **250**:1048-1054.

Chiu SH and Huskey SW (1998) Species differences in N-glucuronidation. *Drug Metab Dispos* **26**:838-847.

Cingi C, Toros SZ, Ince I, Ertugay CK, Gurbuz MK, Cakli H, Erdogmus N, Karasulu E, and Kaya E (2013) Does desloratadine alter the serum levels of montelukast when administered in a fixed-dose combination? *Laryngoscope* **123**:2610-2614.

- Ciotti M, Lakshmi VM, Basu N, Davis BB, Owens IS, and Zenser TV (1999) Glucuronidation of benzidine and its metabolites by cDNA-expressed human UDP-glucuronosyltransferases and pH stability of glucuronides. *Carcinogenesis* **20**:1963-1969.
- Conrad KA, Byers JM, 3rd, Finley PR, and Burnham L (1983) Lidocaine elimination: effects of metoprolol and of propranolol. *Clin Pharmacol Ther* **33**:133-138.
- Cotreau MM, von Moltke LL, Beinfeld MC, and Greenblatt DJ (2000) Methodologies to study the induction of rat hepatic and intestinal cytochrome P450 3A at the mRNA, protein, and catalytic activity level. *J Pharmacol Toxicol Methods* **43**:41-54.
- Dai D, Zeldin DC, Blaisdell JA, Chanas B, Coulter SJ, Ghanayem BI, and Goldstein JA (2001) Polymorphisms in human CYP2C8 decrease metabolism of the anticancer drug paclitaxel and arachidonic acid. *Pharmacogenetics* **11**:597-607.
- Davies B and Morris T (1993) Physiological parameters in laboratory animals and humans. *Pharm Res* **10**:1093-1095.
- Davit B, Reynolds K, Yuan R, Funmilayo A, Conner D, Fadiran E, Gillespie B, Sahajwalla C, Huang S, and Lesko LJ (1999) FDA evaluations using in vitro metabolism to predict and interpret in vivo metabolic drug-drug interactions: impact on labeling. *J Clin Pharmacol* **39**:899-910.

Davydov DR, Davydova NY, Sineva EV, and Halpert JR (2015) Interactions among Cytochromes P450 in Microsomal Membranes: Oligomerization of cytochromes P450 3A4, 3A5 and 2E1 and its functional consequences. *J Biol Chem* **290**:3850-3864.

Davydov DR, Davydova NY, Sineva EV, Kufareva I, and Halpert JR (2013) Pivotal role of P450-P450 interactions in CYP3A4 allostery: the case of alpha-naphthoflavone. *Biochem J* **453**:219-230.

de la Grandmaison GL, Clairand I, and Durigon M (2001) Organ weight in 684 adult autopsies: new tables for a Caucasoid population. *Forensic Sci Int* **119**:149-154.

Delaforge M, Pruvost A, Perrin L, and Andre F (2005) Cytochrome P450-mediated oxidation of glucuronide derivatives: example of estradiol-17beta-glucuronide oxidation to 2-hydroxy-estradiol-17beta-glucuronide by CYP2C8. *Drug Metab Dispos* **33**:466-473.

Devillier P, Roche N, and Faisy C (2008) Clinical pharmacokinetics and pharmacodynamics of desloratadine, fexofenadine and levocetirizine : a comparative review. *Clin Pharmacokinet* **47**:217-230.

Di L, Atkinson K, Orozco CC, Funk C, Zhang H, McDonald TS, Tan B, Lin J, Chang C, and Obach RS (2013) In vitro-in vivo correlation for low-clearance compounds using hepatocyte relay method. *Drug Metab Dispos* **41**:2018-2023.

Di L, Trapa P, Obach RS, Atkinson K, Bi YA, Wolford AC, Tan B, McDonald TS, Lai Y, and Tremaine LM (2012) A novel relay method for determining low-clearance values. *Drug Metab Dispos* **40**:1860-1865.

Di Marco A, Yao D, and Laufer R (2003) Demethylation of radiolabelled dextromethorphan in rat microsomes and intact hepatocytes. Kinetics and sensitivity to cytochrome P450 2D inhibitors. *Eur J Biochem* **270**:3768-3777.

Dridi D and Marquet P (2013) Kinetic parameters of human P450 isoforms involved in the metabolism of the antiallergic drug, loratadine. *Int J Bio Biol Sci* **2**:19-27.

EMA (2013) Guideline on the investigation of drug interactions, European Medicines Agency, London, UK.

Emoto C, Yamazaki H, Yamasaki S, Shimadace N, Nakajima M, and Yokoi T (2000) Characterization of cytochrome P450 enzymes involved in drug oxidations in mouse intestinal microsomes. *Xenobiotica* **30**:943-953.

Ermondi G, Lorenti M, and Caron G (2004) Contribution of ionization and lipophilicity to drug binding to albumin: a preliminary step toward biodistribution prediction. *J Med Chem* **47**:3949-3961.

Fahmi OA, Hurst S, Plowchalk D, Cook J, Guo F, Youdim K, Dickins M, Phipps A, Darekar A, Hyland R, and Obach RS (2009) Comparison of different algorithms

for predicting clinical drug-drug interactions, based on the use of CYP3A4 in vitro data: predictions of compounds as precipitants of interaction. *Drug Metab Dispos* **37**:1658-1666.

FDA (1997) Drug Metabolism/Drug Interaction Studies in the Drug Development Process: Studies In Vitro, U.S. Food and Drug Administration, Center for Drug Evaluation and Research (CDER), Rockville, MD.

FDA (2012) Draft Guidance for Industry: Drug Interaction Studies—Study Design, Data Analysis, and Implications for Dosing and Labeling, U.S. Food and Drug Administration, Center for Drug Evaluation and Research (CDER), Rockville, MD.

Floreani M and Carpenedo F (1990) Inhibition of rat liver monooxygenase activities by 2-methyl-1,4-naphthoquinone (menadione). *Toxicol Appl Pharmacol* **105**:333-339.

Foster JA, Houston JB, and Hallifax D (2011) Comparison of intrinsic clearances in human liver microsomes and suspended hepatocytes from the same donor livers: clearance-dependent relationship and implications for prediction of in vivo clearance. *Xenobiotica* **41**:124-136.

Foti RS, Rock DA, Pearson JT, Wahlstrom JL, and Wienkers LC (2011) Mechanism-based inactivation of cytochrome P450 3A4 by mibefradil through heme destruction. *Drug Metab Dispos* **39**:1188-1195.

Fujiwara R, Nakajima M, Yamanaka H, Katoh M, and Yokoi T (2008) Product inhibition of UDP-glucuronosyltransferase (UGT) enzymes by UDP obfuscates the inhibitory effects of UGT substrates. *Drug Metab Dispos* **36**:361-367.

Fuse E, Tanii H, Kurata N, Kobayashi H, Shimada Y, Tamura T, Sasaki Y, Tanigawara Y, Lush RD, Headlee D, Figg WD, Arbuck SG, Senderowicz AM, Sausville EA, Akinaga S, Kuwabara T, and Kobayashi S (1998) Unpredicted clinical pharmacology of UCN-01 caused by specific binding to human alpha1-acid glycoprotein. *Cancer Res* **58**:3248-3253.

Fuse E, Tanii H, Takai K, Asanome K, Kurata N, Kobayashi H, Kuwabara T, Kobayashi S, and Sugiyama Y (1999) Altered pharmacokinetics of a novel anticancer drug, UCN-01, caused by specific high affinity binding to alpha1-acid glycoprotein in humans. *Cancer Res* **59**:1054-1060.

Gao Y, Liu D, Wang H, Zhu J, and Chen C (2010) Functional characterization of five CYP2C8 variants and prediction of CYP2C8 genotype-dependent effects on in vitro and in vivo drug-drug interactions. *Xenobiotica* **40**:467-475.

Geha RS and Meltzer EO (2001) Desloratadine: A new, nonsedating, oral antihistamine. *J Allergy Clin Immunol* **107**:751-762.

Gemzik B, Halvorson MR, and Parkinson A (1990) Pronounced and differential effects of ionic strength and pH on testosterone oxidation by membrane-bound and

purified forms of rat liver microsomal cytochrome P-450. *J Steroid Biochem* **35**:429-440.

Gentile DM, Tomlinson ES, Maggs JL, Park BK, and Back DJ (1996) Dexamethasone metabolism by human liver in vitro. Metabolite identification and inhibition of 6-hydroxylation. *J Pharmacol Exp Ther* **277**:105-112.

Gerlowski LE and Jain RK (1983) Physiologically based pharmacokinetic modeling: principles and applications. *J Pharm Sci* **72**:1103-1127.

Gertz M, Harrison A, Houston JB, and Galetin A (2010) Prediction of human intestinal first-pass metabolism of 25 CYP3A substrates from in vitro clearance and permeability data. *Drug Metab Dispos* **38**:1147-1158.

Gertz M, Kilford PJ, Houston JB, and Galetin A (2008) Drug lipophilicity and microsomal protein concentration as determinants in the prediction of the fraction unbound in microsomal incubations. *Drug Metab Dispos* **36**:535-542.

Ghosal A, Gupta S, Ramanathan R, Yuan Y, Lu X, Su AD, Alvarez N, Zbaida S, Chowdhury SK, and Alton KB (2009) Metabolism of loratadine and further characterization of its in vitro metabolites. *Drug Metab Lett* **3**:162-170.

Ghosal A, Yuan Y, Hapangama N, Su ADI, Narciso A, Chowdhury SK, Alton KB, Patrick JE, and Zbaida S (2004) Identification of human UDP-glucuronosyltransferase

enzyme(s) responsible for the glucuronidation of 3-hydroxydesloratadine.

Biopharm Drug Dispos **25**:243-252.

Gill KL, Houston JB, and Galetin A (2012) Characterization of in vitro glucuronidation clearance of a range of drugs in human kidney microsomes: comparison with liver and intestinal glucuronidation and impact of albumin. *Drug Metab Dispos* **40**:825-835.

Gillette JR (1973) Overview of drug-protein binding. *Ann N Y Acad Sci* **226**:6-17.

Godoy P, Hewitt NJ, Albrecht U, Andersen ME, Ansari N, Bhattacharya S, Bode JG, Bolleyn J, Borner C, Bottger J, Braeuning A, Budinsky RA, Burkhardt B, Cameron NR, Camussi G, Cho CS, Choi YJ, Craig Rowlands J, Dahmen U, Damm G, Dirsch O, Donato MT, Dong J, Dooley S, Drasdo D, Eakins R, Ferreira KS, Fonsato V, Fraczek J, Gebhardt R, Gibson A, Glanemann M, Goldring CE, Gomez-Lechon MJ, Groothuis GM, Gustavsson L, Guyot C, Hallifax D, Hammad S, Hayward A, Haussinger D, Hellerbrand C, Hewitt P, Hoehme S, Holzhutter HG, Houston JB, Hrach J, Ito K, Jaeschke H, Keitel V, Kelm JM, Kevin Park B, Kordes C, Kullak-Ublick GA, LeCluyse EL, Lu P, Luebke-Wheeler J, Lutz A, Maltman DJ, Matz-Soja M, McMullen P, Merfort I, Messner S, Meyer C, Mwinyi J, Naisbitt DJ, Nussler AK, Olinga P, Pampaloni F, Pi J, Pluta L, Przyborski SA, Ramachandran A, Rogiers V, Rowe C, Schelcher C, Schmich K, Schwarz M, Singh B, Stelzer EH, Stieger B, Stober R, Sugiyama Y, Tetta C, Thasler WE, Vanhaecke T, Vinken M, Weiss TS, Widera A, Woods CG, Xu JJ, Yarborough

KM, and Hengstler JG (2013) Recent advances in 2D and 3D in vitro systems using primary hepatocytes, alternative hepatocyte sources and non-parenchymal liver cells and their use in investigating mechanisms of hepatotoxicity, cell signaling and ADME. *Arch Toxicol* **87**:1315-1530.

Gonzalez FJ, Coughtrie M, and Tukey RH (2011) Drug Metabolism, in: *Goodman & Gilman's The Pharmacological Basis of Therapeutics* (Brunton LL ed), pp 123-143, McGraw-Hill, Inc., New York City, NY.

Griffin SJ and Houston JB (2004) Comparison of fresh and cryopreserved rat hepatocyte suspensions for the prediction of in vitro intrinsic clearance. *Drug Metab Dispos* **32**:552-558.

Grimm SW, Einolf HJ, Hall SD, He K, Lim H-K, Ling K-HJ, Lu C, Nomeir AA, Seibert E, Skordos KW, Tonn GR, Van Horn R, Wang RW, Wong YN, Yang TJ, and Obach RS (2009) The Conduct of in Vitro Studies to Address Time-Dependent Inhibition of Drug-Metabolizing Enzymes: A Perspective of the Pharmaceutical Research and Manufacturers of America. *Drug Metab Dispos* **37**:1355-1370.

Gupta S, Banfield C, Kantesaria B, Flannery B, and Herron J (2004) Pharmacokinetics/pharmacodynamics of desloratadine and fluoxetine in healthy volunteers. *J Clin Pharmacol* **44**:1252-1259.

- Gupta S, Banfield C, Kantesaria B, Marino M, Clement R, Affrime M, and Batra V (2001) Pharmacokinetic and safety profile of desloratadine and fexofenadine when coadministered with azithromycin: a randomized, placebo-controlled, parallel-group study. *Clin Ther* **23**:451-466.
- Gupta SK, Kantesaria B, and Wang Z (2007) Multiple-dose pharmacokinetics and safety of desloratadine in subjects with moderate hepatic impairment. *J Clin Pharmacol* **47**:1283-1291.
- Hakooz N, Ito K, Rawden H, Gill H, Lemmers L, Boobis A, Edwards R, Carlile D, Lake B, and Houston J (2006) Determination of a human hepatic microsomal scaling factor for predicting in vivo drug clearance. *Pharm Res* **23**:533-539.
- Hakooz N and Salem, II (2012) Prevalence of desloratadine poor metabolizer phenotype in healthy Jordanian males. *Biopharm Drug Dispos* **33**:15-21.
- Hallifax D, Foster JA, and Houston JB (2010) Prediction of human metabolic clearance from in vitro systems: retrospective analysis and prospective view. *Pharm Res* **27**:2150-2161.
- Hallifax D and Houston JB (2006) Binding of drugs to hepatic microsomes: comment and assessment of current prediction methodology with recommendation for improvement. *Drug Metab Dispos* **34**:724-726; author reply 727.

Hallifax D and Houston JB (2012) Evaluation of hepatic clearance prediction using in vitro data: emphasis on fraction unbound in plasma and drug ionisation using a database of 107 drugs. *J Pharm Sci* **101**:2645-2652.

Hallifax D, Rawden HC, Hakooz N, and Houston JB (2005) Prediction of metabolic clearance using cryopreserved human hepatocytes: kinetic characteristics for five benzodiazepines. *Drug Metab Dispos* **33**:1852-1858.

Hanioka N, Matsumoto K, Saito Y, and Narimatsu S (2010) Functional characterization of CYP2C8.13 and CYP2C8.14: catalytic activities toward paclitaxel. *Basic Clin Pharmacol Toxicol* **107**:565-569.

Haupt LJ, Kazmi F, Smith BD, Leatherman S, and Parkinson A (2011) Can K_i values for direct inhibition of CYP enzymes be reliably estimated from IC_{50} values? *Drug Metab Rev* **43**:(S2)105.

Henz BM (2001) The pharmacologic profile of desloratadine: a review. *Allergy* **56 Suppl 65**:7-13.

Hichiya H, Tanaka-Kagawa T, Soyama A, Jinno H, Koyano S, Katori N, Matsushima E, Uchiyama S, Tokunaga H, Kimura H, Minami N, Katoh M, Sugai K, Goto Y, Tamura T, Yamamoto N, Ohe Y, Kunitoh H, Nokihara H, Yoshida T, Minami H, Saijo N, Ando M, Ozawa S, Saito Y, and Sawada J (2005) Functional

characterization of five novel CYP2C8 variants, G171S, R186X, R186G, K247R, and K383N, found in a Japanese population. *Drug Metab Dispos* **33**:630-636.

Hinderling PH (1997) Red blood cells: a neglected compartment in pharmacokinetics and pharmacodynamics. *Pharmacol Rev* **49**:279-295.

Howgate EM, Rowland YK, Proctor NJ, Tucker GT, and Rostami-Hodjegan A (2006) Prediction of in vivo drug clearance from in vitro data. I: impact of inter-individual variability. *Xenobiotica* **36**:473-497.

Huang SM, Strong JM, Zhang L, Reynolds KS, Nallani S, Temple R, Abraham S, Habet SA, Baweja RK, Burckart GJ, Chung S, Colangelo P, Frucht D, Green MD, Hepp P, Karnaukhova E, Ko HS, Lee JI, Marroum PJ, Norden JM, Qiu W, Rahman A, Sobel S, Stifano T, Thummel K, Wei XX, Yasuda S, Zheng JH, Zhao H, and Lesko LJ (2008) New era in drug interaction evaluation: US Food and Drug Administration update on CYP enzymes, transporters, and the guidance process. *J Clin Pharmacol* **48**:662-670.

Hyland R, Osborne T, Payne A, Kempshall S, Logan YR, Ezzeddine K, and Jones B (2009) In vitro and in vivo glucuronidation of midazolam in humans. *Br J Clin Pharmacol* **67**:445-454.

Idle JR, Mahgoub A, Lancaster R, and Smith RL (1978) Hypotensive response to debrisoquine and hydroxylation phenotype. *Life Sci* **22**:979-983.

Ito K, Brown HS, and Houston JB (2004) Database analyses for the prediction of *in vivo* drug-drug interactions from *in vitro* data. *Br J Clin Pharmacol* **57**:473-486.

Ito K and Houston BJ (2004) Comparison of the use of liver models for predicting drug clearance using *in vitro* kinetic data from hepatic microsomes and isolated hepatocytes. *Pharm Res* **21**:785-792.

Ito K, Iwatsubo T, Kanamitsu S, Ueda K, Suzuki H, and Sugiyama Y (1998) Prediction of pharmacokinetic alterations caused by drug-drug interactions: metabolic interaction in the liver. *Pharmacol Rev* **50**:387-412.

IUPAC (1997) Ionic Strength, in: *Compendium of Chemical Terminology, 2nd ed (the "Gold Book")* (McNaught AD and Wilkinson A eds), Blackwell Scientific Publications, Oxford, doi: 10.1351/goldbook.I03180.

Jiang F, Desta Z, Shon JH, Yeo CW, Kim HS, Liu KH, Bae SK, Lee SS, Flockhart DA, and Shin JG (2013) Effects of clopidogrel and itraconazole on the disposition of efavirenz and its hydroxyl metabolites: exploration of a novel CYP2B6 phenotyping index. *Br J Clin Pharmacol* **75**:244-253.

Jiang H, Zhong F, Sun L, Feng W, Huang ZX, and Tan X (2011) Structural and functional insights into polymorphic enzymes of cytochrome P450 2C8. *Amino Acids* **40**:1195-1204.

Johnson TN, Tucker GT, Tanner MS, and Rostami-Hodjegan A (2005) Changes in liver volume from birth to adulthood: a meta-analysis. *LiverTranspl* **11**:1481-1493.

Jones DB, Ching MS, Smallwood RA, and Morgan DJ (1985) A carrier-protein receptor is not a prerequisite for avid hepatic elimination of highly bound compounds: a study of propranolol elimination by the isolated perfused rat liver. *Hepatology* **5**:590-593.

Jones HM and Houston JB (2004) Substrate depletion approach for determining in vitro metabolic clearance: time dependencies in hepatocyte and microsomal incubations. *Drug Metab Dispos* **32**:973-982.

Joseph DP, Guengerich PF, and Miners JO (2005) "Phase I and Phase II" drug metabolism: terminology that we should phase out? *Drug Metab Rev* **37**:575-580.

Kaivosaari S, Finel M, and Koskinen M (2011) N-glucuronidation of drugs and other xenobiotics by human and animal UDP-glucuronosyltransferases. *Xenobiotica* **41**:652-669.

Kato Y, Izukawa T, Oda S, Fukami T, Finel M, Yokoi T, and Nakajima M (2013) Human UDP-glucuronosyltransferase (UGT) 2B10 in drug N-glucuronidation: substrate screening and comparison with UGT1A3 and UGT1A4. *Drug Metab Dispos* **41**:1389-1397.

Kazmi F, Barbara JE, Yerino P, and Parkinson A (2015) A Long-Standing Mystery Solved: The Formation of 3-Hydroxydesloratadine is Catalyzed by CYP2C8 but Prior Glucuronidation of Desloratadine by UGT2B10 is an Obligatory Requirement. *Drug Metab Dispos* **43**:523-533.

Kazmi F, Buckley DB, Yerino P, Ogilvie BW, and Parkinson A (2009) Effects of plasma on cytochrome P450 (CYP) inhibition studies in human liver microsomes (HLM): Consequences on in vitro-in vivo extrapolations (IVIVE). *Drug Meta Rev* **41 (S3)**:192.

Kazmi F, Haupt LJ, Horkman JR, Smith BD, Buckley DB, Wachter EA, and Singer JM (2014a) In vitro inhibition of human liver cytochrome P450 (CYP) and UDP-glucuronosyltransferase (UGT) enzymes by rose bengal: system-dependent effects on inhibitory potential. *Xenobiotica* **44**:606-614.

Kazmi F, Hensley T, Pope C, Funk RS, Loewen GJ, Buckley DB, and Parkinson A (2013) Lysosomal sequestration (trapping) of lipophilic amine (cationic amphiphilic) drugs in immortalized human hepatocytes (Fa2N-4 cells). *Drug Metab Dispos* **41**:897-905.

Kazmi F, Smith B, Hvenegaard M, Bendahl L, Gipson A, Buckley DB, Ogilvie BW, and Parkinson A (2010) Identification of a novel carbamoyl glucuronide as a metabolism-dependent inhibitor of CYP2C8. *Drug Metab Rev* **42 (S1)**:143.

- Kazmi F, Yerino P, Ogilvie BW, Usuki E, Chladek J, and Buckley DB (2014d) Assessment under initial rate conditions of the selectivity and time course of cytochrome P450 inactivation in pooled human liver microsomes and hepatocytes: Optimization of inhibitor conditions used for reaction phenotyping studies. *Drug Metab Rev* **In Press**.
- Kilford PJ, Gertz M, Houston JB, and Galetin A (2008) Hepatocellular binding of drugs: correction for unbound fraction in hepatocyte incubations using microsomal binding or drug lipophilicity data. *Drug Metab Dispos* **36**:1194-1197.
- Kilford PJ, Stringer R, Sohal B, Houston JB, and Galetin A (2009) Prediction of drug clearance by glucuronidation from in vitro data: use of combined cytochrome P450 and UDP-glucuronosyltransferase cofactors in alamethicin-activated human liver microsomes. *Drug Metab Dispos* **37**:82-89.
- Kim J-S, Ahn T, Yim S-K, and Yun C-H (2002) Differential Effect of Copper (II) on the Cytochrome P450 Enzymes and NADPH-Cytochrome P450 Reductase: Inhibition of Cytochrome P450-Catalyzed Reactions by Copper (II) Ion. *Biochemistry* **41**:9438-9447.
- Kirby BJ and Unadkat JD (2010) Impact of ignoring extraction ratio when predicting drug-drug interactions, fraction metabolized, and intestinal first-pass contribution. *Drug Metab Dispos* **38**:1926-1933.

- Kochansky CJ, Xia Y-Q, Wang S, Cato B, Creighton M, Vincent SH, Franklin RB, and Reed JR (2005) Species differences in the elimination of a peroxisome proliferator-activated receptor agonist highlighted by oxidative metabolism of its acyl glucuronide. *Drug Metab Dispos* **33**:1894-1904.
- Kudo T, Ozaki Y, Hotta E, Matsubara A, and Ito K (2014) Effect of buffer conditions on CYP2C8-mediated 6 α -hydroxylation of paclitaxel by human liver microsomes. *Drug Metab Rev* **In press**.
- Kumar S, Samuel K, Subramanian R, Braun MP, Stearns RA, Chiu SH, Evans DC, and Baillie TA (2002) Extrapolation of diclofenac clearance from in vitro microsomal metabolism data: role of acyl glucuronidation and sequential oxidative metabolism of the acyl glucuronide. *J Pharmacol Exp Ther* **303**:969-978.
- Li C and Benet L (2003) Mechanistic role of acyl glucuronides, in: *Drug-Induced Liver Disease* (Kaplowitz N and DeLeve L eds), pp 151-181, Marcel Dekker, Inc., New York.
- Li XQ, Andersson TB, Ahlstrom M, and Weidolf L (2004) Comparison of inhibitory effects of the proton pump-inhibiting drugs omeprazole, esomeprazole, lansoprazole, pantoprazole, and rabeprazole on human cytochrome P450 activities. *Drug Metab Dispos* **32**:821-827.

- Lowry OH, Passonneau JV, Schulz DW, and Rock MK (1961) The measurement of pyridine nucleotides by enzymatic cycling. *J Biol Chem* **236**:2746-2755.
- Lu C, Li P, Gallegos R, Uttamsingh V, Xia CQ, Miwa GT, Balani SK, and Gan LS (2006) Comparison of intrinsic clearance in liver microsomes and hepatocytes from rats and humans: evaluation of free fraction and uptake in hepatocytes. *Drug Metab Dispos* **34**:1600-1605.
- Lu C, Miwa GT, Prakash SR, Gan L-S, and Balani SK (2007) A novel model for the prediction of drug-drug interactions in humans based on in vitro cytochrome p450 phenotypic data. *Drug Metab Dispos* **35**:79-85.
- Ludden LK, Ludden TM, Collins JM, Pentikis HS, and Strong JM (1997) Effect of albumin on the estimation, in vitro, of phenytoin Vmax and Km values: implications for clinical correlation. *J Pharmacol Exp Ther* **282**:391-396.
- Mackenzie PI, Walter BK, Burchell B, Guillemette C, Ikushiro S, Iyanagi T, Miners JO, Owens IS, and Nebert DW (2005) Nomenclature update for the mammalian UDP glycosyltransferase (UGT) gene superfamily. *Pharmacogenet Genomics* **15**:677-685.
- Maenpaa J, Hall SD, Ring BJ, Strom SC, and Wrighton SA (1998) Human cytochrome P450 3A (CYP3A) mediated midazolam metabolism: the effect of assay

conditions and regioselective stimulation by alpha-naphthoflavone, terfenadine and testosterone. *Pharmacogenetics* **8**:137-155.

Mahgoub A, Idle JR, Dring LG, Lancaster R, and Smith RL (1977) Polymorphic hydroxylation of Debrisoquine in man. *Lancet* **2**:584-586.

Mao J, Mohutsky MA, Harrelson JP, Wrighton SA, and Hall SD (2012) Predictions of cytochrome p450-mediated drug-drug interactions using cryopreserved human hepatocytes: comparison of plasma and protein-free media incubation conditions. *Drug Metab Dispos* **40**:706-716.

Margolis JM and Obach RS (2003) Impact of nonspecific binding to microsomes and phospholipid on the inhibition of cytochrome P4502D6: implications for relating in vitro inhibition data to in vivo drug interactions. *Drug Metab Dispos* **31**:606-611.

McGinnity DF, Soars MG, Urbanowicz RA, and Riley RJ (2004) Evaluation of fresh and cryopreserved hepatocytes as in vitro drug metabolism tools for the prediction of metabolic clearance. *Drug Metab Dispos* **32**:1247-1253.

McLure J, Miners J, and Birkett D (2000) Nonspecific binding of drugs to human liver microsomes. *Br J Clin Pharmacol* **49**:453-461.

- Miners JO, Knights KM, Houston JB, and Mackenzie PI (2006) In vitro-in vivo correlation for drugs and other compounds eliminated by glucuronidation in humans: Pitfalls and promises. *Biochem Pharmacol* **71**:1531-1539.
- Miners JO, Mackenzie PI, and Knights KM (2010a) The prediction of drug-glucuronidation parameters in humans: UDP-glucuronosyltransferase enzyme-selective substrate and inhibitor probes for reaction phenotyping and in vitro-in vivo extrapolation of drug clearance and drug-drug interaction potential. *Drug Metab Rev* **42**:189-201.
- Miners JO, Polasek TM, Mackenzie PI, and Knights KM (2010g) The In Vitro Characterization of Inhibitory Drug–Drug Interactions Involving UDP-Glucuronosyltransferase, in: *Enzyme- and Transporter-Based Drug-Drug Interactions* (Pang KS, Rodrigues AD, and Peter RM eds), pp 217-236, Springer New York.
- Mistry M and Houston J (1987) Glucuronidation in vitro and in vivo. Comparison of intestinal and hepatic conjugation of morphine, naloxone, and buprenorphine. *Drug Metab Dispos* **15**:710-717.
- Molimard M, Diquet B, and Benedetti MS (2004) Comparison of pharmacokinetics and metabolism of desloratadine, fexofenadine, levocetirizine and mizolastine in humans. *Fundam Clin Pharmacol* **18**:399-411.

Monahan BP, Ferguson CL, Killeavy ES, Lloyd BK, Troy J, and Cantilena LR, Jr. (1990) Torsades de pointes occurring in association with terfenadine use. *JAMA* **264**:2788-2790.

Murphy SE, Park SS, Thompson EF, Wilkens LR, Patel Y, Stram DO, and Le Marchand L (2014) Nicotine N-glucuronidation relative to N-oxidation and C-oxidation and UGT2B10 genotype in five ethnic/racial groups. *Carcinogenesis* **35**:2526-2533.

Muszkat M, Blotnik S, Elami A, Krasilnikov I, and Caraco Y (2007) Warfarin metabolism and anticoagulant effect: a prospective, observational study of the impact of CYP2C9 genetic polymorphism in the presence of drug-disease and drug-drug interactions. *Clin Ther* **29**:427-437.

Nagar S and Korzekwa K (2012) Commentary: nonspecific protein binding versus membrane partitioning: it is not just semantics. *Drug Metab Dispos* **40**:1649-1652.

Naritomi Y, Terachita S, Kimura S, Suzuki A, Kagayama A, and Sugiyama Y (2001) Prediction of human hepatic clearance from in vivo animal experiments and in vitro metabolic studies with liver microsomes from animals and humans. *Drug Metab Dispos* **29**:1316-1324.

Nielsen TL, Rasmussen BB, Flinois JP, Beaune P, and Brosen K (1999) In vitro metabolism of quinidine: the (3S)-3-hydroxylation of quinidine is a specific marker

reaction for cytochrome P-450A4 activity in human liver microsomes. *J Pharmacol Exp Ther* **289**:31-37.

Nishimura M and Naito S (2006) Tissue-specific mRNA expression profiles of human phase I metabolizing enzymes except for cytochrome P450 and phase II metabolizing enzymes. *Drug Metab Pharmacokinet* **21**:357-374.

Nordell P, Svanberg P, Bird J, and Grime K (2013) Predicting metabolic clearance for drugs that are actively transported into hepatocytes: incubational binding as a consequence of in vitro hepatocyte concentration is a key factor. *Drug Metab Dispos* **41**:836-843.

Obach RS (1996) The importance of nonspecific binding in in vitro matrices, its impact on enzyme kinetic studies of drug metabolism reactions, and implications for in vitro-in vivo correlations. *Drug Metab Dispos* **24**:1047-1049.

Obach RS (1997) Nonspecific binding to microsomes: impact on scale-up of in vitro intrinsic clearance to hepatic clearance as assessed through examination of warfarin, imipramine, and propranolol. *Drug Metab Dispos* **25**:1359-1369.

Obach RS (1999) Prediction of human clearance of twenty-nine drugs from hepatic microsomal intrinsic clearance data: An examination of in vitro half-life approach and nonspecific binding to microsomes. *Drug Metab Dispos* **27**:1350-1359.

Obach RS, Lombardo F, and Waters NJ (2008) Trend analysis of a database of intravenous pharmacokinetic parameters in humans for 670 drug compounds. *Drug Metab Dispos* **36**:1385-1405.

Obach RS, Walsky RL, Venkatakrishnan K, Gaman EA, Houston JB, and Tremaine LM (2006) The utility of in vitro cytochrome P450 inhibition data in the prediction of drug-drug interactions. *J Pharmacol Exp Ther* **316**:336-348.

Ogilvie BW, Usuki E, Yerino P, and Parkinson A (2008) In vitro approaches for studying the inhibition of drug-metabolizing enzymes and identifying the drug-metabolizing enzymes responsible for the metabolism of drugs (Reaction Phenotyping) with emphasis on cytochrome P450, in: *Drug-Drug Interactions* (Rodrigues AD ed), pp 231-358, Informa Healthcare USA Inc., New York, NY.

Ogilvie BW, Yerino P, Kazmi F, Buckley DB, Rostami-Hodjegan A, Paris BL, Toren P, and Parkinson A (2011) The proton pump inhibitor, omeprazole, but not lansoprazole or pantoprazole, is a metabolism-dependent inhibitor of CYP2C19: implications for coadministration with clopidogrel. *Drug Metab Dispos* **39**:2020-2033.

Ogilvie BW, Zhang D, Li W, Rodrigues AD, Gipson AE, Holsapple J, Toren P, and Parkinson A (2006) Glucuronidation converts gemfibrozil to a potent, metabolism-dependent inhibitor of CYP2C8: Implications for drug-drug interactions. *Drug Metab Dispos* **34**:191-197.

- Omura T and Sato R (1964) The Carbon Monoxide-Binding Pigment of Liver Microsomes. I. Evidence for Its Hemoprotein Nature. *J Biol Chem* **239**:2370-2378.
- Ortiz de Montellano PR (2008) Mechanism and role of covalent heme binding in the CYP4 family of P450 enzymes and the mammalian peroxidases. *Drug Metab Rev* **40**:405-426.
- Paine MF, Hart HL, Ludington SS, Haining RL, Rettie AE, and Zeldin DC (2006) The human intestinal cytochrome P450 "pie". *Drug Metab Dispos* **34**:880-886.
- Palm K, Stenberg P, Luthman K, and Artursson P (1997) Polar molecular surface properties predict the intestinal absorption of drugs in humans. *Pharm Res* **14**:568-571.
- Paris BL, Ogilvie BW, Scheinkoenig JA, Ndikum-Moffor F, Gibson R, and Parkinson A (2009) In vitro inhibition and induction of human liver cytochrome P450 (CYP) enzymes by milnacipran. *Drug Metab Dispos* **37**:2045-2054.
- Parkinson A, Kazmi F, Buckley DB, Yerino P, Ogilvie BW, and Paris BL (2010) System-dependent outcomes during the evaluation of drug candidates as inhibitors of cytochrome P450 (CYP) and uridine diphosphate glucuronosyltransferase (UGT) enzymes: human hepatocytes versus liver microsomes versus recombinant enzymes. *Drug Metab Pharmacokinet* **25**:16-27.

- Parkinson A, Kazmi F, Buckley DB, Yerino P, Paris BL, Holsapple J, Toren P, Otradovec SM, and Ogilvie BW (2011) An Evaluation of the Dilution Method for Identifying Metabolism-dependent Inhibitors (MDIs) of Cytochrome P450 (CYP) Enzymes. *Drug Metab Dispos* **39**:1370-1387.
- Parkinson A, Mudra DR, Johnson C, Dwyer A, and Carroll KM (2004) The effects of gender, age, ethnicity, and liver cirrhosis on cytochrome P450 enzyme activity in human liver microsomes and inducibility in cultured human hepatocytes. *Toxicol Appl Pharmacol* **199**:193-209.
- Parkinson A, Ogilvie BW, D.B. B, F. K, M. C, and O. P (2013) Biotransformation of Xenobiotics, in: *Casarett & Doull's Toxicology: The Basic Science of Poisons* (Klaassen CD ed), pp 185-367, McGraw-Hill, Inc., New York City, NY.
- Pearce RE, McIntyre CJ, Madan A, Sanzgiri U, Draper AJ, Bullock PL, Cook DC, Burton LA, Latham J, Nevins C, and Parkinson A (1996a) Effects of freezing, thawing, and storing human liver microsomes on cytochrome P450 activity. *Arch Biochem Biophys* **331**:145-169.
- Pearce RE, Rodrigues AD, Goldstein JA, and Parkinson A (1996c) Identification of the human P450 enzymes involved in lansoprazole metabolism. *J Pharmacol Exp Ther* **277**:805-816.

Peltoniemi MA, Saari TI, Hagelberg NM, Reponen P, Turpeinen M, Laine K, Neuvonen PJ, and Olkkola KT (2011) Exposure to oral S-ketamine is unaffected by itraconazole but greatly increased by ticlopidine. *Clin Pharmacol Ther* **90**:296-302.

Pope LE, Khalil MH, Berg JE, Stiles M, Yakatan GJ, and Sellers EM (2004) Pharmacokinetics of dextromethorphan after single or multiple dosing in combination with quinidine in extensive and poor metabolizers. *J Clin Pharmacol* **44**:1132-1142.

Poulin P and Haddad S (2011) Microsome composition-based model as a mechanistic tool to predict nonspecific binding of drugs in liver microsomes. *J Pharm Sci* **100**:4501-4517.

Poulin P, Kenny JR, Hop CE, and Haddad S (2012) In vitro-in vivo extrapolation of clearance: modeling hepatic metabolic clearance of highly bound drugs and comparative assessment with existing calculation methods. *J Pharm Sci* **101**:838-851.

Prenner B, Kim K, Gupta S, Khalilieh S, Kantesaria B, Manitpisitkul P, Lorber R, Wang Z, and Lutsky B (2006) Adult and paediatric poor metabolisers of desloratadine: an assessment of pharmacokinetics and safety. *Expert Opin Drug Saf* **5**:211-223.

Price PS, Conolly RB, Chaisson CF, Gross EA, Young JS, Mathis ET, and Tedder DR (2003) Modeling interindividual variation in physiological factors used in PBPK models of humans. *Crit Rev Toxicol* **33**:469-503.

Pryde DC, Dalvie D, Hu Q, Jones P, Obach RS, and Tran TD (2010) Aldehyde oxidase: an enzyme of emerging importance in drug discovery. *J Med Chem* **53**:8441-8460.

Ramanathan R, Alvarez N, Su AD, Chowdhury S, Alton K, Stauber K, and Patrick J (2005) Metabolism and excretion of loratadine in male and female mice, rats and monkeys. *Xenobiotica* **35**:155-189.

Ramanathan R, Duen Su A, Alvarez N, Feng W, Chowdhury SK, Stauber K, Reyderman L, Alton KB, Wirth M, and Patrick JE (2006) Metabolism and excretion of desloratadine (Clarinet®) in mice, rats, monkeys and humans. *Drug Metab Rev* **38 (S2)**:160.

Ramanathan R, Reyderman L, Su AD, Alvarez N, Chowdhury SK, Alton KB, Wirth MA, Clement RP, Statkevich P, and Patrick JE (2007) Disposition of desloratadine in healthy volunteers. *Xenobiotica* **37**:770-787.

Ramanathan R, Su AD, Alvarez N, Blumenkrantz N, Chowdhury SK, Alton K, and Patrick J (2000) Liquid chromatography/mass spectrometry methods for

distinguishing N-oxides from hydroxylated compounds. *Anal Chem* **72**:1352-1359.

Ramanathan V and Vachharajani N (2010) Protein Binding in Drug Discovery and Development, in: *Evaluation of Drug Candidates for Preclinical Development: Pharmacokinetics, Metabolism, Pharmaceutics, and Toxicology* (Han C, Davis CB, and Wang B eds), pp 135-167, John Wiley & Sons, Inc., Hoboken, NJ.

Rawden HC, Carlile DJ, Houston B, Tindall A, Hallifax D, Galetin A, Ito K, and Houston JB (2005) Microsomal prediction of in vivo clearance and associated interindividual variability of six benzodiazepines in humans. *Xenobiotica* **35**:603 - 625.

Reese MJ, Wurm RM, Muir KT, Generaux GT, St John-Williams L, and McConn DJ (2008) An in vitro mechanistic study to elucidate the desipramine/bupropion clinical drug-drug interaction. *Drug Metab Dispos* **36**:1198-1201.

Reiss PD, Zuurendonk PF, and Veech RL (1984) Measurement of tissue purine, pyrimidine, and other nucleotides by radial compression high-performance liquid chromatography. *Anal Biochem* **140**:162-171.

Remesy C, Demigne C, and Fafournoux P (1986) Control of ammonia distribution ratio across the liver cell membrane and of ureogenesis by extracellular pH. *Eur J Biochem* **158**:283-288.

Richter T, Murdter TE, Heinkele G, Pleiss J, Tatzel S, Schwab M, Eichelbaum M, and Zanger UM (2004) Potent mechanism-based inhibition of human CYP2B6 by clopidogrel and ticlopidine. *J Pharmacol Exp Ther* **308**:189-197.

Ridgway D, Tuszynski JA, and Tam YK (2003) Reassessing models of hepatic extraction. *J BiolPhys* **29**:1-21.

Riley RJ, McGinnity DF, and Austin RP (2005) A unified model for predicting human hepatic, metabolic clearance from in vitro intrinsic clearance data in hepatocytes and microsomes. *Drug Metab Dispos* **33**:1304-1311.

Roberts MS (2010) Drug structure-transport relationships. *J Pharmacokinetic Pharmacodyn* **37**:541-573.

Roberts MS and Rowland M (1986a) Correlation between in-vitro microsomal enzyme activity and whole organ hepatic elimination kinetics: analysis with a dispersion model. *J Pharm Pharmacol* **38**:177-181.

Roberts MS and Rowland M (1986b) A dispersion model of hepatic elimination: 1. Formulation of the model and bolus considerations. *J Pharmacokinetic Biopharm* **14**:227-260.

Roberts MS and Rowland M (1986d) A dispersion model of hepatic elimination: 2. Steady-state considerations--influence of hepatic blood flow, binding within

blood, and hepatocellular enzyme activity. *J Pharmacokinet Biopharm* **14**:261-288.

Roberts MS and Rowland M (1986f) A dispersion model of hepatic elimination: 3. Application to metabolite formation and elimination kinetics. *J Pharmacokinet Biopharm* **14**:289-308.

Routledge PA, Chapman PH, Davies DM, and Rawlins MD (1979) Pharmacokinetics and pharmacodynamics of warfarin at steady state. *Br J Clin Pharmacol* **8**:243-247.

Rowland A, Elliot DJ, Knights KM, Mackenzie PI, and Miners JO (2008a) The "albumin effect" and in vitro-in vivo extrapolation: sequestration of long-chain unsaturated fatty acids enhances phenytoin hydroxylation by human liver microsomal and recombinant cytochrome P450 2C9. *Drug Metab Dispos* **36**:870-877.

Rowland A, Gaganis P, Elliot DJ, Mackenzie PI, Knights KM, and Miners JO (2007) Binding of inhibitory fatty acids is responsible for the enhancement of UDP-glucuronosyltransferase 2B7 activity by albumin: implications for in vitro-in vivo extrapolation. *J Pharmacol Exp Ther* **321**:137-147.

Rowland A, Knights KM, Mackenzie PI, and Miners JO (2008c) The "albumin effect" and drug glucuronidation: bovine serum albumin and fatty acid-free human serum albumin enhance the glucuronidation of UDP-glucuronosyltransferase (UGT) 1A9

substrates but not UGT1A1 and UGT1A6 activities. *Drug Metab Dispos* **36**:1056-1062.

Rowland A, Knights KM, Mackenzie PI, and Miners JO (2009) Characterization of the binding of drugs to human intestinal fatty acid binding protein (IFABP): potential role of IFABP as an alternative to albumin for in vitro-in vivo extrapolation of drug kinetic parameters. *Drug Metab Dispos* **37**:1395-1403.

Rowland A, Mackenzie PI, and Miners JO (2015) Transporter-mediated uptake of UDP-glucuronic acid by human liver microsomes: assay conditions, kinetics, and inhibition. *Drug Metab Dispos* **43**:147-153.

Rowland M, Leitch D, Fleming G, and Smith B (1984) Protein binding and hepatic clearance: discrimination between models of hepatic clearance with diazepam, a drug of high intrinsic clearance, in the isolated perfused rat liver preparation. *J Pharmacokinet Biopharm* **12**:129-147.

Rowland M and Tozer TN (2011) *Clinical Pharmacokinetics and Pharmacodynamics: Concepts and Applications*. Lippincot Williams & Wilkins, Baltimore, MD.

Schary WL and Rowland M (1983) Protein binding and hepatic clearance: studies with tolbutamide, a drug of low intrinsic clearance, in the isolated perfused rat liver preparation. *J Pharmacokinet Biopharm* **11**:225-243.

Schering-Plough (2001) Clarinex [package insert], Schering Corporation, Kenilworth, NJ.

Sem DS and Kasper CB (1993) Enzyme-substrate binding interactions of NADPH-cytochrome P-450 oxidoreductase characterized with pH and alternate substrate/inhibitor studies. *Biochemistry* **32**:11539-11547.

Shand DG, Cotham RH, and Wilkinson GR (1976) Perfusion-limited of plasma drug binding on hepatic drug extraction. *Life Sci* **19**:125-130.

Shitara Y, Hirano M, Sato H, and Sugiyama Y (2004) Gemfibrozil and its glucuronide inhibit the organic anion transporting polypeptide 2 (OATP2/OATP1B1:SLC21A6)-mediated hepatic uptake and CYP2C8-mediated metabolism of cerivastatin: analysis of the mechanism of the clinically relevant drug-drug interaction between cerivastatin and gemfibrozil. *J Pharmacol Exp Ther* **311**:228-236.

Silverman RB (1995) Mechanism-based enzyme inactivators. *Methods in Enzymology* **249**:240-283.

Skaggs SM, Foti RS, and Fisher MB (2006) A streamlined method to predict hepatic clearance using human liver microsomes in the presence of human plasma. *J Pharmacol Toxicol Methods* **53**:284-290.

Smith DA and Dalvie D (2012) Why do metabolites circulate? *Xenobiotica* **42**:107-126.

Smith R, Jones RD, Ballard PG, and Griffiths HH (2008) Determination of microsome and hepatocyte scaling factors for in vitro/in vivo extrapolation in the rat and dog. *Xenobiotica* **38**:1386-1398.

Soars MG, Burchell B, and Riley RJ (2002) In vitro analysis of human drug glucuronidation and prediction of in vivo metabolic clearance. *J Pharmacol Exp Ther* **301**:382-390.

Soars MG, Grime K, Sproston JL, Webborn PJ, and Riley RJ (2007) Use of hepatocytes to assess the contribution of hepatic uptake to clearance in vivo. *Drug Metab Dispos* **35**:859-865.

Soars MG, Webborn PJ, and Riley RJ (2009) Impact of hepatic uptake transporters on pharmacokinetics and drug-drug interactions: use of assays and models for decision making in the pharmaceutical industry. *Mol Pharm* **6**:1662-1677.

Sohlenius-Sternbeck A-K (2006) Determination of the hepatocellularity number for human, dog, rabbit, rat and mouse livers from protein concentration measurements. *Toxicology in Vitro* **20**:1582-1586.

Storb R, Buckner CD, Dillingham LA, and Thomas ED (1970) Cyclophosphamide regimens in rhesus monkey with and without marrow infusion. *Cancer Res* **30**:2195-2203.

Strober W (2001) Trypan blue exclusion test of cell viability. *Curr Protoc Immunol*
Appendix 3:Appendix 3B.

Sun H, Liu L, and Pang KS (2006) Increased estrogen sulfation of estradiol 17beta-D-glucuronide in metastatic tumor rat livers. *J Pharmacol Exp Ther* **319**:818-831.

Tamura M, Yubisui T, and Takeshita M (1988) The opposite effect of bivalent cations on cytochrome b5 reduction by NADH:cytochrome b5 reductase and NADPH:cytochrome c reductase. *Biochem J* **251**:711-715.

Tang C, Lin Y, Rodrigues AD, and Lin JH (2002) Effect of albumin on phenytoin and tolbutamide metabolism in human liver microsomes: an impact more than protein binding. *Drug Metab Dispos* **30**:648-654.

Thummel KE, Shen DD, Podoll TD, Kunze KL, Trager WF, Bacchi CE, Marsh CL, McVicar JP, Barr DM, Perkins JD, and et al. (1994a) Use of midazolam as a human cytochrome P450 3A probe: II. Characterization of inter- and intraindividual hepatic CYP3A variability after liver transplantation. *J Pharmacol Exp Ther* **271**:557-566.

Thummel KE, Shen DD, Podoll TD, Kunze KL, Trager WF, Hartwell PS, Raisys VA, Marsh CL, McVicar JP, and Barr DM (1994b) Use of midazolam as a human cytochrome P450 3A probe: I. in vitro-in vivo correlations in liver transplant patients. *J Pharmacol Exp Ther* **271**:549-556.

Tornio A, Filppula AM, Kailari O, Neuvonen M, Nyronen TH, Tapaninen T, Neuvonen PJ, Niemi M, and Backman JT (2014) Glucuronidation converts clopidogrel to a strong time-dependent inhibitor of CYP2C8: a phase II metabolite as a perpetrator of drug-drug interactions. *Clin Pharmacol Ther* **96**:498-507.

Tornio A, Niemi M, Neuvonen M, Laitila J, Kalliokoski A, Neuvonen PJ, and Backman JT (2008) The effect of gemfibrozil on repaglinide pharmacokinetics persists for at least 12 h after the dose: evidence for mechanism-based inhibition of CYP2C8 in vivo. *Clin Pharmacol Ther* **84**:403-411.

Trainor G (2007) Chapter 31 Plasma Protein Binding and the Free Drug Principle: Recent Developments and Applications. *Annual Reports in Medicinal Chemistry* **42**:489-502.

Tran TH, Von Moltke LL, Venkatakrishnan K, Granda BW, Gibbs MA, Obach RS, Harmatz JS, and Greenblatt DJ (2002) Microsomal protein concentration modifies the apparent inhibitory potency of CYP3A inhibitors. *Drug Metab Dispos* **30**:1441-1445.

- Traylor MJ, Chai J, and Clark DS (2011) Simultaneous measurement of CYP1A2 activity, regioselectivity, and coupling: Implications for environmental sensitivity of enzyme-substrate binding. *Arch Biochem Biophys* **505**:186-193.
- Tseng E, Walsky RL, Luzietti RA, Jr., Harris JJ, Kosa RE, Goosen TC, Zientek MA, and Obach RS (2014) Relative contributions of cytochrome CYP3A4 versus CYP3A5 for CYP3A-cleared drugs assessed in vitro using a CYP3A4-selective inactivator (CYP3cide). *Drug Metab Dispos* **42**:1163-1173.
- Turner DB, Rostami-Hodjegan A, Tucker GT, and Yeo KR (2007) Prediction of nonspecific hepatic microsomal binding from readily available physicochemical properties. *Drug Metab Rev* **38(S1)**:162.
- Turpeinen M, Tolonen A, Uusitalo J, Jalonen J, Pelkonen O, and Laine K (2005) Effect of clopidogrel and ticlopidine on cytochrome P450 2B6 activity as measured by bupropion hydroxylation. *Clin Pharmacol Ther* **77**:553-559.
- Uchaipichat V, Winner LK, Mackenzie PI, Elliot DJ, Williams JA, and Miners JO (2006) Quantitative prediction of in vivo inhibitory interactions involving glucuronidated drugs from in vitro data: the effect of fluconazole on zidovudine glucuronidation. *Br J Clin Pharmacol* **61**:427-439.

Veech RL, Eggleston LV, and Krebs HA (1969) The redox state of free nicotinamide-adenine dinucleotide phosphate in the cytoplasm of rat liver. *Biochem J* **115**:609-619.

Walsky RL, Gaman EA, and Obach RS (2005) Examination of 209 drugs for inhibition of cytochrome P450 2C8. *J Clin Pharmacol* **45**:68-78.

Wattanachai N, Polasek TM, Heath TM, Uchaipichat V, Tassaneeyakul W, Tassaneeyakul W, and Miners JO (2011) In vitro-in vivo extrapolation of CYP2C8-catalyzed paclitaxel 6 α -hydroxylation: effects of albumin on in vitro kinetic parameters and assessment of interindividual variability in predicted clearance. *Eur J Clin Pharmacol* **67**:815-824.

Wattanachai N, Tassaneeyakul W, Rowland A, Elliot DJ, Bowalgaha K, Knights KM, and Miners JO (2012) Effect of albumin on human liver microsomal and recombinant CYP1A2 activities: impact on in vitro-in vivo extrapolation of drug clearance. *Drug Metab Dispos* **40**:982-989.

Wilkinson GR (2005) Drug metabolism and variability among patients in drug response. *N Engl J Med* **352**:2211.

Williams JA, Hyland R, Jones BC, Smith DA, Hurst S, Goosen TC, Peterkin V, Koup JR, and Ball SE (2004) Drug-drug interactions for UDP-glucuronosyltransferase

substrates: a pharmacokinetic explanation for typically observed low exposure (AUC_i/AUC) ratios. *Drug Metab Dispos* **32**:1201-1208.

Windberger U, Bartholovitsch A, Plasenzotti R, Korak KJ, and Heinze G (2003) Whole blood viscosity, plasma viscosity and erythrocyte aggregation in nine mammalian species: reference values and comparison of data. *Exp Physiol* **88**:431-440.

Wright JN, Slatcher G, and Akhtar M (1991) 'Slow-binding' sixth-ligand inhibitors of cytochrome P-450 aromatase. Studies with 19-thiomethyl- and 19-azido-androstenedione. *Biochem J* **273 (Pt 3)**:533-539.

Yamazaki H, Gillam EM, Dong MS, Johnson WW, Guengerich FP, and Shimada T (1997) Reconstitution of recombinant cytochrome P450 2C10(2C9) and comparison with cytochrome P450 3A4 and other forms: effects of cytochrome P450-P450 and cytochrome P450-b5 interactions. *Arch Biochem Biophys* **342**:329-337.

Yang J, Jamei M, Yeo KR, Rostami-Hodjegan A, and Tucker GT (2007) Misuse of the well-stirred model of hepatic drug clearance. *Drug Metab Dispos* **35**:501-502.

Yao C, Kunze KL, Kharasch ED, Wang Y, Trager WF, Ragueneau I, and Levy RH (2001) Fluvoxamine-theophylline interaction: gap between in vitro and in vivo inhibition constants toward cytochrome P4501A2. *Clin Pharmacol Ther* **70**:415-424.

Youdim KA, Zayed A, Dickins M, Phipps A, Griffiths M, Darekar A, Hyland R, Fahmi O, Hurst S, Plowchalk DR, Cook J, Guo F, and Obach RS (2008) Application of CYP3A4 in vitro data to predict clinical drug-drug interactions; predictions of compounds as objects of interaction. *Br J Clin Pharmacol* **65**:680-692.

Yumibe N, Huie K, Chen KJ, Clement RP, and Cayen MN (1995) Identification of human liver cytochrome P450s involved in the microsomal metabolism of the antihistaminic drug loratadine. *Int Arch Allergy Immunol* **107**:420.

Yumibe N, Huie K, Chen KJ, Snow M, Clement RP, and Cayen MN (1996) Identification of human liver cytochrome P450 enzymes that metabolize the nonsedating antihistamine loratadine. Formation of descarboethoxyloratadine by CYP3A4 and CYP2D6. *Biochem Pharmacol* **51**:165-172.

Zhang L, Zhang YD, Strong JM, Reynolds KS, and Huang SM (2008) A regulatory viewpoint on transporter-based drug interactions. *Xenobiotica* **38**:709-724.

Zhang QY, Dunbar D, Ostrowska A, Zeisloft S, Yang J, and Kaminsky LS (1999) Characterization of human small intestinal cytochromes P-450. *Drug Metab Dispos* **27**:804-809.

Zhou D, Guo J, Linnenbach AJ, Booth-Genthe CL, and Grimm SW (2010) Role of human UGT2B10 in N-glucuronidation of tricyclic antidepressants, amitriptyline, imipramine, clomipramine, and trimipramine. *Drug Metab Dispos* **38**:863-870.

Zhou SF (2009a) Polymorphism of human cytochrome P450 2D6 and its clinical significance: Part I. *Clin Pharmacokinet* **48**:689-723.

Zhou SF (2009b) Polymorphism of human cytochrome P450 2D6 and its clinical significance: part II. *Clin Pharmacokinet* **48**:761-804.

Zi J, Liu D, Ma P, Huang H, Zhu J, Wei D, Yang J, and Chen C (2010) Effects of CYP2C9*3 and CYP2C9*13 on Diclofenac Metabolism and Inhibition-based Drug-Drug Interactions. *Drug Metab Pharmacokinet* **25**:343-350.

Zientek M, Jiang Y, Youdim K, and Obach RS (2010) In Vitro-in Vivo Correlation for Intrinsic Clearance for Drugs Metabolized by Human Aldehyde Oxidase. *Drug Metab Dispos.*

Zomorodi K, Carlile DJ, and Houston JB (1995) Kinetics of diazepam metabolism in rat hepatic microsomes and hepatocytes and their use in predicting in vivo hepatic clearance. *Xenobiotica* **25**:907-916.

APPENDIX I: PERMISSION FOR ARTICLE REPRODUCTION (CHAPTER 5)



Council

Annette E. Fleckenstein
President
University of Utah

Kenneth E. Thummel
President-Elect
University of Washington

Richard R. Neubig
Past President
Michigan State University

Paul A. Insel
Secretary/Treasurer
University of California – San Diego

Dennis C. Marshall
Secretary/Treasurer-Elect
Ferring Pharmaceuticals, Inc.

Sandra P. Welch
Past Secretary/Treasurer
Virginia Commonwealth University

Charles P. France
Councilor
University of Texas Health Science
Center - San Antonio

Margaret E. Gnegy
Councilor
University Michigan Medical School

John D. Schuetz
Councilor
St. Jude Children's Research Hospital

Mary Vore
Board of Publications Trustees
University of Kentucky

Brian M. Cox
FASEB Board Representative
Uniformed Services University
of the Health Sciences

Scott A. Waldman
Program Committee
Thomas Jefferson University

Judith A. Siuciak
Executive Officer

February 2, 2015

Faraz Kazmi
XenoTech, LLC
16825 West 116th St
Lenexa, KS 66219

Email: fkazmi@xenotechllc.com

Dear Faraz Kazmi:

This is to grant you permission to include the following article in your dissertation tentatively titled "System-dependent drug metabolism of cytochrome P450 substrates: The mechanistic basis of why microsomes are vastly superior to hepatocytes at metabolizing midazolam but vastly inferior at metabolizing desloratadine" for the University of Kansas:

Faraz Kazmi, Joanna E Barbara, Phyllis Yerino, and Andrew Parkinson, A Long-Standing Mystery Solved: The Formation of 3-Hydroxydesloratadine is Catalyzed by CYP2C8 but Prior Glucuronidation of Desloratadine by UGT2B10 is an Obligatory Requirement, *Drug Metab Dispos* 2015, doi:10.1124/dmd.114.062620

On the first page of each copy of this article, please add the following:

Reprinted with permission of the American Society for Pharmacology and Experimental Therapeutics. All rights reserved.

In addition, the original copyright line published with the paper must be shown on the copies included with your thesis.

Sincerely yours,

Richard Dodenhoff
Journals Director